Involvement of Human DNA Polymerase Kappa in Nucleotide Excision Repair

A thesis submitted to the University of Sussex for the degree of Doctor of Philosophy

by

Ross Alexander John Cloney

April 2011

I hereby declare that this thesis has not been and will not be submitted in whole or in part of another university for the award of any other degree. The work described herein in my own work except where otherwise stated.

Ross Alexander John Cloney

April 2011

Acknowledgements

"But there's no sense crying over every mistake.
You just keep on trying till you run out of cake.

And the Science gets done."

- GlaDOS, **Portal**[1]

I would like to acknowledge and thank everyone who has helped me get this far, friends and family who aided me along the way with their guidance and assistance; Alan for offering me the opportunity to do a D.Phil. in his laboratory, Tomoo for kick-starting this project and mentoring me at the start of my D.Phil., Simone, Jess, Atsuko, Anna and all the members of the lab and write-up area for their seemingly endless (if sometimes contradictory) advice.

In particular I would like to note the role Justin Harbottle has played throughout the course of my D.Phil. His unquestioning and limitless support and counsel has meant far more to me than I could ever write down here.

My work throughout my D.Phil. has been supported by the Medical Research Council.

[1] (2007) Portal. Half-Life, Valve Corporation Microsoft Game Studios: Single-player puzzle-platform.

Table of Contents

List of Figures

List of Tables

List of Abbreviations

6-4PP	(6-4) pyrimidine photoproducts
ALD	Accumulation at Local Damage
APS	ammonium persulfate
ATP	adenosine triphosphate
BER	Base Excision Repair
BSA	Bovine Serum Albumin
CPD	Cyclobutane pyrimidine dimer
CS	Cockayne Syndrome
DMEM	Dulbecco's Modified Eagle's Media
DMSO	dimethyl sulfoxide
DNA	Deoxyribonucleic Acid
DSB	Double Strand Break
EDTA	Ethylenediamine tetraacetic acid
FACS	Fluorescent Activated Cell Sorting
GFP	Green Fluorescent Protein
GGR	Global Genomic Repair
HU	Hydroxyurea
IP	Immunoprecipitation
IR	Ionising Radiation
kDa	Kilo Dalton
NER	Nucleotide Excision Repair
PAD	Polymerase Associated Domain
PBS	Phosphate Buffered Saline
PCNA	Proliferating Cell Nuclear Antigen
PCR	Polymerase Chain Reaction
Pol	Polymerase
RNAPII	Ribonucleic Acid Polymerase II

RPM	Revolutions Per Minute
SDM	Site-Directed Mutagenesis
SDS	Sodium Dodecyl Sulphate
SDS-PAGE	Sodium Dodecyl Sulphate Polyacrylamide Gel Electrophoresis
SSB	Single Strand Break
TEMED	Tetramethyl-ethylenediamine
TCR	Transcription Coupled Repair
TLS	Translesion Synthesis
TTD	Tricothiodystrophy
UBZ	Ubiquitin Binding Zinc Finger Domain
UV	Ultraviolet
XP	Xeroderma Pigmentosum
XPV	Xeroderma Pigmentosum Variant

Abstract

Nucleotide excision repair is one of the major repair pathways responsible for identifying and removing lesions in the DNA double helix. In higher eukaryotes, nucleotide excision repair is a coordinated response of over 30 proteins recruited in an ordered procession with distinct roles in the recognition, removal and repair of said lesions. A key step in the completion of the repair process is the resynthesis of the excised strand using the undamaged partner as a template. DNA polymerase kappa (polκ), a member of the Y-family, has been shown to have a role in nucleotide excision repair distinct from its traditional role in translesion synthesis. Cell lines lacking polκ showed clear defects in nucleotide excision repair and increased ultraviolet light sensitivity. Building on this established work, conserved residues were identified in the C-terminus of human polκ and mutated to alanines. Under transient expression, mutations in the ubiquitin binding domains severely impaired the recruitment to sites of damage. Cell lines defective in polκ that stably expressed these mutant polymerases showed sensitivity to ultraviolet radiation following exposure; intriguingly, this defect seems confined to the global genomic repair pathway as no substantial defect in transcription-coupled repair was observed. Following on from these observations, immunoprecipitation of the polymerase and partner proteins was investigated in an attempt to identify interactions disrupted by the mutations to the ubiquitin binding domains. These experiments indicated impairment in binding to ubiquitinated PCNA in the mutants. In further work, the recruitment of wild-type human polκ was shown to be independent of the 3' incision by the nuclease XPG during the repair process, consistent with a recently proposed model for NER.

Introduction

1.1 General Overview of DNA Damage

Paramount to the survival of the cell is the preservation of the integrity of the genetic information encapsulated in the DNA carried in the nucleus of the cell. However, this inheritance is constantly exposed to agents that can alter or break the structure of DNA or impede vital biological processes, to the detriment of the cell, the organism and its descendents. The exposure of the cell to DNA damaging agents comes from a variety of sources, both internal and external. DNA bases will spontaneously undergo hydrolysis, resulting in depurination that can result in the loss of a guanine or adenine and deamination that changes a cytosine to a uracil. The price of oxidative respiration is the generation of reactive oxygen species (ROS) that include superoxide anions, hydrogen peroxide, hydroxyl radicals and downstream products generated by the interaction of ROS with other cellular components. These highly reactive free radical species will readily attack DNA, leading to the formation of oxidative lesions in the DNA (Wang, 2007). Other potentially mutagenic effects arise from incorporation of mis-matched base pairs during DNA replication or the intentional generation of double-strand breaks (DSB) in the DNA during the V(D)J recombination of genes to generate antibody diversity (Bassing et al., 2002) or during meiosis. From external sources, the cell is exposed to ultraviolet (UV) radiation, ionising radiation (IR) and external chemical hazards. UV radiation generates helix distorting lesions such as cyclobutane pyrimidine dimers (CPD) and pyrimidine(6-4)pyrimidone photoproducts (6-4PP) by exciting electrons to high energy states and allowing bonds to form between neighbouring bases in the DNA (Herrlich et al., 2008); these distortions can block DNA replication and transcription. IR from the products of radioactive decay, alpha-, beta- and gamma-rays, strikes the double helix with enough energy to generate a DSB. Chemical sources of DNA damage include those found naturally in the environment, such as the bulky hydrocarbon by-products of combustion that can create helix distorting lesions. Examples are benzo[a]pyrene or a variety of synthetic chemicals often used in anti-cancer therapy including the cross-linking agent cisplatin and the DNA-cleaving agent bleomycin. In single-celled organisms, damage to the genetic

material can have consequences for the viability of the cell. In multicellular eukaryotes, the danger of DNA damage comes not from the loss of a single cell but from the mutational effects that can increase the risk of a cell turning cancerous. The extent of the assault the genome is under on a daily basis is difficult to fully grasp. It has been estimated that every day each human cell will be required to deal with ten thousand depurination events, over six thousand methylation or oxidation events and, depending on location, up to a hundred thousand lesions resulting from sunlight exposure (reviewed in (Ciccia and Elledge, 2010). This level of damage represents a background level to which the cell has had to evolve solutions. Life style decisions such as smoking or the environmental exposures common to the modern world, such as air travel and medical scans, add further pressures onto the repair machinery. Though due to the sheer size of the human genome, thousands of daily incidences of damage affects only a small portion of the overall genome, if unrepaired they could potentially be catastrophic events. The types of DNA damage are exemplified through the repair mechanisms evolved to deal with them and can be divided into the following categories: Direct Reversal, Base Excision Repair (BER), Mismatch Repair (MMR), Homologous Recombination (HR), Non-homologous End-Joining (NHEJ) and Nucleotide Excision Repair (NER). BER is responsible for minor helical distortions, MMR can correct insertion, deletions and misincorporation of bases, while NHEJ and HR can correct double strand breaks in the DNA helix and NER deals with the removal of a variety of bulky DNA lesions (Hoeijmakers, 2001).

1.1.1 Ubiquitination

The coordination of the cellular responses to DNA damage is regulated through a variety of mechanisms but a key tool at the disposal of the cell is the ability to modify proteins post-translationally in response to changing conditions. These range from the frequent and well-characterised modification by phosphorylation, where upon a phosphate group is covalently bound to a serine, threonine or tyrosine residue of a target protein by a kinase and removed by a phosphatase, to other modifications less encountered in DNA damage

response and repair such as gycosylation of proteins where carbohydrate groups are attached to the target protein. Post-translational modifications often function to change the activity of a target protein. One of the common modifications is the use of small modifying proteins attached to their target. The best characterised is the 8kDa protein ubiquitin, though several small modifying proteins exist that function in similar manners, such as SUMO (*S*mall *U*biquitin-like *Mo*difier), NEDD (or RUB – *R*elated to *Ub*iquitin) amongst others (Jentsch and Pyrowolakis, 2000) . For the purposes and intent of what follows in this thesis, ubiquitin and its usage will be focused on below.

Ubiquitin, as the name suggests, is a ubiquitous protein among the eukaryotes and has been extremely highly conserved. In the long evolutionary divergence between yeast and humans, only three residues out of 76 have changed. Ubiquitin is a protein present in many essential biological processes: mediating degradation of proteins via the proteasome system, protein modifications to signal DNA damage and recruit response factors, protein transport and endocytosis amongst others.

Ubiquitin is conjugated to its target proteins through a series of reactions involving a cascade of proteins. Firstly, an 'E1' protein uses the energy of ATP to activate ubiquitin. Then the ubiquitin is handed off to an 'E2' ubiquitin conjugating protein that functions in conjunction with an 'E3' ligase to transfer the ubiquitin from the serine residue of the E2 onto a lysine residue of the target substrate. Typically, species have a single or limited set of E1 proteins, a handful of E2 proteins and a diverse array of E3 proteins for the wide range of substrates to which ubiquitin can be conjugated (reviewed in (Pickart and Eddins, 2004; Weissman, 2001). A key reaction in the DNA damage response is the addition of ubiquitin to the eukaryotic sliding clamp PCNA. This is facilitated by the E2 Rad6 and the E3 Rad18 and allows the switch to damage tolerance pathways (Kannouche et al., 2004) and is mediated through the interaction of RAD18 with the ssDNA binding protein RPA (Davies et al., 2008). Other proteins can interact with ubiquitin modified substrates through specialised domains that recognise the ubiquitin modification. These domains

vary from each other in their structure depending on the role the protein performs. As will be expanded upon later, two important ubiquitin-interaction motifs for DNA damage tolerance are the ubiquitin zinc finger (UBZ) domains, which coordinate a zinc ion with conserved histidines and cysteines, and ubiquitin binding motifs (UBM) (Hurley et al., 2006).

1.1.2 Mismatch Repair

Given the breadth and extent of the genome, numbering close to an estimated three billion base pairs in humans, it is remarkable that replication can proceed as accurately as it does to minimise the risk of potentially threatening mutagenic events. The replicative polymerases δ and ε, responsible for the lagging and leading strand of the replication fork respectively, are capable of adding nucleotides to the elongating DNA strand at a rate of thousands per second. This speed is matched with an accuracy of one mistake in every few million newly incorporated nucleotides (Lindahl, 1996). Such accuracy is possible due to their tightly constrained active site and proof-reading capabilities. However, even with this rarity of mistakes, the size of the genomes found in the higher eukaryotes would still lead to an unacceptable incorporation of several hundred mispaired bases per replication cycle. It is the ability of the cell to recognise mismatched bases and correct the mistakes that lowers the rate of inaccurate replication from one mistake in a million to one or two mistakes per billion.

In *Escherichia coli*, mismatch repair is carried out by the actions of MutS, MutL and MutH. The mismatch is initially recognised by a MutS homodimer which then, in the presence of ATP, recruits a MutL homodimer. Together, these proteins activate the endonuclease MutH that cleaves the DNA strand up- or down-stream of the lesion, up to a kilobase away. The specificity for nicking only the strand containing the lesion is due to *E. coli* being able to distinguish template DNA from newly synthesised DNA based on its methylation status. The MutH protein cleaves at unmethylated GATC sites. If the excision takes place 5' of the mismatched base pair, then the 5'-3' nucleases RecJ or ExoVII digest away the DNA until

the erroneous base is removed. If MutH cleaves downstream of the lesion, the 3'-5' exonucleases ExoI or ExoX remove the DNA strand. Following this, the strand is restored by DNA pol III and DNA ligase (reviewed in (Schofield and Hsieh, 2003).

In eukaryotic organisms, a broadly similar mechanism is at work though the number of proteins involved is greatly expanded and specialised. Eukaryotes have homologues of the MutS (MSH1-MSH6) and MutL (MLH1-MLH3, PMS2) proteins found in prokaryotes. The differing MSH proteins have evolved to specialise in the detection of different mismatches by working as heterodimers. MSH2 and MSH6 can detect a mismatched base and insertion or deletion loops that result in a 1-3 nucleotide offset. MSH2 and MSH3 function together to detect larger loops of 2-8 nucleotides, while MSH1 appears to have a role in mitochondrial mismatch repair. The two remaining MutS homologues in eukaryotes, MSH4 and MSH5 have meiosis specific roles independent of DNA repair. The MLH proteins function as heterodimers as well, with MLH1 being the most common component. A heterodimer of MLH1 and PMS2 functions as the key MutL homologue for repair after replication (reviewed in (Modrich, 2006; Schofield and Hsieh, 2003). As of yet, no homologue for MutH has been identified in eukaryotes nor do eukaryotes discriminate DNA strands based on methylation status of GATC sequences. In eukaryotes strand discrimination is based on nicks in DNA. On the lagging strand, these nicks are readily available from the synthesis of multiple Okazaki fragments. The exonuclease ExoI degrades the mismatch containing strand and the DNA is restored by the replication machinery and LigI. On the continuous leading strand, discriminating the newly synthesised strand is more complicated. PMS2 acts as an endonuclease to nick DNA 5' of a mismatch to allow access by ExoI and digestion (reviewed in (Moldovan et al., 2007)) (Fig 1.1).

1.1.3 Base Excision Repair

The structure of the nucleotides in the genome is not static but a dynamic interplay between chemical attack and repair. As previously mentioned, there are a variety of

Figure 1.1 - Mismatch Repair

In prokaryotic systems, the MutS protein recognises the mismatched base and recruits MutL. This activates the nuclease MutH which nicks the newly synthesised strand. Exonucleases degrade the error containing strand and the DNA is replaced by the actions of Pol III and DNA Ligase.

In eukaryotes, MSH dimers recognise different mismatches, insertion loops or deletion loops. Analogous to prokaryotes, MLH proteins are then recruited. The mismatch containing strand is degraded by ExoI and the replication machinery restores the gap in the DNA before it is finally sealed by the ligase LigI.

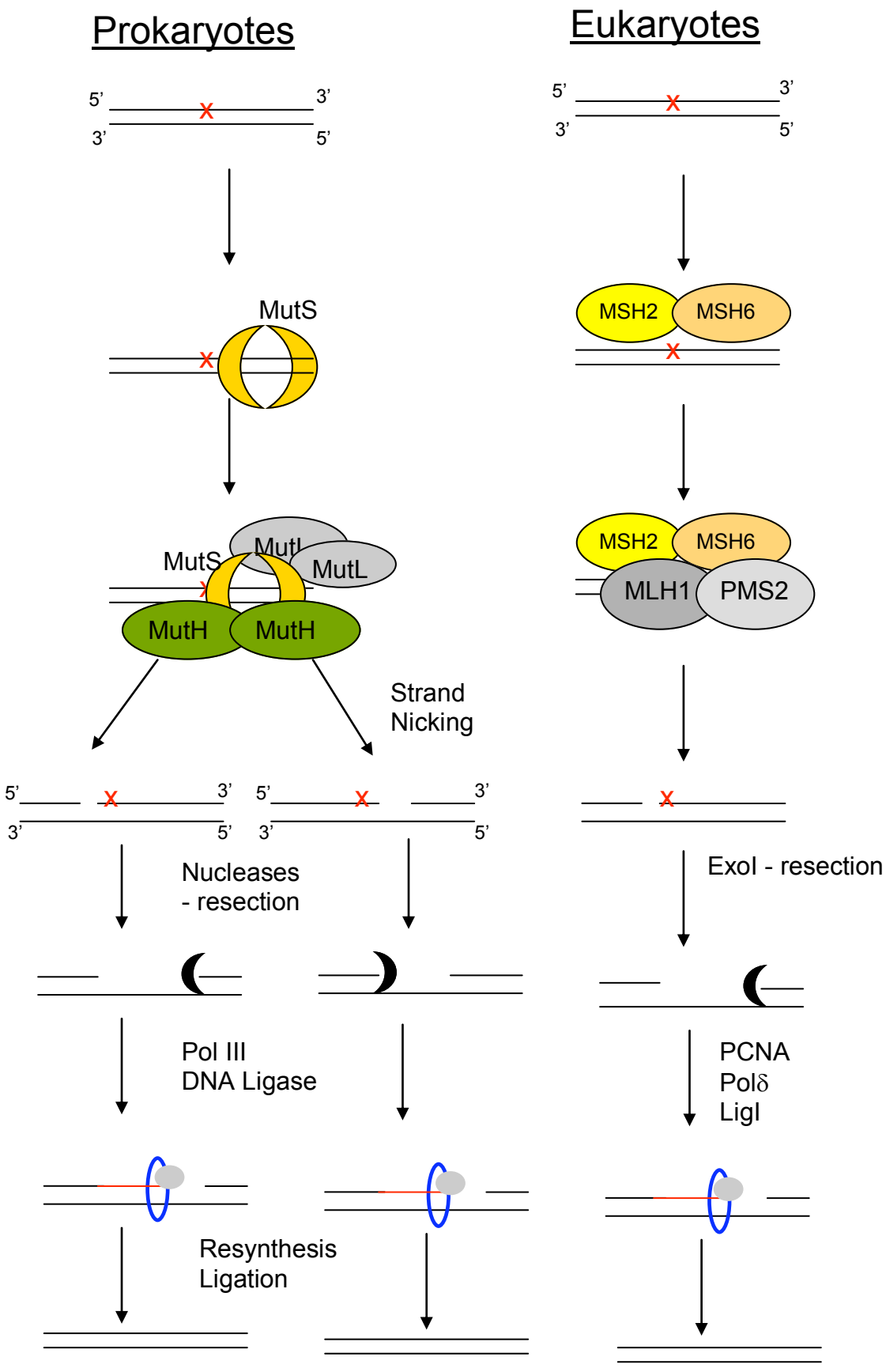
Prokaryotes
Eukaryotes
5'
3'
3'
5'
MutS
MSH2
MSH6
MutS
MutL
MutL
MutH
MutH
MLH1
PMS2
Strand
Nicking
Nucleases
- resection
ExoI - resection
Pol III
DNA Ligase
PCNA
Polδ
LigI
Resynthesis
Ligation

endogenous and exogenous events that can alter the composition of the bases. Spontaneous hydrolysis of cytosine to uracil can cause a C:G to T:A transition if replication proceeds across the incorrect base. Several proteins can recognise uracil in DNA with one of the best characterised being uracil-DNA glycosylase (UNG). The inclusion of thymine in DNA instead of uracil as in RNA presents an elegant evolutionary adaptation to distinguish valid genetic information from progressive incorporation of entropic noise. Other DNA glycosylases are able to distinguish other varieties of modified bases resulting from such environmental hazards as ROS; OGG1 recognises the oxidised base 8-oxoguanine and MPG recognises alkylated DNA bases (reviewed in (Barnes and Lindahl, 2004). Following identification of an altered base, BER can proceed down a short-patch repair pathway or a long-patch repair pathway. In short-patch repair, after identification the damaged base is cleaved producing an abasic site. An AP endonuclease is recruited to cut 5' of the abasic site, generating a nick in the DNA backbone and generating an available hydroxyl group at the 3' terminus for DNA synthesis. Some DNA glycosylases can also possess bifunctional properties. In addition to their ability to remove the damaged base, they can function as AP lyases. This activity cleaves 3' of the abasic site, generating an available 5' phosphate group for subsequent ligation. This allows access by DNA polymerase β and the scaffolding protein XRCC1 which correctly inserts a new base into the gap opposite the template strand. DNA polβ also possesses 5' dRPase activity that can remove a 5' sugar-phosphate residue to generate a 5' phosphate group (Lindahl, 2000). The DNA strand is then resealed by DNA Ligase III in prokaryotes and LigIII or LigI in eukaryotes (Kubota et al., 1996). In long-patch repair, the incision by the AP endonuclease leads to the recruitment of DNA polymerase β, DNA polymerase δ, PCNA, the flap structure-specific endonuclease I FEN1 and LigI. Actions by the polymerases displace a tract of DNA leading to a overhanging flap structure that is excised by FEN1 before the newly synthesised strand is ligated to the original DNA backbone (Klungland and Lindahl, 1997) (Fig 1.2).

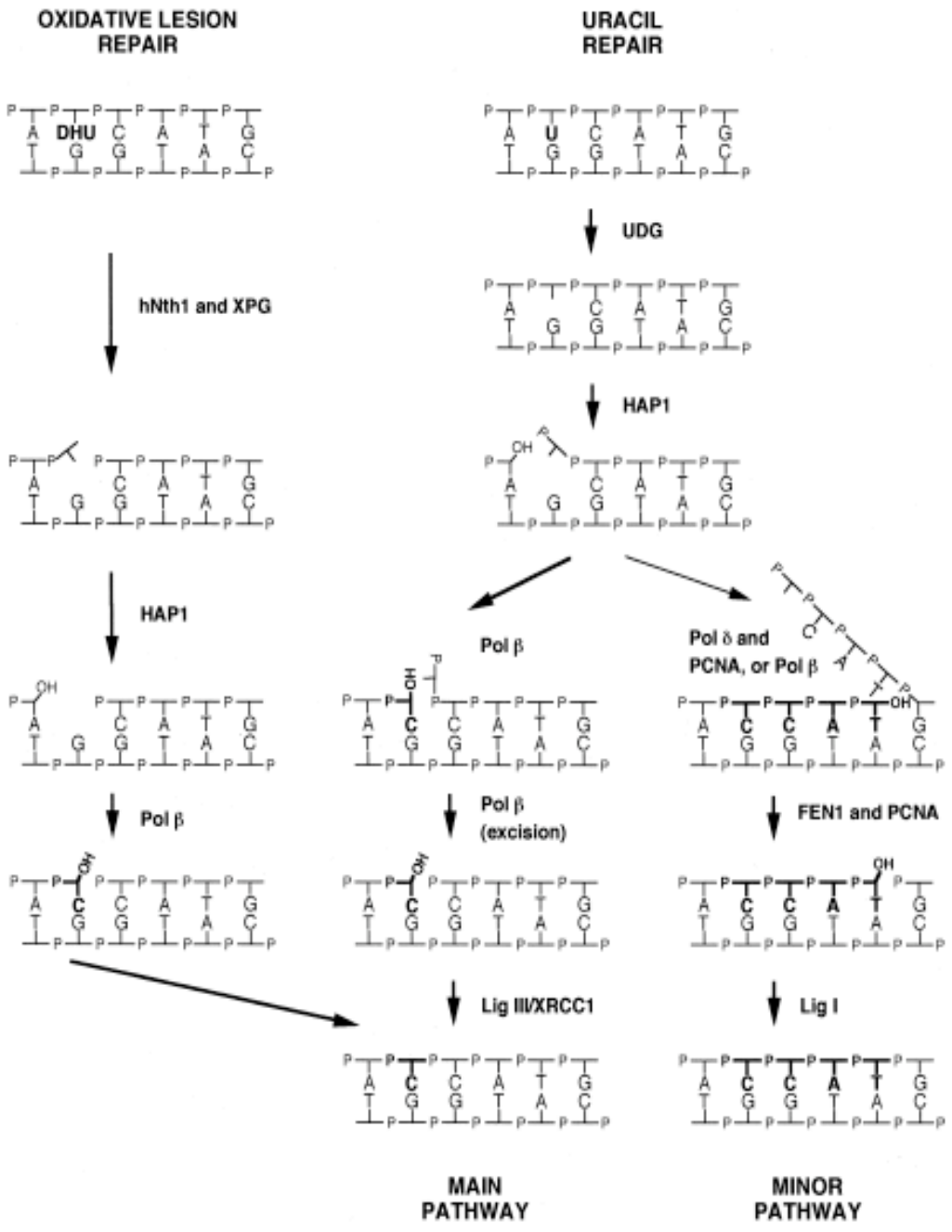

Figure 1.2 - Base Excision Repair

Recognition of the lesion or spontaneous uracil leads to a the generation of an abasic site. Processing generates a 3'-OH group for resynthesis of the single base by polβ. This resynthesis step can either be 'short-patch' by filling in the single base with the actions of LigIII/XRCC1 or 'long-patch' over several bases with the involvement of polδ, PCNA and FEN1 to degrade the displaced strand before ligation with LigI. Adapted from Lindahl (2000) *Mutation Research*

1.1.4 Single Strand Break Repair

It is not just the component bases of DNA that can be damaged by cellular processes and the environment. The sugar-phosphate backbone is also vulnerable. Breaks to the DNA backbone are an extremely frequent insult but also potentially dangerous as they can be converted into highly dangerous double-strand breaks if they are encountered by the replication machinery. As such, the detection of a single strand break is an extremely rapid event. Within seconds of a break occurring, poly(ADP-ribose) polymerase (PARP) 1 and PARP2 are recruited to the break through their zinc-finger domains and synthesise long chains of poly(ADP-ribose) (PAR) on PARP1, histones H1 and H2A. These chains of PAR recruit XRCC1 and LIG3 to reseal the break. XRCC1 acts as a scaffold for end processing proteins required to 'clean-up' DNA ends that are not directly ligatable, such as APE1, APLF, APTX and PNK. Breaks that not directly adjunct to each other have the intervening gap filled in by polymerase β prior to ligation. The enzyme PARG hydrolyses the PAR chains, completing the cycle of repair within minutes of the initial damage (reviewed in (Caldecott, 2008; Schreiber et al., 2006) (Fig 1.3).

1.1.5 Double Strand Break Repair

Of all the varieties of DNA damaging events, the creation of a break in both DNA strands represents one of the potentially most cytotoxic possibilities that must be addressed swiftly by the repair machinery. Double strand breaks can be created through radiation damage, chemical attack from drugs such as bleomycin or the replication fork colliding with unrepaired single strand breaks, lesions or cross-links. Failure to properly repair the complete severing of the DNA helix can result in large scale restructuring of the genome such as Gross Chromosomal Re-arrangements or propel the cell down apoptotic pathways. Unsurprisingly, in recent years the knowledge of the complexity of the response to double strand breaks has grown rapidly. Each new protein discovered gives the field a better

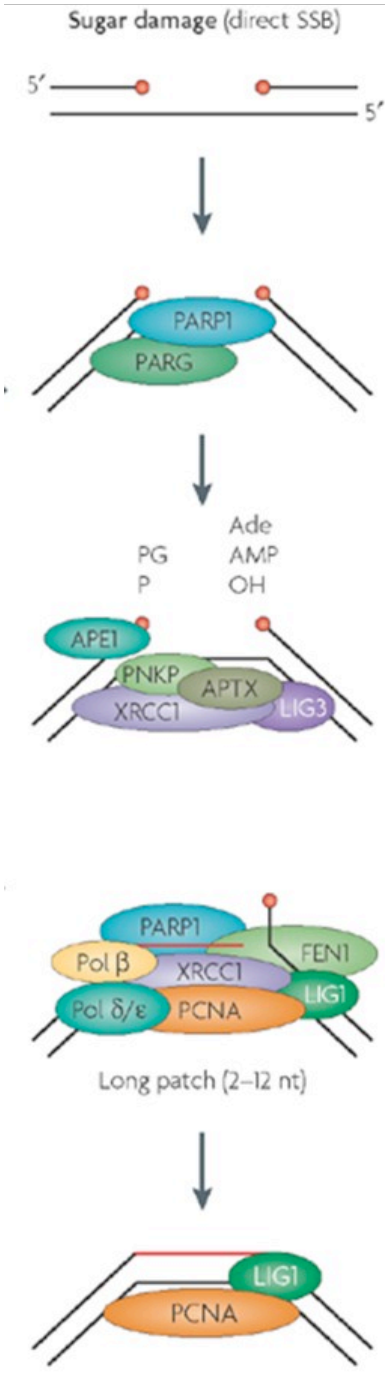

Fig 1.3 - Single Strand Break Repair

Recognition of the single strand break is followed by end processing and the assembly of gap filling machinery alongside the scaffolding protein XRCC1. Following gap filling, the DNA backbone is sealed with a ligase. Adapted from Caldecott (2008) *Nature Reviews Genetics*

representation of the level of feedback and signal amplification required of this repair response.

Upon the creation of a double strand break, the eukaryotic cell has two major pathways to repair available to it. Non-Homologous End-Joining (NHEJ) offers a rapid repair with no safeguards against the degradation or loss of genetic information. Homologous recombination (HR) allows for error-free repair but is dependent on the presence of a complementary template in the form of a sister chromatid. Two further variations on this method of repair are also available, alternative-NHEJ and single strand annealing (SSA).

1.1.5.1 Non-Homologous End Joining

During phases of the cell cycle where there is no available sister chromatid to ensure accurate repair the severed ends of the double helix must be directly religated to each other. Seconds after creation of double strand breaks, the Ku heterodimer is recruited to the sites of the break. The heterodimer is composed of Ku70 and Ku80 subunits. These subunits form a ring structure, with the central aperture wide enough to accommodate the DNA double helix (Walker et al., 2001). Each end of the break can have multiple Ku heterodimers loaded onto it as they slide down the DNA helix. Recently, Ku70/80 has been shown to have a degree of DNA end processing ability (Roberts et al., 2010). Ku70/80 proceeds to then load the catalytic subunit of DNA-PK and activate it (Yoo and Dynan, 1999). This synaptic complex of Ku70/80 and DNA-PK recruits DNA Ligase IV, XRCC4 and XLF to religate the ends of the DNA (reviewed in (Mahaney et al., 2009). Limited end processing by the nuclease Artemis and other factors such as APLF and the PNK kinases is used to prepare ends unsuitable for direct ligation (Povirk et al., 2007) (Fig 1.4). NHEJ can either proceed through the described pathway, which leads to the rapid repair of DSBs, or NHEJ can proceed through a slower repair pathway. The local chromatin structure distinguishes between rapid or slow repair. The slower repair pathway is dependent on the ATM signalling cascade.

Fig 1.4 - Non-Homologous End-Joining

Initial recognition of the Double Strand Break by the Ku70/80 heterodimer is followed by recruitment of DNA-PKcs and factors including XRCC4, XLF, and DNA Ligase IV to resect the DNA ends and ligate. In a heterochromatic region, KAP1 is phosphorylated to open up chromatin structure and repair requires the involvement of ATM and Artemis.

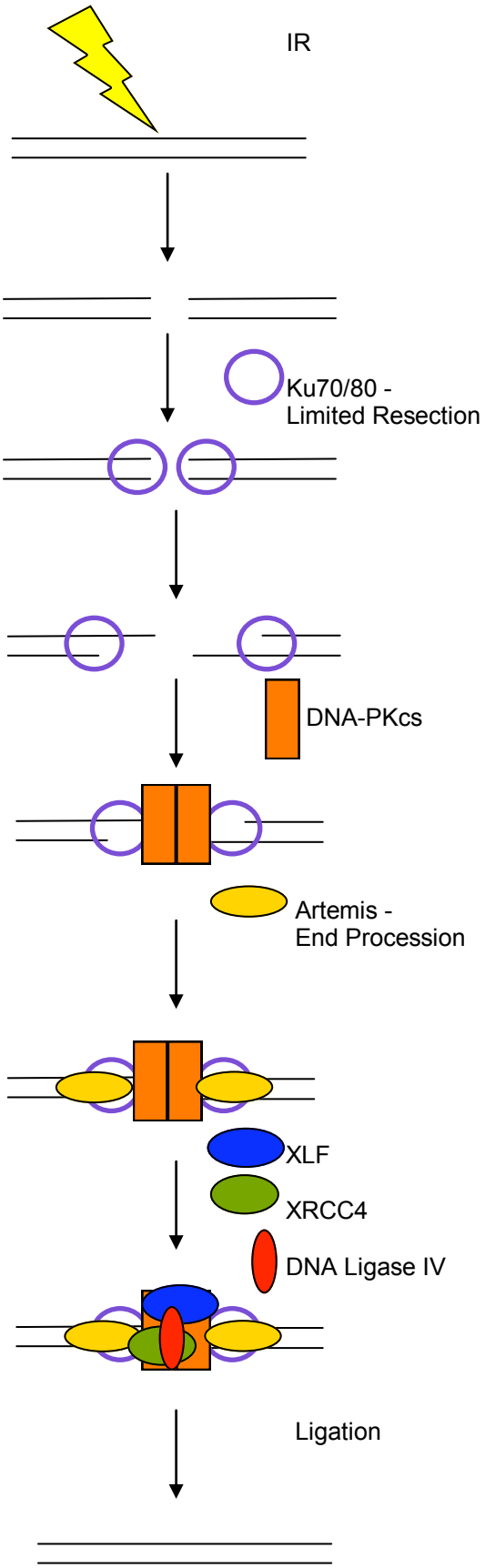
IR
Ku70/80 -
Limited Resection
DNA-PKcs
Artemis -
End Procession
XLF
XRCC4
DNA Ligase IV
Ligation

The recruitment and activation of the kinase ATM is an essential step in the response to a double-strand break as it is responsible for the phosphorylation and activation of many downstream proteins. In undamaged cells, ATM exists as an inactive dimer but following DNA damage, ATM autophosphorylates on serine 1981 and is present as a catalytically active monomer (Bakkenist and Kastan, 2003). ATM is responsible for the phosphorylation of histone H2AX, a common variant of histone H2A, on serine 139 (Rogakou et al., 1998). γ-H2AX acts as signal and scaffold platform for further downstream factors required for DNA repair and the histone phosphorylation can spread over many megabases from the site of the initial break. γ -H2AX recruits MDC1 through MDC1's BRCT repeats, which further recruits ATM and propagates the signal. MDC1 acts as a platform for the recruitment of various downstream proteins such as 53BP1 and the ubiquitin ligase RNF8, which ubiquitinate H2A and H2AX in a K63 linked manner. These ubiquitin chains recruit the ubiquitin ligase RNF168 creating further K63 linked ubiquitin chains. RAP80 interacts with the ubiquitin chains and serves to recruit the BRCA1 complex (Huen et al., 2007; Mailand et al., 2007). The exact nature of the BRCA1 complex is still being elucidated, though ubiquitin binding and deubiquitinating activities have been reported for its subunits (Wang et al., 2009)

In eukaryotes, DNA is condensed into chromatin which can be divided into the accessible euchromatin and the highly condensed heterochromatin. In the latter, access to repair factors is hindered by the compact structure of the chromatin. For NHEJ to ligate DNA ends in this context, the chromatin must be relaxed. This requires the actions of ATM to phosphorylate the heterochromatin building factor KAP-1. This signal is initially genome wide and then persists at sites of DSB; this persistence is dependent on the presence of 53BP1. In cells lacking 53BP1, KAP-1 and ATM foci fail to form at heterochromatic regions. The relaxed chromatin structure allows access to the DNA ends by Artemis for end-processing before repair of the DSB (Goodarzi et al., 2008; Noon et al., 2010).

1.1.5.2 Homologous Recombination

The presence of a sister chromatid during S-phase and G2 allows the eukaryotic cell a route to error-free repair of double-strand breaks by using the genetic information on the homologue as a template for the damaged chromatid. The double-strand break is recognised through the MRN complex, composed of MRE11-RAD50-NBS1. MRE11 possessed endonuclease and exonuclease activities that could point to a role in beginning the processing of the DNA ends for HR, however any nuclease activity is limited and may be limited to 'cleaning up' ends before more extensive resection by other nucleases. RAD50 interacts with MRE11 through its ATPase domains and helps to stabilise the DNA ends in preparation for HR. NBS1 interacts with MRE11 and, through its C-terminus, with ATM (reviewed in (Mimitou and Symington, 2009; Williams et al., 2007). The ATM signalling cascade has previously been outlined in the proceeding section.

A limited degree of resection is accomplished by CtIP but much more extensive resection of the DNA ends is accomplished by the exonuclease EXO1. This exposes a large region of single-stranded DNA that is rapidly coated with the single-strand binding protein RPA (Bolderson et al., 2010; Sartori et al., 2007). This protein coat needs to be displaced to allow recombination and is accomplished by BRCA2 and the recombinase RAD51, the latter which forms a nucleofilament with the DNA and conducts a search for homology with the sister chromatid (Sigurdsson et al., 2001). Strand invasion and extension leads to the formation of a double Holliday Junction, that then undergoes 'dissolution' by the actions of Bloom helicase and TOPOIIIα leading to a non-crossover (Wu and Hickson, 2003). Crossover and non-crossover resolutions can be achieved through the actions of MUS81 (Chen et al., 2001) or through the actions of the resolvase GEN1 (Ip et al., 2008) (Fig 1.5).

1.1.6 Direct Reversal of Photo-Products

A common and elegant solution that has evolved to deal with the DNA damage generated by exposure to sunlight is the direct reversal of the lesion by a dedicated family of proteins

Figure 1.5 - Homologous Recombination

Following the generation of a double strand break, the MRN complex detects the break and helps to recruit the kinase ATM. ATM initiates a cascade of events including the phosphorylation of H2AX which is proceeded by a series of protein modifications and recruitment that includes the proteins Mdc1, 53BP1, RNF8, RNF168, CtIP, BRCA1, BRCA2, RAD51 amongst others. The DNA ends are resected and the exposed single strand is coated with Rad51 which searches the sister chromatid for homology. This is followed by strand invasion and the formation of Holliday Junctions that can then either be resolved in a crossover or non-crossover manner.

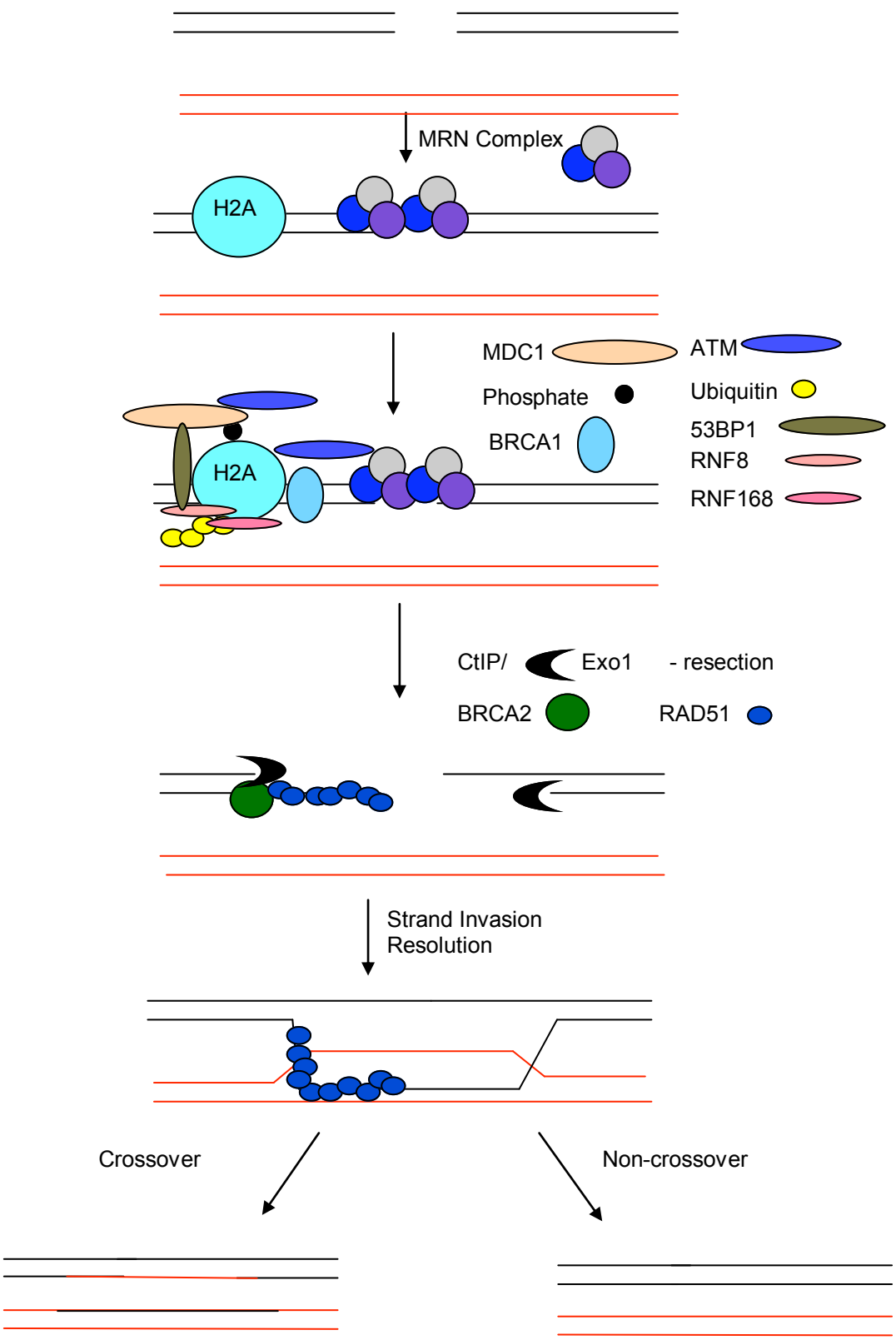
MRN Complex
H2A
MDC1
ATM
Phosphate
Ubiquitin
BRCA1
53BP1
RNF8
H2A
RNF168
CtIP/
Exo1
- resection
BRCA2
RAD51
Strand Invasion
Resolution
Crossover
Non-crossover

known as the photolyases. These proteins use the energy of visible light to repair the damage caused by UV light. These proteins are found nearly ubiquitously across life and are related to the circadian proteins that regulate the internal clock of organisms. While CPDs and 6-4PP are detected by different photolyases, the manner in which they function is similar. The lesion is generated by high-energy UV wavelengths. After detection, the proteins utilise the energy of blue or near-UV sunlight to excite an electron in their chromophore. This electron is used to reduce a FAD group and passed along to the pyrimidine ring of the linked bases. This in turn destabilises the ring and it collapses, breaking the bonds holding the base pairs together. The electron is finally passed back to the photolyase to return its chromophore to a ground state. Intriguingly, the placental mammals lack photolyase proteins, despite their presence in all the other branches of life, including the non-placental mammals. Though the reasons of this evolutionary loss are unclear, the placental mammals are able to utilise photolyases if they are induced to transgenically express the proteins or are treated with topical applications. In the absence of functional photolyases, the placental mammals are entirely dependent on the functions of nucleotide excision repair to remove the DNA damage induced by sunlight exposure (reviewed in (Eker et al., 2009)).

There are other methods of direct reversal dealing with other forms of DNA damage. For example, exposure to alkylating agents can add undesirable methyl groups to bases producing lesions including O^6-methylguanine (O^6-meG). These alterations if unrepaired are mutagenic by virtue of producing G:C -> A:T transitions during replication. Direct repair of these damaged bases is handled by methyl- and alkyltransferases. To illustrate, O^6-meG is repaired by the actions of O^6-meG-DNA methyltransferase (MGMT) which transfers the methyl group on to itself, de-activating itself in the process (reviewed in (Eker et al., 2009)). Though a fascinating topic these methods of direct repair will not be further discussed in this thesis.

1.2 Nucleotide Excision Repair

The nucleotide excision repair pathway is a highly conserved, highly versatile DNA repair pathway capable of removing a diverse range of helix-distorting DNA lesions, particularly the UV photoproducts, by removing a stretch of nucleotides, typically 22-28 base pairs long in eukaryotes and 12 base pairs in prokaryotes, containing the damage. In *E.coli*, NER is a coordinated response involving six proteins: UvrA, UvrB, UvrC and UvrD to remove the damage, Pol I to fill the DNA gap and finally DNA Ligase to reseal the strand. Eukaryotic NER is divided into two broad areas of function, Global Genomic Repair (GGR) and Transcription Coupled Repair (TCR). TCR is initiated when an actively transcribing RNA Polymerase II (RNAP II) encounters a DNA lesion it cannot accommodate. GGR monitors the entire genome, which includes transcribed and non-transcribed regions, for lesions produced during normal cellular activities and from DNA-damaging agents. The NER process is a multi-step, multi-enzyme procedure that involves: damage recognition, DNA processing and gap-filling. While GGR and TCR begin with different proteins due to their different methods of damage detection, the two processes then converge to complete NER.

When NER proteins are defective, three diseases can result: Xeroderma Pigmentosum (XP), Cockayne syndrome (CS) and Tricothiodystrophy (TTD). XP is characterised by predisposition to skin cancers, sunlight-induced pigmentation changes and, depending on the complementation group, present with extreme sun-sensitivity and neurological abnormalities. XP can be subdivided into different complementation groups based on which protein in GGR is compromised (XP-A through XP-G though NER is not compromised in XP-V). CS patients show mental and physical abnormalities and premature aging while TTD patients have brittle hair, growth retardation and neurological abnormalities (Lehmann, 2003).

1.2.1 NER in prokaryotes

The NER system in prokaryotes, using *E. coli* as a model system, is a six enzyme process. These enzymes have functional equivalents in eukaryotic systems, though as with most biological processes, the eukaryotic NER process involves many more proteins. UvrA forms a heterotrimer or heterotetramer with UvrB ($UvrA_2UvrB$ or $UvrA_2UvrB_2$ respectively) in an ATP-dependent manner (Truglio et al., 2006). This complex binds to DNA and scans along until it encounters damage. Upon damage recognition, UvrA dissociates from the complex. Interaction with UvrC brings this into the complex, where it cleaves the damaged strand of DNA approximately 4 nucleotides 3' of the damage and approximately 7 nucleotides on the 5' side, creating a 12-15 nucleotide gap. UvrD (DNA helicase II) unwinds the DNA duplex, releasing the incised strand. Finally, DNA Polymerase I fills in the gap, releasing UvrB and DNA ligase seals new DNA to the existing DNA (reviewed in (Truglio et al., 2006)). The prokaryotic NER pathway is summarised overleaf (Fig 1.6). Intriguingly there is evidence from *E. coli* that natural NER processes can lead to spontaneous mutagenic events. While NER serves to repress UV induced mutagenesis, under undamaged growth conditions there is an increase in spontaneous mutagenesis in NER-proficient strains compared to NER-deficient strains. NER-overproducing strains in turn showed a greater increase in the bacterial SOS response (Hasegawa et al., 2008). This raises the possibility that NER machinery can incorrectly recognise normal DNA structures as damage and prompt their excision, a mechanism that might also prevail in a mammalian context.

1.2.2 NER in eukaryotes

The process of NER, like many biological processes that have evolved to address problems common to all domains of life, in the eukaryotes bears mechanistic similarities to the process as it is done in the prokaryotes, with a marked increase in the number and complexity of proteins involved given, the vastly more complex genomic landscape that

Figure 1.6 - Prokaryotic Nucleotide Excision Repair

The heterotrimer $UvrA_2UvrB$ binds to the DNA and scans along until it encounters a lesion. Binding of UvrB kinks the DNA helix,UvrA disassociates from the heterotrimer and UvrC is recruited. UvrC makes incisions 5' and 3' around the lesion. The helicase UvrD releases the incised 12bp fragment of DNA containing the lesion. Repair synthesis factors are recruited, Pol I and DNA Ligase, to seal the gap that has been generated by the actions of the NER machinery.

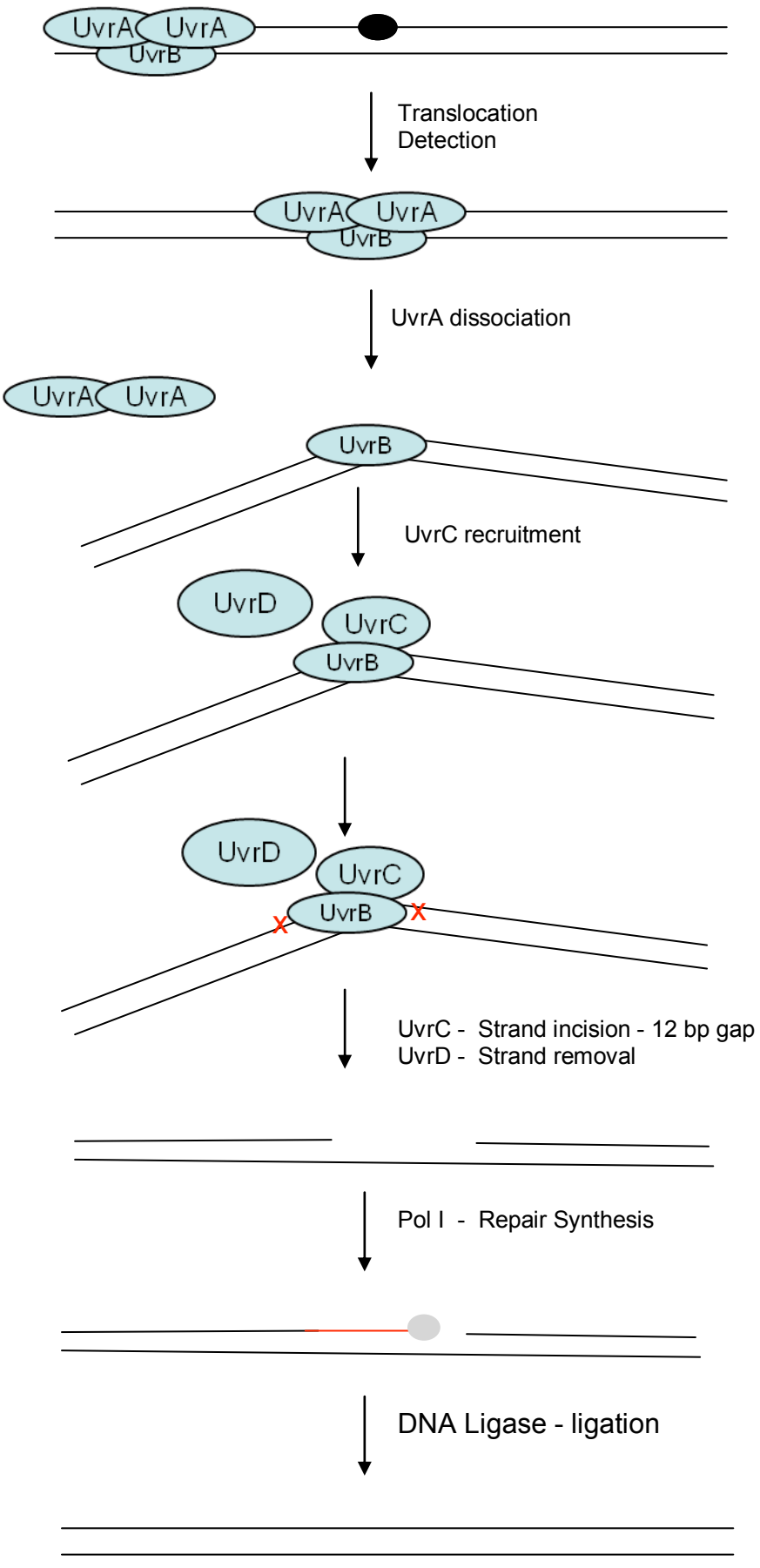
UvrA
UvrA
UvrB
Translocation
Detection
UvrA
UvrA
UvrB
UvrA dissociation
UvrA
UvrA
UvrB
UvrC recruitment
UvrD
UvrC
UvrB
UvrD
UvrC
UvrB
X
X
UvrC - Strand incision - 12 bp gap
UvrD - Strand removal
Pol I - Repair Synthesis
DNA Ligase - ligation

the eukaryota have evolved. Briefly, there are two damage recognition pathways that either scan the genome as a whole or are specifically tied to interruptions in active transcription. Following damage recognition, the pathways merge as the DNA duplex is locally melted by helicase activity and the damage is verified. The lesion containing strand is then incised 5' in front of the lesion and 3' behind it and is fully excised from the DNA. The lost genetic information is refilled using the undamaged strand as a template before the local chromatin topology is restored. Given the focus of this thesis, the model of NER detailed in the following sections will focus on mammalian repair though it should be noted that there are homologues for the majority of repair proteins in yeast. These are summarised in Table 1: Summary of NER Factors and Homologues at the end of this section and in the following figure (Fig 1.7).

1.2.2.1 CSA and CSB

Following UV irradiation, cells exhibit a decline in their levels of RNA transcription resulting from stalling of RNAPII at sites of damage. Recovery of RNA synthesis is dependent on the functions of the Cockayne Syndrome (CS) proteins and downstream NER. In the absence of functional CS proteins or NER, RNA transcription levels stay depressed (Mayne and Lehmann, 1982). It has been observed that repair of lesions on transcribed strands of DNA is carried out at a faster rate than damage located in the bulk of non-transcribed DNA. This transcription-coupled repair serves to rapidly remove lesions from actively transcribed genes (Mellon et al., 1987) In TCR, the initial recognition of the damage to the DNA occurs when an elongating RNAP II encounters a lesion that halts its progress. CSB is a member of the SWI2/SNF2 DNA-dependent ATPase family that during the course of normal elongation forms transient complexes with the elongation machinery. Encountering DNA damage stabilises this complex, initiating TCR (Boom et al., 2004), recruiting the other NER factors and associated proteins (save XPC-Rad23B and XPE-DDB1 which are uninvolved in this branch of NER) and the CSA-DDB1 complex (Fousteri et al., 2006). Successful initiation of TCR is dependent upon a ubiquitin binding

Figure 1.7 - Eukaryotic (Mammalian) Nucleotide Excision Repair

A) Damage is sensed through either the detection of a stalled RNA polymerase by the CS proteins (Transcription coupled repair) or through the detection of helical distortions by XPE and/or XPC (Global Genomic Repair). Chromatin remodelers (omitted for simplicity) are involved in reshaping the chromatin landscape to facilitate downstream processes.

B) The two pathways converge with the recruitment of TFIIH, carrying the helicases XPB and XPD which serve to unwind the double helix and allowing the recruitment of RPA, XPA and XPG.

C) The nucleases XPF-ERCC1 and XPG coordinate their incisions on the lesion containing strand with the 5' incision by XPF preceding the 3' incision by XPG (5' and 3' are in relation to the position of the lesion).

D) The resulting gap in the DNA double helix is then resynthesised by DNA polymerases, polδ, polε, and polκ. This is then followed by ligation and the restoration of the chromatin structure. The choice of polymerase and ligase is influenced by whether the cell is actively cycling or in a non-cycling state.

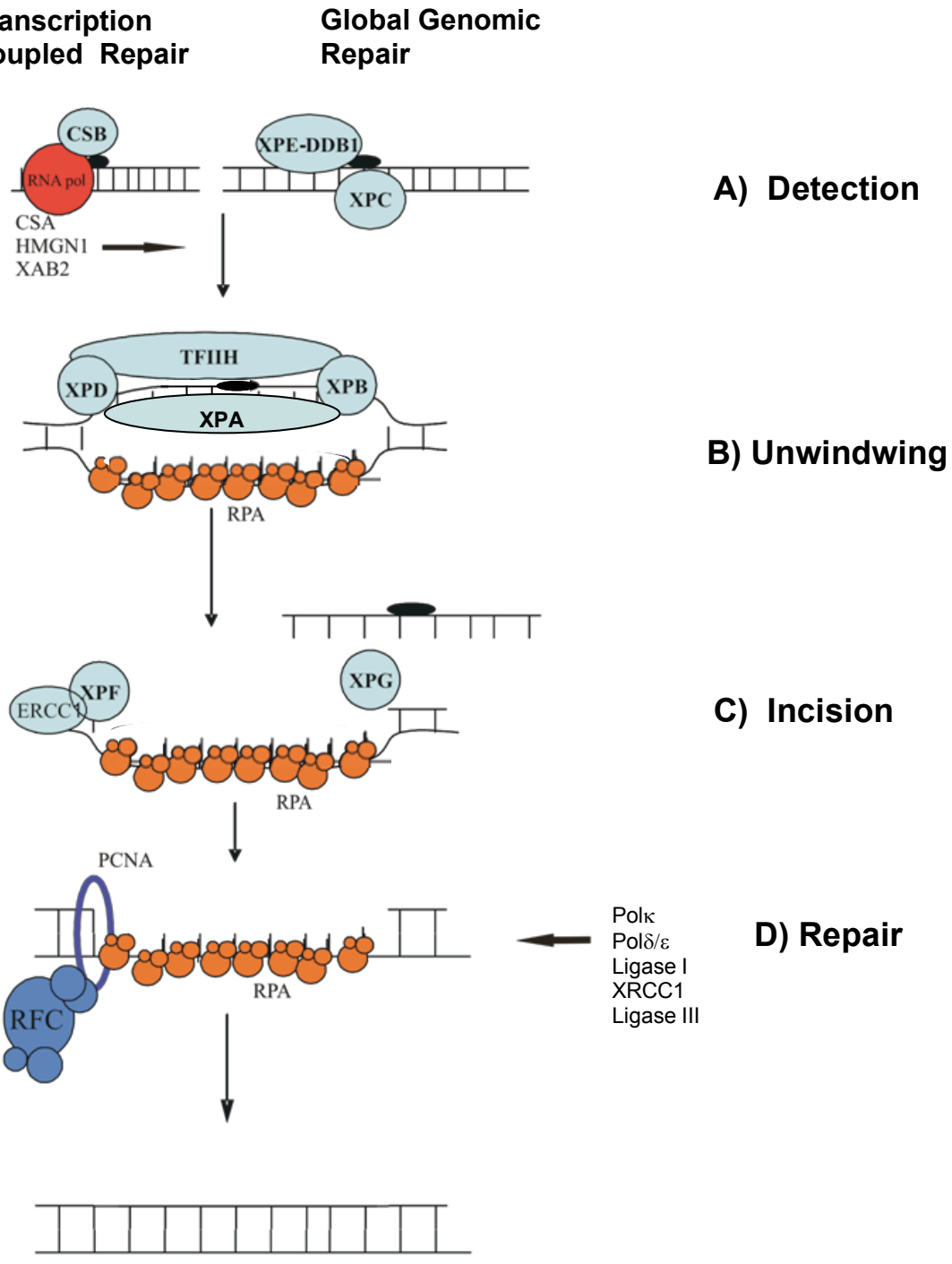
Transcription Coupled Repair
Global Genomic Repair
CSB
RNA pol
CSA
HMGN1
XAB2
XPE-DDB1
XPC
A) Detection
TFIIH
XPD
XPB
XPA
RPA
B) Unwindwing
XPF
ERCC1
XPG
RPA
C) Incision
PCNA
RFC
RPA
Polκ
Polδ/ε
Ligase I
XRCC1
Ligase III
D) Repair

domain (UBD) of CSB, though presently the ubiquitinated substrate with which it interacts is unknown (Anindya et al., 2010).

CSB also has an important role in the resumption of RNA transcription following UV irradiation, except for p53 responsive genes that are regulated post-UV independently of CSB (Proietti-De-Santis et al., 2006). CSA contains several WD-40 protein-protein interaction motifs and interacts with a ubiquitin ligase complex of DDB1, Cullin 4A and ROC1/Rbx1 (Fousteri and Mullenders, 2008). This complex recruits other factors such as HMGN1, XAB2 to engage in chromatin remodelling and TFIIS to restart transcription following repair (Fousteri and Mullenders, 2008).

1.2.2.2 XPC-Rad23B and XPE-DDB1

In GGR, the majority of the damage recognition step is carried out by XPC in complex with hRAD23B and centrin2. There are two forms of hRad23 expressed in human cells, hRAD23A and hRAD23B with the latter being in a complex with XPC (Masutani et al., 1994). The inclusion of hRAD23B in the XPC complex appears to stimulate its NER activities (Sugasawa et al., 1996). This complex binds to damaged DNA with a stronger affinity than undamaged DNA however it is less able than XPE-DDB1 to detect CPDs which only cause minor helical distortions (Shuck et al., 2008). The detection of CPDs is enhanced by cooperation with another protein complex known as the UV-DDB complex. The UV-DDB complex is composed of DDB1 and XPE/DDB2; it is associated with Cullin 4A, Roc1 and the COP9 signalsome (CNS) (Groisman et al., 2003) The UV-DDB complex has a thousand-fold higher affinity for UV-damaged DNA than XPC-RAD23B (Batty et al., 2000). In contrast to XPC, XPE-DDB1 does not recognise the helical distortion but binds directly to the lesion. DDB1 is composed of three WD40 β-propeller structures, BPA, BPB and BPC. XPE binds at the interface of BPA and BPC. The lesion is flipped into a binding pocket in XPE which restricts detection to UV-photoproducts only. The binding of XPE-DDB1 further distorts the DNA helix. CUL4, the ubiquitin ligase component of the complex is able to move through a 120° arc around the bound XPE-DDB1 complex, establishing a ‘zone of

ubiquitination' (Scrima et al., 2008). When XPE-DDB1 complex binds to a lesion on DNA, the regulatory partner CSN is released promoting the ubiquitination activity of the complex (Takedachi et al., 2010). UV-DDB is able to ubiquitinate XPC and be ubiquitinated itself, this ubiquitination increases XPC's affinity for DNA and results in the degradation of UV-DDB itself (Sugasawa et al., 2005). This ubiquitination process is regulated through interaction with both XPC and Ku. As mentioned previously, Ku, composed of Ku70 and Ku80, is a major component in the NHEJ repair pathway. Whereas the interaction with XPC serves to prompt the ubiquitination activity of the XPE-DDB1 complex, Ku acts as a negative regulator of its activity (Takedachi et al., 2010). The XPE-DDB1 complex shares many components with the complex of proteins that CSA interacts with for TCR. This may point toward a shared role above and beyond XPE's ability to recognise CPDs, potentially in the reorganisation of chromatin. XPE-DDB1-CUL4-ROC1 has been shown to ubiquitinate histones following damage and recognition of the lesion, and such histone modifications act a manner that, *in vitro*, is able to interact with the downstream factor XPA and may serve as a method of recruitment to damage sites (Takedachi et al., 2010). Once the lesion has been recognised, XPC-RAD23B acts as a recruitment factor for the downstream proteins by bringing Transcription Factor IIH (TFIIH) into the assembling incision complex.

Intriguingly, XPC does not bind itself to the damage but instead detects the distortion in the helix caused by the presence of the lesion. Crystal structure evidence from the yeast homologue, Rad4, duplexed with damage containing DNA shows the binding of the protein takes place on the opposing strand to the one containing damage. A β-hairpin is inserted between the two strands and two base pairs are flipped out of normal orientation and into a binding pocket able to accommodate any of the four bases, thus not limiting the detection of damage to any particular sequence specificity (Min and Pavletich, 2007). This does raise the notion that XPC might be able to bind to naturally occurring, but damage free, distortions in the double helix, such as those present for events such as transcription or replication. Several experiments have shown that XPC will bind 5' to DNA structures such as loops and bubbles regardless if there is damage present

or not (Sugasawa et al., 2001; Sugasawa et al., 2002) It has been demonstrated that XPC can bind several dozen base pairs away from a lesion if presented with a greater distortion to the DNA helix (Sugasawa et al., 2009). In conjunction with TFIIH and XPA, XPC can then scan downstream of its initial binding to find the lesion, at which point the complex stalls and NER can fully engage. This scanning and stalling emerges as an interesting mechanism for verifying damage and distinguishing it from normal structures independently of requiring exact lesion recognition specificity from XPC. Is this scanning and stalling a physiologically relevant method of detection? As a method of monitoring the genome, a complex of XPC/TFIIH/XPA translocating along DNA would bear strong similarities to how $UvrA_2$UvrB scans for DNA damage in prokaryotes. However, in the *in vitro* studies done by Sugasawa *et al* excluded the XPE-DDB1 complex which is more sensitive for the detection of UV lesions that produce minor helical distortions than XPC. *In vivo* systems may see markedly less requirement for translocation along the DNA if interaction with XPE-DDB1 recruits XPC directly to the lesion. Also, a translocating complex would require a method of stopping and verifying the presence of a lesion. It had been suggested that stalling of XPD might fulfil this role though, as will be discussed later, data conflicts whether XPD is blocked by the presence of lesions.

A rapidly expanding area of interest is the chromatin context within which NER must be taking place. *In vitro* reconstitution of the NER pathway has been an invaluable aid in exploring the mechanism and sequence of repair. However, experiments *in vitro* carried out on naked DNA sidesteps the issue that within the living cell, DNA is highly packaged and organised into chromatin. Starting from the basic wrap of DNA around a nucleosome and building up to the chromosomal level, NER takes place within a dynamic but regulated structural landscape. Studies have shown that repair is delayed on nucleosome bound DNA compared to the more accessible linker region (Smerdon and Thoma, 1990). In the budding yeast *Saccharomyces cerevisiae* a general acetylation of histones has been observed following UV irradiation and differing rates of repair dependent on whether the damaged strand was accessible to transcription-coupled repair, where the chromatin

landscape had presumably been relaxed to allow access by the transcription machinery, or whether it was dependent on global-genomic repair (Teng et al., 2002). The histone acetylase Gcn5 was shown to affect rates of repair and its mammalian homologue, in conjunction with a partner transcription factor E2F1, co-localises to sites of NER damage and is required for the localisation of downstream core NER factors (Guo et al., 2010). Additionally, other chromatin modifying factors have recently been shown to impact on the NER process. INO80, a chromatin remodelling complex, is required for the efficient repair of damage and for the correct localisation of the factors XPC and XPA (Jiang et al., 2010). Additionally, XPC has been shown to interact with subunits of the SWI/SNF complex involved in chromatin remodelling (Ray et al., 2009; Zhao et al., 2009). These studies are leading toward a model of repair where the chromatin landscape must first be opened up to allow access to NER factors that can then complete repair unhindered by topological restraints. As will be detailed more fully in a proceeding section, following this repair the chromatin landscape must be restored to finalise the process of repair.

Since remodelling is required to allow the NER machinery access to damaged DNA in chromatin, it begs the question about whether this has any implications for the detection of the damage. Does chromatin remodelling proceed first or is damage detection still the initiating event? Could the chromatin remodelling proteins have damage detection ability? This seems unlikely for several reasons. XPC and XPE complexes have evolved to detect helical distortions and CPDs respectively. Jiang *et al* demonstrated an interaction between XPE-DDB1 complex and INO80 through co-immunoprecipitation techniques. Also, Ray *et al* showed a requirement for XPC for the recruitment of SWI/SNF remodelers. It would appear that following detection of damage, chromatin remodelers are recruited by NER factors, allowing a change in local chromatin to grant access to the rest of the NER machinery. In contrast to this, the work on GCN5 in human cells demonstrated an impairment of NER factor recruitment in the absence of the histone acetyltransferase. However, a physical interaction between GCN5 and NER factors was not investigated. While GCN5 may be able to localise to sites of DNA damage and acetylate histones, thus

relaxing the chromatin and helping to expose the damage, any subsequent damage detection, verification and removal is dependent on NER factors recruited through separate means.

1.2.2.3 TFIIH

With roles in both transcription and NER of damaged DNA, the ten protein complex TFIIH contains two DNA helicases with opposite polarity, XPB and XPD. These were thought to unwind the DNA duplex exposing regions of single stranded DNA; XPB is a 3'-5' helicase (Schaeffer et al., 1993) and XPD has 5'-3' helicase activity (Schaeffer et al., 1994). Two distinct roles for the two XP subunits have recently been discovered. Though both XPB and XPD contain classical helicase motifs, only mutations in the Walker A ATP-binding motif of XPB impair its function in NER while mutations in the helicase domains leave it functional; contrastingly, mutations in the helicase domains of XPD impair its repair activities (Coin et al., 2007). The ATPase activity of XPB is stimulated by its association with the p52 subunit of TFIIH. These distinct roles lead to the model where XPB uses its ATPase activity to locally separate the DNA double helix and act as a 'wedge' to separate them while XPD functions as a classical helicase and unwinds the DNA (Coin et al., 2007). The solving of the structure of an archaeal XPD helicase has given invaluable insights into how it functions and how mutations in one protein can give rise to a range of distinct clinical symptoms. XPD possesses a Fe-S stabilised core that separates the strands of DNA and the single stranded DNA is drawn through the two motor domains (Liu et al., 2008). The helicase can unwind bubble structures and appears to be unaffected in its translocation by damaged DNA (Rudolf et al., 2010), though it should be noted that the *S. cerevisiae* homologue of XPD is unable to translocate past damage (Naegeli et al., 1992). Recently work by Mathieu *et al* has shown that human XPD can stall at UV induced damage, in contrast to the findings of Rudolf *et al.* Whereas Rudolf *et al* worked with the archaeal XPD and relatively short oligonucleotide substrates, Mathieu *et al* used the human XPD and longer fragments of DNA. Their work could represent a more accurate representation of the movement and stalling of the helicase in human cells (Mathieu et al.,

2010). This stalling of the helicase could potentially be a method of damage verification. The sequence similarity in conserved domains between archaeal and eukaryotic XPD helicases allows known human mutations to be mapped onto the archaeal structure. From this investigation, mutations responsible for Xeroderma Pigmentosum syndromes appear to be clustered in the helicase domains, abolishing the function of the subunit but preserving the structure of the protein. Mutations giving rise to combined CS/XP patients and TTD patients appear to disrupt interaction between the subunit and the TFIIH complex or disrupt the subunit structure directly (Fan et al., 2008; Liu et al., 2008; Wolski et al., 2008).

1.2.2.4 XPA, RPA

At the centre of the NER system sits the repair protein XPA. The protein interacts with various other NER factors including ERCC1, TFIIH and RPA (Park et al., 1995; Park and Sancar, 1994). XPA was originally believed to be the damage recognition protein but has since been relegated by the discovery and characterisation of XPC and XPE. However, XPA is undoubtedly a crucial component of the NER pathway as deficiencies in XPA result in severe repair deficiencies in cells and clinical symptoms in patients. The function that XPA performs is still under debate, though several suggestions have been put forward: a function as a damage verification step; licensing the excision step of NER; fine-tuning the NER pathway; or serving to link the NER process to the checkpoint safeguards in the cell. It has been shown that, XPA prompts the dissociation of the CAK subunit for TFIIH, allowing TFIIH to locally melt the DNA around the lesion and for NER to proceed to the excision step (Coin et al., 2008) but also there is a requirement for XPA for appropriate checkpoint activation. Following exposure to UV light, XPA has been reported to be phosphorylated by ATR on serine 196 which causes its localisation to the nucleus, where it co-localises with the kinase (Wu et al., 2006). It has also been observed that an inhibition of ATR prevents the proper removal of the UV damage products CPDs and 6-4PP during S-phase (Auclair et al., 2008) The links between XPA, ATR and the checkpoint response will be explained more fully below. XPA may have several roles in the NER process or roles

independent of its NER activities. Recent investigations from some laboratories have pointed to a central role of XPA in NER by showing that it functions as the rate limiting step of excision repair and this rate of repair is controlled in a circadian specific manner. In mouse tissues, XPA is most highly expressed during the day portion of a 12hr alternating day/night cycle and is dependent on the activities of the clock protein CYC1 (Kang et al., 2010b). This would align the highest rate of XPA expression with the greatest exposure to UV damage inducing sunlight, though care should probably be taken extrapolating to humans given that mice are naturally nocturnal mammals. At a post-translational level, XPA is regulated by phosphorylation, as has been mentioned, but also by ubiquitination and acetylation. Ubiquitination is controlled by the HERC2 subunit of the HERC ubiquitin ligase complex and targets XPA for degradation by the proteasome. Following UV irradiation, XPA is localised away from association with HERC2 and its protein half-life increases from 2-4 hrs to over 12, greatly increasing the amount of XPA for the excision of even the minor distorting lesions such as CPDs (Kang et al., 2010a). It has recently been reported that XPA is also acetylated on residues K63 and K67 and this serves to inactivate the protein (Fan and Luo, 2010). However, reports differ on the amount of XPA acetylated and therefore the overall impact of acetylation on XPA activity and regulation. These roles and functions of XPA have been chiefly reported by individual groups and, while intriguing, require further experimental investigation to confirm.

RPA is a trimeric protein consisting of 70 kDa, 32 kDa and 14 kDa subunits that binds to exposed regions of single-stranded DNA and is a crucial and common component of many DNA repair pathways and other biological processes involving DNA. Following many forms of DNA damage, RPA is hyper-phosphorylated in an ATR dependent manner (Carty et al., 1994). In NER, RPA protects the unwound undamaged single-stranded DNA from attack by nucleases and recruits the remaining factors while stabilising the assembling incision complex (Park and Choi, 2006). Though XPA and RPA are recruited to sites of damage independently and XPA is not required for the loading of RPA, the interaction between the proteins is necessary for successful NER. In *in vitro* and *in vivo* systems that included XPA

with mutations that prevented binding to the RPA32 subunit, there was a decrease in incision activity and cell viability (Saijo et al., 2011). There is also some evidence that RPA functions as another damage recognition protein due to its higher affinity for damaged DNA over non-damaged DNA, though the extent to which this competes with or complements the other recognition factors is debatable. In the context of NER, XPE-DDB1 complex shows the highest affinity for minor helical distortions with XPC, XPA and RPA showing preferences for damaged DNA in a declining order of sensitivity. Several proteins may exhibit *in vitro* ability to bind damaged DNA that may or may not be related to their *in vivo* functions and roles. Recent evidence has emerged that RPA may play a role in regulating the initiation and completion of repair events, while serving to separate NER into two phases: a pre-incision complex assembly and post-incision complex assembly. In cells unable to initiate the 5' incision event, pre-incision repair factors, such as XPC, XPA, TFIIH subunits and RPA, assemble but are dynamic and able to re-associate at new sites of damage. Post-incision repair factors, such as PCNA, polδ, etc, are unable to be recruited to the NER event. If incision is able to proceed, but repair synthesis is halted through the use of polymerase inhibitors, then the post-incision factors are recruited but, along with RPA, become immobile and unable to be redirected to other sites of damage. Without the presence of RPA, the pre-incision complex, which includes the nucleases, is unable to make the 5' incision. Thus RPA appears to serve to link the pre- and post-incision events. While pre-incision factors are dynamic in their ability to associate and de-associate from DNA lesions, full excision is unable to take place until RPA is released by the completion of repair synthesis. This presumably ensures that NER fully completes repair of a DNA lesion before initiating another while essential factors are indisposed elsewhere. If this system was not regulated, the NER machinery could generate single-stranded gaps in the DNA before resynthesis factors were recruited to resynthesise the excised genetic material, potentially leading to erroneous checkpoint activation or genetic instability (Green and Almouzni, 2003; Overmeer et al., 2011; Staresincic et al., 2009). By regulating the transitions between phases of NER, it is conceivable that a single-stranded gap in DNA is never actually generated or exists only as a very short lived intermediate.

1.2.2.5 XPG and XPF-ERCC1

XPG is recruited to the site of damage due to association with TFIIH but is stabilised by interactions with XPA and RPA (Park and Choi, 2006). XPG is a nuclease that cuts the strand of DNA containing the lesion 3' to the damage (O'Donovan et al., 1994). XPF-ERCC1 is brought into the complex by interactions with XPA (Li et al., 1994; Park and Sancar, 1994). ERCC1 localises the XPF nuclease by interaction with ssDNA, allowing XPF to cleave 5' of the lesion (Bunick and Chazin, 2005). The characterisation of the order of the incisions had been a matter of debate in the literature, with some groups reporting 5' incision in the absence of 3' incision and vice versa (Evans et al., 1997; Wakasugi et al., 1997) Recent work has more precisely elucidated the coordination between the two nucleases, requiring the initial cut be made by XPF before XPG is induced to cleave DNA. However, in a further layer of coordination of the excision process, XPG is physically required to license the XPF incision before making its own. A catalytically dead mutant of XPG has been shown to be able to prompt the excision by XPF while unable to make its own incision into the DNA strand 3' of the lesion (Staresincic et al., 2009) In the absence of a catalytically active XPF, no incision takes place and the repair complex is indefinitely stalled (Staresincic et al., 2009).

As mentioned above, the incision event provides a divider between the pre-incision events of damage detection and assembly of incision factors and the post-incision event of repair synthesis. There is evidence that alongside RPA, XPG has a role to play in the correct assembly of post-incision factors. *In vitro* studies have shown that RPA serves to recruit the clamp loader RF-C and in turn PCNA is stabilised by the XPG, which also shields PCNA from inhibition by the p21 cyclin-dependent kinase inhibitor. XPG incision activity is greatly stimulated once polδ is recruited, which also serves to release the nuclease, and gap-filling resynthesis can proceed (Mocquet et al., 2008).

1.2.2.6 Checkpoints and NER

It is through this unwinding of the helix and excision of the damage containing strand, that an intermediate product of single stranded DNA coated in RPA could be generated. Such regions are involved in the activation of a variety of responses when they are identified by the cellular damage response mechanism. As will be detailed below, these strands of DNA interact with Rad18, which modifies proteins through its E3 ubiquitin ligase activity. They also function as recruiters for the kinase ATR (Mec1 in yeast) which functions to initiate a checkpoint response. Though these single stranded DNA structures are only a few dozen nucleotides long and are expected to be short-lived in NER since the excision and repair synthesis processes appear to be highly coordinated (Staresincic et al., 2009), the potential for recruitment still exists.

Several studies have pointed towards a link between NER and the checkpoints that the cell uses to slow cell cycle progression and protect against premature progression with potentially disastrous consequences. In yeast, it has been observed that functional NER is required to activate Mec1 and that the XPA homologue, Rad14, physically interacts with the Ddc1-Rad17-Mec3 complex (Giannattasio et al., 2004), homologue of the mammalian RAD9-RAD1-HUS1 (9-1-1) complex. XPA has been implicated in a role that ties together the checkpoint responses and NER by several studies, though there is still uncertainty in the literature as contradictory results have been reported. For example, some studies have seen that during S-phase, XPA deficiency reduced the co-localisation of ATRIP, the ATR interaction protein, with damage and a deficiency of CHK1 phosphorylation (Bomgarden et al., 2006). This is supported by another group who reported that XPA deficient fibroblasts were unable to properly activate the G_2/M checkpoint (Marini et al., 2006). However, where these studies differ is in the requirement for other NER factors. Bomgarden *et al.* saw no defect in XPC defective cells that were unable to initiate GGR but Marini *et al.* observed a XPC linked defect (Bomgarden et al., 2006; Marini et al., 2006). These differences may be attributable to differences in sensitivity of the quantifying assay, with Bomgarden *et al.* being able to observe CHK1 phosphorylation with western blot

techniques that may be missed by the immunofluoresence used by Marini *et al.* The studies differ again on the S-phase requirement of XPA, with Marini *et al.* not detecting an S-phase checkpoint defect in the absence of XPA which differs from the observations of Bomgarden *et al.* The requirement for XPA outside of S-phase is supported by observations that show that the lack of NER activity in serum starved cells prevents the phosphorylation of the histone variant H2AX (γ-H2AX) in a GGR dependent manner (O'Driscoll et al., 2003). Agreeing with this observation, Matsumoto *et al.* observed in quiescent cells a dependency on NER for the generation of γ-H2AX and theorised that this may be due to a prolonged existence of the single stranded DNA intermediates by a disruption in the repair synthesis step, possibly driven by low cellular concentrations of accessory factors such as PCNA and polδ. This could be mimicked by treating cells with β-D-arabinofuranoside which inhibits the replicative polymerases (Matsumoto et al., 2007). Conversely, other groups have observed that the ATR dependent checkpoint response is heightened in cells unable to carry out functional NER. Jiang *et al* argues that in light of the recruitment of DNA damage checkpoint proteins in the absence of XPA, ATR is able to directly bind to damaged DNA (Jiang and Sancar, 2006). While seeing the same checkpoint response in NER-deficient cell lines, other groups have argued against ATR being able to directly detect damaged DNA. Vrouwe *et al* have shown that the endonuclease APE1 is able to nick the DNA backbone 5' of a 6-4PP. This nick could then be converted into a stretch of single-stranded DNA by the actions of other nucleases, stretches of DNA sufficient to activate the checkpoint (Vrouwe et al., 2011)

In yeast a role for the nuclease exonuclease I (ExoI) has been unearthed that may help explain how the relatively small gapped NER intermediates can play a role in the checkpoint response. In *Δexo1* yeast strains, defects are seen in G1 checkpoint activation and phosphorylation of Mec1 targets compared to wild-type cells. Use of electron microscopy showed long stretches of single stranded DNA generated in an ExoI dependent manner following UV irradiation if the repair synthesis step of NER was inhibited. Following the 5' incision by Rad1-Rad10, the flap structure might present an inviting

substrate for Exo1 digestion but is out competed by the repair synthesis step. If the latter is delayed, ExoI processing may take over, generating the long stretches of single stranded DNA required to activate a checkpoint response (Giannattasio et al., 2010).

In mammalian cells a similar requirement of EXO1 appears evident. EXO1 is present as two isoforms in human cells, hEXO1a and hEXO1b where the only difference is an extra 43 amino acids on the C-terminus of hEXO1b. Both isoforms have been observed to behave in the same manner. Human EXO1 co-localises with NER factors following localised UV damage and a physical interaction between XPA and EXO1 has been observed. In the absence of the NER factor XPA, hEXO1 did not accumulate at localised UV damage. Cells that have had their levels of EXO1 reduced through siRNA treatment show reduced gap-filling of DNA following UV exposure and a reduced checkpoint response. In both yeast and mammalian cells, there appears to be a minority of events where the 3' incision is impaired. This leads to processing by EXO1 which can generate a stretch of single-stranded DNA which is then followed by the activation of the checkpoint (Steric *et al*, manuscript in print).

1.2.2.6 Gap filling, ligation and restoration of chromatin structure

Following removal of the lesion-containing strand of DNA, the resulting gap in the double helix must be filled in. This is accomplished by the same protein factors that are used to replicate DNA under normal conditions. Replication Factor C (RFC) loads the homotrimeric protein proliferating cell nuclear antigen (PCNA) onto the DNA. PCNA is a ring shaped protein that encircles the double helix and acts as a platform for DNA polymerases to function, enhancing their processivity by preventing dissociation from the DNA (Maga and Hübscher, 2003). It has been widely accepted, by evidence from *in vitro* studies, that a replicative polymerase such as polδ or polε is involved to correctly incorporate nucleotides into the nascent DNA. This fills the gap left by the NER incision before finally being sealed by a DNA ligase, though as will be detailed later this situation is more complex than previously thought. The choice of ligase is dependent on what

conditions and phase of the cell cycle the cell is in while attempting repair. In cycling cells during S-phase, there appears to be a preference for using polε to fill in the NER gap and seal the nick with Lig1, however in G1 and G0 cells, polδ and XRCC1-LIG3 are required to seal the DNA backbone (Moser et al., 2007). Following UV irradiation, the chromatin assembly factor 1 (CAF-1) is recruited to sites of NER (Green and Almouzni, 2003) and there is evidence that Ino80, in yeast, is also required for the restoration of chromatin structure, though opposing results have been observed in mammalian NER (Jiang et al., 2010; Sarkar et al., 2010). This recruitment is required for the deposition of the histones H3.1 and ubiquitinated H2A as markers of repair and restoration of the chromatin structure (Zhu et al., 2009).

Use of immunofluorescent techniques has elucidated whether the NER proteins in human cells form a complex to repair DNA damage or whether the enzymes are sequentially recruited to the sites of damage (Volker et al., 2001). This study confirms that XPC-hRAD23B is the initial damage recognition component in GGR followed by the recruitment of TFIIH, XPG, XPA-RPA and ERCC1-XPF to remove the damage before the process is completed by the actions of a DNA polymerase and ligase. In TCR, the initiating event is the recognition of a stalled RNA polymerase II by the protein CSB. Further investigations have shown a role for XPE-DDB1 in detection of UV lesions before XPC.

1.2.3 Diseases of Defective Nucleotide Excision Repair

Given the importance and versatility of NER in removing a wide range of helix-distorting lesions it comes as no surprise that defects in various points in the pathway of repair can give rise to multiple severe pathological conditions. The diseases of defective NER are Xeroderma Pigmentosum (XP), Cockayne Syndrome (CS), Trichothiodystrophy (TTD) and UV Sensitivity Syndrome. They are diverse in the range of their severity and symptoms and stem from different defects along the NER pathway.

XP is a disease of global genome repair and its symptoms can range from the mild to the extremely severe depending on which protein function in the GGR pathway has been impaired. It is characterised by greatly increased pre-disposition to skin pigmentation changes and skin cancer development if precautions against sunlight exposure are not taken, an elevated risk of other cancers and, in some cases, neurological abnormalities. (Kraemer et al., 1987) XP-E and XP-F patients typically have rather mild conditions, though in the case of the latter there remains the possibility that protein levels are not abolished but severely impaired, leaving a small population of viable protein for competent NER. Also it should be noted that in the case of XP-F that the original patients represented mis-sense mutations and more recently patients have been diagnosed with more severe phenotypes (Lehmann, personal communication; Matsumura et al., 1998; Niedernhofer et al., 2006). XP-C patients display a greater severity of skin symptoms, as they lack the GGR damage sensor. However their functional TCR seems sufficient to protect XP-C patients from neurological defects perhaps because TCR can still remove lesions from neurologically active genes. XPA null mutations give rise to severe and wide ranging clinical manifestations of Xeroderma Pigmentosum as without XPA there is no possibility of either NER pathway proceeding to successful completion (reviewed in (Lehmann, 2003).

CS results from defects in transcription-coupled repair and patients' exhibit severe growth and neurological defects but, unlike XP patients, show no increased risk of cancer development. These differences are can be attributed to retaining a fully functional GGR branch of NER able to eventually remove lesions located anywhere in the genome but, by having defective TCR, they are unable to rapidly repair lesions blocking transcription. This explains the lack of cancer predisposition, as GGR is still able to repair lesions before they can result in downstream mutagenic events. However, CS cells are unable to rapidly repair lesions found in transcribed DNA which can be highly detrimental, particularly in highly transcriptionally active cells such as those found in neuronal tissue (reviewed in (Lehmann, 2003)).

Mutations affecting XPB, XPD, and XPG can present clinically with combined XP and CS symptoms. While XP symptoms on their own appear to be related to mutations that affect the catalytic functions of the proteins, combined XP/CS symptoms arise from mutations in XPD that detrimentally affect the stability of the TFIIH complex and its interactions with other NER factors. This is the case, as previously mentioned, for XPD. Mutations that negatively affect the helicase function of the protein present with XP characteristics while those that affect the stability of the over-all protein complex also show CS characteristics. Truncation mutations in the XPG C-terminus can also give a combined XP/CS phenotype. The C-terminus of XPG interacts with TFIIH CAK subunit. In the absence of this stabilising interaction, the CAK unit dissociates and the complex is destabilised (reviewed in (Schärer, 2008).

TTD is characterised by brittle hair, ichthyotic skin, growth deficiencies and neurological development abnormalities. The proteins defective in TTD are restricted to the XPB helicase, the XPD helicase and the TFIIH subunit TTD-A (Giglia-Mari et al., 2004). Given its confinement to mutations in the TFIIH subunits, it has been suggested that TTD is not strictly a defect in NER but broadly a transcription syndrome as clinical features result from subtle transcription deficiencies (reviewed in (Bergmann and Egly, 2001)).

UV sensitivity syndrome (UVSS) is a poorly characterised syndrome that presents with mild symptoms, making accurate diagnosis difficult. As the name implies, patients are sensitive to UV radiation but do not display enhanced predisposition to cancer or neurodegenerative effects typically seen in patients with XP or Cockayne Syndrome. Work indicates a link between UVSS and aspects of transcription coupled repair and at a cellular level, UVSS cells are indistinguishable from CS cells (Nardo et al., 2009) and results from the involvement of CSA, CSB or the recently discovered gene *uvssa* . However, it should also be noted that the extreme mildness of the symptoms may lead to a reduced rate of diagnosis and therefore the rarity of the syndrome comparative to the other diseases

caused by NER deficiencies may represent an underestimate of its occurrence. The different diseases that develop from defecting NER are presented overleaf (Fig 1.8).

A summary of necessary NER proteins identified in XP and CS complementation groups and their functions is presented below:

Table 1 Summary of Core NER Factors and Homologues

E. coli	*S. cerevisiae*	*S. pombe*	*H. sapiens*	Function
			XPE	GGR Damage Detection
		ddb1	DDB1	
	Rad4	rhp41/rhp42	XPC	
	Rad23	rhp23	RAD23B	
			RAD23A	
UvrA				
	Rad28		CSA	TCR Damage Detection
mfd	Rad26	rhp26	CSB	
UvrB				DNA Helix Unwinding
	Rad25	ercc3sp	XPB	
	Rad3	rad15	XPD	
	Kin28		CDK7	Kinase Subunit
	p62, p44, p34, p52, p8, MAT1			TFIIH Subunits
	Rad14	rhp14	XPA	Damage Verification?
UvrC				Strand Incision
	Rad1-Rad10	rad16-swi10	XPF-ERCC1	
	Rad2	rad13	XPG	

Figure 1.8 - Disease of Defective Nucleotide Excision Repair

A) Xeroderma Pigmentosum : Characterised by sunlight sensitivity, predisposition to skin cancer and in some instances neurological defects. Subdivided into seven complementation groups (XP-A to XP-G). XP-V is not due to a defect in NER but displays several similar clinical characteristics.

B) Cockayne Syndrome : Characterised by sunlight sensitivity but no increased risk of skin cancers. Patients display growth and neurological abnormalities. Results from defects in transcription coupled repair proteins CSA and CSB.

C) Trichothiodystropy - Characterised by brittle hair, icythotic skin, the blood defect b-thalassaemia trait and neurological defects. Results from defects in TFIIH subunits XPD, XPB and TTDA with transcriptional defects.

D) UV sensitivity syndrome - Characterised by mild photosensitivity. No growth or neurological defects, no cancer predisposition. Displays transcription coupled repair defect. Results from defects in CSA, CSB and a UV sensitivity syndrome gene (UVSSA)

Images adapted from Lehmann (2001) (A-C) and
Nardo *et al* (2009) (D)

Xeroderma Pigmentosum

A)

B) Cockayne Syndrome

C) Trichothiodystrophy

D) UV Sensitivity Syndrome

1.3 Translesion Synthesis Polymerases

All three domains of life contain a diverse collection of DNA polymerases adapted to specific tasks required for the replication of genetic material. The eukaryotic replicative polymerases, polymerase delta (pol δ) on the lagging strand and polymerase epsilon (pol ε) on the leading strand, are capable of copying DNA with incredible speed and accuracy, typically only making only one misincorporation in several tens of thousands of bases (Kunkel and Burgers, 2008). The price to be paid for such accuracy is an inability to replicate past helix distorting lesions in the DNA, since these obstructions are unable to fit into the active site of the polymerase (Lehmann, 2002). Upon encountering such a lesion, the replication fork may stall or ultimately collapse, generating a potentially genotoxic double strand break. A family of polymerases, the Y-family, is adapted to replicating past lesions on the DNA helix. This family includes polymerase eta (polη), polymerase iota (polι), Rev1 and polymerase kappa (pol κ) (Friedberg et al., 2002). Although not sharing sequence similarity to the replicative polymerases, the translesion synthesis (TLS) polymerases do share similar structural features including the palm, thumb and fingers features but also include a 'little finger' domain (Friedberg et al., 2002). These polymerases possess poor fidelity and processivity when compared to the replicative polymerases. They are able to replicate past DNA lesions by having a less constrained active site, able to accommodate the helix distorting damage (Pagès and Fuchs, 2002).

1.3.1 Recruitment – Ubiquitinated PCNA

To enable the switch from replicative polymerase to TLS polymerase, eukaryotic cells rely on post-translational modification of PCNA. Like many proteins, PCNA can be modified with small accessory molecules to change its function. Upon encountering a DNA lesion the replication machinery stalls, exposing stretches of single-stranded DNA which is then coated with RPA. The RPA acts as a signal to recruit the ubiquitin ligase RAD18 which interacts with the ubiquitin conjugator Rad6 (Davies et al., 2008). PCNA is ubiquitinated by the RAD18/RAD6 complex on lysine 164. While long chains of ubiquitin are commonly

added to lysine residues on proteins to prompt degradation via the proteasome, this monoubiquitination of PCNA allows the replicative polymerase to be displaced by the TLS polymerase to be recruited (Lehmann et al., 2007). The balance between modified and unmodified PCNA in human cells is kept in check by the de-ubiquitinating enzyme (DUB) USP1. While it was previously thought that Usp1 was autocatalytically cleaved following doses of UV radiation (Huang et al., 2006), new evidence points toward the autocleavage being a continual event and the decline in Usp1 levels following DNA damage attributable to a shut down in transcription of *USP1* (Cohn et al., 2007). The TLS polymerases, except REV1, possess PCNA interacting motifs (PIP Boxes) a consensus sequence of QxxLxxFF (Warbrick, 2006) that allows association between the polymerase and the PCNA platform (Warbrick, 2000). TLS polymerases also possess ubiquitin binding domains that can recognise ubiquitinated PCNA, enhancing this association (Bienko et al., 2005). Thus the ubiquitination of PCNA at a stalled replication fork recruits polymerases capable of bypassing the impeding damage (Kannouche et al., 2004) (Fig 1.9 – right branch). Polyubiquitination of PCNA by actions of the Ubc13-Mms2 and Rad5 proteins can allow DNA repair to proceed down an error-free route as opposed to the potentially mutagenic TLS pathway (Chiu et al., 2006). The mechanism of selecting the polymerase more accurately suited for the lesion is still debated though there is strong evidence from polη and polι that polymerases transiently interact with the replication machinery and are chosen for bypass based on efficiency of incorporation, stabilised by the interaction with ubiquitinated PCNA. Polη is highly mobile in the nucleus during S-phase and accumulates transiently at replication foci. The residence time in foci is increased by over-expression of Rad18 or by relaxing the chromatin structure (Sabbioneda et al., 2008).

1.3.2 Pol η

Polη is one of the best characterised of the Y-family polymerases and has served as a model for the other members of the Y-family. Like all Y-family polymerases, on undamaged templates Polη exhibits low fidelity and accuracy and is highly distributive

Figure 1.9 - Translesion Synthesis

Following the replication fork encountering unrepaired DNA damage, the cell can circumvent a collapse of the fork by the use of specialised polymerases to bypass the damage and repair it later (a process known as postreplication repair). This is believed to happen in one of two pathways:

A) 'On-the-fly' : Translesion synthesis happens directly at the replication fork in a manner dependent on Rev1 and prevents stalling of the replication fork. Rev1 acts as an adaptor between the translesion synthesis polymerases and the sliding clamp PCNA (Edmunds, C. E *et al* 2008).

B) 'Gap-filling': The blockage of the replication fork leads to repriming downstream of the lesion and reinitiation of the replicative machinery. The stalled PCNA becomes a target for ubiquitination due to the recruitment of Rad18/Rad6 ubiquitin ligases by the RPA coated exposed single stranded DNA. PCNA is eventually deubiquitinated by the actions of the DUB USP1 with UAF1, however ubiquitinated PCNA is detectable for several hours following damage (Niimi, A., *et al* 2008).

Through a poorly understood mechanism, polyubiquitination of PCNA by Rad5/ Mms2/Ubc13 leads down an error-free pathway involving a non-crossover and resolution event (not shown).

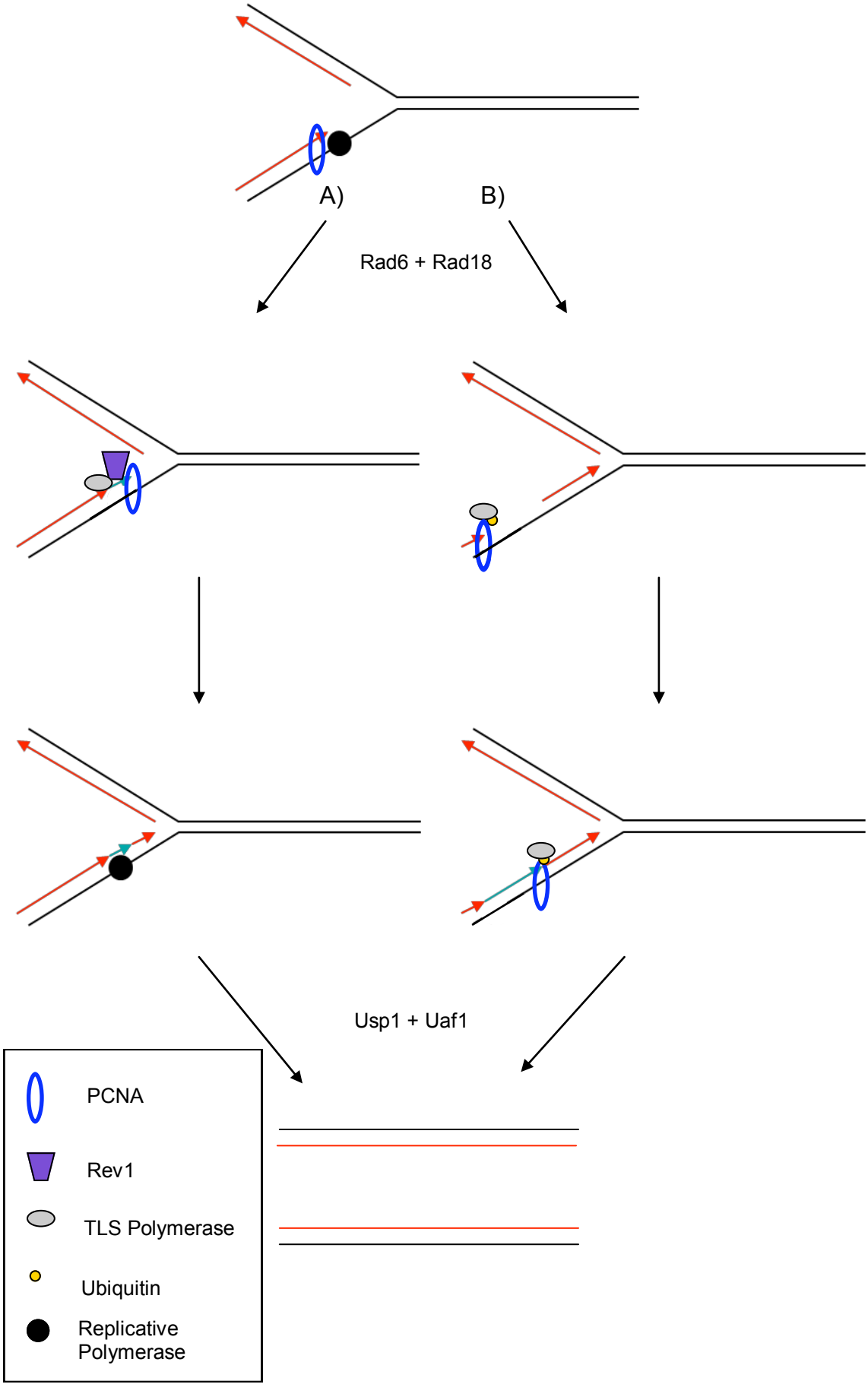
A)
B)
Rad6 + Rad18
Usp1 + Uaf1
PCNA
Rev1
TLS Polymerase
Ubiquitin
Replicative Polymerase

(Ohmori et al., 2001). However, the Y-family polymerases have not been adapted to replicate along undamaged DNA like the replicative polymerases but instead have evolved for replication across unrepaired lesions. Polη can accurately insert the correct base opposite CPDs, a minor helical distorting lesion that is slowly repaired by the NER machinery (McCulloch et al., 2004). Unrepaired CPDs, like other unrepaired lesions, can lead to a stalling of the replication fork and, if not dealt with, fork collapse. Despite the risk of a mutagenic insertion, that is a preferable outcome to a far more disastrous event of replication fork collapsing, which may lead to the far more cytotoxic event of a double-strand break in the DNA helix. The importance of Polη in tolerating UV light damage that has evaded repair is evident in the clinical features of the disease Xeroderma Pigmentosum variant (XP-V). Lack of functional protein gives rise to XP-V, which displays the same clinical features as the other XP complementation groups but without any impairment of the NER pathway (Masutani et al., 1999). This predisposition to cancer and extreme sensitivity to sunlight induced skin changes results from the inability to bypass unrepaired photodamage accurately. In the absence of Polη, other polymerases attempt to bypass the damage. This was assumed to be the sole responsibility of Polι but work has shown that the mutagenic emergence is due to the attempts by polκ/polζ and polι to bypass the damage (Ziv et al., 2009). It has been proposed that the 'polymerase switch' was indicative of how polη gained access to the DNA template upon the replication fork encountering damage. Polη has been shown to interact with mono-ubiquitinated PCNA (Kannouche et al., 2004) and this interaction is required for a switch away from polδ in favour of polη *in vitro* (Zhuang et al., 2008). Further experimental investigations have shown increasingly that the recruitment of polη is more complex than initially proposed. The UBZ domains of polη are essential for its recruitment to replication foci, but this recruitment is not necessarily dependent on ubiquitinated PCNA (Sabbioneda et al., 2008; Sabbioneda et al., 2009). Polη is mono-ubiquitinated and this could allow the polη UBZ domains to form an intramolecular interaction and prevent inappropriate interactions with PCNA until required (Bienko et al., 2010). To be recruited to replication forks, polη interacts with the phosphorylated species of Rad18 (Day et al., 2010; Watanabe et al.,

2004) Following UV irradiation, polη is phosphorylated on serine 601 by the kinase ATR in a manner dependent on Rad18 but not ubiquitinated PCNA. The prevention of polη phosphorylation renders the cells sensitive to UV and defective in post-replication repair (Göhler et al., 2011).

1.3.3 Pol ι

The polymerase Polι is closely related to Polη in sequence and polη may serve to help target polι to stalled replication forks (Kannouche et al., 2003), though only a sub-population may interact *in vivo* and transiently (Sabbioneda et al., 2008). A prevailing theory for translesion synthesis across certain lesions is that the process is a two-step mechanism, where an initial polymerase inserts a base opposite a lesion which can then be used as a primer by another TLS polymerase to extend from by additional nucleotide insertion. Polι is remarkably able to extend synthesis over short distances from a wide variety of mismatched termini (Vaisman et al., 2001) A notable feature of Polι is that the polymerase does not align incoming nucleotides with the template by conventional Watson-Crick base pairing but instead the Hoogsteen alignment. The Hoogsteen alignment uses alternative hydrogen bond donors/acceptors on the purine rings and results in an altered geometry of the double helix. This gives greater flexibility in the incorporation of base pairs though it can result in inappropriate matches. Due to this unconventional flexibility, the accuracy of Polι can vary nearly a thousand-fold depending on the template DNA from which the polymerase is attempting synthesis (Tissier et al., 2000). The exact biological role of polι is still debated. The idea that polι might be used in somatic hypermutation due to its lack of fidelity in DNA synthesis was discarded after knockout mice showed no defect (Shimizu et al., 2005). Recent evidence has shown a role for polι in the repair of oxidative damage through BER. Polι is recruited to sites of oxidative damage following laser tracking in a manner dependent on its nuclear localisation domain and ubiquitin binding domains. Polι has also been shown to interact with other BER factors such as XRCC1. When polι is knocked down through siRNA

treatment, cells are rendered sensitive to hydrogen peroxide, which generates free oxygen radicals (Petta et al., 2008).

1.3.4 REV1

REV1 is a dCMP transferase capable of efficiently inserting a base opposite an abasic site and opposite other forms of damaged bases with declining efficiencies (Nelson et al., 1996a). Intriguingly, the catalytic activities of REV1 are not required for DNA damage tolerance. While the N-terminus is required for proper nuclear localisation of the protein, the BRCT domains and the catalytic activity are not required to rescue UV or cisplatin sensitivity in a *REV1* DT40 cell line (Ross et al., 2005). The other Y-family polymerases have been shown to have REV1 interacting regions and, for polκ, this interacting region is important for the ability of cells to survive genotoxic damage (Ohashi et al., 2009; Ohashi et al., 2004). There is evidence from the avian cell line DT40 that REV1 serves to temporally separate the activity of TLS into an 'on-the-fly' activity done at the replication fork and reliant on REV1 and a post-replication gap filling completed after bulk DNA replication, where the replication machinery re-primes downstream of an unrepaired lesion (Edmunds et al., 2008) (Fig 1.9 – left branch). The 'on-the-fly' TLS also requires the Werner Syndrome helicase WRN to bypass the unrepaired lesion (Phillips and Sale, 2010). In other cell lines PCNA has been shown to persist in a ubiquitinated state for hrs following damage (Niimi et al., 2008). The temporal division of TLS could be dependent on the biological environment upon encountering the lesion, with some situations more amenable to 'on-the-fly' synthesis while others would stall the replication machinery long enough for it to re-prime downstream. Alternatively, TLS may function in different ways dependent on which strand the lesion is found on. The lagging strand, which has re-priming continuously as each Okazaki fragment is generated, could favour the accumulation of ubiquitinated PCNA while the leading strand would favour a process that does not interrupt the progression of the replication fork.

More recently, a role for REV1 in maintaining epigenetic information has been revealed. *REV1* DT40 cells lose the epigenetic information at repressed loci that contain G4-DNA quartets. These structures in single-stranded DNA, where four guanines can form a secondary structure through non-canonical base pair binding, are impediments to the replication machinery. It is hypothesised that on the leading strand the dCMP transferase activity of REV1 can destabilise the quartet through the insertion of a cytosine opposite a guanine and allowing progression of the fork. This would ensure incorporation of histones and maintaining the epigenetic information. On the lagging strand, the replication fork would reprime downstream of the quartet. The gap would then be filled by TLS dependent on the ubiquitination of PCNA. While the epigenetic information would be lost in the area of the gap, the surrounding areas would allow recovery of the lost information. However, in *REV1* cells, repeated use of post-replicative gap filling results in the loss of the epigenetic information (Sarkies et al., 2010).

1.3.5 Pol ζ

Unlike the polymerases mentioned previously, polymerase zeta (polζ) is not a member of the Y-family of DNA polymerases. Instead, polζ is a member of the B-family of polymerases. This polymerase consists of two core subunits: the catalytic subunit Rev3 and the subunit Rev7 in yeast (Nelson et al., 1996b) and REV3L and REV7 in higher eukaryotes. Intriguingly, disruption of polζ by deletion, in yeast, or depletion in mammals resulted in a lowering of the incidence of mutagenesis following exposure to DNA damaging agents, a property also observed for Rev1. Polζ interacts with Rev1 through Rev7 and the BRCT domains of Rev1 (Masuda et al., 2003). Human cells lacking polζ showed increased sensitivity to cross-linking reagents such as cisplatin (Wu et al., 2004). This pointed towards a role of polζ as an error-prone TLS polymerase with a role in the bypass of cross-linked DNA strands. *In vitro* studies have shown that polζ is a good extender from bases inserted opposite lesions by other polymerases (Johnson et al.,

2000b) and more recent *in vivo* work has shown that it plays a part in bypass of unrepaired photolesions, along with polι and polκ, in XP-V patient cells (Ziv et al., 2009)

1.4 Polymerase Kappa

The human Y-family polymerase, polκ is a homologue of the *E.coli* DNA polymerase IV (Gerlach et al., 1999; Ogi et al., 1999), encoded for by the genes *polκ* and *dinB* in eukaryotes and *E.coli* respectively. Human *polκ* was discovered by a homology search for genes related to the yeast TLS polymerase *RAD30* (Johnson et al., 2000a). Compared to the error rate of proof-reading polymerases, such as polδ with a rate of misincorporation around 10^{-6}, polκ is typical of other TLS polymerases in being error prone with poor processivity and fidelity. However, its error rate of 10^{-3} is the most accurate among the TLS polymerases (Johnson et al., 2000a). The commonly introduced mutations by polκ include inserting a cytosine opposite a thymine (Ohashi et al., 2000a) and preferential incorporation of an adenine across from an abasic site when incubated with single nucleotides. However, when incubated with four dNTPs and a template containing an abasic site, the polymerase 'slips' which can result in a -1 frameshift mutation if the context of the DNA sequence stabilises the misincorporation (Ohashi et al., 2000b).

1.4.1 Polκ Structure and Regulation

The N-terminal domain of polκ shares many features with the other Y-family polymerases. Crystal structure analysis has been invaluable in determining where similarity is shared and where proteins differ. Along with the other members of the family, human polκ has a 'hand' structure consisting of the palm, fingers, thumb and the Y-family unique 'little finger' or PAD domain (Uljon et al., 2004) The palm domain contains a mixed β-sheet and three α-helices along with the catalytic residues D30, D155 and E156 similar to polη whereas the finger domain is composed solely of three β-sheets and α-helices and is much shorter than the corresponding region on polη (Uljon et al., 2004). The palm and fingers domain interact with the replicative end of the template-primer, with the fingers over the

newly fashioned base pair being created in the catalytic site of the palm (Lone et al., 2007). Intriguingly, the polκ active site is more highly constrained than polη, which may contribute to its reduced rate of errors and inability to bypass photodamage (Uljon et al., 2004). The thumb domain again differs from other Y-family polymerases. In the structure of polκ the sixth α-helix is longer than observed in polη, allowing possible interaction with the DNA (Uljon et al., 2004). In DNA synthesis, the thumb of polκ appears to interact with the minor groove of DNA (Lone et al., 2007). Finally, the orientation of the little finger domain differs in comparison to polη. Where the latter polymerase links its little finger domain to the finger domain, polκ has it tucked under the palm domain (Uljon et al., 2004). When in complex with DNA, the little finger domain swings out by 50 Å and interacts with the major groove of the DNA helix (Lone et al., 2007). Polκ also differs from other Y-family polymerases by the inclusion of an N-clasp that makes additional contact with the DNA template. Thus, polκ fully encircles the DNA template when it is in contact with it, which may assist with its noted higher fidelity than other Y-family polymerases (Lone et al., 2007). Human polκ also possesses a 'molecular brake' at residue F171 that serves to restrict TLS across adducts produced by chemicals such as benzo[a]pyrene, though the reasons for the evolution of this molecular brake are not clear. When this residue is mutated to an alanine, an increase in efficiency of bypass was observed (Sassa et al., 2011). This is at first counter-intuitive, given the sensitivity to benzo[a]pyrene in polκ$^{-/-}$ murine cells. The authors suggest that, given the relatively recent appearance of benzo[a]pyrene and other industrial hydrocarbons as genotoxic agents, polκ has evolved to bypass endogenous bulky lesions produced by cellular metabolism. Only with industrialisation has the ability of polκ to bypass exogenous hydrocarbons become important. However, the error-free mechanism of polκ bypass of benzo[a]pyrene adducts seems too specialised to be a recent adaptation. While industrial pollutants are a modern phenomenon, hydrocarbon combustion and by-products (i.e., fire and smoke) have been environmental hazards throughout evolution. The nature of the 'molecular brake' remains to be elucidated.

The C-terminus of polκ contains several motifs that allow it to replace an error-free replicative polymerase at stalled replication forks. These include two C2HC zinc cluster domains that recognise ubiquitin (ubiquitin binding domains or UBZs), a PCNA binding box and a nuclear localisation signal, responsible for the import of polκ into the nucleus after synthesis (Ogi et al., 2005). These features allow polκ to interact with ubiquitinated PCNA at the site of a stalled replication fork. Mouse polκ is observed to be ubiquitinated *in vivo* in a manner dependent on its UBZ domains (Guo et al., 2008). These same UBZ domains have been shown to interact, as one would expect, with ubiquitin and this interaction is required for the proper localisation of polκ into foci (Guo et al., 2008). Human polκ also has been shown to form a complex with PCNA and this interaction, along with the clamp loader RFC and the single-strand DNA binding protein RPA, strongly simulate the DNA polymerase activity of polκ *in vitro* (Haracska et al., 2002) (Fig 1.10).

The expression of *polκ* had been observed in several tissues in mice. Of note, *polκ* was seen to be expressed in the testis and ovaries, the adrenal cortex of the kidneys, the epithelial cells of the skin and several tissues of the eye (Velasco-Miguel et al., 2003). Following the discovery of expression in the testis, it was questioned if polκ played a role in spermatogenesis. Intriguingly, *polκ* contains two transcription start sites, P1a and P1b, of which P1b seems to be exclusive for expression in the testis, though this exclusivity gave no insights into any role polκ might have in spermatogenesis (Ogi et al., 2001). However, when *polκ* deficient mice were generated by gene targeting and deletion of exon 6, they were still fertile (Schenten et al., 2002).

The expression of *polκ* in B lymphocytes, sites of antibody generation, offered the intriguing idea that the polymerase might in some manner be involved in the generation of extreme diversity seen in antibodies through an involvement in somatic hypermutation. However, no defect was found between control mice and ones that had the *polκ* gene targeted (Shimizu et al., 2003). However, the possibility was raised that another polymerase may be compensating for the deficiency in polκ and vice versa. The

Figure 1.10 - Structural Features of Human Polymerase Kappa

The structure features of human polκ can be divided between the highly conserved N-terminal region containing the catalytic domain and the unconserved C-terminal region. The C-terminal region contains the Ubiquitin Binding Zinc Fingers (UBZ) domains, the PCNA Interaction Region (PIP box) and the Nuclear Localisation Signal (NLS). The N-terminal region contains the key catalytic domain structures of Thumb, Palm, Fingers and the Little Finger (or Polymerase Associated Domain (PAD)). Also included is the N-Clasp that contributes to the increased fidelity compared to other Y-family polymerases. Just after the catalytic region is the Rev1-Interaction Region (RIR) which facilitates interaction with the Y-family dCMP transferase Rev1 (Ohashi *et. al.* 2009)

Partially adapted from Lone (2007) *Molecular Cell*.

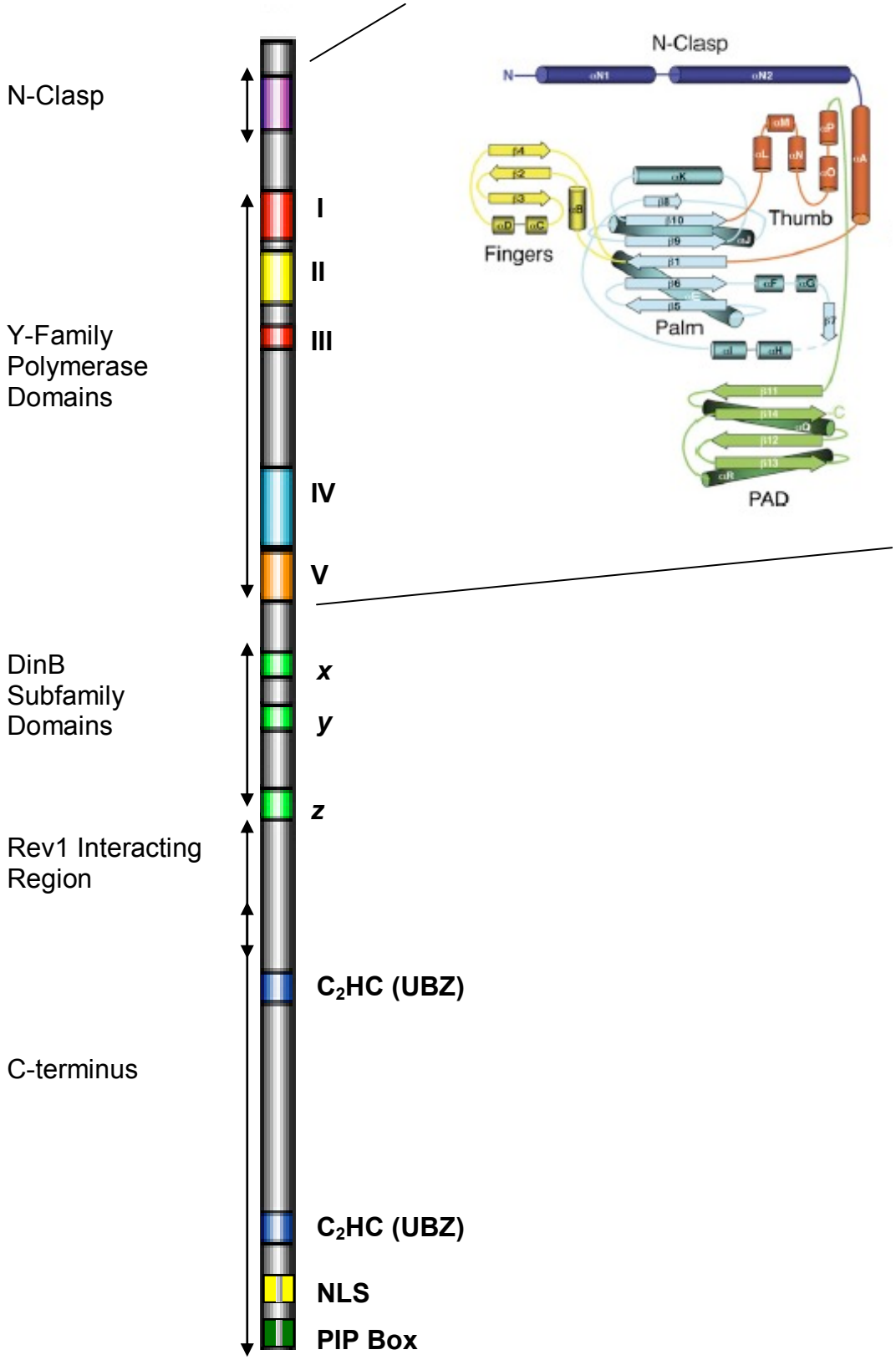

N.B. : The domains and structure of human polκ are not shown in scale to each other. The colour coding is adapted from different figures and do not relate to each other.

generation of polκ-polι double-deficient mice which showed no defect in immunoglobulin diversity generation and a growing understanding of the role of polη in somatic hypermutation, has pointed away from a primary role for polκ in antibody development (Shimizu et al., 2005).

In accordance with the role of polκ in replicating past bulky polycyclic hydrocarbon DNA lesions such as benzo[a]pyrene adducts and oxidised steroids, the *polk* gene's promoter region contains two xenobiotic binding sites for the aryl hydrocarbon receptor (Ogi et al., 2001). Fittingly given the presence of bulky hydrocarbons in cigarette smoke, *polκ* is over-expressed in lung tumours. This over-expression is not due to any chromosomal abnormalities common to cancerous cells, such as gene duplication. Given the mutagenic properties of polκ, the over-expression may indicate a role in the oncogenesis of the lung cancer (O-Wang et al., 2001). Conversely, *polκ* expression has been shown to be down regulated in colorectal cancer cells, specifically through downregulation of *cis*-acting proteins CREB and SP1 (Lemée et al., 2007). It is suggested that this may involve a down-regulation of polκ in its *accurate* repair roles as opposed to its *mutagenic* aspects. Thus the regulation of a Y-family polymerase, presumably carefully controlled in healthy cells, can either be up- or down-regulated in cancerous tissue depending on what role the protein is performing.

A deficiency in polκ has several notable phenotypic characteristics of which some were not predictable from *in vitro* experimental results. Mouse embryonic stem cells that had been rendered *polκ*$^{-/-}$ by deletion of exon 5 and 6 of the gene, which contains the sequence for key catalytic residues, showed enhanced sensitivity to the bulky adduct forming damaging agent benzo[a]pyrene but also displayed sensitivity to UV irradiation that would not have been predicted based on *in vitro* work (Ogi et al., 2002). Another group generated *polκ*$^{-/-}$ mice by targeting specifically exon 6 and screened for mutation frequency using the Big Blue system. These mice, as previously mentioned, displayed no impairment of embryonic development or defect in antibody diversification (Schenten et

al., 2002). Intriguingly, these mice do show reduced survival at later ages compared to wild-type littermates, though further examination showed no obvious abnormalities post-autopsy (Stancel et al., 2009). The mice also showed a spontaneous mutator phenotype in tissues responsible for metabolism of major polycyclic compounds, the kidneys and the liver. These tissues exhibited a G:C>T:A and G:C>C:G mutational spectrum and a less pronounced incidence of mutation from G:C>A:T was observed in mouse lung tissue (Stancel et al., 2009). Unfortunately despite observations of polκ accumulation in the adrenal cortex, a prominent site of biosynthesis (Velasco-Miguel et al., 2003), not enough material was able to be gathered to investigate the effect of a deficiency of polκ.

1.4.2 Polκ Function in Translesion Synthesis

Before more recent roles were unearthed for the polymerase, polκ was primarily characterised as a member of the Y-family of translesion synthesis polymerases. As polη evolved to specialise in the accurate bypass of photodamage, polκ can accommodate DNA that has been damaged by bulky hydrocarbon lesions (Ogi et al., 2002). Polκ shows the ability *in vitro* to replicate past abasic sites, 8-oxoguanine residues or benzo[a]pyrene adducts without introducing errors (Ohashi et al., 2000b). So suited is polκ to the bypass of benzo[a]pyrene adducts that in its absence, cells are unable to recover from the intra-S phase checkpoint after treatment (Bi et al., 2006). The polymerase can inefficiently replicate past acetylaminofluorene guanine (AAF-G) adducts and is unable to bypass *in vitro* upon encountering the CPD and 6-4PP lesions generated by DNA exposure to UV irradiation but is able to extend replication from termini inserted by other polymerases (Carlson et al., 2006). However, polκ has recently been implicated in having a limited ability to bypass photoproducts *in vivo*. In XP-V patients, the lack of functional polη for efficient and error-free bypass of CPDs forces a reliance on a three polymerase interaction between polζ, polι and polκ for translesion synthesis past the lesion in a mutagenic manner (Ziv et al., 2009).

In common with the other Y-family polymerases, polκ interacts with PCNA and this interaction enhances the activity of the polymerase (Haracska et al., 2002). This interaction was tested through an *in vitro* pull-down and may be missing other modifications required for effective *in vivo* function of polκ. Indeed, analysis using localisation of eGFP-tagged protein showed that proper accumulation of mouse polκ required intact UBZ domains, which corresponded with an interaction between polκ and ubiquitin seen in a yeast two-hybrid analysis (Guo et al., 2008). Deletion of the UBZ domains abolished the observed *in vitro* and *in vivo* interactions (Guo et al., 2008). Intriguingly, the localisation of human polκ differed from what was expected based off knowledge of how another Y-family polymerase, polη, localised following damage. Initially it had been reported that polκ localised with other replication factors such as PCNA in a manner similar to polη (Bergoglio et al., 2002). However, when repeated with more thorough controls, including side-by-side comparisons with eGFP-polη against eGFP-polκ, polκ only accumulated in foci in 25% of cells following damage (5% of cells showed foci without damage, compared to 80% with damage and 20% without for polη foci). These polκ foci also poorly colocalised with PCNA foci and polκ foci were often absent in cells strongly showing PCNA foci (Ogi et al., 2005). While surprising, these results also confirmed the importance of the UBZ domains and the PIP box of polκ for localisation into foci, along with the NLS for proper import and retention into the nucleus (Ogi et al., 2005).

In addition to a role in bypassing bulky hydrocarbon adducts, there is a growing body of evidence for a role of polκ in the bypass of interstrand cross-linked DNA adducts. The resolution of lesions resulting from the cross-linking of DNA is a complex process, involving aspects of both NER and TLS (Sarkar et al., 2006) . As had been previously mentioned, polζ plays a major role in the correct bypass of interstrand cross-links. As also mentioned previously, polκ displays the ability to bypass monoadducts attached to the N^2 of guanine, such as benzo[a]pyrene adducts (Ogi et al., 2002). These adducts do not differ greatly from unhooked interstrand cross-links formed between the N^2 of opposing guanines and polκ might be expected to be able to accommodate these lesions as well.

Accordingly, polκ was shown to be able to bypass such unhooked N^{2-} N^{2-}guanine interstrand lesions (Minko et al., 2008). Thus polκ may play a role in being able to efficiently bypass cross-links once unhooked that resemble the other DNA lesions it can bypass in TLS.

1.4.3 Polκ Involvement in NER

Roles for TLS polymerases in non-bypass functions, such as role of polη in gene conversion (Seki et al., 2005), was already established when a role for polκ in NER was discovered (Ogi and Lehmann, 2006). Despite the inability of polκ to replicate DNA past the UV generated DNA lesions of 6-4PP and CPD, *polk* disruption increases the UV sensitivity of cultured cells (Ogi et al., 2002). Ogi showed that complementation of *polk* deficient MEF/ES cells with wild-type *polk* of mouse or human origin could rescue UV sensitivity. Rescue was dependent on the polymerase activity of polκ being intact, as a D198N polymerase-dead mutant showed no recovery of UV sensitivity. It might be tempting, as some have done, to assume that this is a poorly explored role of polκ in TLS, with some recent evidence supporting such an *in vivo* role (Ziv et al., 2009). However, in cells lacking polκ, defects were shown in specific and dependable assays that are classic measurements of NER. Following UV irradiation polκ was shown to be involved in both TCR, observed by the recovery of RNA synthesis, and GGR, observed by unscheduled DNA synthesis (Ogi and Lehmann, 2006). To further confirm the role of polκ in NER, repair replication was measured by observing the incorporation of ^{3}H-thymidine and bromodeoxyuridine (BrdU) in the presence of the dNTP depleting agent hydroxyurea. BrdU incorporation into long stretches of DNA from replication would be significantly denser than DNA containing only short patches of incorporated BrdU from repair synthesis. *Polκ* deficient mutants again showed a large reduction in repair synthesis that was then restored by complementation with human *polk* cDNA (Ogi and Lehmann, 2006). Removal of photoproducts was measured by dot-blot procedures with antibodies to both CPD and 6-4PP. Wild-type cells showed efficient repair of 6-4PP, with 50% removal in five hrs whereas *polκ* deficient

mutants showed 50% removal after fifteen hrs but could be restored to wild-type levels of repair by transfection with *polκ* cDNA. These results supported the hypothesis that polκ was able to carry out the gap-filling step in NER instead of, or complementing, replicative polymerases such as polδ or polε (Ogi and Lehmann, 2006). In *E.coli*, the Y-family polymerases pol IV and pol V can take over from the replicative polymerase following hydroxyurea (HU) treatment (Godoy et al., 2006). After HU treatment, the pool of dNTPs in the *E.coli* cell falls to 10μM from its untreated level of 100μM. The replicative polymerases, with a K_m in the range of 3-40μM, function inefficiently at these nucleotide concentrations. The Y-family polymerases are much more tolerant of low nucleotide levels. *E.coli* pol IV, when associated with the β clamp, a PCNA homologue, has a K_m of 5 μM and pol V has a K_m of 0.08 μM when associated with RecA (Tang et al., 2000). It is possible that an analogous situation occurs in mammalian cells, where polκ, with a K_m of between 0.28 – 2.2 μM when inserting bases in an error-free manner, can take over from other polymerases in situations of low nucleotide concentrations, such as in non-dividing cells. Indeed, further work has developed the role of polκ in the NER process. Work done by Ogi *et al.* has shown that a knock-down of polκ can reduce the unscheduled synthesis of DNA by 50%, similar to the levels achieved by knocking down the subunits of polδ with no further increase in a dual knock-down (Ogi et al., 2010). Furthermore, it was shown that the involvement of polκ was dependent upon ubiquitinated PCNA and the scaffold protein XRCC1 (Ogi et al., 2010) (Figure 1.11). This interaction and involvement in NER was especially pronounced in quiescent cells, furthering the hypothesis that polκ maybe particularly involved when nucleotide concentrations are low. Though mutagenic, polκ has an error rate of 1 in 1000 and the cell may have evolved to 'take the risk' and use polκ to start synthesising a gap of 30 nucleotides as under strenuous conditions as opposed to leaving it unrepaired. This emerging role of polκ in the NER process prompts further investigation into the structural features that allow the polymerase to take part and regulate its role.

Figure 1.11: A Model for Human Polκ Involvement in NER

Following damage detection and positioning of the nucleases, NER can proceed down one of two pathways. 50% of the time incision will be complete and the gap rapidly sealed by the actions of polε. For the other 50%, repair synthesis is coordinated between polκ, dependent on XRCC1 and ubiquitinated PCNA, and polδ. The PCNA ubiquitination is achieved through the independent recruitment of RAD18 prior to the assembly of the NER complex. Model adapted from Ogi *et al.* (2010) *Molecular Cell*

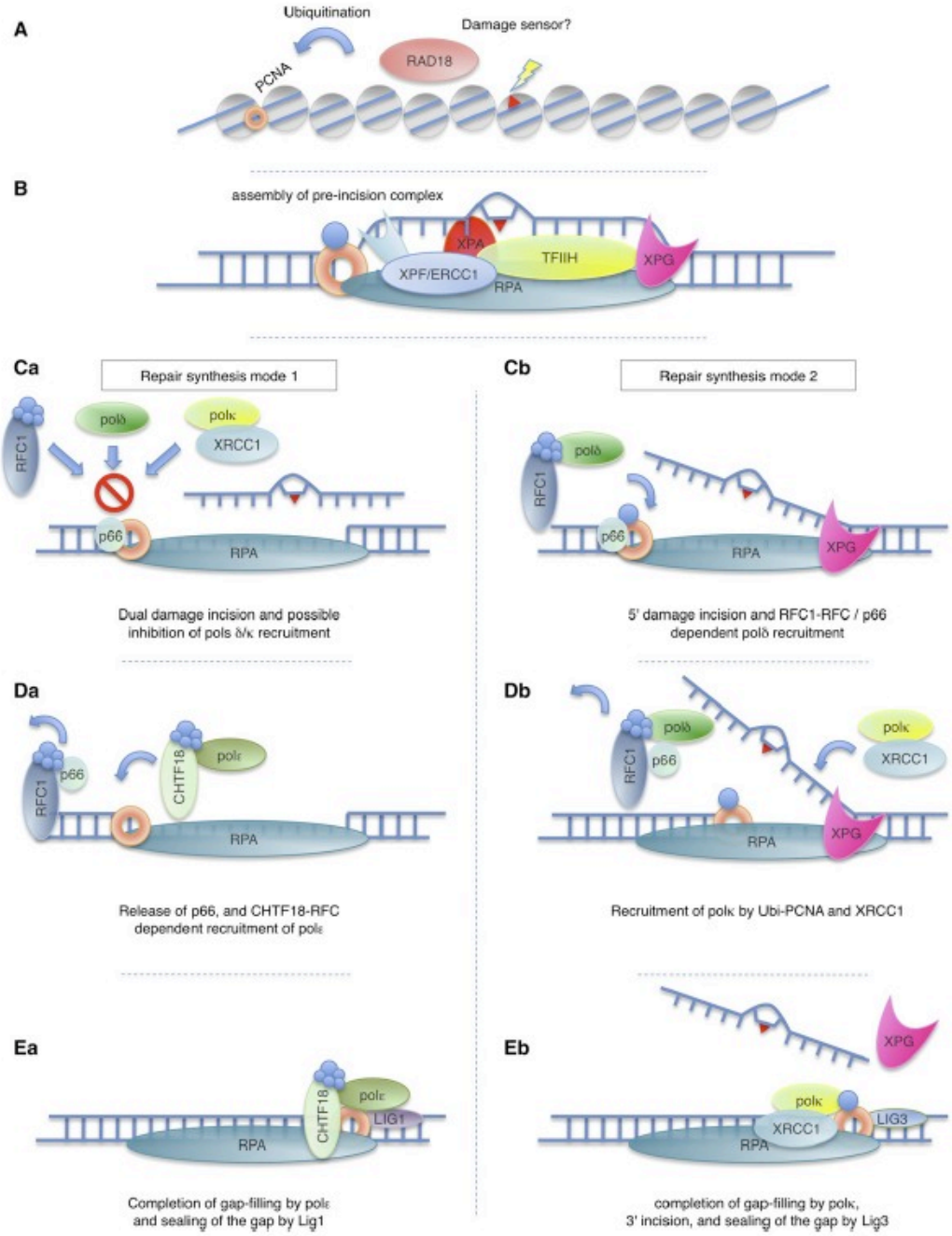
A
Ubiquitination
Damage sensor?
RAD18
PCNA
B
assembly of pre-incision complex
XPA
TFIIH
XPG
XPF/ERCC1
RPA
Ca
Repair synthesis mode 1
polδ
polκ
XRCC1
RFC1
p66
RPA
Dual damage incision and possible inhibition of pols δ/κ recruitment
Cb
Repair synthesis mode 2
polδ
RFC1
p66
RPA
XPG
5' damage incision and RFC1-RFC / p66 dependent polδ recruitment
Da
p66
RFC1
CHTF18
polε
RPA
Release of p66, and CHTF18-RFC dependent recruitment of polε
Db
polδ
p66
RFC1
polκ
XRCC1
RPA
XPG
Recruitment of polκ by Ubi-PCNA and XRCC1
Ea
CHTF18
polε
LIG1
RPA
Completion of gap-filling by polε and sealing of the gap by Lig1
Eb
XPG
polκ
XRCC1
LIG3
RPA
completion of gap-filling by polκ, 3' incision, and sealing of the gap by Lig3

As part of that investigation, the thesis that follows will detail experiments that were conducted to explore the role of conserved residues found in an otherwise unconserved region of human DNA polκ. The effects of mutating these residues on the behaviour and function of the protein as observed by localisation, sensitivity to damage and ability to recover from damage will be addressed. In addition, affects on protein-protein interactions and recruitment to the NER process are investigated.

Chapter 2: Materials and Methods

2.1 Commonly Used Reagents

2x HBS – 275mM NaCl, 3mM Na_2HPO_4 anhydrous, 55mM HEPES in a final volume of 500ml of distilled water. The pH is brought to 7.0. Stored at -20°C

3x Laemmli Buffer – 20% glycerol (v/v), 15% β-mercaptoethanol (v/v), 4.5% SDS (v/v); 15mM Tris.HCl pH 6.8; a grain of bromophenol blue. Stored at -20°C.

10x Running Buffer – 250mM Tris-Base, 2M glycine, 35mM SDS, brought up to final volume (4l) with distilled water. Stored at room temperature.

Developing Solution – 0.04% formaldehyde in 2% sodium carbonate in distilled water. Make fresh prior to use.

Fixation Solution – 50 : 5 : 45 v/v/v methanol : acetic acid : water. Make fresh prior to use.

IP Buffer - 1.25mM NaCl, 50mM Tris pH 7.5, 1x Protease Inhibitor Tablet (Roche), brought up to final volume (50ml) with distilled water. Stored at -20°C.

Lysis Buffer – 0.5% NP40, 40mM NaCl, 50mM HEPES, 2mM $MgCl_2$, 1mM NEM, 2x Protease Inhibitor (Roche), 20mM imidazole, 1µl/ml benzonase, brought up to final volume (1ml) with distilled water. Made fresh prior to each use.

Sensitising Solution – 0.02% sodium thiosulfate in distilled water. Make fresh prior to use.

Transfer Buffer – 50mM Tris base, 40mM glycine, 0.0375% SDS, 20% ethanol, brought up to final volume (1l) with distilled water. Stored at room temperature.

Wash Buffer – 1.25mM NaCl, 50mM HEPES, 2x Protease Inhibitor Tablet (Roche), 20mM imidazole, made up to final volume (50ml) with distilled water. Made fresh prior to use.

2.1.1 Commonly Used Reagents – In House

Supplies of the following used reagents were produced in-house by support staff:

0.5 M EDTA – 250mM Na_2EDTA, 250mM Na_4EDTA, brought up to final volume (1l) with distilled water. pH 8.0, sterilise by autoclave, store at room temperature.

PBS – 137mM NaCl, 0.3mM KCl, 10mM Na_2HPO_4, 1.7mM KH_2PO_4 made up to final volume (1l) with distilled water, pH to 7.4 with HCl. Sterilise by autoclaving, stored at room temperature.

LB – 1% bacto-tryptone (w/v), 0.5% bacto-yeast extract (w/v), 171mM NaCl made up to final volume (1l) with distilled water, pH to 7.0 with NaOH. Sterilise by autoclaving, stored at room temperature.

10% (w/v) SDS in water

2.1.2 Commonly Used Reagents – Tissue Culture

Cell Culture Medium - Dulbecco's Modified Eagle Medium supplemented with 10% (v/v) foetal calf serum, 1% (v/v) glutamine, 1% (v/v) penicillin-streptomycin and 1% (v/v) non-essential amino acids. Store at 4°C, use at 37°C.

Cell Culture Starvation Medium - Dulbecco's Modified Eagle Medium supplemented with 0.5% (v/v) foetal calf serum, 1% (v/v) glutamine, 1% (v/v) penicillin-streptomycin and 1% (v/v) non-essential amino acids. Store at 4°C, use at 37°C.

4.1% EDTA – 0.5mM Na_2EDTA, 0.7mM Na_4EDTA brought up to final volume (1l) and sterilised by autoclaving.

Trypsin-EDTA – 0.25% (w/v) trypsin, 0.6% EDTA (v/v), a final volume of 200ml in PBS. Store at 4°C, use at 37°C.

FACS Cell Preparation Solution – 2mM EDTA in PBS. Store at 4°C, use at 37°C.

2.2 Preparation of Plasmid DNA

2.2.1 Miniprep

A colony was picked off a plate by sterile pipette tip and placed in 5ml of LB media containing the appropriate selective antibiotic. This was grown overnight at 37°C with shaking. The plasmid was then purified using a Qiagen miniprep kit following the supplied protocol. The plasmid was eluted in 50µl of elution buffer and then spectroscopically

analysed for DNA concentration by measuring absorbance at 260nm on a spectrophotometer.

2.2.2 Midiprep

A colony was picked as previously described and grown in 1ml of LB with selective antibiotic for 5 hrs at 37°C with shaking. This starter culture was then added to 100ml of LB with selective antibiotic and grown overnight at 37°C with shaking. The plasmid was purified using a Qiagen midiprep kit following the supplied protocol. The purity and concentration of the DNA was analysed as previously described.

2.3 Generating polκ mutants for single amino acid changes:

2.3.1 PCR site-directed Mutagenesis

Complementary PCR primers were designed using the Stratagene Primer Design software available on the Stratagene website. They included no more than two or three base pair changes to alter a single amino acid residue at a time from its starting codon to one encoding an alanine. The mutational mismatch was contained in the centre of each primer with between 15-20 base pairs either side that were complementary to the region of *polk* that was to be mutated. The PCR was carried out with KOD polymerase with the following setup:

Table 2: PCR Site Directed Mutagenesis Components

Reagent	Volume	Final Concentration
Template DNA (eGFP-C3 polκ/pMSCV GFP-polκ)	1 µl at 10ng/µl	0.2ng/µl
Forward Mutagenic Primer	1.5 µl at 10pmol/µl	0.3µM
Reverse Mutagenic Primer	1.5 µl at 10pmol/µl	0.3µM
dNTPs (2mM)	5 µl	0.2mM
10x KOD Buffer	5 µl	1x
Magnesium Sulfate (25mM)	3.5 µl	1.5mM
100% DMSO[2]	2.5 µl	5%
milliQ H2O	29 µl	-
KOD polymerase (1U/µl)	1 µl	0.02U/ µl
Final Volume	50 µl	-

The PCR machine was programmed to run through the following cycle:

Table 3: PCR Parameters for Site Directed Mutagenesis

Step	Temperature (°C)	Time	Cycles
	95	1 min	1
Denaturing	95	1 min	18
Annealing	55	1 min	
Extension	70	1 min/kilobase	
	70	10 min	1

[2] DMSO was occasionally included to a total concentration of 5% since better results in successfully generating mutants had been obtained with its addition.

2.3.2 Degradation of unmutated template plasmid

1 µl of *dpn* I (20,000 U/µl) (New England Biolabs) was added to the PCR products and put at 37°C in a water bath for one hr to digest the methylated, unmutated template plasmid.

2.3.3 Ethanol Precipitation of PCR product

To increase the efficacy of obtaining successful mutant clones, the entire PCR amplified plasmid was used in the transformations. To concentrate the DNA into a workable volume, it was first precipitated using ethanol. A volume of 3M sodium acetate (pH 5.2) equivalent to $1/10^{th}$ the volume of the PCR reaction was added to the PCR mixture following Dpn1 digestion. A volume of -20°C 100% ethanol equivalent to twice the reaction mixture with sodium acetate included was added and the mixture was pulse vortexed before being stored at -20°C for 1 hr. Afterwards, the solution was centrifuged at 13,000 RPM in a standard tabletop centrifuge for 10 min. The supernatant was removed and the pellet of DNA was washed twice with room temperature 70% ethanol. The pellet was allowed to air dry for 10 min before being resuspended in 10 µl of elution buffer.

2.3.4 Transformation of DH5α competent cells

DH5α competent cells were thawed on ice and a 50µl aliquot was transferred to a 14ml thin walled tube. Between 1µl to 5µl of DNA, depending on DNA concentration, with lower volumes used for more highly concentrated DNA and vice versa, was added to the tube and mixed gently. The tubes were put on ice for 30 min before being heat shocked for 45s at 42°C and then returned to ice for an additional 2 min. 450µl of room temperature LB was added and the tubes were put in a water bath at 37°C for 1 hr. Afterwards, between 100µl to 250µl was plated out onto agar plates with the appropriate selection antibiotics and placed overnight at 37°C. To get maximum number of colonies from low-yield transformations as with a mutagenised plasmid, the 450µl suspension of

cells was spun in a centrifuge at 3,000 rpm for 5 min, the pellet was resuspended in 100µl of LB and the entire volume was plated onto agar plates with appropriate selection antibiotics before being incubated overnight at 37°C.

2.4 Generating polκ mutants with multiple amino acid changes:

2.4.1 Fusion PCR

Complementary PCR primers were designed using the Stratagene Primer Design software. They included multiple base pair alterations. The mutational mismatches were contained in the centre of each primer with between 15-20 base pairs either side that were complementary to the region of *polk* that was to be mutated. In addition, forward and reverse primers, upstream and downstream of the region of mutagenesis respectively, were designed that included appropriate restriction digest sites to aid subcloning back into the empty vector. The PCR was carried out with KOD polymerase with the following setup:

Table 4: Fusion PCR Components

First PCR Product			Second PCR Product		
Reagent	Volume	Final Concentration	Reagent	Volume	Final Concentration
Template DNA (eGFP-C3 polκ)	1 µl at 10ng/µl	0.2ng/µl	Template DNA (eGFP-C3 polκ)	1 µl at 10ng/µl	0.2ng/µl
Forward Primer	1.5 µl at 10pmol/µl	0.3µM	Forward Mutagenic Primer	1.5 µl at 10pmol/µl	0.3µM
Reverse Mutagenic Primer	1.5 µl at 10pmol/µl	0.3µM	Reverse Primer	1.5 µl at 10pmol/µl	0.3µM
dNTPs (2mM)	5 µl	0.2mM	dNTPs (2mM)	5 µl	0.2mM
10x KOD Buffer	5 µl	1x	10x KOD Buffer	5 µl	1x
Magnesium Sulfate (25mM)	3.5 µl	1.5mM	Magnesium Sulfate (25mM)	3.5 µl	1.5mM
milliQ H2O	31.5 µl	-	milliQ H2O	31.5 µl	-
KOD polymerase (1U/µl)	1 µl	0.02U/ µl	KOD polymerase (1U/µl)	1 µl	0.02U/ µl
Final Volume	50 µl	-	**Final Volume**	50 µl	-

The PCR machine was programmed to run through the following cycle:

Table 5: PCR Parameters for Fusion PCR

Step	Temperature (°C)	Time	Cycles
	95	1 min	1
Denaturing	95	1 min	30
Annealing	55	1 min	
Extension	70	15s/kilobase	

The size of the bands was checked on a 1% agarose gel before moving onto the fusion step:

Table 6: Fusion PCR Components for Fusion of the Two Fragments

Reagent	Volume	Final Concentration
Template DNA (Forward PCR product)	1 µl at 1/50 dilution	-
Template DNA (Reverse PCR product)	1 µl at 1/50 dilution	-
Forward Primer	1.5 µl at 10pmol/µl	0.3µM
Reverse Primer	1.5 µl at 10pmol/µl	0.3µM
dNTPs (2mM)	5 µl	0.2mM
10x KOD Buffer	5 µl	1x
Magnesium Sulfate (25mM)	3.5 µl	1.5mM
milliQ H2O	28 µl	-
KOD polymerase (1U/µl)	1 µl	0.02U/ µl
Final Volume	50 µl	-

Since the two PCR products from the first round contain complementary ends, they can act as primers for each other. The next round of PCR fuses the two fragments together into a single PCR product containing the mutations.

Table 7: PCR Parameters for Fusion PCR to Fuse the Two Fragments

Step	Temperature (°C)	Time	Cycles
	95	1 min	1
Denaturing	95	1 min	30
Annealing	55	1 min	
Extension	70	15s/kilobase	

2.4.2 TA cloning into pGEMT-easy vector

The fusion PCR product was purified using a Qiagen PCR cleanup column as according to the provided protocol. The bound DNA was eluted by incubating with Elution Buffer for 1 min and then being spun at 13,000 rpm. The eluted DNA was then was incubated with TAQ polymerase for 30 min at 70°C as per the kit protocol to generate 3' A overhangs. This product was ligated into the pGEMT-easy vector as per the Promega protocol. The 3' adenine overhangs impart directionality and limited complementariness to the linear pGEMT-easy vector. The vector and insert were incubated together in Rapid Ligation Buffer with T4 DNA Ligase at room temperature for 1 hr. After this, the ligated plasmids were inoculated with DH5α *E.coli* and the bacteria were transformed as described previously. The transformed *E.coli* was plated onto LB-Agar plates coated with IPTG and X-Gal to allow blue-white screening for successful insertions. White colonies, positive for the insertion of the PCR product, were picked and grown overnight for a miniprep.

2.4.3 Digest and Gel extraction

Plasmids were digested with NEB restriction enzymes in appropriate buffer as per the NEB protocols for 2 hrs at 37°C. An additional microlitre of restriction enzymes used was added and incubated for an additional hr. They were then electrophoresed on a 1% agarose gel for 1 hr. Bands of appropriate size were visualised under the UV

transilluminator box and excised with a clean scalpel. DNA was purified from the gel slices using a Qiagen Gel Extraction Kit and following the supplied protocol. The DNA was eluted by incubating with Elution Buffer for 1 min before being spun at 13,000 rpm. The concentration and purity of the extracted DNA was checked by measuring absorbance at 260nm on a spectrometer.

2.4.4 Ligation

Vector plasmids and mutant *polκ* inserts from the fusion PCR obtained via insertion into and extraction from the pGEMT-easy vector were combined in a 1:3 ratio and the volume was increased to 10µl with distilled water. 10µl of NEB 2x Quick Ligase buffer was added, the solution was mixed and 1µl of Quick Ligase was added. The solution was incubated at 4°C overnight. 5µl of the mixture was used the following day to transform DH5α cells as described above. For ligation into the pMSCV vector, the insert was blunt-ended following restriction digest from the pGEMT-easy plasmid using T4 polymerase by incubating for 1 hr at 37°C. The insert was then recovered by a Qiagen Gel Extraction Kit as described above. The pMSCV vector was cut with a blunt-end restriction enzyme as described above and dephosphorylated with calf alkaline phosphatase by incubating for 1 hr at 37°C. The insert and vector were ligated together as described above.

2.5 Sequencing to Verify Presence of Mutations and Correct Ligations

Sequencing was carried out by GATC Biotech on samples of plasmid DNA at a concentration of 100 ng/µl and a total volume of 30 µl. Plasmids were sequenced with primers synthesised in house by GATC Biotech and designed to cover the length *of GFP-polκ* to ensure correct creation of the mutation and lack of secondary mutations due to the PCR amplification for the site-directed mutagenesis, the correct directionality of insertion and the ligation of insert DNA into vector plasmid respectively.

2.6 Cellular Transfection of Plasmids and siRNA

2.6.1 Transfection of cell lines with plasmid DNA using Fugene 6

A glass coverslip was placed in each well of a 6 well plate and suspension of 1 x 10^5 cells was placed onto it. 2ml of DMEM supplemented with 10% FCS was added and the cells were allowed to adhere to the coverslip in a 37°C incubator with 5% CO_2. 24 hrs later, the cells were transfected with 3µl Fugene 6 to 2ug DNA ratio in 97 µl serum-free media per well following the Fugene 6 protocol. The cells were returned to the incubator for 48 hrs before continuing the assay.

2.6.2 Transfection of cell lines with plasmid DNA and siRNA using Metafectene Pro

To use the MRC5 derived cell line expressing 6xHis-PCNA with the K164R mutation that prevents the protein from being ubiquitinated by Rad18/Rad6 following UV induced damage, it was necessary to simultaneously knock down the endogenous PCNA while transfecting in GFP-polκ wild-type. Fugene 6 and Hiperfect, alone and in combination, proved either unable to accomplish the task or toxic to the cells. Metafectene Pro is marketed as a transfection reagent able to accomplish such double transfections with comparatively less toxicity to the cells.

5x10^4 cells per well in suspension were plated into the wells of a 24 well plate and allowed to adhere by incubating at 37°C overnight in DMEM supplemented with 10% FCS. The next day, the cells were transfected with 2µl of Metafectene Pro and either target siRNA or non-targeting control siRNA in 60µl PBS to a final volume of 100nM siRNA per well. The cells were left for 48 hrs at 37°C. At the end of this incubation, the medium was removed from the cells and the cells were trypsinised off the well. The trypsinised cells were moved into a 6 well plate with a coverslip included and fresh medium was added. The knockdown was repeated as described, with volumes scaled up accordingly but included 2µg of plasmid DNA per transfection. The cells were incubated at 37°C overnight before processing the next day.

2.6.3 Transfection of cell lines with plasmid DNA using Calcium Phosphate Precipitation

The XPCS1RO and XP2YO cell lines, and their derivatives, were refractory to successful transfection using Fugene 6 or other lipid-based transfection reagents. Higher efficiencies of transfection could be achieved using calcium phosphate precipitation. A coverslip was placed into a 10cm dish and a suspension of approximately 1 x 10^6 cells in 10ml of DMEM supplemented with 10% FCS was added. 24 hrs later a precipitate of calcium phosphate and plasmid DNA was prepared: One eppendorf contained 0.5ml of room-temperature 2x HBS and in a separate eppendorf plasmid DNA, 2M calcium chloride and water were combined and brought to a total volume of 0.5ml with distilled water. Using a glass Pasteur pipette and an electric pipette, the 2x HBS solution was gently bubbled as the DNA:calcium chloride solution was added drop wise. The full 1ml was evenly distributed across the 10cm dish which was then returned to the incubator. 24 hrs later, the medium was taken off, the dish washed with warmed PBS and fresh medium added. The dish was then returned to the incubator for a further 24 hrs before the assay was continued. For the transfection of HEK293 cells, the same protocol was used with the exception that the coverslip was omitted from the 10cm dish.

2.7 MG132 Inhibition of the Proteasome

20µl of 5mM MG132 (100x final concentration) was added to 1.98ml of 10% FCS in DMEM in the wells of a 6 well plate that contained coverslips plated with cells as previously described. The cells were incubated with this medium for 2-6 hrs at 37°C. The cover slips were removed and UV irradiated as described below. This was followed by 2 hrs of incubation in fresh medium with MG132. The remaining cells in the well were washed with PBS and prepared for western blotting as previously described.

2.8 Immunofluorescent Staining for Localised Damage

2.8.1 Local UV irradiation and 10mM hydroxyurea treatment

The medium was aspirated off the cells and they were washed twice with PBS. The coverslips were transferred onto a parafilm covered lid of a 10cm dish and a 5um polycarbonate filter was laid on to the coverslip. The coverslips were exposed to 40 J/m2 of UV radiation before being transferred to 6 well plates containing 2ml of 10mM hydroxyurea in medium. The plates were placed in a 37°C incubator with 5% CO_2 for 45 min.

2.8.2 Fixation and Permeabilisation of the cells

The coverslips were washed with PBS to remove all traces of medium. 2ml of 2% PFA in PBS was added and the coverslips were incubated at room temperature for 15 min. The coverslips were washed with PBS to remove all traces of PFA. 2ml of 0.5% Triton-X in PBS was added to permeabilise the cells for 10 min. The coverslips were washed with PBS to remove all traces of Triton-X 100.

2.8.3 Immunofluoresence Microscopy

The fixed cells on the coverslips were blocked for 30 min at room temperature in 10% BSA in PBS, 100µl per coverslip. After blocking, excess BSA was removed and the coverslips transferred to a parafilm lined tray. 100µl of primary antibody diluted in PBST was added per coverslip and left for 2 hrs at room temperature or at 4°C overnight, shielded from the light in both cases. The coverslips were washed 3 times, 5 min per wash, in PBST. 100µl of appropriate secondary antibody diluted 1 in 1000 in PBST was added per coverslip and left for 1 hr at room temperature. The coverslips were washed 3 times in PBST, 5 min per wash.

The coverslips were gently touched edge-wise against absorbent paper to blot away any excess of PBST from the previous set of washes. The prepared coverslips were mounted

onto standard laboratory slides, cell side down, with 15µl of ProLong Gold with DAPI. They were stored at 4°C until analysis using a Leica DM5000 microscope with a 100x oil-immersion objective. Images were analysed using ImageJ or Photoshop software.

2.9 Creation of Stable Cell Lines

Polk mutants recreated in the pMSCV vector as described above were used to create stably expressing cell lines in the M6 (MEF *polk*$^{-/-}$) background. 1 x 10^5 cells were seeded into the wells of a 6 well plate and incubated overnight at 37℃ with 5% CO_2 in 2ml of 10% FCS containing DMEM. The next day cells were transfected with Fugene 6 and the desired plasmid as described above and incubated for 24 hrs. The following day, 3µg - 5µg of puromycin per ml of medium was added to the wells and cells were incubated for 7-10 days. Puromycin levels were increased up to 5µg/ml to ensure complete death of untransfected cells. Surviving cells were trypsinised off the well surface and replated into 100mm plates with 10ml of 10% FCS DMEM and 3µg/ml puromycin to maintain selection. After 7-10 days, colonies were picked off the dish with 3mm cloning discs soaked in trypsin. The cloning discs were placed into the wells of a 24 well plate with 500µl of medium. Cells that grew to confluence were trypsinised and the cells seeded into a T25 flask with appropriate medium. After cells had reached confluence, they were trypsinised and resuspended in 5ml of medium. 1ml was taken to test for expression of GFP-polκ by Western Blotting for GFP and the rest was frozen down.

2.10 Freezing cells for long-term storage

Cells for long-term storage were trypsinised from their flask and resuspended with DMEM supplemented with 10% FCS. The cells were spun out of suspension at 1,500 rpm for 5 min. The supernatant was removed and the cell pellet was resuspended in DMEM supplemented with 10% FCS with 10% DMSO and aliquoted into the desired number of cryotubes. The tubes were frozen in cryobombs at -80°C before being transferred to liquid nitrogen storage tanks.

2.11 Western Blotting

2.11.1 Preparation of Western Blot Samples

Cells on the surface of a well of a 6 well plate or a 35mm dish were scraped in 50µl of Laemmli Buffer. The suspension was sonicated in a chilled ultrasonic bath at 4°C for 10 min and boiled in a water bath for 10 min. For samples of the stable cell lines, cells were suspended in lysis buffer (50ul) and treated for 30 min with benzonase at 4°C. The solution was spun down and the supernatant was removed. A 2µl sample of the supernatant was combined with 200µl of Bradford Reagent and 800µl of distilled water. Protein levels were determined on the spectrophotometer at an absorbance of 600 nm. Absorbance values were used to equalise the samples to equivalent of the least concentrated sample. 3x Laemmli Buffer was added to give a 1x final concentration and the sample was boiled for 10 min. Samples that had been obtained from pulldown off NiNTA- or Dyna-beads were prepared in a similar manner.

2.11.2 Western Blotting for Protein Expression

SDS-PAGE gels were prepared by combining distilled water and 30% acrylamide/bis-acrylamide with 1.3 ml of 1.5M Tris (pH 8.8), 0.05 ml of 10% SDS and 0.05 ml of 10% ammonium persulfate. The stacking gel was prepared with fixed amounts, so that every 1ml of stacking gel is composed of: 0.68ml distilled water, 0.17 ml 30% acrylamide/bis-acrylamide, 0.13 ml 1.0 Tris (pH 6.8), 0.01 ml 10% SDS and 0.01ml 10% ammonium persulfate. The polymerisation reaction was initiated by adding 2µl TEMED for every 5ml gel and the main body of the gel was poured between two glass plates sandwiched together. The top of the gel was covered with butanol to protect it from oxygen. Once set, the butanol was removed and the stacking gel was prepared in a similar manner, with the inclusion of well dividers. Once set, the well dividers were removed and the gel was

placed into a BD-Gel Running Tank and prepared for usage by completing the electro-chemical circuit by addition of running buffer.

10µl of size marker was loaded along with prepared samples and run down the gel. Proteins were transferred to a HiBond nitro-cellulose membrane using a semi-dry transfer system by assembling a stack consisting of a sheet of Biorad Extra Thick Filter Paper wetted with transfer buffer, a nitrocellulose membrane wetted with distilled water, the SDS-PAGE gel and a final layer of Filter Paper wetted with transfer buffer. This was run at 20V for 20 min for 0.75mm thick gels and 20V for 60 min for 1mm thick gels. The stack was disassembled and the paper and gel discarded. The membrane was blocked in 5% milk powder in PBST for 30 min and then incubated overnight at 4°C in the appropriate primary antibody. The membrane was washed 3 x 5-10 min in PBST and incubated for an hr in the appropriate secondary antibody. The membrane was washed 3 x 5-10 min in PBST and developed with Western Lightening reagents. X-ray film was exposed and developed to visualise the protein bands.

2.12 siRNA knockdown of protein expression

For cells that required co-transfection with siRNA and plasmid DNA, 5 x 10^4 cells were first plated into the well of a 24-well plate and treated with siRNA in a complex with Metafectene Pro. After 48hrs, the cells were trypsinised and replated into the well of a 6-well plate and co-transfected with siRNA and 2 µg of plasmid DNA in a complex with Metafectene Pro. Protein expression was checked 24hrs later.

2.13 Fluorescence Assisted Cell Sorting of Stable Cell Lines

Cell lines requiring sorting for expression were grown to confluency in a T75 flask. The FACS Aria was calibrated as per the start-up protocol. Cells were trypsinised off the flask and resuspended in media. Cells were spun into a pellet by centrifuging at 1,500 rpm for 5 min and resuspended in 0.5ml of PBS with 2mM EDTA. The suspension was passed

through a BD Cell Strainer into a FACS tube to break up any clumps of cells. 1ml of complete medium was added to an empty tube, ensuring the medium coated the sides, to collect the sorted cells in. Cells were sorted based on their expression of GFP either for immediate use in proceeding experiments or to remove cells that had lost expression. Cell sorting occurs by interrogation of a single cell by a trio of lasers at 488nm, 633nm and 408nm wavelengths. These are used to obtain information about forward and side scatter of laser light and fluorescence. The scattered light or fluorescence is passed though longwave and bandpass filters to photomultiplier tube detectors. The detected event is then broken off from the stream into a single droplet and then, based on user designed gates, can then be collected into a pre-designated collection tube or passed to waste collection by passing by two deflection plates with 12,000V difference between them.

2.14 Recovery of RNA Synthesis Measured by Incorporation of ^{3}H-uridine

6 x 10^5 cells stably expressing GFP-polκ wild-type or the C-terminal mutants or the control cell lines M1 (MEF *polκ*$^{+/+}$) and M6 (MEF *polκ*$^{-/-}$) were sorted for near physiological levels of expression. The cells were then transferred to a new 20ml universal tube and centrifuged at 1500 RPM for 5 min. The medium was removed and the cells resuspended in 8ml of fresh DMEM with 10% FCS media. Approximately 0.75 x 10^5 cells in 1ml of medium were seeded onto a 35mm dish. This was repeated for a total of 8 dishes per cell line. The dishes were returned to the incubator and the cells were allowed to recover from sorting for a full day. 36 hrs later, the medium was removed thoroughly by tilting the plates at an angle so the wells were nearly dry, washed with PBS and drained thoroughly again. The medium was then replaced with 1ml of 0.5% FCS supplemented DMEM per dish. The cells were starved in this manner for three days. Following this, the medium was once again thoroughly removed in the same fashion. The dishes were irradiated with UV-C radiation at the following doses, two plates per dose: 0 J/m^2, 5 J/m^2, 10 J/m^2, and 15 J/m^2. Cells were incubated for a minimum of 16 hrs in a 37°C incubator. The medium was once again thoroughly removed from the plates, which were incubated at 37°C for 4 hrs with fresh DMEM supplemented with 0.5% FCS, 5μCi/ml ^{3}H-uridine. After

the 4 hrs, the medium was thoroughly removed and the cells were scraped in 250µl of 2% SDS in PBS. A strip of grade 17 chromatography paper was divided into 16 sections, two sections per plate, a total of four sections per dose. 100µl duplicate samples from each plate were spotted onto the chromatography paper. Two strips of paper were kept separate to use as a measurement of background radioactivity. The strips of paper were fixed in 5% TCA for 5 min, washed in IMS for 5 min and then washed again in separate IMS for 5 min followed by air-drying overnight. The next day, the strips of chromatography paper were cut into individual sections and placed into scintillation tubes with 1ml of Eco-Scint. The tubes were loaded into a liquid scintillation counter and counts of decay events were obtained over a four min period per tube.

2.15 Time course of Recovery of RNA Synthesis Measured by Incorporation of ^{3}H-uridine

6 x 10^5 cells stably expressing GFP-polκ wild-type or the C-terminal mutants or the control cell lines M1 (MEF Polκ$^{+/+}$) and M6 (MEF Polκ$^{-/-}$) were sorted for near physiological levels of expression of polκ. The cells were then transferred to a new 20ml universal tube and centrifuged at 1500 RPM for 5 min. The media was removed and the cells resuspended in 8ml of fresh DMEM with 10% FCS media. Approximately 0.75 x 10^5 cells in 1ml of medium were plated onto a 35mm dish. This was repeated for a total of 8 dishes per cell line, two dishes per planned dose of UV radiation. Cells were allowed to recover and prepared for irradiation as described above. The dishes were irradiated with either UV-C radiation 4 J/m^2 or 0 J/m^2 and cells were incubated for 30 min, 2.5 hrs, 5 hrs or 8 hrs in a 37°C incubator. At the end of each time point the media was once again thoroughly removed from and the plates were incubated at 37°C for 30 min with DMEM supplemented with 0.5% FCS, 5µCi/ml ^{3}H-uridine. After the 30 min, samples were prepared for the liquid scintillation counter as described above.

2.16 Clonogenic UV Survival

Cells stably expressing GFP-polκ wild-type or the C-terminal mutants or the control cell lines MEF Polκ$^{+/+}$ and MEF Polκ$^{-/-}$ were sorted for near physiological levels of expression. Cells were plated in triplicate onto 10cm plates for four different UV doses. The plates were returned to the incubator overnight. The next day, the medium was removed and the plates were washed with PBS. The PBS was removed and cells were UV irradiated at 0 J/m^2, 5 J/m^2, 10 J/m^2 and 15 J/m^2. 10% FCS supplemented DMEM was added to the plates with 3μg/ml of puromycin included if necessary. The plates were then incubated for 10 days after irradiation. At the end of the incubation period, 2ml of methylene blue in water was added directly to the medium in the plates and gently swirled to ensure complete coverage. The plates were incubated at room-temperature for 1 hr, followed by the removal of the media and gently washing with distilled water. After overnight drying, the numbers of colonies per plate per dose were counted and the average percentage survival was plotted. A colony was counted if it contained 50 or greater cells.

2.17 Purification of Proteins from Cell Lysates

2.17.1 Pulldown of 6xhis-Ubiquitin containing complexes using NiNTA Agarose Beads

One or more confluent T125 flasks of HEK293 cells were trypsinised, centrifuged and resuspended in 20 ml of DMEM with 10% FCS. 1ml of suspension was diluted into 9ml of medium and plated onto a 10cm plate. This was repeated for a total of five plates per individual pulldown. The plates were placed in a 37°C incubator. The next day, the cells were transfected using calcium phosphate as previously described. The plates were returned to the incubator overnight. The next day, the medium was aspirated off the plates, which were then washed with warm PBS and the medium was replaced. The plates were returned to the incubator overnight. The next day, the medium was removed and plates designated for the post-UV samples were UV irradiated at 20 J/m^2. The medium on all plates was replaced with fresh DMEM supplemented with 10% FCS and 10mM HU and returned to the 37°C incubator for 45 min. Following incubation, the

medium was removed from the plates and they were washed once with PBS. Cellular material was cross-linked by the addition of 4ml 1% formaldehyde in PBS to each plate followed by 10 min room temperature incubation. The fixant was removed, the plate washed once with PBS and then with 0.1M glycine (pH 7.4) in PBS. 200 µl of lysis buffer was added to each plate and the cells were scraped into the buffer. Dependent on cellular confluency, this gave a final volume between 300 and 400 µl per plate. Cellular extracts were pooled with their co-treated plates to give a final volume per sample of 1.5 ml to 2 ml. These pooled samples were incubated with benzonase and rotated on a wheel at 4°C for 30 min. The samples were spun down for 15 min at 13000 RPM at 4°C and the supernatant was removed. Protein concentration was determined as described in the previous section. Each sample was equalised to the least concentrated sample and a volume from each was removed as *Input*. Meanwhile, the stock of NiNTA beads were vortexed and 20 µl of NiNTA beads per 500 µl of individual sample were removed from suspension. The beads were spun down at 3000 RPM for 3 min and the ethanol was removed. The beads were resuspended back to their original volume in wash buffer. Equal volumes of each sample were incubated with the NiNTA beads, 20 µl per 500 µl of sample, for 2 hrs at 4°C. At the end of the incubation, the samples were spun down at 3000 RPM for 3 min at 4°C and the supernatant was removed as the *Unbound* sample. The beads were washed 3 times with 600 µl of wash buffer containing 20mM imidazole, spun down in between each wash with *Wash* samples being taken. After the final wash, the beads were incubated in elution buffer containing 100 mM imidazole for 1 min and finally spun down again. The supernatant was removed as the final *Elution* sample.

2.17.2 Immunoprecipitation of GFP-tagged protein

The *Elution* sample obtained from incubating the lysate of transfected cells with the NiNTA beads was increased to a final volume of 500 µl by the addition of IP buffer. This was now designated *IP Input* for the immunoprecipitation of GFP-tagged proteins from the elution. The *IP Input* was incubated for 1 hr at 4°C with 1 µl of anti-GFP antibody raised in rabbits. After incubation, the inputs were spun down at 13,000 rpm at 4°C to

collect any aggregates. The supernatants were transferred to new 1.5 ml eppendorf tubes. At the same time, 50 μl of Dynabeads per sample were prepared: The beads were immobilised on a magnetic rack and the supernatant was removed. The beads were washed three times with 250 μl of ice cold IP buffer, each time re-immobilised on a magnetic rack. Non-specific interactions were blocked by incubating the Dynabeads in 500 μl of 1% bovine serum albium in IP buffer for 30 min at 4°C on a rotating wheel. This was followed by immobilisation on a magnetic rack and washing as before. The beads were finally resuspended in a volume of ice cold IP buffer to give a final volume of 50 μl per sample. The beads were added to the input samples and incubated overnight at 4°C on a rotating wheel. The next day, the beads were immobilised on a magnetic rack and the supernatant removed as the *IP Unbound* fraction. The beads were washed three times with 250 μl of IP buffer, immobilised on magnetic beads after each wash. Following the third wash, the beads were resuspended in 250 μl of IP buffer and transferred to a new tube and one final wash was performed. To elute the captured proteins from the beads, the supernatant was removed from the beads and the beads were resuspended in 50 μl of 1x SDS loading buffer before being boiled for 15 min. This was collected as the *Bound* fraction.

2.17.3 Immunoprecipitation of GFP-tagged Proteins using Chromotek GFP-Trap Magnetic Beads

Elutions from cell lysates purified for 6xhis-tagged proteins by incubating with NiNTA beads were prepared for immunoprecipitation as before by diluting the elutions to a final volume of 500μl in IP buffer. In accordance with the Chromotek GFP-Trap protocol, the IP buffer for this experiment was supplemented with 0.5mM EDTA. Chromotek GFP-Trap beads, 20μl per sample, were prepared by immobilising on a magnetic rack in 250μl of ice-cold buffer and the supernatant was removed. The beads were washed twice with 250μl of ice cold buffer. Beads were resuspended and added to cell lysates. The lysates were incubated overnight at 4°C. The next day the beads were immobilised on a magnetic rack

and the supernatant was removed and kept as the *IP Unbound* sample. The beads were washed twice in 250µl of ice cold IP buffer. After the final wash, the supernatant was removed and the beads were resuspended in 50 µl of 1x SDS loading buffer before being boiled for 15 min. This was collected as the *Bound* fraction.

2.18 Silver Staining SDS-PAGE Gels for Protein Detection

SDS-PAGE gels were prepared as previously described. After samples were run on these gels, they were fixed by incubating in the Fixation Solution for 30 min. The gel was then washed twice with distilled water, 2 min per wash. After the second wash, the gel was incubated in distilled water at room temperature for 1 hr. The water was then removed and the gel was sensitised by incubating with Sensitising Solution for 2 min. The solution was discarded and the gel was washed twice with distilled water, 10 s per wash. The gel was then incubated with 4°C 0.1% silver nitrate ($AgNO_3$) for 30 min. The solution was discarded and the gel was washed twice with distilled water, 30 s per wash. The water was discarded and the gel was developed by the addition of Developing Solution. As the solution yellowed, it was replaced with fresh solution. Developing was halted by discarding the Developing Solution and replacing with 1% acetic acid. The gel was washed several times in 1% acetic acid before being stored at 4°C in 1% acetic acid.

Chapter 3: Role of Conserved C-terminal Residues in Recruitment to site of Nucleotide Excision Repair

The work by Ogi *et al.* established the previously unsuspected role of human DNA polκ in the nucleotide excision repair process. A lack of polκ rendered both DT40 chicken cells and mouse ES cells sensitive to the lethal effects of UV irradiation (Ogi et al., 2002; Okada et al., 2001). This was unexpected as polκ is unable to bypass UV induced photodamage *in vitro* (Ohashi et al., 2000b). While more recent work had shown a role for polκ in damage bypass in XP-V cells that lacked polη (Ziv et al., 2009), the NER specific assays performed by Ogi *et al.* cemented the role performed in NER by the polymerase (Ogi and Lehmann, 2006; Ogi et al., 2010)

Polκ and its homologues are represented in each of the major kingdoms of life; DinB in the prokaryotes and Dpo4 in the archaea. Though absent in *S. cerevisiae*, it is conserved in *S. pombe* and higher eukaryotes. The N-terminal region of the protein contains the catalytic site of the polymerase and is highly conserved between different organisms. Conversely, the C-terminal end of the protein exhibits poor conservation between species and has only a few known structural motifs. These include two zinc finger ubiquitin-binding domains (UBZ), a nuclear localisation signal to import the protein from the cytoplasm and a PCNA binding motif (PIP) box.

When the C-terminal regions of Polκ from different higher eukaryotes are aligned, these areas of conservation are clearly seen. As expected, motifs reported to be required for the correct function of Polκ are highly conserved. These include the UBZ domains necessary for interaction with ubiquitin, the PIP box for the interaction between polymerase and sliding clamp and the NLS, required for the correct localisation of Polκ to the nucleus of the cell. Outside of the motifs the sequence identity is negligible, roughly 10% identity between mice and humans. Intriguingly however, several other residues

appear to have been conserved throughout the evolution of the higher eukaryotes but lay outside the characterised regions. These residues have not currently been ascribed specific functions (Figure 3.1). To more fully explore this role it was decided to explore the structural features of human polκ that might contribute to its involvement in NER.

3.1 Site-Directed Mutagenesis for mutation to alanines

To investigate the role, if any, these conserved residues (whether located inside the identified domain regions or outside them) could play in the role of polκ in NER, they were independently mutated to alanines through the use of site-directed mutagenesis. Complementary primers were designed incorporating the desired mutation(s) and were used to introduce the alteration into *polκ* that had been cloned from cDNA into the eGFP-C3 vector plasmid that is then able to express a GFP-polκ construct when transfected into mammalian cells. Though versatile, site-directed mutagenesis can be cumbersome when it is necessary to introduce many mutations in close proximity, due to increased destabilisation of the primer-template pair due to nucleotide mismatches and the increased length of complementary regions necessary to overcome this. Alternatively, repeated rounds of PCR, verification and plasmid preparation with multiple primers as a new pair would be required for each new mutation. To overcome this, fusion PCR was used to generate the $IQEL_{807\text{-}810}AAAA$ mutations. This involves two outer primer pairs and two inner, complementary primer pairs containing all the required mutations and with the plasmid containing the wild-type gene is used as the template. Two initial, separate, rounds of PCR generate two overlapping fragments. In the second round of PCR, the two fragments are annealed together and used as both template and primers for the first cycle. The outer primer pairs are then used to fuse these two together, creating a single PCR product that can be cloned into the wild-type gene (Figure 3.2B).

3.2 Transfection of MRC5 and ALD assay

To explore the localisation of wild-type GFP-polκ and the C-terminal mutants during the NER process, MRC5V1 cells plated onto a coverslip were transfected with of plasmid DNA

Fig 3.1 - Polκ C-terminus and Alignment of Conserved Residues

A) An illustration of the general outline of the C-terminus of human polκ with known domains highlighted. The residue 590 marks the beginning of the C-terminal region.

B) An alignment of the C-terminus amino acid sequence of polκ from various higher eukaryotes. Identical residues are highlighted in black, similar residues in grey. Residues identified for mutagenesis are highlighted in blue. The domains of the C-terminus are underscored as indicated.

A)


590
870
N-terminus
UBZ 1
UBZ 2
NLS
PIP

B)

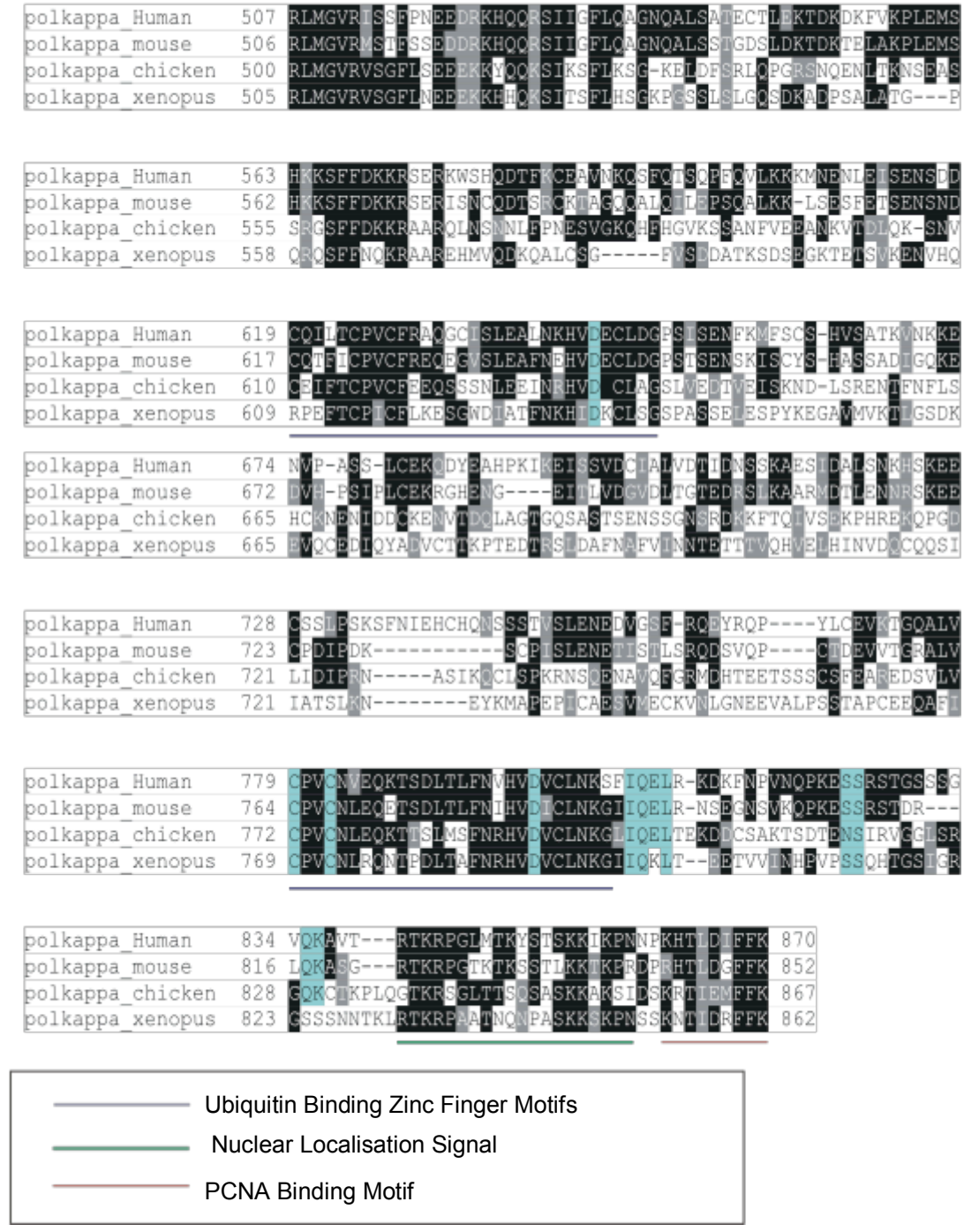
polkappa_Human 507 RLMGVRISSFPNEEDRKHQQRSIIGFLQAGNQALSATECTLEKTDKDKFVKPLEMS
polkappa_mouse 506 RLMGVRMSIFSSEDDRKHQQRSIIGFLQAGNQALSSTGDSLDKTDKTELAKPLEMS
polkappa_chicken 500 RLMGVRVSGFLSEEEKKYQQKSIKSFLKSG-KELDFSRLQPGRSNQENLTKNSEAS
polkappa_xenopus 505 RLMGVRVSGFLNEEEKKHHQKSITSFLHSGKPGSSLSLGQSDKAQPSALATG---P
polkappa_Human 563 HKKSFFDKKRSERKWSHQDTFKCEAVNKQSFQTSQPFQVLKKKMNENLEISENSDD
polkappa_mouse 562 HKKSFFDKKRSERISNCQDTSRCKTAGQQALQILEPSQALKK-LSESFETSENSND
polkappa_chicken 555 SRGSFFDKKRAARQLNSNNLFPNESVGKQHFHGVKSSANFVEEANKVTDLQK-SNV
polkappa_xenopus 558 QRQSFFNQKRAAREHMVQDKQALCSG-----PVSDDATKSDSEGKTETSVKENVHQ
polkappa_Human 619 CQILTCPVCFRAQGCISLEALNKHVDECLDGPSISENFKMFSCS-HVSATKVNKKE
polkappa_mouse 617 CQTFICPVCFREQDGVSLEAFNEHVDECLDGPSTSENSKISCYS-HASSADIGQKE
polkappa_chicken 610 CEIFTCPVCFEEQSSSNLEEINRHVD CLAGSLVEDTVEISKND-LSRENIFNFLS
polkappa_xenopus 609 RPEFTCPICFLKESGWDIATFNKHIDKCLSGSPASSELESPYKEGAVMVKILGSDK
polkappa_Human 674 NVP-ASS-LCEKQDYEAHPKIKEISSVDCIALVDTIDNSSKAESIDALSNKHSKEE
polkappa_mouse 672 DVH-PSIPLCEKRGHENG----EITLVDGVDLTGTEDRSIKAARMCLENNRSKEE
polkappa_chicken 665 HCKNENIDDCKENVTDQLAGTGQSASTSENSSGNSRDKKFTQIVSGKPHREKQPGD
polkappa_xenopus 665 FVQCPDIQYAEVCTTKPTEDTRSLDAFNAFVINNTETTTVQHVELHINVDQCQQSI
polkappa_Human 728 CSSLPSKSFNIEHCHQNSSSTVSLENEDVGSF-RQEYRQP----YLCEVKTGQALV
polkappa_mouse 723 CPDIPDK----------SCPISLENETISTLSRQDSVQP----CTDEVVTGRALV
polkappa_chicken 721 LIDIPRN-----ASIKQCLSPKRNSQENAVQFGRMDHTEETSSSCSFPAREDSVLV
polkappa_xenopus 721 IATSLKN--------EYKMAPEPICAESVMECKVNLGNEEVALPSSTAPCEEQAFI
polkappa_Human 779 CPVCNVEQKTSDLTLFNVHVDVCLNKSFIQELR-KDKFNPVNQPKESSRSTGSSSG
polkappa_mouse 764 CPVCNLEQETSDLTLFNIHVDICLNKGIIQELR-NSECNSVKQPKESSRSTDR---
polkappa_chicken 772 CPVCNLEQKTTSLMSFNRHVDVCLNKGLIQELTEKDDCSAKTSDTENSIRVGGLSR
polkappa_xenopus 769 CPVCNLRQNTPDLTAFNRHVDVCLNKGIIQKLT--EETVVIKHPVPSSQHTGSIGR
polkappa_Human 834 VQKAVT---RTKRPGLMTKYSTSKKIKPNNPKHTLDIFFK 870
polkappa_mouse 816 LQKAEG---RTKRPGTKTKSSTLKKTKPRDPRHTLDGFFK 852
polkappa_chicken 828 GQKCTKPLQGTKRSGLTTSQSASKKAKSIDSKRTIEMFFK 867
polkappa_xenopus 823 GSSSNNTKLRTKRPAATNQNPASKKSKPNSSKNTIDRFFK 862
Ubiquitin Binding Zinc Finger Motifs
Nuclear Localisation Signal
PCNA Binding Motif

Fig 3.2 - Generation of Mutants through SDM and Fusion PCR

A) Schematic of Site-Directed Mutagenesis. Complementary, mutagenic primers are used via PCR to introduce base pair changes to the plasmid.

B) Schematic of Fusion PCR to generate large base pair changes. Sets of primers are used to initially generate two fragments containing mutations and then to fuse the two fragments together before ligation back into the original vector

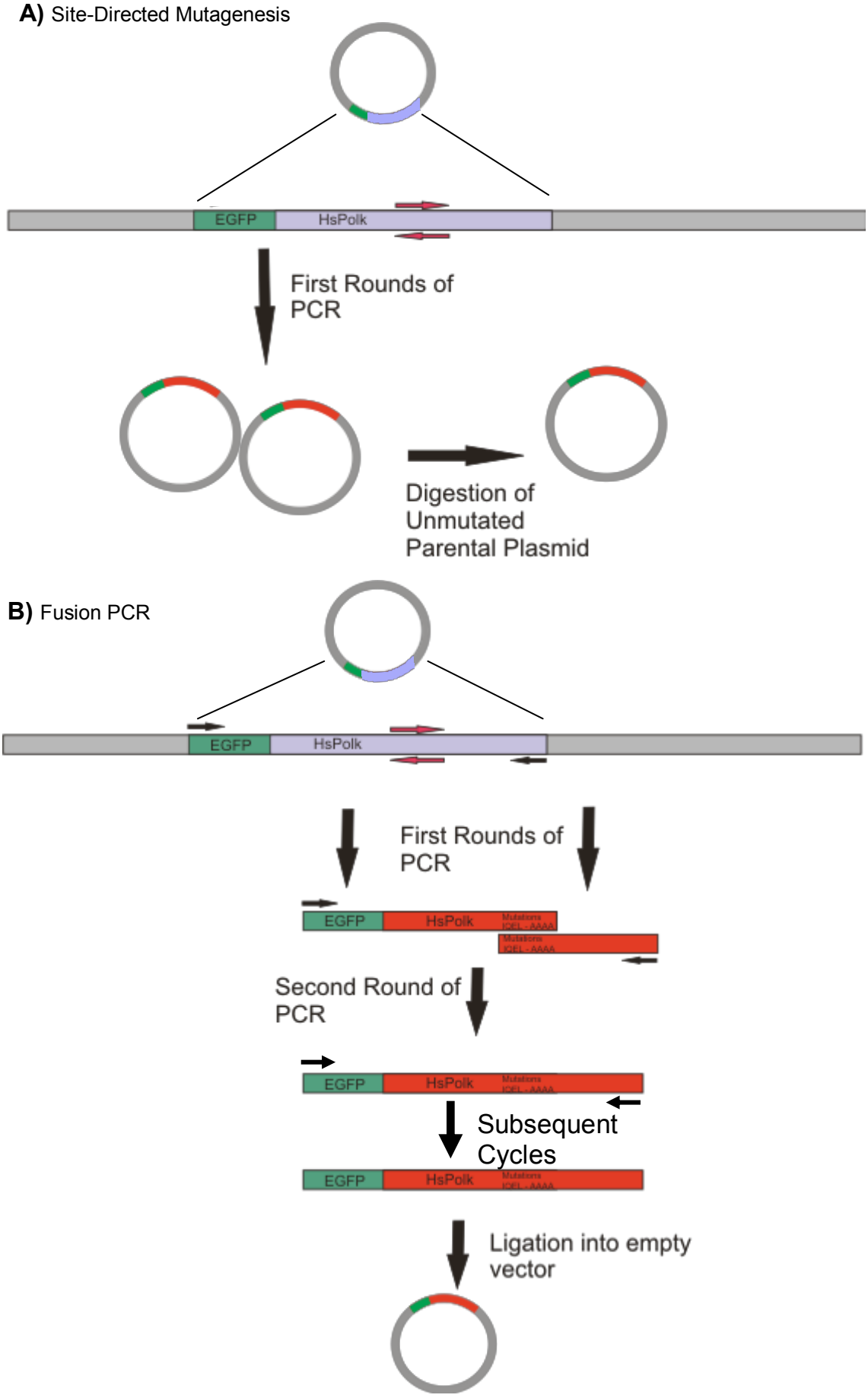
A) Site-Directed Mutagenesis
EGFP
HsPolk
First Rounds of PCR
Digestion of Unmutated Parental Plasmid
B) Fusion PCR
EGFP
HsPolk
First Rounds of PCR
EGFP
HsPolk
Second Round of PCR
EGFP
HsPolk
Subsequent Cycles
EGFP
HsPolk
Ligation into empty vector

using Fugene 6 transfection reagent. A day later, the cells were exposed to localised UV irradiation using a polycarbonate filter with 5μm pores as first pioneered by Volker *et al* (Volker et al., 2001). This restricts the incidences of damage to where there are pores in the filter, allowing discrete visualisation of areas of NER activity. Following irradiation, the coverslips are placed back into medium supplemented with 10mM hydroxyurea. This serves to deplete the nucleotide pool available to the cells by inhibiting ribonucleotide reductase and has been observed to increase the accumulation of GFP-polκ at sites of damage (Ogi et al., 2010).

Following fixation of the cells, they were stained with fluorescently labelled antibodies for RPA. RPA is a heterotrimeric protein composed of three subunits that is involved in the NER process and is involved in two phases of NER, pre- and post-incision (Overmeer et al., 2011). This protects the DNA from degradation by nucleases. By staining for RPA, a positive control for localised damage is provided to distinguish between actual non-accumulation of GFP-polκ and instances where there was no damage. The use of RPA as an internal control is repeated throughout the experiments described in this chapter.

3.3 Wild-type GFP-polκ is recruited to sites of local damage

Analysis of MRC5V1 cells transfected with wild-type GFP-polκ and then exposed to localised UV irradiation shows that the construct protein accumulates at these sites of damage and co-localises with RPA at the same site. Conversely, transfection with GFP alone leads to no change in pan-nuclear distribution of the protein and no co-localisation with RPA. The expression of free GFP and its inability to localise to sites of UV-induced damage rules out any unintended role the GFP might play in the accumulation of the construct proteins. (Figure 3.3)

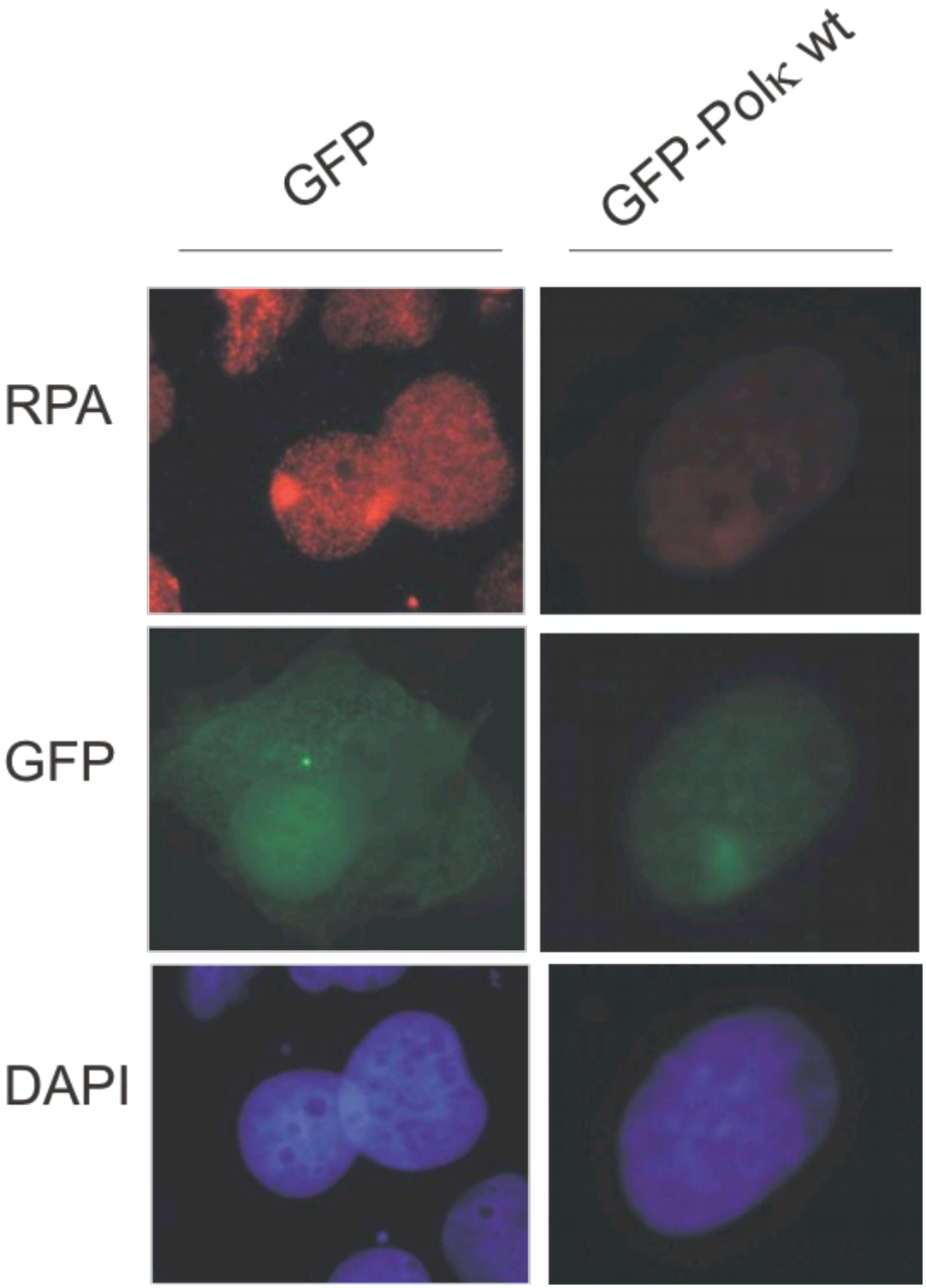

Figure 3.3 - Wt GFP-polκ accumulates at sites of local UV damage

MRC5 cells were transiently transfected with plasmid expressing either GFP or wild-type GFP-polκ and subsequently exposed to UV irradiation though a 5μm pore filter. After fixation, cells were stained for accumulation of RPA with an anti-RPA mouse antibody and for DNA by incubating with DAPI.

3.4 GFP-polκ with mutations outside the UBZ domains is recruited to sites of local damage

Having shown that the wild-type protein accumulates at sites of local damage, I was then able to investigate the accumulation of the GFP-polκ constructs with mutations in their C-termini. Proteins with mutations created in the C-terminus in the areas of conservation outside the UBZ domains were assayed for their ability to accumulate following localised UV damage. Intriguingly, despite their high levels of conservation, these mutations had no effect on the ability to recruit GFP-polκ to sites of NER repair. Even mutations affecting several amino acid residues, all highly conserved, such as the GFP-polκ $IQEL_{807\text{-}810}AAAA$ construct, had no effect on the ability of polκ to be recruited to damage (Figure 3.4).

3.5 GFP-polκ UBZ mutants are not recruited to sites of local damage

Conversely, when the mutations were created inside the UBZ domains, this did adversely affect the ability of GFP-polκ to accumulate at sites of localised UV damage. The single mutations D644A and D799A in conserved aspartic acid residues in two different zinc finger motifs both prevented accumulation following UV. As expected, when both mutations are present in the same construct of GFP-polκ no recruitment of the polymerase is observed. Having either single mutation appears to be as disruptive to the accumulation of GFP-polκ as possessing both mutations. In a similar vein, the double mutant C778C782A, which disrupts the second UBZ domain with two internal mutations, also showed similar levels of impairment (Figure 3.5). From this, it appears that the accumulation of GFP-polκ following UV is reliant on intact and functional UBZ domains in the C-terminus of the polymerase.

Figure 3.4: GFP-polκ Non-UBZ mutants accumulate at local UV damage

MRC5 cells were transiently transfected with plasmid expressing either GFP-polκ wt or the indicated GFP-polκ constructs with mutations in the C-terminus of the protein and subsequently exposed to UV irradiation though a 5μm pore filter. After fixation, cells were stained for accumulation of RPA with an anti- RPA mouse antibody and for DNA by incubating with DAPI.

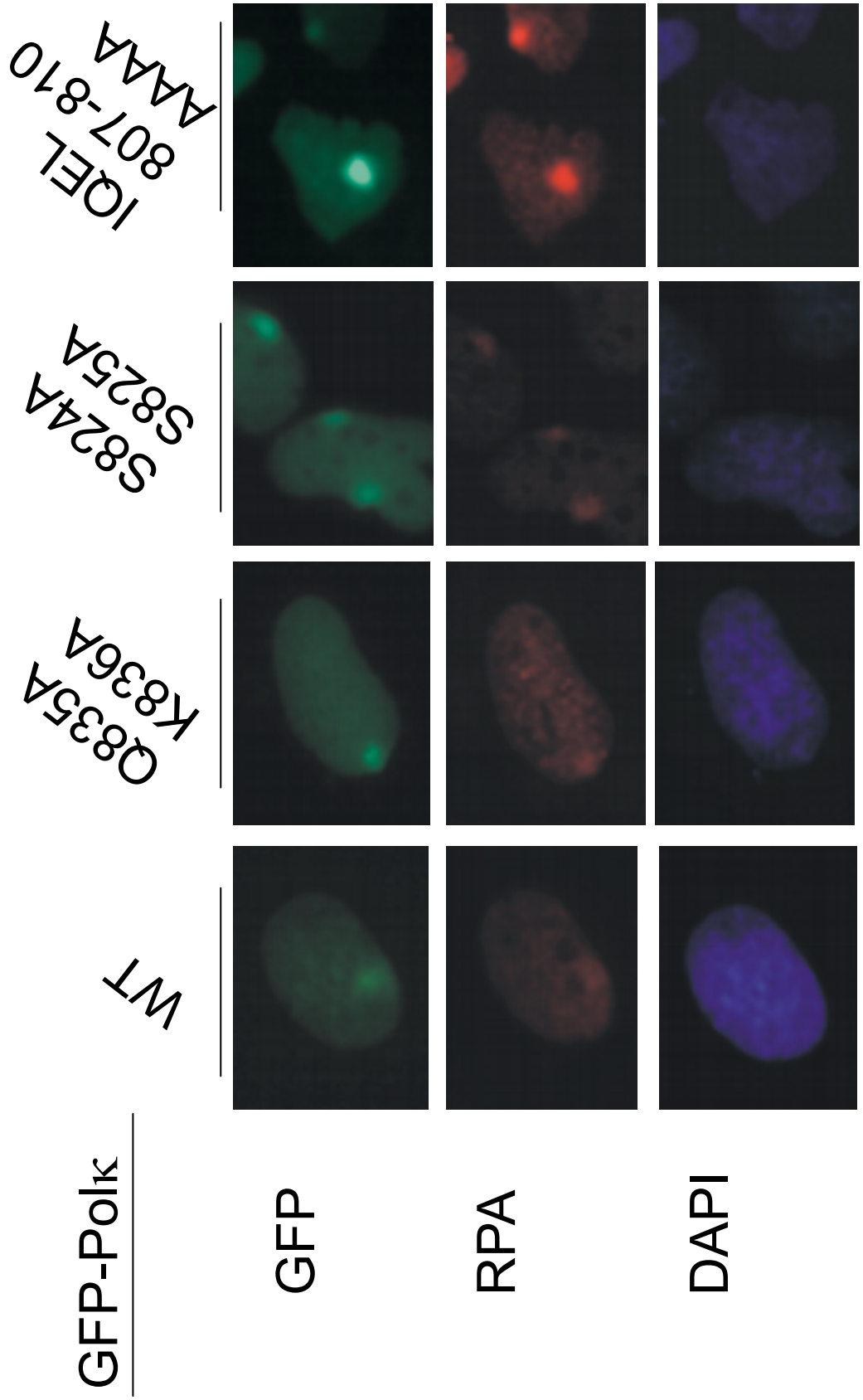
GFP-Polκ
WT
Q835A K836A
S824A S825A
IQEL 807-810 AAAA
GFP
RPA
DAPI

Figure 3.5: GFP-polk UBZ mutants do not accumulate at local UV damage

MRC5 cells were transiently transfected with plasmid expressing either GFP-Polk wt or the indicated GFP-polk constructs with mutations in the C-terminus of the protein and subsequently exposed to UV irradiation though a 5μm pore filter. After fixation, cells were stained for accumulation of RPA with an anti- RPA mouse antibody and for DNA by incubating with DAPI.

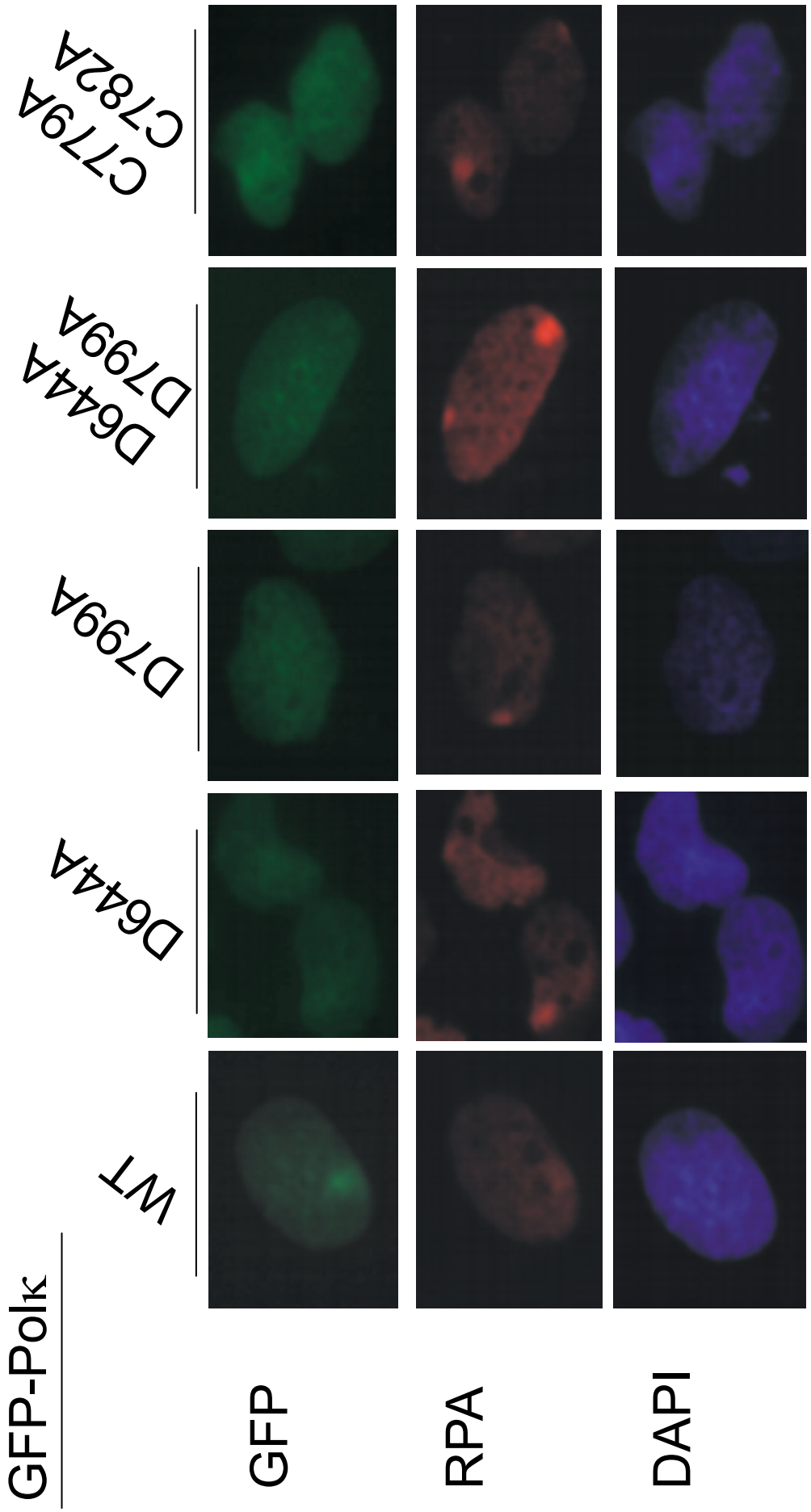
GFP-Polκ
WT
D64A
D799A
D64A D799A
C779A C782A
GFP
RPA
DAPI

3.6 UBZ mutants show greatly reduced accumulation after local damage

The previous results gave a qualitative observation of how mutations to conserved residues affected the localisation of GFP-polκ to sites of UV induced damage. A quantification of the percentage of cells showing an overlap of GFP-polκ accumulation with RPA accumulation re-enforced the previous observations (Figure 3.6). Each bar represents the average of three independent experiments. Due to low rates of transfection an average of 30-60 cells were scored in each experiment. This quantification of co-localisation shows the consistency of wild-type and non-UBZ accumulation and the inability of the UBZ mutant constructs to accumulate. Residual levels of co-localisation seen in the UBZ mutants could be reasonably explained by their remaining functional motifs that are able to interact with factors known to be at the NER site, such as an intact PIP box interacting with PCNA (Figure 3.6). It was observed informally that when accumulation was seen in these transfections, the intensity of the GFP-polκ was less than the intensity observed with the accumulation of wild-type polymerase.

3.7 Differences in accumulation are not due to differences in level of expression after transfection

It was important to rule out the possibility that differences seen in the accumulation of GFP-polκ constructs may have been due to differences in the level of expression of individual constructs following transfection into the MRC5V1 cell line. All the constructs used in the transient transfections are under the CMV promoter, a strong promoter commonly used for over-expression of plasmid genes. Therefore, any differences in expression between individual constructs were unlikely. However, the possibility remained that the mutant protein was less stable, leading to lower levels of protein. To rule this out, MRC5V1 cells were transiently transfected with wild-type GFP-polκ or the mutant versions and then one day later, levels of protein were quantified using the FACS CANTO flow cytometer system. The FACS CANTO functions in a manner similar to the

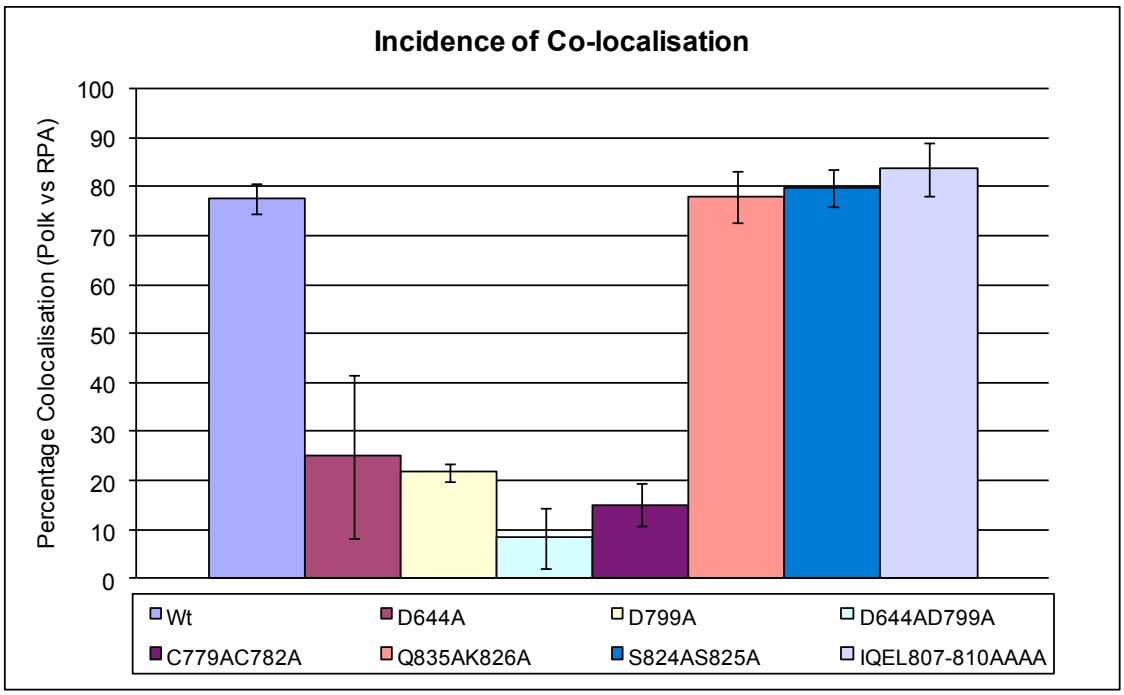

Fig 3.6: Quantification of accumulation at local UV damage

Cells that had been transfected with variants of GFP-polκ were locally damaged with UV and co-stained for RPA. For each construct, cells were counted to determine the presence of localised RPA signal and localised GFP-polκ signal. Only cells that demonstrated expression of GFP were counted as positive cells for the purposes of quantification, irrespective of RPA accumulation. Data points are the average of three independent experiments per construct. N=30 cells per experiment counted The error bars represent the standard deviation of three independent experiments.

FACS ARIA as described in section 2.12 with the exception that the analysed cells are discarded. This gave relative levels of protein expression based on GFP fluorescence. As can be seen from the FACS profiles, there is only a two-fold difference in levels of expression between the lowest expressing construct and the highest expressing. Furthermore, the construct showing the highest levels of over-expression is the GFP-polκ C779C782AA mutant, one that was consistently observed to not accumulate at sites of local damage. Thus over-expression of the mutants does not seem to be linked to ability to accumulate following damage (Figure 3.7).

3.8 Polκ needs to interact with an ubiquinated substrate to be recruited

The reduction in accumulation of the UBZ mutant constructs of GFP-polκ after localised UV damage implies that this accumulation was due to the interaction of GFP-polκ with an ubiquitinated partner protein. To test a dependence on the presence of an ubiquitinated protein being responsible for the accumulation of GFP-polκ, the pool of free ubiquitin was depleted before local UV irradiation and the accumulation of GFP-polκ was quantified. The free ubiquitin pool was depleted by treating the cells with the proteasome inhibitor MG132, which inhibits the 26S proteasome by behaving as a substrate analogue and inhibiting the transition-state of the chymotrypsin-like activities of the proteasome (Lee and Goldberg, 1998). By preventing protein degradation, ubiquitin that had been used to 'tag' proteins for destruction is not recycled back into the pool of available ubiquitin. Thus an effective block on protein degradation prevents subsequent post-translational modifications involving ubiquitin in non-degradation processes.

As can be seen, MG132 treatment reduces the ubiquitination of known targets such as PCNA following UV irradiation (Fig 3.8A, compare lanes 1, 2 with 4, 5). It also substantially reduces the accumulation of GFP-polκ and quantification of co-localisation with RPA accumulation shows a consistent reduction of about 40% compared to a control treated with DMSO (Figure 3.8B, bottom panel). The residual accumulation can be reasonably accounted for by the presence of ubiquitinated targets that were post-translationally

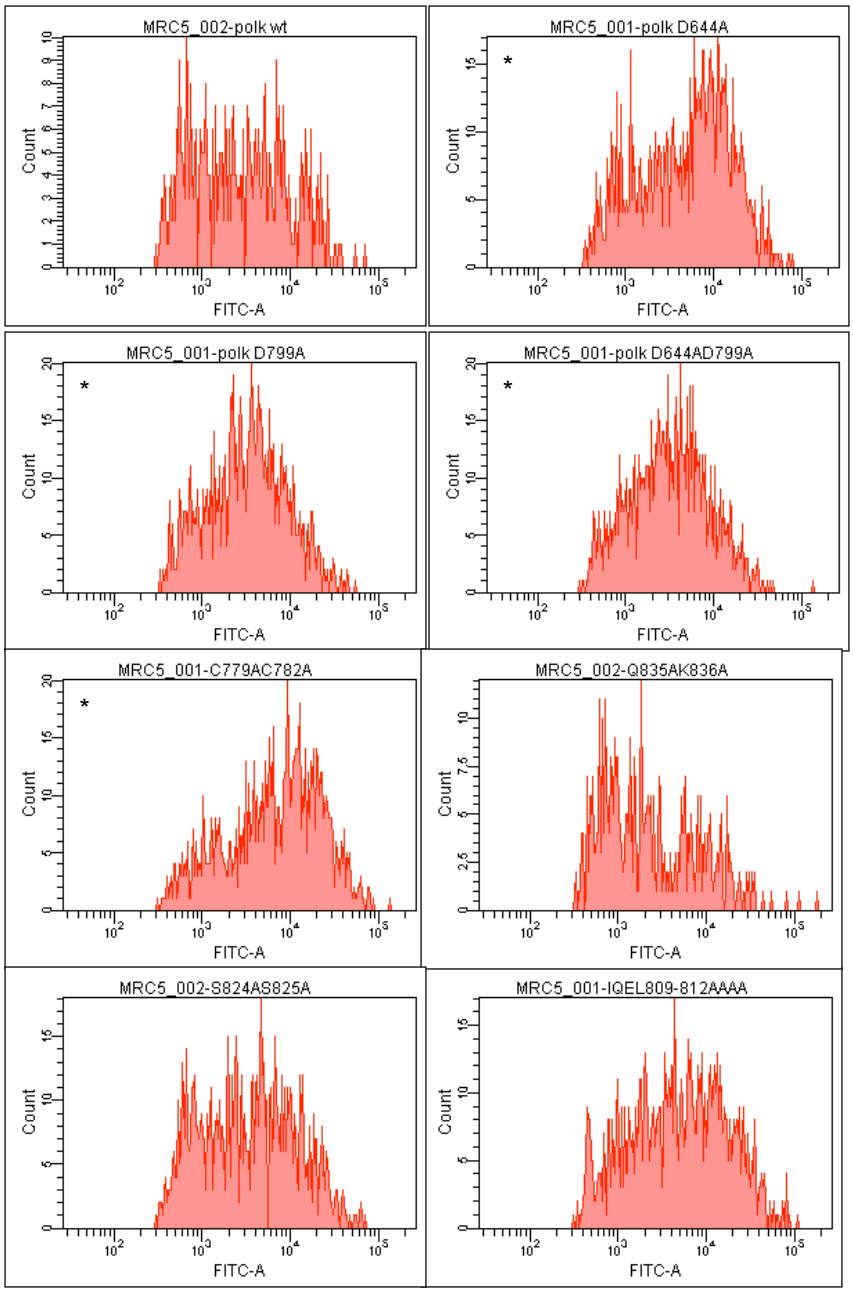

Figure 3.7: FACS Analysis of GFP-polκ Expression: All constructs of GFP-polκ express at similar levels independent of accumulation at local UV damage

MRC5V1 cells were transfected with plasmid for expression of GFP-Polk wild type or the indicated mutations. 24 hours later they were analysed on a FACS Canto for expression of GFP and plotted as events against expression. Non-transfection related fluorescence was removed by analysing a non-transfected sample of MRC5V1 and gating for its exclusion (data not shown). Mutations inside the UBZ domains are marked out with a star.

modified prior to the treatment with MG132. This can be seen in a residual ubiquitinated-PCNA band on the western blot that is still present following treatment. However, this band does not increase in intensity following UV irradiation comparative to the control conditions (Figure 3.8).

3.9 Role of PCNA in recruiting Polκ to sites of NER activity

The interaction between the sliding clamp protein PCNA and the translesion synthesis polymerases in their conventional roles bypassing unrepaired damage during S-phase is fairly well established. The TLS polymerases contain PIP boxes and ubiquitin binding domains that interact with the ubiquitinated form of PCNA. PCNA is ubiquitinated following many genotoxic insults and in keeping with this, UV exposure prompts a rapid and prolonged accumulation of ubiquitinated PCNA (Niimi et al., 2008).

The experiments above suggest that an ubiquitinated partner protein is required for accumulation of polκ at local damage. Polκ has been shown to interact physically with both PCNA (Haracska et al., 2002) and with ubiquitin in separate experiments (Guo et al., 2008). To determine whether ubiquitinated PCNA itself was the partner required by Polκ, I attempted to assess the accumulation of local damage under conditions in which PCNA cannot be ubiquitinated. PCNA is ubiquitinated exclusively on K164. Mutations to this highly conserved lysine residue effectively abolish PCNA's ability to be ubiquitinated following DNA damaging events. MRC5-Sv cells stably expressing 6xhis-tagged PCNA^{K164R}, refractory to siRNA silencing, alongside endogenous PCNA had been constructed by Atsuko Niimi. The cell line was plated into separate wells of a 24 well plate and the endogenous PCNA was knocked down using 100nM of siRNA against PCNA using the transfection reagent Metafectene Pro. After 48 hrs, the cells were trypsinised and replated onto coverslips in a 6 well dish. The cells were dual transfected with GFP-polκ and siRNA against endogenous PCNA. The next day, the coverslips were locally UV irradiated as previously described and western blot samples were prepared from wells that had been treated in parallel. As can be seen in Figure 3.9, despite a moderately

Fig 3.8: Inhibition of GFP-polκ Accumulation at Local Damage by MG132 Treatment:

A) MRC5 cells were pre-treated for the indicated times with either MG132 or DMSO prior to being UV irradiated with 40 J/m^2. Cells were scraped into Laemmli buffer and the Western Blot was probed with anti-PCNA. Treatment with MG132 prevents ubiquitination after 2hrs incubation prior toUV irradiation. Longer periods of incubation saw no further inhibition of ubiquitination.

B) MRC5 cells were transiently transfected on a coverslip with GFP-polκ using Fugene 6. Coverslips were treated with MG132 or DMSO before being locally irradiated through a 5µm filter with 40J/m2 of UV light. Coverslips were incubated in 10mM HU for 45 min before fixation and staining with anti-RPA antibody as an indicator of NER damage.

C) Quantification of GFP-polκ Accumulation at Local Damage (ALD) co-localising with RPA ALD shows a 40% reduction after MG132 treatment. Cells positive for GFP expression were counted to determine polκ accumulation and the RPA accumulation. Data are expressed as the percentage of localised polκ against localised RPA. Each data point is the average of three independent experiments, n=30 cells counted per experiment. The error bars represent the standard deviation of the three independent experiments.

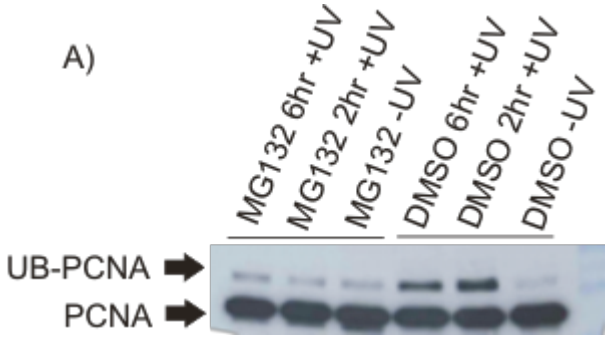
A)
MG132 6hr +UV
MG132 2hr +UV
MG132 -UV
DMSO 6hr +UV
DMSO 2hr +UV
DMSO -UV
UB-PCNA
PCNA

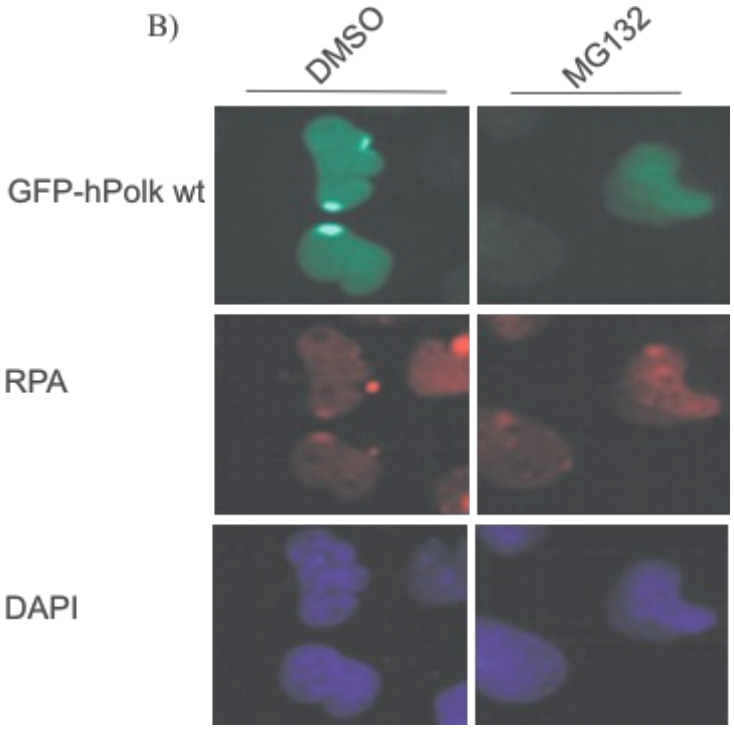
B)
DMSO
MG132
GFP-hPolk wt
RPA
DAPI

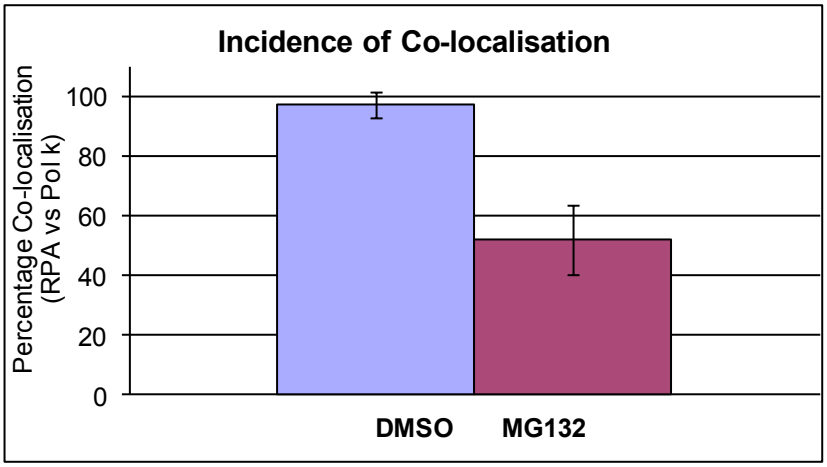
Incidence of Co-localisation
Percentage Co-localisation (RPA vs Pol k)
100
80
60
40
20
0
DMSO
MG132

successful knockdown of endogenous PCNA (Figure 3.9 B), GFP-polκ was still seen to accumulate at sites of local damage in the $PCNA^{K164R}$ cells (Figure 3.9 A). When these results are quantified by counting cells positive for GFP-polκ expression and comparing the co-localisation of accumulation of GFP-polκ with the accumulation of the RPA control, no difference was observed in the incidence of co-localisation (Figure 3.9 C).

3.10 Discussion

The involvement of human DNA polκ in the nucleotide excision repair process was unexpected. Even though sensitivity toward UV irradiation had been noted before in polκ deficient cell lines, it was assumed that this role was contingent on the polymerase functioning in a translesion synthesis pathway, similar to its role in helping the cell to tolerate unrepaired hydrocarbon lesions (Ogi et al., 2002). The involvement of the polymerase in NER was dependent on the polymerase activity in the highly conserved N-terminus. However, the C-terminus has not been subjected to the same strict evolutionary conservation and has diverged in sequence amongst the higher eukaryotes. An alignment of polκ C-termini from model organisms among the higher eukarya showed islands of conservation of which four corresponded to previously identified motifs, the two ubiquitin binding domains, the PCNA interaction motif and the nucleus localisation signal. Three other conserved sets of residues had not been identified in any role. To explore the role of these conserved residues, they were mutated to the codons for alanines. Following the creation of these mutant polymerases, the initial investigation was to see if any localisation was affected following exposure to damaging UV radiation.

Mutations to different areas of conservation affected the localisation of the polymerase in two differing ways. Mutations constructed outside the UBZ domains appear to have no affect on accumulation to sites of NER. Conversely, mutations inside the UBZ domains negatively affect the localisation of the polymerase following damage and the extent of accumulation is greatly reduced in these mutants (compare Fig 3.4 with Fig 3.5). The polymerase appears to require two intact UBZ domains to properly localise to damage, as

Fig 3.9: : siRNA Knockdown of PCNA and Effect on GFP-polκ Accumulation - siRNA knockdown of PCNA has a negligible affect on wt GFP-polκ accumulation at local UV damage

A) MRC5V1 K164R cells were seeded on a coverslip and treated with 100nM of either a NTC siRNA or siRNA against endogenous PCNA. 48 hours later the cells were transfected with a plasmid carrying wt GFP-polκ and another round of siRNA treatment. 24 hours later the cells were damaged with local UV followed by fixation and staining for RPA.

B) Western blot samples were prepared from cells growing in the same well as the coverslips and therefore treated in parallel with the same conditions. Samples were run on a 10% gel and the resultant membrane was probed with antibody against PCNA (PC10).

C) Cells that were positive for expression of GFP were quantified for the co-localisation of wt GFP-Polκ and RPA to the areas of local damage. Due to the detrimental effects of the transfection protocol on the cells, the data is an aggregate of two experiments with a total cell count of n=70.

A)

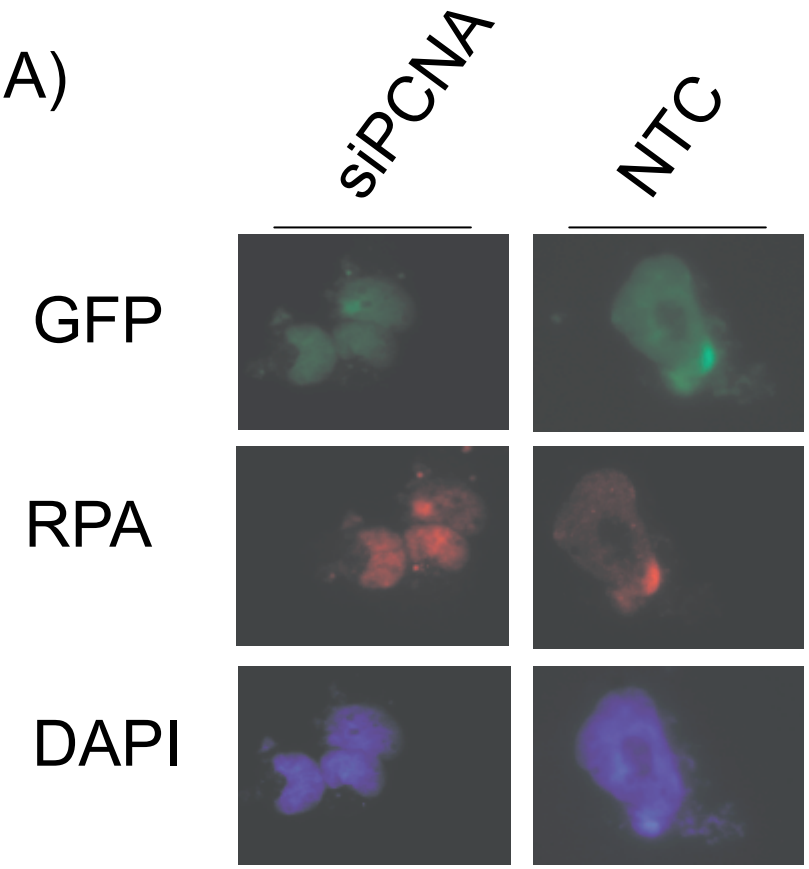
siPCNA
NTC
GFP
RPA
DAPI

B)

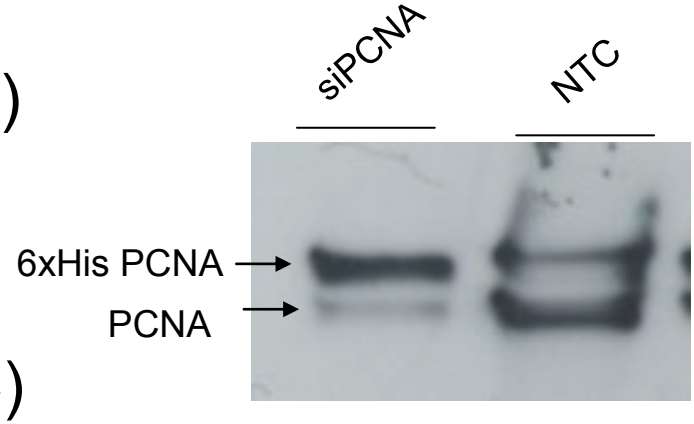
siPCNA
NTC
6xHis PCNA
PCNA

C)

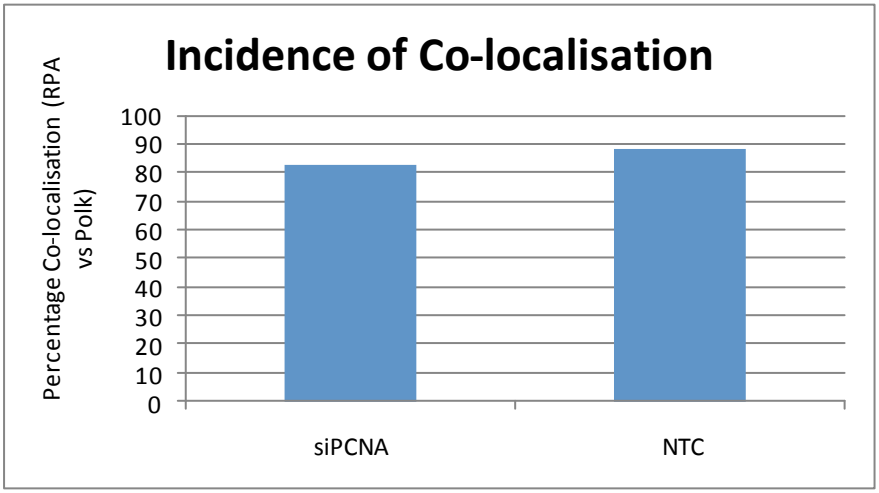
Incidence of Co-localisation
Percentage Co-localisation (RPA vs Polk)
100
90
80
70
60
50
40
30
20
10
0
siPCNA
NTC

the mutations D644A, D799A and C779AC782A were all confined to a single UBZ domain and all showed the same reduction as the mutation D644AD799A which contained a mutation in each domain. Based off the characterisation of the human polη UBZ domains, these mutations disrupt the zinc-finger in two different ways: the D644A, D799A and the combined mutation affect the aspartic acid residues that interact with amide groups in ubiquitin, while the C779AC782A mutation affects the cysteine residues that interact with the zinc ion (Bomar et al., 2007). All these localisation experiments took place under conditions of 10mM HU exposure and cells were fixed 45 min following initial exposure to UV. Though not systematically investigated, observations taken at earlier (30 min) or later (1hr) time points did not show a difference in localisation of polκ. The inclusion of HU was based on earlier work by Ogi *et al* where they observed that the inclusion of HU resulted in a more pronounced signal and supports the work of Overmeer *et al* who showed that treatment with HU stalls the repair synthesis components. The HU acts as an inhibitor of ribonucleotide reductase, which serves as the limiting step in the biosynthesis of deoxyribonucleotide triphosphates (dNTP) for the synthesis of DNA. The treatment with HU serves to deplete cellular dNTP levels, which might affect GFP-polκ localisation in one of either two ways: the lowered levels of dNTPs would inhibit DNA repair synthesis, causing stalling of the polymerase and enhancing the amount of time spent at the resynthesis step of NER, and/or under the conditions of low dNTP polκ might take preference over and above the replicative polymerases which are more intolerant of low dNTP concentrations for synthesis. As the experiment was concerned solely with the recruitment of polκ to sites of NER and not with its efficiency of function once there, the inclusion of HU should not affect the different mutant polymerases in a manner different from wild-type.

On preparation of these data for publication, a concern had been raised by a reviewer that the accumulation of GFP-polκ might have been a possible artefact caused by different levels of expression. If the UBZ mutants were expressed at significantly lower levels than the non-UBZ mutants, they might not be seen to accumulate following damage whereas

highly over-expressed mutants might be driven to accumulate to an artificial degree. The GFP-polymerase constructs were all made in the same plasmid background under the CMV promoter. CMV is a strong promoter leading to over-expression of proteins but presumably all constructs were over-expressed to the same degree. Furthermore, the cells were transfected with equivalent amounts of plasmid and several cells across several experiments showed no comparable differences irrespective of plasmid. However, to experimentally rule out this objection, the levels of expression of each polymerase following transient transfection into the MRC5V1 cell lines were measured by flow cytometry. The level of expression bore no correlation to the accumulation seen in the cell lines. The difference between the lowest expressed construct, Q835AK836A, and the highest expressed construct, C779AC782A, was only two-fold. Furthermore, the latter was repeatedly seen not to accumulate at sites of local damage. Thus I concluded that the level of expression had no effect on whether or not the GFP-polκ mutant was able to be recruited to sites of NER (Fig 3.7).

The experiments concerning the localisation of the mutants showed a requirement for the UBZ domains of polκ for efficient localisation to NER sites. These UBZ domains had been shown to interact with ubiquitin and be required in murine polκ for foci formation following UV. Was there a similar role of interacting with an ubiquitinated substrate to allow the participation of human polymerase in an NER context? To test this, the proteasome was chemically inhibited with MG132. Proteins in the cell are targeted for recycling by being covalently bonded to ubiquitin through lysine linkages and accumulate a dense, K48-branched ubiquitin modification to allow recognition by the proteasome complex. However, this modification occurs independently of cellular recycling, so if the cell is prevented from degrading old proteins, the ubiquitin moieties are not recycled back into a pool of free ubiquitin. It would be this pool of free ubiquitin that non-degradation specific post-translational modifications would also draw on. The treatment with MG132 is a fast, chemical method to achieve a reduction in free ubiquitin that would be difficult to achieve by other techniques such as siRNA knockdown. When cells are treated with

MG132 before exposure to UV irradiation, the levels of accumulation of wild-type GFP-polκ at sites of NER was drastically reduced compared to the control cells treated with DMSO. This reduction is not as severe as seen in the polymerases with the UBZ mutations. It is possible that there is still some level of free ubiquitin left in the cell following treatment which can be used to post-translationally modify target proteins, even though no increase in the level of ubiquitinated PCNA was seen following UV in the MG132 treated cells while a strong increase was seen in the control cells. Alternatively, as can be noted in the western blot, there was a level of ubiquitinated species of PCNA present before treatment. The existence of a residual level of ubiquitinated proteins might be sufficient to recruit some polκ to sites of NER in a limited manner (Fig 3.8).

The shortcoming of MG132 treatment is that all post-translational modifications involving ubiquitin would be inhibited, thus offering no specificity to detail which specific protein the polymerase would be interacting with. Given that polκ interacts with ubiquitinated PCNA during TLS, and PCNA is present during the NER resynthesis step, it was an attractive target for a role in recruitment of the polymerase to the damage sites. Furthermore, Ogi *et al* has shown that Rad18, the E3 ligase that ubiquitinates PCNA, is required for the accumulation of polκ at sites of local UV damage (Ogi et al., 2010). To explore this, a cell line constructed by Atsuko Niimi was employed. This cell line was derived from the MRC5V1 cell line but stably expresses a histidine tagged mutant of PCNA that differs from wild-type in two important aspects: firstly, the primary sequence contains several nucleotide changes that render the mRNA transcript refractory to knockdown by siRNA treatment; secondly, the PCNA has a mutation which changes the lysine 164 to an arginine. This lysine is the site of ubiquitination by the Rad18/Rad6 complex in TLS and the K164R mutation renders cells sensitive to DNA damaging agents and inhibits interaction with the TLS polymerases. To test any reliance of ubiquitinated PCNA on the recruitment of GFP-polκ, this cell line was treated with either siRNA that targeted the still expressed endogenous PCNA or a non-targeting control oligo. Following knockdown, a plasmid carrying e*gfp-polκ wt* was transfected in and cells were exposed to DNA damage.

There was a degree of technical difficulty that impaired some aspects of this experiment. Treatment with siRNA was at a high concentration of 100nM to achieve the knockdowns observed, restricting the ability to use more siRNA to attempt a more thorough knockdown of endogenous PCNA. Moreover, the treatment conditions involving two separate transfection reagents were found to be toxic to the cells and were only partly solved by using a single reagent, Metafectene Pro. Due to limited cell survival, the experiment was performed multiple times and the results aggregated to obtain quantification of accumulation at local damage. When this was performed, despite seeing a reduction in the levels of endogenous PCNA, no changes were seen in the accumulation of GFP-polκ to sites of damage (Fig 3.9). While this may be seen as a refutation of a role for ubiquitinated PCNA in recruiting polκ to sites of NER activity, the data must be carefully interpreted. Firstly, the structure of PCNA should be recalled; as a homotrimer PCNA is normally composed of three identical subunits. However, in this instance, the cells were expressing two versions of PCNA with presumably no preference for which monomer gets incorporated into the trimer. Secondly, although the knock down of PCNA was highly successful, it was not a 100% complete depletion of the endogenous PCNA. While no siRNA treatment will ever completely remove the target protein, in this experiment the outcome may be highly susceptible to a residual level of endogenous protein. The population of PCNA in the treated cells may be composed of a significant portion containing a mix of monomers, some K164R and unable to be ubiquitinated and others wild-type. If the recruitment of polκ is dependent on only a single monomer being ubiquitinated, then a signification portion of PCNA available in the cell would still be functionally modified for recruitment. Finally, a single spot of immunofluoresence signifying an area of local damage can represent several distinct instances of NER at several different points along the repair pathway. Thus is it not surprising that, in such a scenario, no observable differences were seen in the $PCNA^{K164R}$ expressing cell-line? In the absence of a $PCNA^{K164R}$ knock-in cell line only expressing monomers unable to be ubiquitinated, it is difficult to rule out a role for ubiquitinated PCNA in recruiting polκ to sites of NER, especially in the light of what is known about the interaction of polκ with

ubiquitinated PCNA during TLS, the role of Rad18 in the accumulation of polκ at local UV damage and the observed impairment of accumulation following mutations of the UBZ domains.

Chapter 4– Phenotypes of GFP-polκ Stable Expression Cell lines in NER assays

The initial starting observation that led to the elucidation of the involvement of human polκ in the nucleotide excision repair process was the sensitivity of mouse embryonic fibroblasts unable to express endogenous polymerase to the lethal effects of ultraviolet radiation. This was further supported by observable differences in the ability of the cells to incorporate radioactively labelled nucleotides either as a measure of repair synthesis or recovery of RNA synthesis following the upstream NER activities of lesion detection and removal (Ogi and Lehmann, 2006)

As has been detailed in the previous chapter, mutations to conserved residues in the C-terminus of human polκ can differently affect the recruitment of the GFP-tagged protein to sites of NER following ultraviolet irradiation. Any mutations made outside the known motifs were still able to accumulate at sites of damage in the same manner as the wild-type protein. However, mutations inside the ubiquitin binding zinc fingers (UBZ) domains abrogated the ability to accumulate at local damage. To explore whether these mutations had a phenotypic effect in keeping with their observed effect on protein accumulation, it was decided to create a set of cell lines that could stably express GFP-polκ, either as the wild-type version of the protein or as the C-terminal mutant variants. These could be used to determine more fully the implications of mutations to conserved residues in polκ.

4.1 Creation of Cell lines Expressing Polκ from a Polκ$^{-/-}$ Background

Mouse embryonic fibroblasts (MEF) cells in which the exons of endogenous polκ that contain the conserved catalytic residues had been deleted in the M6 cell line (Ogi et al., 2002), were used to derive MEF cell lines stably expressing an individual GFP-polκ construct: either the wild-type, one of the UBZ mutants or one of the non-UBZ mutants. Given that mutation to either aspartic acid residue in the zinc fingers prevented

accumulation at localised UV damage equally, a cell line stably expressing the double mutation GFP-polκ D644D779AA was chosen for phenotypic analysis.

M6 cells were transfected with the pMSCV plasmid carrying *GFP-polκ,* either wild-type or with the necessary mutations introduced through SDM as described previously, and the puromycin-resistance gene as a selectable marker. It was necessary to move the e*gfp-polκ* into this new vector as the eGFP-C3 vector carried resistance against G418, to which the M6 cell lines were already resistant due to the method of their construction (Ogi et al., 2002). After the majority of the cells had died off, the survivors were replated and allowed to grow into colonies that were then picked and expanded again (Figure 4.1).

Clones of each stable cell line were screened for GFP-polκ expression initially by immunoblotting and probing samples from each clone with an antibody raised against GFP. This allowed the clones that had successfully incorporated and expressed GFP-polκ to be distinguished from clones that had only acquired the puromycin resistance (Fig 4.2). Following this, clones that displayed acceptable levels of expression were chosen to be expanded while the remainder of the positive clones were frozen down. The chosen clones were sorted and analysed on the BD-Flow Assisted Cell Sorter (FACS ARIA) machine. Figure 4.3A shows data from a clone of the stable cell line expressing wild-type GFP-polκ as a representative example. The M6 line was run on the machine initially to set up areas of gating where expression of the integrated plasmid could be distinguished from background autofluorescence (Fig 4.3-A) The FACS machine was also used to enrich the cell population for cells expressing GFP-tagged protein as determined by fluorescence (Fig 4.3-B). From this, all the selected cell lines could be sorted using the BD-FACS Aria and selectively enriched for GFP-polκ expression to screen out cells that had silenced expression and maintain the stability of the clone (Fig 4.3-C)

This procedure led to the creation of a total of five cell lines expressing GFP-polκ with mutations in the conserved residues. Strongly expressing clones were selected and

Figure 4.1 Creation of stable cell lines in MEF Polκ$^{-/-}$ background

The cell line M6 was seeded into wells and 24 hours later was transfected with plasmid for expression of wild-type GFP-Polκ or a mutant variant. For each set of transfections, a well remained untransfected with plasmid DNA as a control for sensitivity to selection. Following ten days selection with puromycin, surviving cells were trypsinised, replated and allowed to grow into colonies under selection pressure. Colonies were expanded into clonal cell lines which were then analysed for the successful integration of the plasmid by the expression of GFP-Polκ on western blot and GFP expression on the FACS Aria machine.

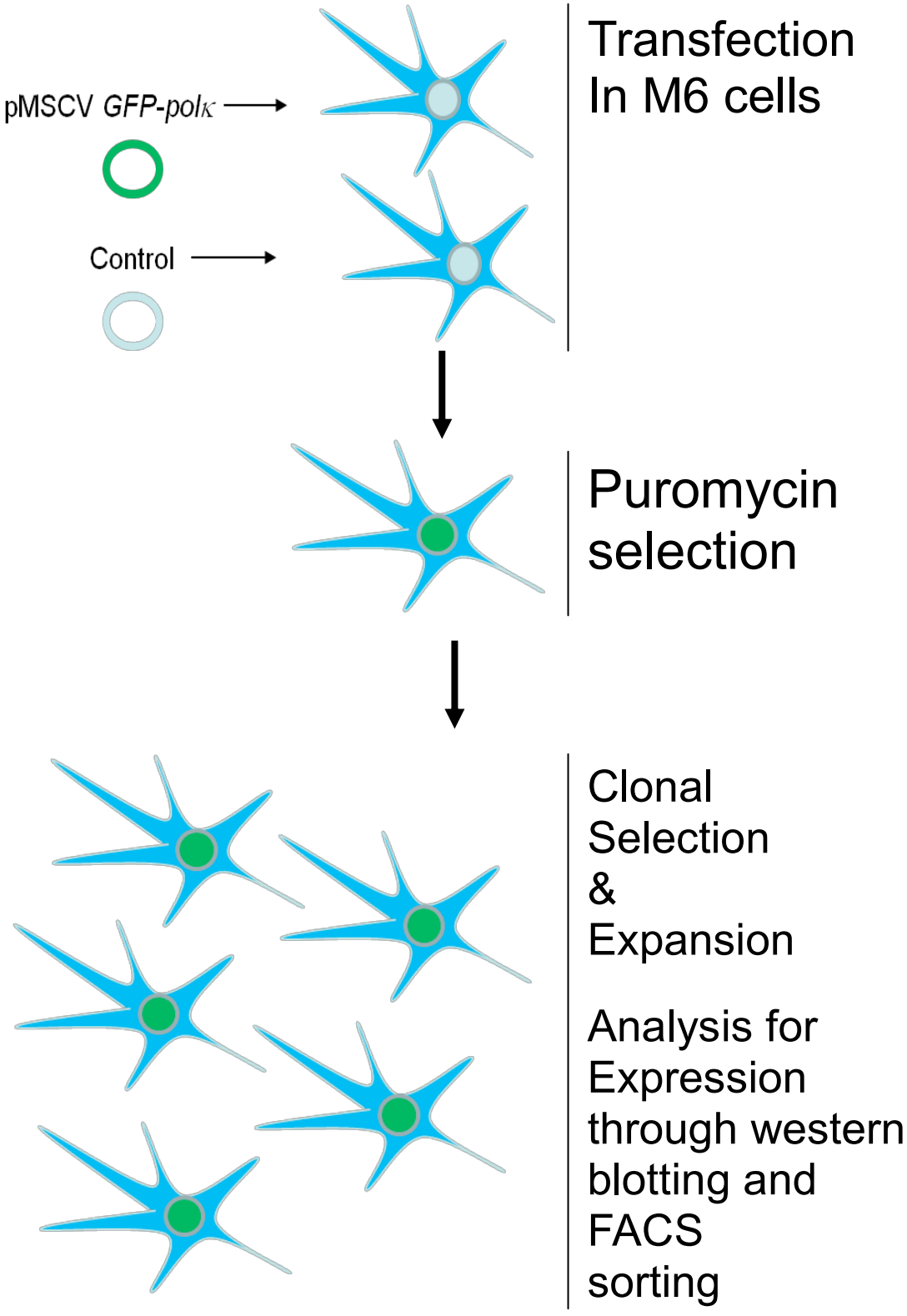
pMSCV GFP-polκ
Control
Transfection
In M6 cells
Puromycin
selection
Clonal
Selection
&
Expansion
Analysis for
Expression
through western
blotting and
FACS
sorting

Figure 4.2: Polκ Expression in the stable cell lines

Samples were taken from the clonal cell lines derived by selection M6 parental cells for puromycin resistance following transfection with plasmid carrying wild-type GFP-polκ or indicated mutants. These samples were run on 8% gels and the membranes probed with antibody raised against GFP to detect the presence of GFP-polκ. Alongside were run either an equivalent sample taken from the M6 line to demonstrate lack of GFP-polκ expression or a sample taken from a cell line overexpressing GFP-tagged polη (Cnt - kind gift from Dr. Sabbionedda. GFP-polη is roughly 100 kDa, compared to GFP-polκ at 130 kDa). Following analysis based on the western blot, positive clones were frozen down. Clones marked out by an asterisk were used in the majority of the proceeding experiments. Clones marked as such (Ŧ) were used as alternative clones in a subset of experiments. The position of GFP-polκ is marked out on the IQEL807-810 blot due to the weakness of expression seen.

GFP-Polκ Construct

WT

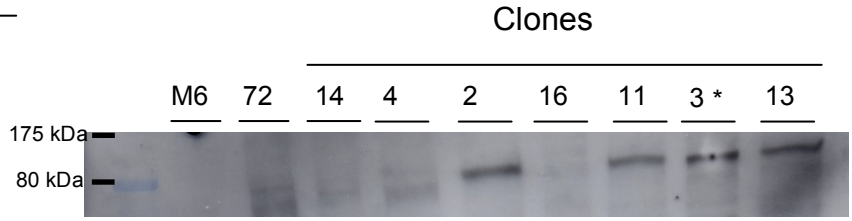

D644A
D799A

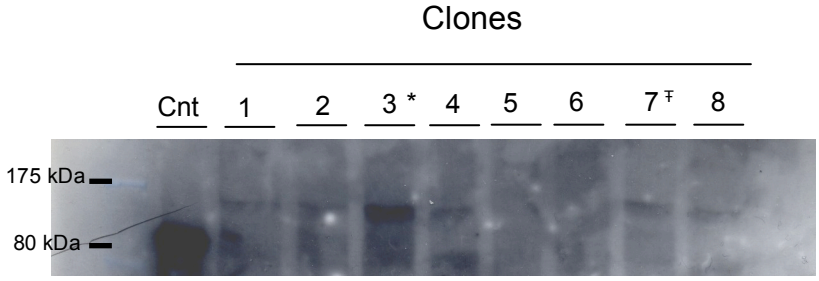

C779A
C782A

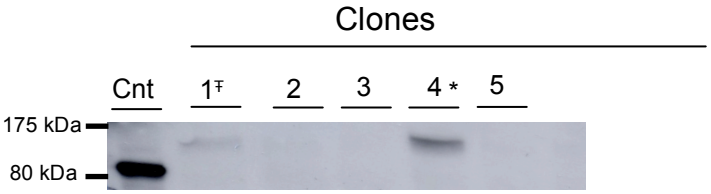

Q835A
K836A

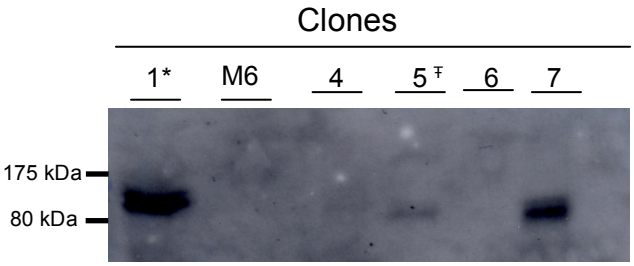

IQEL807-

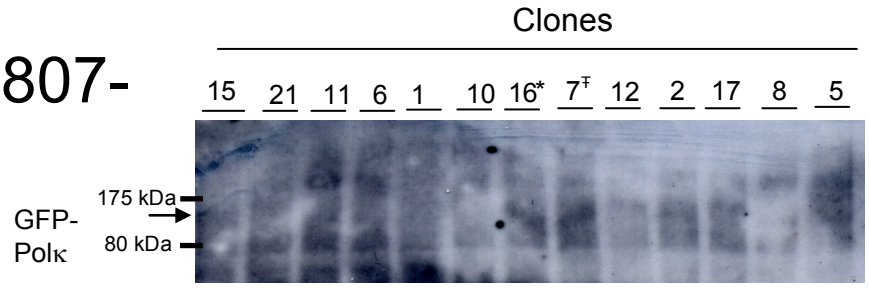

Figure 4.3: Enrichment of the stable cell lines for GFP-polκ expression

A) Clones stably expressing wild-type GFP-polκ or indicated variants were analysed on the BD FACS Aria and selectively enriched for the sub-population with GFP expression. The cell line WT3 (M6 complemented with human wild-type GFP-polκ) is shown compared to the M6 (MEF polκ$^{-/-}$) and M1 (MEF polκ$^{+/+}$) lines as an example.

B) The statistical analysis of the subpopulations expressing GFP highlight the enrichment above background levels of fluorescence.

C) A comparative view of the fluorescence of the main clones of each stable cell line used in proceeding experiments with the control lines M1 and M6 included as indicators of background levels. To demonstrate the enrichment of GFP-positive events only, percentage of events in the P2 Gate only is listed alongside.

Mutations inside the UBZ domains are marked out with a star.

A)

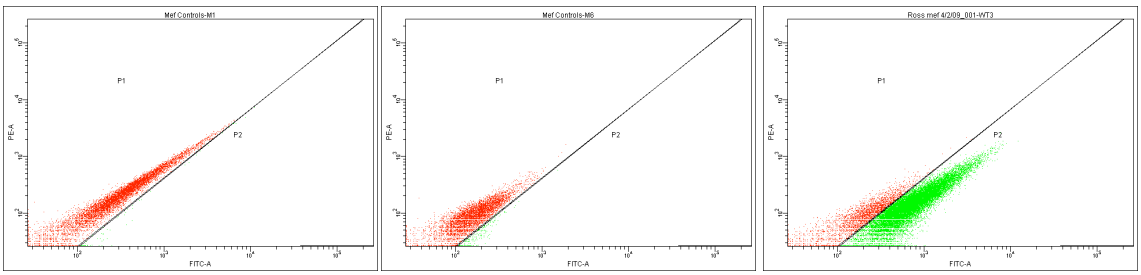

B)

Tube: M1

Population	#Events	%Parent	%Total
All Events	10,000		100.0
P1	9,919	99.2	99.2
P2	58	0.6	0.6

Tube: M6

Population	#Events	%Parent	%Total
All Events	10,000		100.0
P1	9,747	97.5	97.5
P2	189	1.9	1.9

Tube: WT3

Population	#Events	%Parent	%Total
All Events	30,000		100.0
P1	7,470	24.9	24.9
P2	22,263	74.2	74.2

C)

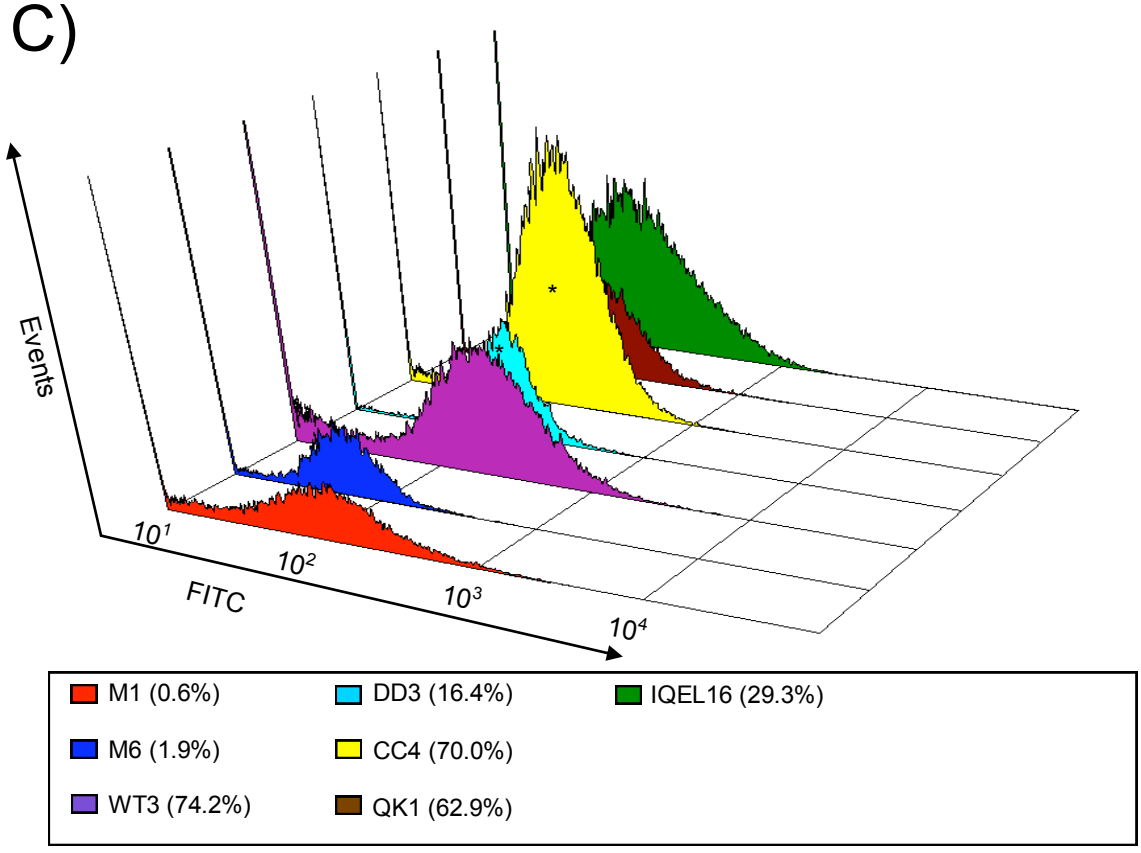

enriched to be used as the basis for future experiments: GFP-polκ wild-type clone 3 (WT3), GFP-polκ D644AD779A clone 3 (DD3), GFP-polκ C799AC782A clone 4 (CC4), GFP-polκ Q835AK836A clone 1 (QK1) and GFP-polκ IQEL809-812AAAA clone 16 (IQEL16). It should be noted that despite repeated attempts to create a M6 derived cell line expressing GFP-polκ S824AS825A, none was successful. Expression was difficult to achieve and was not stable; putative successful clones rapidly lost expression. Attempts to maintain expression through the use of repeated use of the sorting capabilities of the FACS machine proved fruitless. The cell lines are summarised in the table below and in Appendix C.

Table 8: Summary of MEF Cell Lines

Designation	Cell Line	Polκ Status
M1	Mouse Embryonic Fibroblasts	*Polκ*$^{+/+}$
M6	Mouse Embryonic Fibroblasts	*Polκ*$^{-/-}$
WT3 / WT	Mouse Embryonic Fibroblasts (Derived from M6)	Stably expresses GFP-polκ wild-type
DD3 / DD7	Mouse Embryonic Fibroblasts (Derived from M6)	Stably expresses GFP-polκ D644AD799A
CC4 / CC1	Mouse Embryonic Fibroblasts (Derived from M6)	Stably expresses GFP-polκ C779AC782A
QK1 / QK5	Mouse Embryonic Fibroblasts (Derived from M6)	Stably expresses GFP-polκ Q835AK836A
IQEL16 / IQEL7	Mouse Embryonic Fibroblasts (Derived from M6)	Stably expresses GFP-polκ IQEL807-810AAAA

To avoid unintentional artifacts produced by over-expression of the stably integrated GFP-polκ, it was decided to establish gates during the FACS analysis and sorting that would limit GFP-polκ in the MEF cells to close to physiological levels of expression relative to the human cell line MRC5V1. From an initial 'sort layout' that divided the cell population into two areas based on GFP fluorescence (though note that there is always a population of cells expressing GFP at very low levels that is difficult to separate out from non-expressing cells), the gated area for expression P4 was further subdivided. The cell line WT3 was

sorted for GFP expression through use of the FACS Aria cell-sorter and the expression profile was gated into 'all GFP fluorescence' (Gate P4), roughly 'low-medium' (Gate P7), 'low-medium-high' (Gate P3, combining Gates P7 and P5)), 'medium-high' (Gate P5) and 'above high' (Gate P2) areas (Figure 4.4-A). Samples of cells were taken from each gate and prepared for western blotting. The MRC5V1 cell line was chosen as a benchmark line for comparison as it endogenously expressed human polκ. It was necessary to use the MRC5V1 cell line as the anti-polκ antibody does not recognize murine polκ present in the M1 line. Samples from the MRC5V1 line were run alongside samples of the MEF line from each gated region of expression and probed for polκ (Figure 4.4-B). This was followed by subdividing Gate P3 to refine the levels of fluorescence and to exclude Gate P2 from further analysis (Fig 4.4-C) Based on this initial observation, the gates were adjusted slightly to include a higher expressing population in Gate P7 and the experiment was repeated. From this, the level of expression found in Gate P7 was judged to have the greatest number of cells close to physiological levels of expressions (Fig 4.4-D).

4.2 Survival of Stable Cell Lines Following UV Irradiation

To explore the impact of the stable expression of GFP-tagged polκ, whether wild-type or the variants containing the C-terminal mutations, on the cell's ability to carry out successful NER, the cell lines' ability to survive and proliferate following exposure to ultraviolet radiation was assayed. Since expression of GFP by itself was shown by Ogi to have no negative nor positive impact on the survival of cells lacking endogenous Polκ (Ogi and Lehmann, 2006) this cell line was excluded from the assays. The cells that are stably expressing the C-terminal mutations which are located outside the UBZ domains, IQEL16, are as resistant to the effects of ultraviolet radiation as the cell line stably expressing GFP-polκ wt or the M1 cell line that expressed wild-type endogenous polymerase. The QK1 cell line at lower doses initially appears sensitive to UV irradiation but recovers at higher doses (Figure 4.5). Contrastingly, when the cell lines DD3 and CC4 are assayed in this manner, they display sensitivity to UV irradiation similar to the M6 line that lacks functional endogenous polκ, indicating that mutations to the conserved residues inside

Fig. 4.4: Physiologically Equivalent Expression of GFP-Polκ By FACS Analysis and Western Blotting

A) The fluorescence expression profile of the GFP-polκ expressing MEF cell lines were gated and sub-gated according to levels of fluorescense: P4 - all cells expressing fluorescence; P3 - low-medium-high expression; P2 - abovehigh expression; P5 - medium-high expression; P7 - low-medium expression . The population breakdown shows the percentage of the total number of events each gate contains in the cell line WT3, which was used as a representative cell line to establish the parameters.

B) Equivalent numbers of cells were taken from each of the indicated gates and run alongside an MRC5V1 control sample and probed with antibody raised against human polκ. 10x the amount of MRC5V1 control sample was loaded relative to the MEF samples to account for differences in cell number.

C) The P3 gate was subdivided into P5 and P7, with equivalent numbers of cells collected from each gate. Samples were run alongside the MRC5V1 control to compared with endogenous human polκ.

D) After slight alterations to the boundaries of the P7 gate, samples were collected again and run against the MRC5V1 control to confirm levels of GFP-polκ. Samples were also probed for alpha tubulin to compensate for disparate cell numbers between samples.

A)

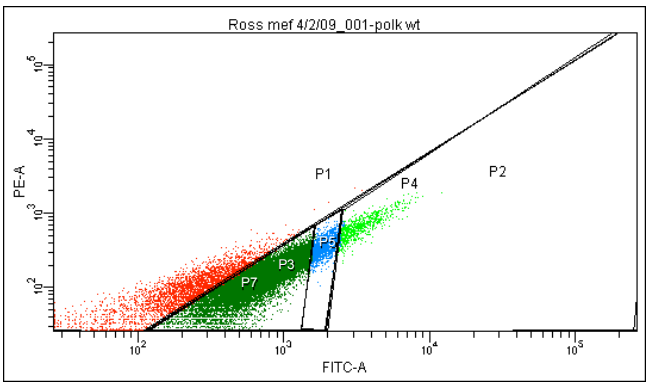

Experiment Name:	ross mefs_001
Specimen Name:	Ross mef 4/2/09_001
Tube Name:	polk wt
Record Date:	17-Jun-2010 10:43:44
$OP:	Ross
GUID:	5df075ce-6055-4c21-aac3-d4dbd90115b3

Population	#Events	%Parent
All Events	30,000	####
P3	20,047	66.8
P7	18,750	62.5
P1	4,291	14.3
P2	871	2.9
P4	20,940	69.8
P5	1,569	5.2

B)

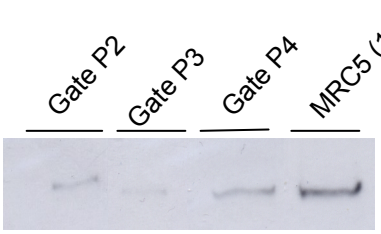

C)

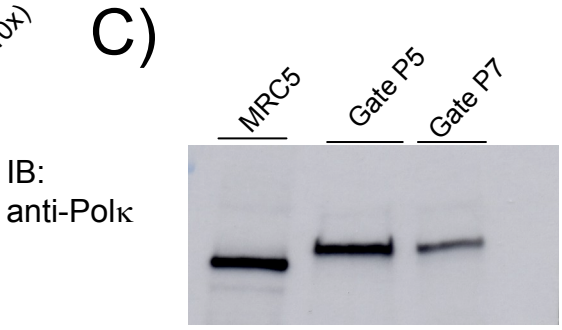

D)

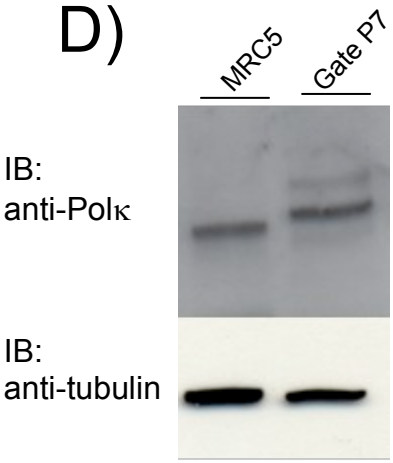

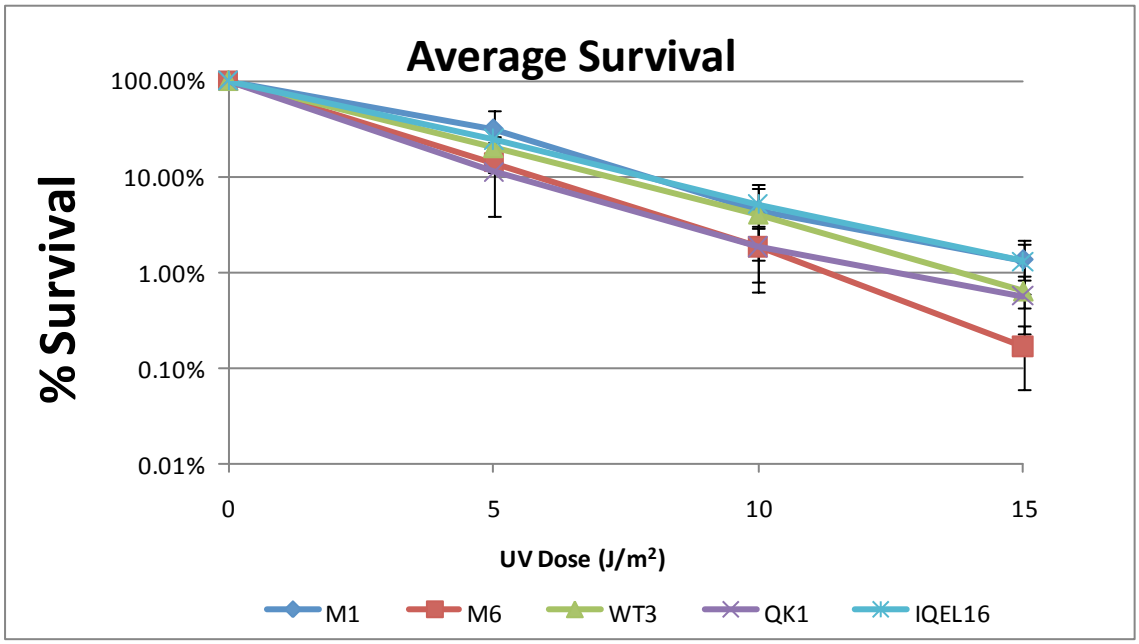

Figure 4.5: GFP-polκ mutations outside the UBZ domains do not show enhanced sensitivity to UV irradiation

MEF cells were sorted according to expression level and plated in triplicate and were exposed to UV at the indicated doses. After ten days, the cells were stained with methylene blue and counted. Data points are expressed as the percentage that survived compared to the unirradiated control plates Each data point is the average of a minimum of three independent experiments. The error bars represent the standard deviation of a minimum of three independent experiments.

the UBZ domains of the protein affect the survival potential of the cells following DNA damage (Figure 4.6). Though the apparent differences between the cell lines do not appear substantial, when the values are normalised against the cell line M1, the cell line expressing endogenous polκ, it is observed that the M6, DD3 and CC4 cell lines all display substantially less survival than M1. Conversely, when the cell lines WT3 and IQEL16 are normalised to M1 in each experiment, they are resistant to the lethal effects of UV irradiation. The cell line QK1, when normalized to M1, now can be seen to have an intermediate response to UV irradiation, sensitive at lower doses but recovering to wild-type levels at the highest dose (Appendix G, Table 8). To ensure that these results are not the artefact of clonal specific variances but are actually dependent on the role and function of polκ, other clones for each stable cell line were sorted according to the same gating as the previous set and also assayed for their sensitivity to ultraviolet radiation. These alternative clones also showed the same pattern of survival, with the cell lines expressing wild-type polymerase or cell lines with mutations to non-UBZ conserved residues more resistant to the lethal effects of UV irradiation than cell lines expressing GFP-polκ with UBZ domain mutations (Figure 4.7 and Figure 4.8 respectively). In this set of survival assays, the cell lines QK5 and IQEL7 now appear to have an intermediate sensitivity. However, this is partially biased due to a substantially greater than average survival of the cell lines M1 and WT than had previously been observed. When then average percentage of survival is compared, the clones of each cell line do not appear to differ greatly (Appendix G, Table 8 and Table 9: compare averages of QK1 with QK5 and IQEL16 with IQEL17).

4.3 Recovery of RNA Synthesis Following UV Irradiation

Though a clear difference was seen between the cell lines that stably expressed GFP-polκ with mutations in the UBZ domains of the protein and the cell lines expressing wild-type protein following UV irradiation, it should be noted that this is only an indirect measurement of NER activity. A more direct measurement of NER can be obtained through an 'Unscheduled DNA Synthesis' assay, wherein serum starved cells are UV

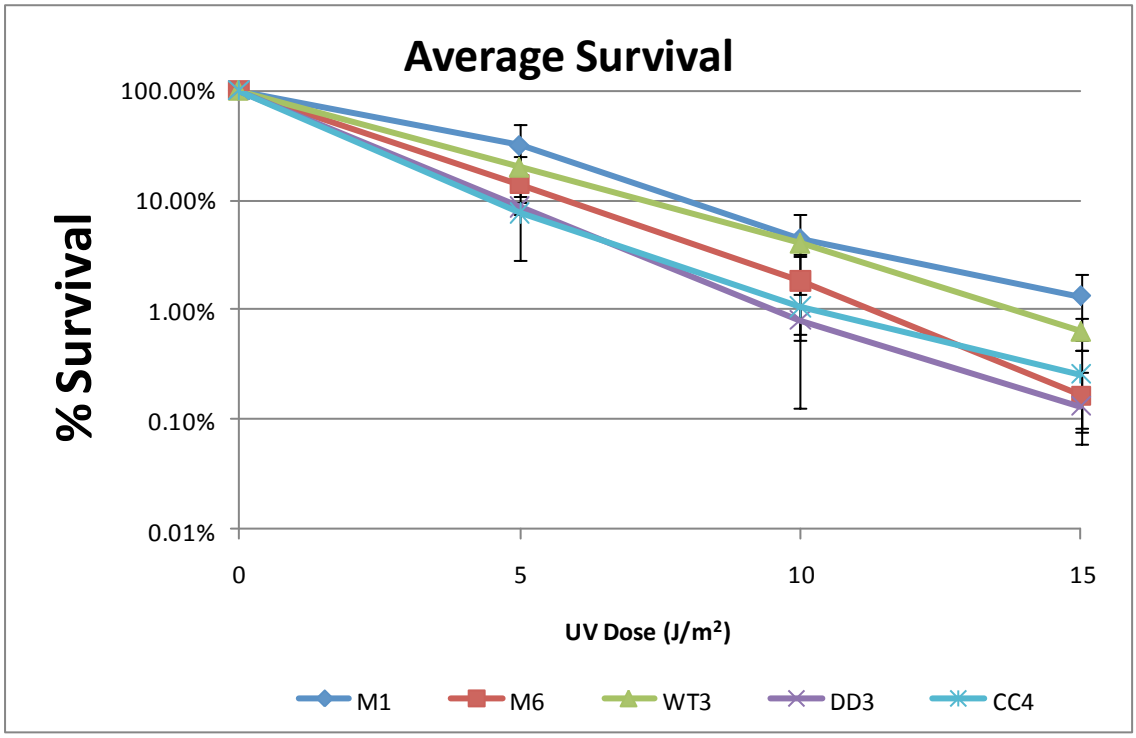

Figure 4.6: GFP-polκ mutations inside the UBZ domains do show enhanced sensitivity to UV irradiation

MEF cells were sorted according to expression level and plated in triplicate and were exposed to UV at the indicated doses. After ten days, the cells were stained with methylene blue and counted. Data points are expressed as the percentage that survived compared to the unirradiated control plates Each data point is the average of a minimum of three independent experiments. The error bars represent the standard deviation of a minimum of three independent experiments.

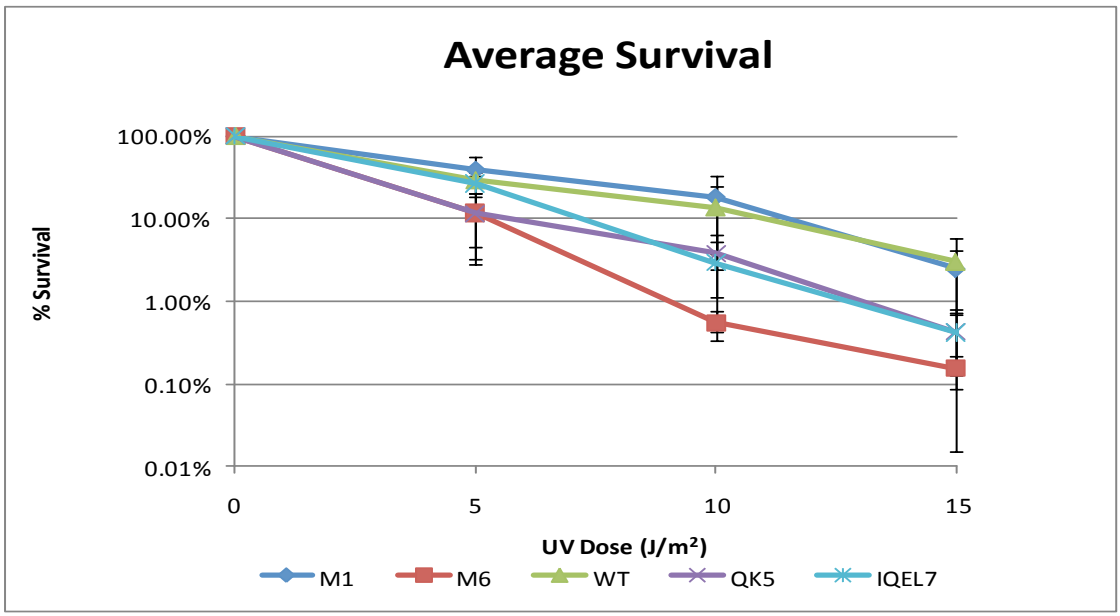

Figure 4.7: UV Survival of non-UBZ Mutants of GFP-Polκ Alternative Clones

MEF cells were sorted according to expression level and plated in triplicate and were exposed to UV at the indicated doses. After ten days, the cells were stained with methylene blue and counted. Data points are expressed as the percentage that survived compared to the unirradiated control plates Each data point is the average of a minimum of three independent experiments. The error bars represent the standard deviation of a minimum of three independent experiments.

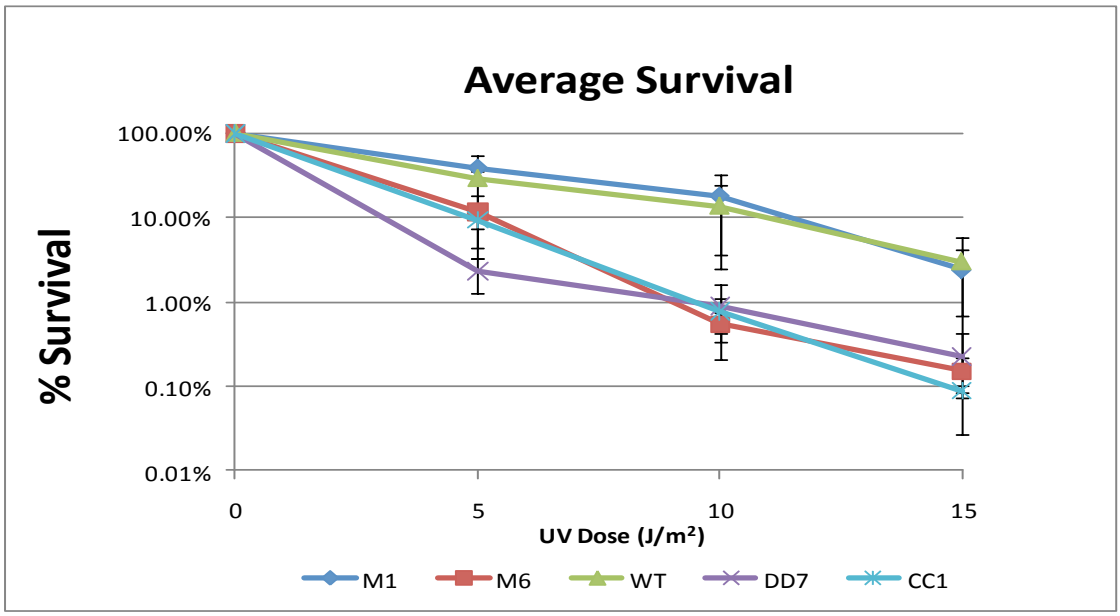

Figure 4.8: UV Survival of UBZ Mutants of GFP-Polκ Alternative Clones

MEF cells were sorted according to expression level and plated in triplicate and were exposed to UV at the indicated doses. After ten days, the cells were stained with methylene blue and counted. Data points are expressed as the percentage that survived compared to the unirradiated control plates Each data point is the average of a minimum of three independent experiments. The error bars represent the standard deviation of a minimum of three independent experiments.

irradiated and then labeled with a radioactively nucleotide or a conjugatable nucleotide analog. Incorporation of the nucleotide into the DNA of the cell is reliant on DNA synthesis and, since the cells are cultured under conditions that inhibit entry into and progress through S-phase and bulk DNA replication, the majority of such incorporation results from repair synthesis of the gaps generated by excising the damage containing strand of the double helix. Using this method based around the incorporation of ^{3}H-thymidine, the NER defect in *polκ*$^{-/-}$ MEF cells was demonstrated in the original work by Ogi and Lehmann (Ogi and Lehmann, 2006). Further work using 5-ethynyl-2'-deoxyuridine (EdU), which is able to be covalently conjugated to a fluorescent tag, further showed a dependence on polκ in 50% of unscheduled DNA synthesis activity human primary fibroblasts (Ogi et al., 2010). To see if the mutations constructed in *polκ* and expressed in the MEF cell line background had any effect on this repair synthesis, both versions of the assay were attempted. Unfortunately, severe technical limitations concerning the effectiveness of serum starvation on immortalised MEF cells made meaningful data difficult to acquire.

Another common assay for the determination of NER activity is to monitor the incorporation of radioactively labeled uridine following UV irradiation. This assay is targeted toward the transcription coupled repair pathway. Following UV, there is a reduction of transcription activity and the CS proteins are required to bring about recovery of transcription. As was detailed in the introduction, CSB serves to detect stalled RNA polymerases and, with CSA, bring about the initialisation of NER to remove the blocking lesion. Inability to properly complete NER results in a failure to recover RNA transcription. By monitoring the recovery of RNA synthesis, the ability of a cell to complete TC-NER can be ascertained. The advantages of this assay are that it does not depend on the cells being in a non-proliferative state. In the first series of experiments, cells were exposed to different doses of UV then incubated for 24hrs to allow recovery of RNA synthesis.

As can be seen, the M6 cell line lacking expression of endogenous polκ displays a reduced ability to recover its levels of RNA synthesis compared to the M1 cell line which does express endogenous polκ. This deficiency can be rescued as seen by the cell line WT3 which is derived from M6 but expresses GFP-tagged polκ wild-type. Expression of GFP-polκ with mutations in the C-terminus outside the known domains also show wild-type levels of recovery; given the previously observed behaviour of QK1 and IQEL16 this was not unexpected (Figure 4.9). The cell line QK1 was also consistently observed to have level of RNA synthesis following 5 J/m^2 higher than the unirradiated control (Figure 4.9, Appendix G: Table 10). Intriguingly, despite having a marked sensitivity to ultraviolet irradiation as measured through clonogenic survival, the cell lines that stably express GFP-polκ carrying mutations inside the UBZ domains, DD3 and CC4, appear to be unhindered in their ability to recovery their RNA synthesis following UV, closely following the same pattern of recovery as the cell lines expressing wild-type protein (Figure 4.10). When normalised against the cell line M1 in each experiment, the M6 cell line displays roughly 50% of the TCR capacity of M1. In comparison, the cell lines WT3, DD3, CC4, QK1 and IQEL16 all display broadly equivalent levels of RNA synthesis recovery (Appendix G, Table 10).

4.4 Time Course of RNA Synthesis Recovery Following UV

The results of monitoring the recovery of RNA synthesis post-UV irradiation, as detailed above indicated no differences between the cell lines that expressed GFP-polκ containing mutations in the UBZ domains and ones that expressed wild-type protein. This was in spite of sensitivities observed in other assays and differences in localisation when the mutant constructs were transiently over-expressed. However, the possibility remained that there were observable differences in the cell lines but not at sixteen hrs post-UV irradiation when the levels of RNA synthesis were assayed. To investigate this, a time-course of RNA synthesis was carried out. This assay was based on one initially devised by Mayne and Lehmann (Mayne and Lehmann, 1982). To initially test the feasibility of monitoring the incorporation of radioactively tagged uridine over a shorter period of time

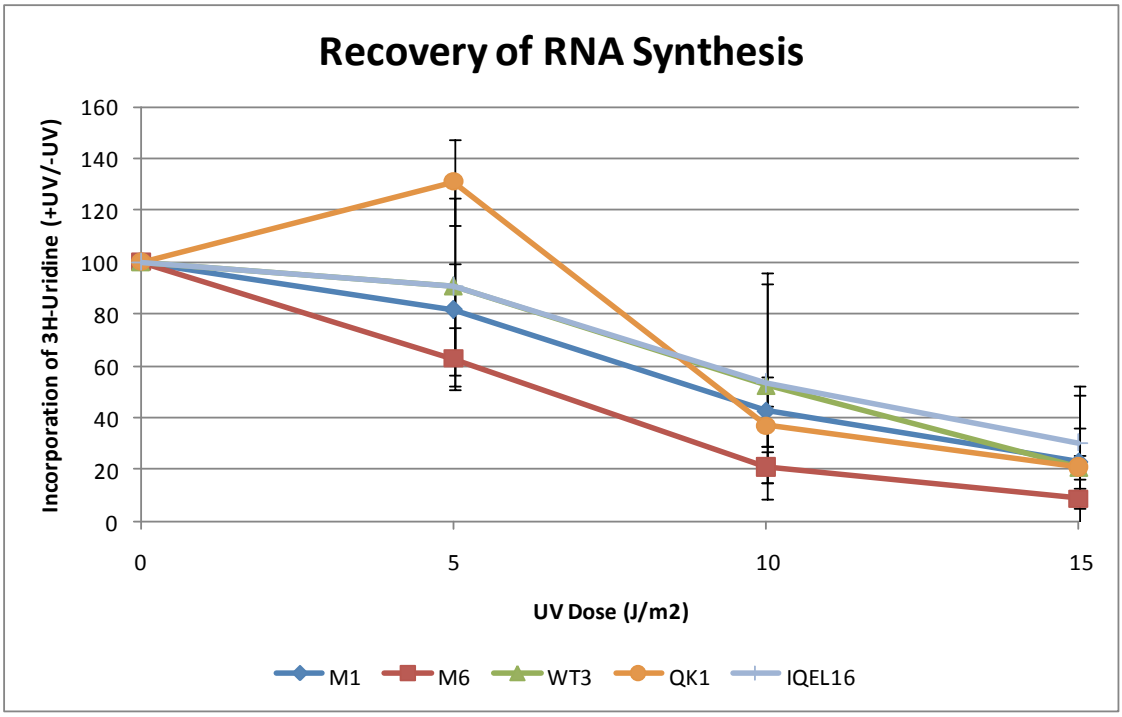

Figure 4.9: GFP-polκ mutations outside the UBZ domain do not show any impairment of RNA synthesis recovery following UV irradiation

MEF cells were sorted for expression and serum starved in DMEM with 0.5% FCS for three days. The cells were then UV irradiated at the stated doses and allowed to recover for 16+ hours. After that, the cells were labelled with 5μCi/ml ^{3}H-uridine for four hours before being processed for analysis. Results are plotted as a percentage of the incorporation of the ^{3}H-Uridine by comparison with unirradiated cells that were processed in parallel. Each data point is the average of a minimum of three independent experiments. The error bars represent the standard deviation of a minimum of three independent experiments.

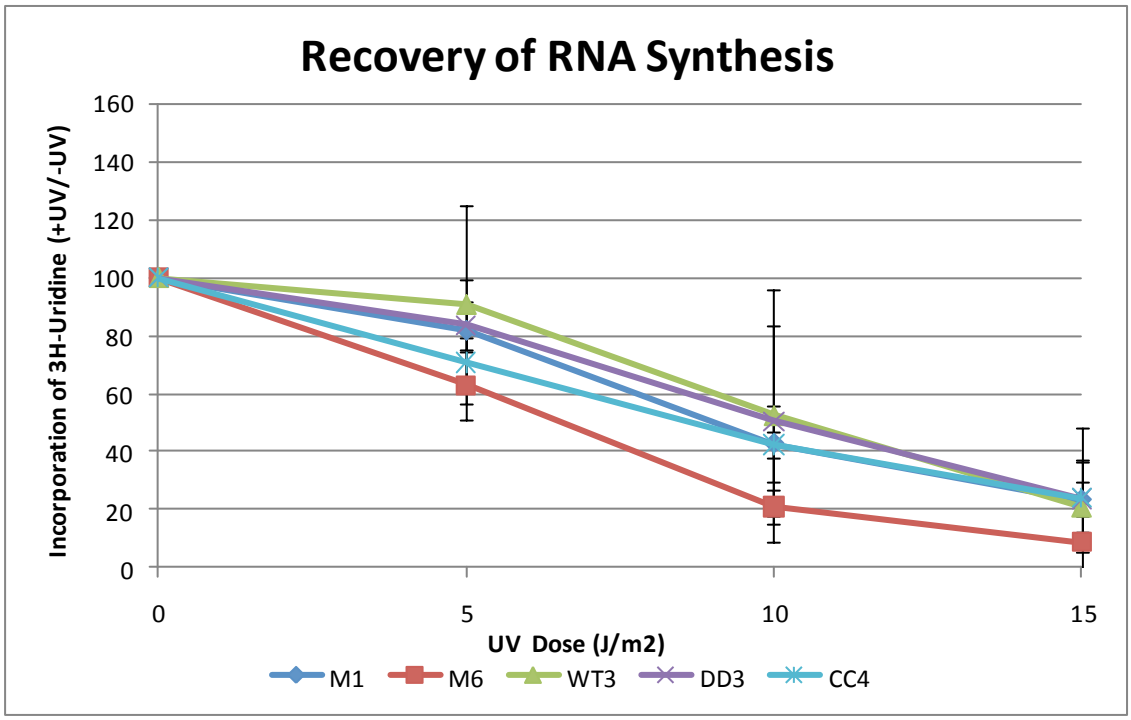

Figure 4.10: GFP-polκ mutations inside the UBZ domain do not show any impairment of RNA synthesis recovery following UV irradiation

MEF cells were sorted for expression and serum starved in DMEM with 0.5% FCS for three days. The cells were then UV irradiated at the stated doses and then allowed to recover for 16+ hours. After that, the cells were labelled with 5μCi/ml ^{3}H-uridine for four hours before being processed for analysis. Results are plotted as a percentage of the incorporation of the ^{3}H-Uridine by comparison with unirradiated cells that were processed in parallel. Each data point is the average of a minimum of three independent experiments. The error bars represent the standard deviation of a minimum of three independent experiments.

than previously attempted in the MEF cell lines, the experiment was trialed with just the cell lines M6 and WT3. Two differing doses of UV radiation were used, 4 J/m^2 and 8 J/m^2, in addition to the unirradiated control. The recovery was monitored as described above. As can be seen, in both repeats of the experiment, a greater recovery can be seen in the WT3 cell line at 4 J/m^2 whilst at the same dose the M6 line does not significantly recover. However, at a dose of 8 J/m^2 of UV, neither cell line showed appreciable levels of recovery over the time period in which the cells were monitored (Figure 4.11). Based on these observations, despite some reservations about the initial levels of impairment following the exposure to UV radiation, it was decided to attempt the experiment with the lines DD3, CC4 and M1 in addition to WT3 and M6 using a dose of 4 J/m^2 (Figure 4.12).

Though there is a considerable amount of variability in the assay a few trends can be deduced. The M6 line consistently displayed a reduced ability to recover RNA synthesis after UV irradiation over the eight hrs, consistent with the displayed impairment of RNA synthesis at sixteen hrs. Meanwhile, the M1 line and WT3, the cell line that stably expresses wild-type protein, displayed a greater degree of RNA synthesis over the course of the assay. In the cell line DD3, there is arguably no difference between DD3 and the cell lines with wild-type polκ. A slight defect is observable in the cell line CC4 at the earlier time points of the assay but recovers normally by 5 hrs. These observations are consistent with the 16 hr post-UV percentage of recovery in which the cell lines that stably express the protein with mutations inside the UBZ domains are as fully able to recover their RNA synthesis after UV as cell lines expressing wild-type protein.

4.5 Discussion

To further investigate the effects of the mutations created inside the C-terminus of human polκ on the behaviour of the protein and in cells that expressed the mutant constructs, a set of stable cell lines were created in the M6 MEF background that had its endogenous polκ disrupted in exon 6. Several stages of selection, screening and enrichment were used since the method of creation involved an entirely random integration event into the cell

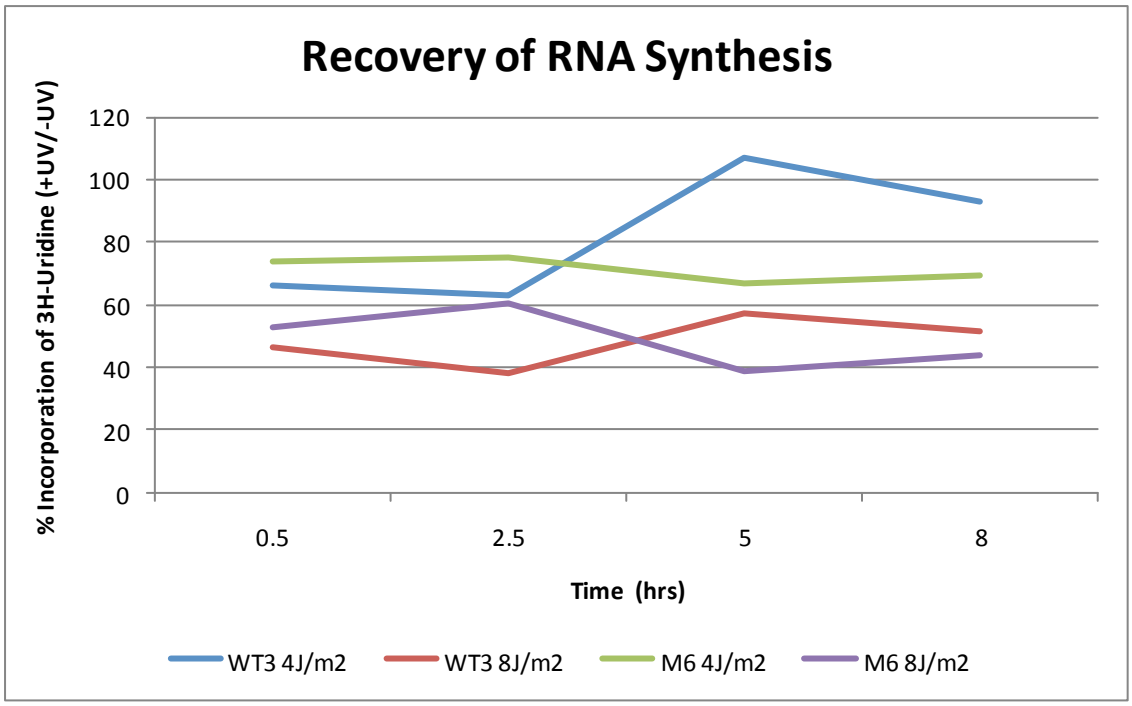

Fig. 4.11: Effect of UV Dosage on Incorporation of ^{3}H-uridine in MEF cell lines

M6 cells and WT3 cells, sorted for expression, were exposed to UV irradiation at the indicated doses and the recovery of RNA synthesis was monitored over the indicated time points by measuring the incorporation of ^{3}H-uridine. Data points are the average of two independent experiments are presented as the level of incorporation as compared with unirradiated control plates labelled and processed in parallel. The results of this experiment were used to select a UV dose to administer in the proceeding experiments.

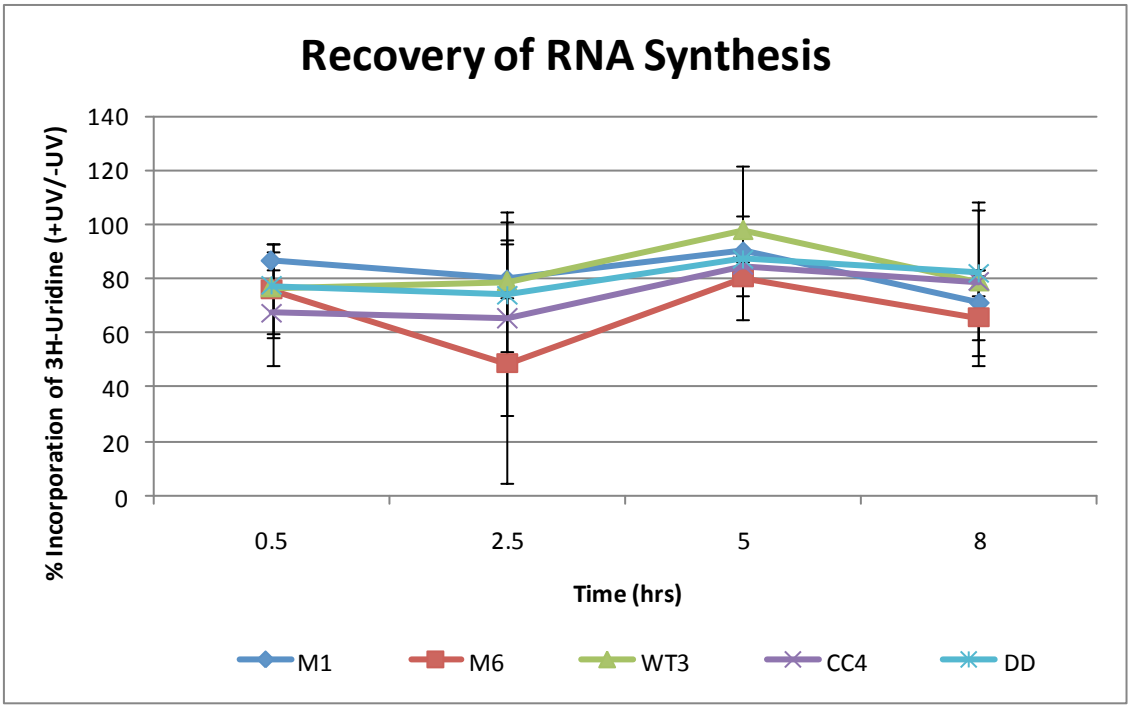

Figure 4.12: GFP-Polκ mutantions inside the UBZ domains do not show any impairment in rate of recovery of RNA synthesis following UV irradiation

MEF cells were sorted according to expression level and subsequently were exposed to UV at 4 J/m^2 The cells were allowed to recover for the indicated times before labelling with 5μCi/ml ^{3}H-uridine for thirty minutes. Cells were then processed and analysed for the incorporation of the nucleotide. The percentage recovery is calculated as the percent incorporation compared to an unirradiated control processed in parallel at each time-point. Each data point is the average of a minimum of three independent experiments. The error bars represent the standard deviation of a minimum of three independent experiments.

genome. As was shown by screening on western blot, clones that survived the antibiotic selection do not always express the target protein but have acquired the selection resistance. Unlike yeast systems, where the gene is targeted to a specific locus and integrated through the favoured pathway of homologous recombination, mammalian systems have no such precision, and control over re-arrangements, silencing and other undesirable effects are limited. Though the data were not shown, the selected clones were also checked to ensure that they did not express free GFP independent of polκ. Though the event is unlikely, it had been noted by other colleagues working with other GFP-tagged chimeric proteins stably integrated into other cell lines. Any expression of free GFP would be a contaminant in the next stage of enrichment, where the cells were selected on the basis of their expression for GFP by sorting through the use of a FACS Aria system. The M6 and M1 cell lines were used as controls to establish a set of gates which would exclude the natural autofluorescence of proteins in the cell and allow selection specifically on GFP-polκ expression. As was noted, it proved impossible to create a stable cell line expressing the constructed mutant GFP-polκ S824AS825A, either as selected clone or as a mixed population of non-clonal cells. The reasons for this are not immediately clear since in Chapter 3, it had been seen that the transiently expressed protein accumulated at sites of localised damage exactly as GFP-polκ wild-type and did not display any significant deviations in expression as observed by FACS analysis. A few tentative explanations could be put forward: the S824AS825A mutation may represent a mutation that is long-term detrimental to the health and viability of the cells, resulting in a selective pressure that rewards cells able to silence the integrated gene. The other stable cell lines, when not regularly sorted for expression on the FACS Aria, were also observed to show a decrease in GFP-polκ expressing cells over the course of time. This effect may simply be more pronounced with the S824AS825A mutation. Alternatively, while the mutant may appear wild-type under transient expression, it may have a dominant negative phenotype, possibly indicating an importance of the conserved residues as a site of modification or interaction. Indeed, a strong accumulation at localised damage could present a problem if the modified polymerase then fails to leave the site of repair once

DNA synthesis has been completed. It would be intriguing to construct a system allowing the expression of the mutant polymerase, possibly under an inducible promoter system, to explore if it did show any phenotypic deficiencies.

This concern about dominant negative phenotypes led to the decision to try to separate the expression of GFP-polκ into distinct 'gates' and select for a level of expression relatively close to the physiological expression of human polκ as observed in another immortalised, but human, cell line. For this, the cell line MRC5V1 was chosen. It had several characteristics in common with the MEF cell line. The MRC5V1 cell line was grown under the same tissue culture conditions as the MEFs, unlike primary human cell lines that required different concentrations of FCS and had different growing rates. The WT3 cell line was chosen as a representative for the stable cell lines as it had shown a consistent and stable level of expression in a significant proportion of cells. Furthermore, the levels of expression varied between cells significantly, allowing comparisons between low, medium and high levels of GFP-polκ expression. Equivalent numbers of cells were collected for each comparison sample and probed for their levels of tagged polymerase. As expected, the higher level of expression showed an amount of polymerase far above the MRC5V1 comparison and was excluded from further consideration. The lower level gates P5 and P7 were closer to physiological expression; it was decided to use the P7 gate as it represented a level of polymerase only twice as abundant as in the comparison cell line yet yielded a far greater number of cells than the P5 gate (Fig. 4.4).

Once the gating had been established for physiological levels of expression, it was possible to test the stable cell lines for phenotypic effects of expressing the different variants of GFP-polκ. It was first decided to test the cell lines for their ability to survive the exposure to UV irradiation. NER deficient cells display marked sensitivity to the lethal effects of UV and it was the initial observation that *polκ*$^{-/-}$ MEF cells are sensitive to UV that led to the work that established the role of the polymerase in NER (Ogi and Lehmann, 2006). When the stable cell lines were exposed to varying doses of UV irradiation, they fell into two

recognisable sets which corresponded with whether or not the polκ mutations had been observed to accumulate at localised damage. The first set of stable cell lines, consisting of WT3 and IQEL16, and to a lesser extent QK1, behaved the same as the positive control line M1. These cells did not display enhanced sensitivity to UV irradiation and also these polκ mutations had been observed not to affect localisation to sites of localised UV damage. The second group aligns itself with the *polκ*$^{-/-}$ cell line M6; consisting of DD3 and CC4, these cells lines display increased sensitivity to UV to the same extent as the M6 line and the polκ mutations had been observed to prevent accumulation at sites of localised UV damage. To ensure that these observations were not simply a set of clone-specific artefacts that happened to agree with predicted observations, a secondary set of clones from each cell line was assayed in the same manner. They all behaved as previously seen in the first set. Normalising the survival percentages against the cell line with expression of endogenous polκ assists in highlighting the lethality observed in the M6, DD3, DD7, CC4 and CC1 cell lines (compare Fig 4.5 with 4.6 and 4.7 with 4.8, compare Table 8 with Table 9 in Appendix G). From this, it appears that the UBZ domains of the polymerase are important for long-term survival following UV irradiation. Given that effects on survival corresponds to the polκ mutation affects localisation following DNA damage, this survival presumably is reliant on the involvement of polκ in NER shortly after the cytotoxic DNA lesions have been generated. Since the UV survival assay requires a ten day window from start to assessment, other assays would be required to observe immediate consequences of the variant polymerases on NER activity.

I initially tried to assay the cell lines using an Unscheduled DNA Synthesis (UDS) assay. Under conditions of serum starvation and HU exposure, the vast majority of replicative DNA synthesis is inhibited and cells do not enter into S-phase. Thereby, when exposed to DNA damaging agents such as UV radiation and provided with modified nucleotides to incorporate into DNA, any DNA synthesis shown by the cells would be reliant on NER activity. UDS assays have been used diagnostically for years to identify patients with Xeroderma Pigmentosum. Classically radioactively labelled thymidine was used on serum

starved cells but recent advances in copper catalysed chemistry have allowed the development of a non-radioactive assay using the conjugation of a fluorescent marker to incorporated uridine analogues, with S-phase cells visually excluded from analysis (Limsirichaikul et al., 2009). Both these attempts were tried with the stable MEF cell lines and the control cell lines. Unfortunately, neither proved adaptable to properly assay the cell lines. These UDS assays are traditionally done on primary human fibroblasts. For both cases, the cells are restricted in their growth abilities and will stop growing upon confluency or low serum condition. However, immortalised cell lines are freed from these restrictions and will not pause or go quiescent even after extensive starvation. Thus S-phase cells were unable to be excluded by starvation or visual identification and attempts to measure UDS on these lines failed to return any usable data. This has been supported by informal conversations with colleagues who developed the fluorescent assay; they found it unusable for immortalised cell lines like MRC5V1. In theory it may be possible to co-stain for a marker of cell cycle phase, such as cyclin A, or for a marker of proliferating cells, such as ki67. However, neither possibility was explored: cyclin A, for instance, is detectable in both S- and G2-phase cells, potentially excluding a significant fraction of non-S-phase cells from analysis; in contrast ki67 will be detectable in any proliferating cell but not in non-proliferating cells. The difficulty with serum starvation and distinguishing S-phase cells from ones in other phases of the cell cycle makes it likely that there were few, if any, truly non-proliferating cells.

The UDS assay as described is admittedly a relatively crude way of demonstrating repair synthesis that proved to be inappropriate for use with the immortalised cell lines. There are more stringent methods for measuring repair synthesis that could be explored. Particularly, a caesium chloride gradient could be used to separate DNA repair from replication. Cells are incubated with ^{3}H-thymidine and excess BrdU. Replicative DNA synthesis incorporates an extensive amount of BrdU which greatly increases its density. Conversely, gap filling for NER incorporates relatively little BrdU, not greatly changing the density of the DNA. By measuring the incorporation of radioactivity in this normal

fraction, a measure of resynthesis of DNA can be ascertained and clearly distinguished from any bulk DNA replication. This method was successfully used by Ogi *et al* to elucidate the repair defect originally seen in polκ deficient MEF cells (Ogi and Lehmann, 2006).

With the UDS assay untenable for use with the immortalised MEF cell lines, an alternative assay was employed; the Recovery of RNA Synthesis (RRS). Following exposure to UV irradiation, there is a general decrease of RNA synthesis. Functional NER is required to recover RNA synthesis back to pre-exposure levels. Cells that are deficient in that NER pathway do not show significant recovery. The assay classically uses the incorporation of radioactively labelled uridine and is used in the diagnosis of Cockayne Syndrome patients. Since results are normalised against a non-irradiated control sample, results are less dependent on cell number to give an accurate result. Following the inability to use the UDS assay due to numerous technical difficulties, it was felt that the RRS assay might help to obtain, at the bare minimum, a crude idea of how the MEF cell lines respond to UV irradiation in an NER specific manner. We expected that the stable cell lines would fall into the same pattern observed for survival post-UV and for accumulation at local damage, with the UBZ mutants deficient in recovery and the non-UBZ mutants in the same category as the wild-type polymerase expressing cells. Surprisingly, I observed that the mutations inside the UBZ domain of polκ had no effect on the ability to recover RNA synthesis. While the polymerase deficient cell line M6 repeatedly showed a defect compared to the proficient M1 cell line, as had previously been observed by Ogi and Lehmann, the cell lines DD3 and CC4 did not show the M6 type deficiency in recovery. Rather they displayed levels of recovery similar to the non-UBZ mutant cell lines WT3, QK1, IQEL16 and M1 (compare Fig. 4.9 with 4.10; Appendix G, Table 10). Intriguingly, the cell line QK1 consistently exhibited an increase in RNA synthesis at 5 J/m^2 before returning to the same levels of RNA synthesis as the other cell lines at higher doses. At the same dosage, this cell line also exhibits sensitivity to UV similar to M6 but again is restored to wild-type levels at higher doses. How can we reconcile the evidence of the behaviour of

this cell line? Polκ is known to be ubiquitinated and K836 might represent a possible site of modification. The role of ubiquitination in regulating the polymerase has been little explored, though if there are parallels with polη it may play a role in preventing inappropriate associations with replication machinery (Bienko et al., 2010). At low doses of UV, GFP-polκ Q835AK836A might be preferentially recruited to involvement in transcription-coupled repair over global genomic repair. However, as the exposure to UV increases in dose, a greater proportion of damage is generated in non-transcribed DNA, since this forms the majority of the genome. This would overcome any preference the mutant construct might show and restore function to unmutated behaviour as observed.

With the unexpected conclusion that mutations to the UBZ domain do not prevent overall recovery of RNA synthesis, the suggestion was raised to look at earlier time points to see if the UBZ domain mutations might cause a delay in recovery of RNA synthesis if not an overall deficiency. The previous assay measured incorporation of radioactive uridine at a point sixteen hrs post UV exposure. With some slight modifications to the experimental protocol, the incorporation of the labelled nucleotide at points 30 min following exposure upwards to 8 hrs after exposure were measured as a percentage of incorporation in un-irradiated control cells. In primary human cell lines, within the first hour of exposure to UV, there is a substantial decrease in the levels of RNA synthesis which over time recovers back to un-irradiated levels (Mayne and Lehmann, 1982). In cells that are deficient in TCR and late stage NER, this drop in synthesis activity never recovers. When the MEF cell lines M1, M6, WT3, DD3 and CC4 were treated in the same manner, two observations were immediately apparent. Firstly, a substantial decrease in RNA synthesis was not uniformly observed. While the M6 cell line and DD3 and CC4 did show a decline in RNA synthesis, it was not as deep as expected. The cell lines that express either wild-type human polymerase, WT3, or murine, M1, did not show as substantial a decrease. Secondly, the M6 line, though not as impaired as expected, did not recover levels of RNA synthesis back to any un-irradiated level. The positive control cell lines did show recovery of RNA synthesis even from their lesser impaired starting points. The cell lines DD3 did not

appear to show any substantive difference comparative to the positive control cell lines, keeping with its behaviour in the RRS assay at 16+ hrs post-UV. The CC4 cell line might show a degree of impairment at the early stages of RNA synthesis recovery, but returned to wild-type levels after roughly three hrs (Fig. 4.10).

Given the sensitivity seen in the cell lines stably expressing mutations inside the UBZ domains of human polκ for long-term survival post-UV, it was surprising to see no defect in an assay for TCR. It would appear that the UBZ domains of the polymerase are not required for its participation in TCR and are therefore required for it to engage in GGR, though it should be noted that GGR was not directly assayed due to the technical problems encountered with the UDS assay. It suggests that this sensitivity is not related to the involvement of polκ in NER but instead result from the involvement of polκ in TLS past photoproducts. Though a UV induced TLS role for polκ has been proposed by other laboratories, there is mitigating evidence against this explanation. As has previously been mentioned, the polymerase is unable to bypass UV photoproducts efficiently *in vitro*, and while a role has been uncovered for the mutagenic bypass of said photoproducts *in vivo*, this has been demonstrated in a XPV background (Ziv et al., 2009), where the cell line in question lacked the far more efficient UV bypass polymerase, polη. The MEF cell lines used in these assays presumably do not lack polη and as such would be unlikely to be dependent on the more inefficient polκ in any post-UV TLS survival manner. Though it would have been desirable to have overcome the technical difficulties of the UDS assay to assay directly for GGR activity, in the light of the UV survival results and the RRS results, it does appear that the UBZ domains of the polymerase are essential for its role in GGR but not for TCR. However, polκ is still necessary for TCR as Ogi *et al* have seen a deficiency in recovery of RNA synthesis in the M6 lines, an observation that was repeated here.

Why might the UBZ domains of polκ be required for GGR but not for TCR? It might be possible that recruitment to sites of NER in GGR requires polκ to interact with an ubiquitinated partner protein but this interaction is not essential for its participation in

TCR, though it is unclear why there would be a difference in recruitment at a point so far down in NER pathway. At the point of repair synthesis, the distinguishing features that separate GGR and TCR, i.e. the different mechanisms for recognising the unrepaired lesion, have long since conjoined into the common NER pathway. The wider environment in which repair is taking place might be an avenue to explore further. The model put forward by Ogi *et al* suggested that the combined involvement of polκ and polδ in NER might take place in areas of steric hindrance due to the chromatin structure. The recruitment of polκ could under those conditions, as suggested by data presented in this thesis, require the intact UBZ domains of the protein (Ogi et al., 2010). Under conditions of TCR, however, the chromatin landscape is already accessible due to the transcription process. Polκ may still bear some responsibility for repair in these conditions but not rely as heavily on the UBZ domains to stabilise its interactions. Instead, recruitment through some still undefined role of XRCC1 may be sufficient for the recruitment of polκ to sites of repair under these conditions.

Chapter 5: Accumulation of Human DNA Polκ Following Localised UV Irradiation in XPF- and XPG-deficient, Wild-type and Nuclease Dead Cell Lines

Following recognition of the damage and a localised melting of the DNA double helix around the lesion, it is then presumed necessary to physically excise the damage-containing strand before repair synthesis is possible. This is accomplished by the two NER nucleases XPF and XPG, which cut 5' and 3' of the lesion respectively. Defects in the action of XPF gives rise to XP complementation group F, a relatively mild instance of the disease if due to a mis-sense mutation but severe if caused by gene deletion, and defective XPG can lead to XP complementation group G and XP/Cockayne Syndrome.

The sequence of action of the nucleases has been a matter of considerable interest and it has long been held that the 3' nuclease XPG made the initial incision as it was recruited first (Volker et al., 2001) followed by the 5' nuclease XPF (Evans et al., 1997). However, recent work has shown the situation to be more subtle. As mentioned previously, it has been suggested recently that it is XPF that makes the first incision into the damage-containing DNA strand but its action is prompted by the physical presence of XPG without the requirement that XPG make the 3' incision into the strand (Staresincic et al., 2009). This separation of actions allows an intriguing issue to be considered. There are two points where the factors necessary for repair synthesis could be recruited: immediately following the 5' incision by XPF when there is a flap of DNA or held off until the incision by XPG when there is a single stranded gap in the DNA helix. In the former case these factors can be recruited following the 5' incision without dependence on the 3' incision. Is polκ recruited at a similar point in the repair process or is it added at a later point following complete incision (Fig 5.1)?

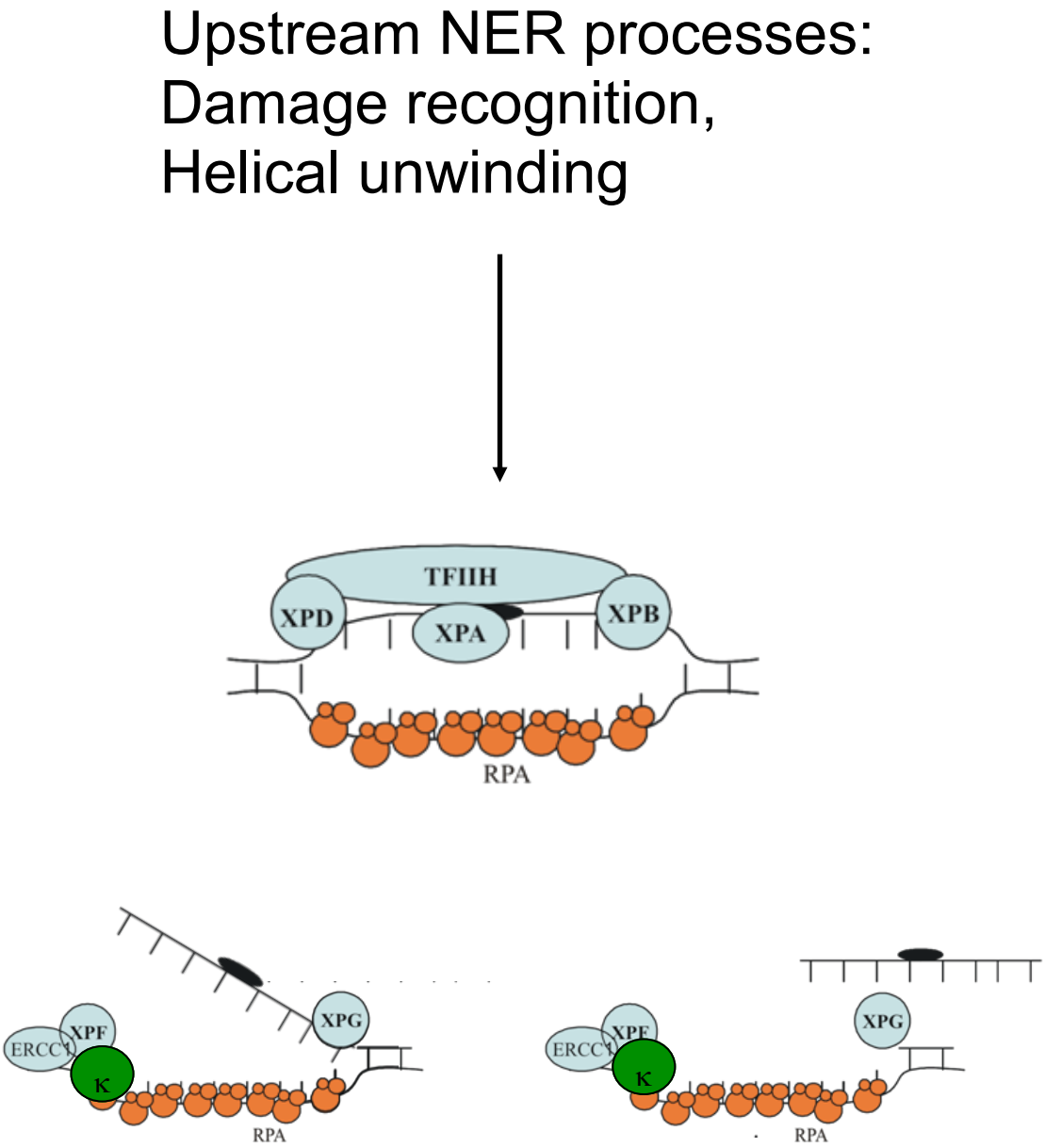

Fig 5.1 Two Possible Models for Polκ Recruitment Post-Incision in NER

Following upstream NER events to recognise the damage and open the DNA helix, two possible routes present themselves to allow the recruitment of polκ. In one, the incision by XPF is enough to allow access to the template strand. In the other, both nucleases must make their incisions to release the damage containing strand and give the polymerase access.

5.1 Accumulation of Endogenous Polκ

To explore these possibilities, cell lines were obtained from the lab of Orlando Schärer. They were as follows: the XP2YO line deficient in XPF, XP2YO XPF WT and XP2YO XPF D676A which carries a catalytically dead XPF nuclease; the XPCS1RO line deficient in XPG, XPCS1RO XPG WT and XPCS1RO XPG E791A which carries a catalytically dead XPG nuclease. The XP2YO cell line, its complemented derivatives, the XPCS1RO cell line and its complemented derivatives proved remarkably difficult to transfect with GFP-polκ using contemporary standard laboratory techniques. Attempts with Fugene 6 and Metafectene Pro produced extremely low levels of transfection in a small proportion of the total population. Further efforts with an Amaxa Nucleofector Kit produced very little improvement in transfection efficacy and were highly detrimental to the subsequent health and viability of the cell population. It should be noted that the original complementation of the parental cell lines XP2YO and XPCS1RO was carried out using a lentiviral system, allowing for much higher transfection efficacy than that usually achieved with chemical techniques such as the lipid micelles of Fugene. Rather than constructing a virus carrying GFP-polκ wild-type, it was decided to look at the accumulation of endogenous polκ after localised UV irradiation through immunofluorescent staining.

To confirm that the polκ antibody used, the rabbit polyclonal SK04 antibody, was suitable for detecting endogenous polκ using immunofluorescent techniques, MRC5V1 cells were seeded onto coverslips and UV irradiated through a 5μm polycarbonate filter. The cells were then fixed and extracted in 2% paraformaldyhde and 0.2% Triton-X 100 in PBS, blocked in 10% BSA for 2 hrs and dual incubated with anti-polκ (rabbit) and anti-RPA (mouse) overnight. The following day, the cells were incubated with the appropriate secondary antibodies and mounted using DAPI containing mounting media. As can be seen in MRC5V1, accumulation of endogenous polκ co-localises with accumulation of RPA following the localised UV damage (Fig 5.2). The procedure was then repeated on the cell lines XP2YO (XPF deficient), XP2YO wild-type (complemented with wild-type XPF), XP2YO

Figure 5.2 Accumulation of Endogenous Polκ is Detectable by Immunofluoresence

MRC5V1 cells were grown on a coverslip and exposed to UV irradiation through at 5μm pore filter. Following fixation, cells were stained for accumulation of endogenous RPA and polκ. In MRC5V1 cells, endogenous polκ co-localises with RPA and is detectable with the polκ antibody SK04. Accumulation of protein is indicated by the white arrow.

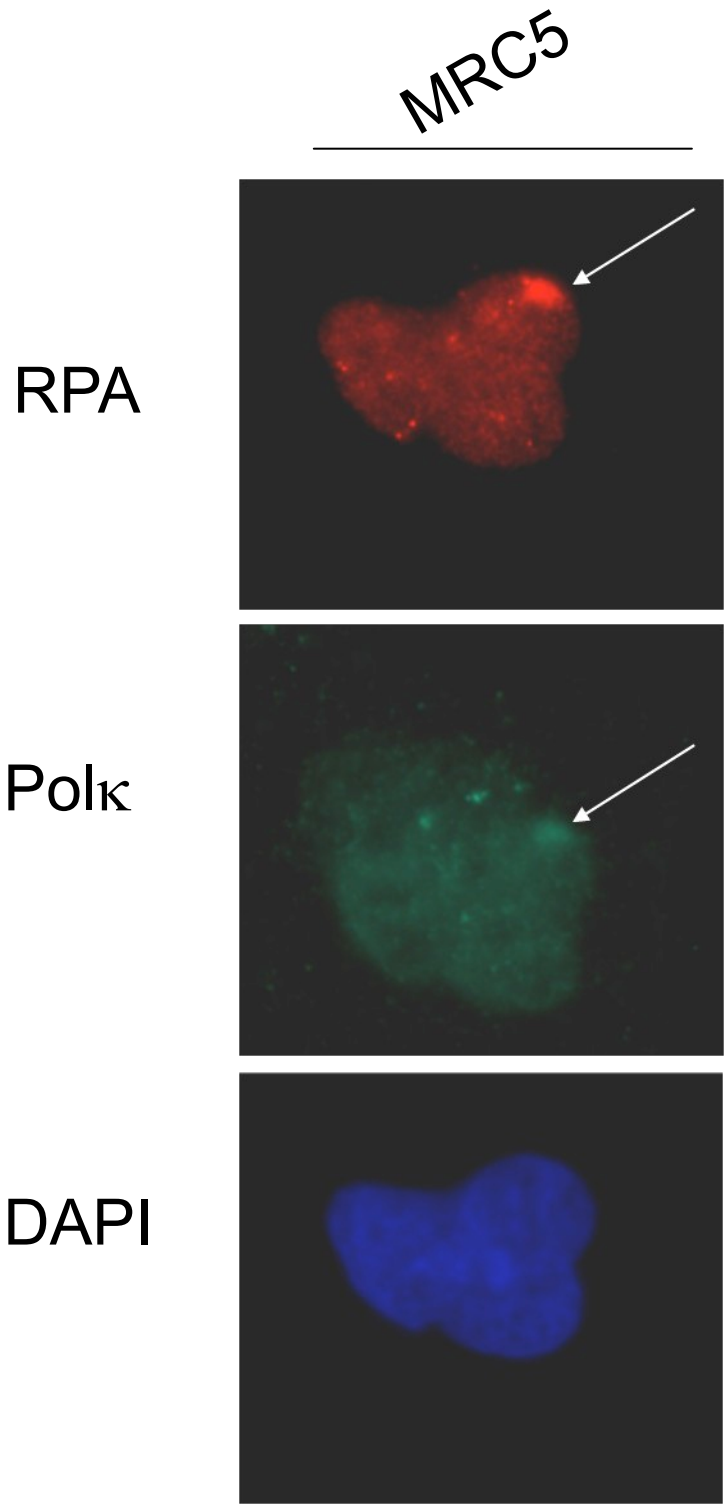
MRC5
RPA
Polκ
DAPI

D676A (complemented with a nuclease defective mutant XPF), XPCS1RO (XPG deficient), XPCS1RO wild-type (complemented with wild-type XPG) and XPCS1RO E791A (complemented with a nuclease defective mutant XPG). As indicated by the white arrows, in some of the cell lines, there is an increased visual concentration of polκ that co-localises with RPA. In XPF cells that are unable to make the 5' incision the accumulation of polκ is not observed (XP2YO, XP2YO D676A), whereas in XPF cells complemented with wild-type XPF, accumulation of polκ is observed (Fig 5.3). In the XPG cells, polκ accumulation is observed even if the 3' incision is still unable to occur (XPCS1RO XPG WT, XPCS1RO E791A). However, if the cell is deficient in XPF then neither incision is possible, consequently no accumulation of polκ is observed (Fig 5.4). However, these accumulations of polκ are not as intense as observed when plasmid carrying GFP-tagged polymerase is transfected in and the polκ antibody results in a large degree of background staining, which was not alleviated by differing extraction/fixation methods or the use of a mouse mono-clonal antibody (data not shown).

5.2 Accumulation of wild-type GFP-polκ following Calcium Phosphate Transfection

Though promising, the results obtained using an antibody against endogenous polκ had high levels of background fluorescence that made firm conclusions on the localisation of the protein in the different cell lines more difficult to obtain. To overcome these shortcomings, transfection with plasmid carrying e*gfp-polκ* was attempted using the traditional technique of calcium phosphate precipitation. This achieved much higher rates of transfection than previously attempted techniques.

To initially test the feasibility of using calcium phosphate to transfect these cell lines, it was first trialled by seeing if the transfection protocol could achieve the successful transfection of a plasmid carrying just *gfp* before moving onto the tagged polymerase construct. The two parental cell lines from which the others were derived, XP2YO and XPCS1RO, were transfected in accordance with the protocol and for this trial, no DNA

Figure 5.3 Accumulation of Endogenous Polκ is Only Observed When XPF is Able to Perform the 5' Incision

XP2YO and derived lines cells were grown on a coverslip and exposed to UV irradiation through at 5μm pore filter. Following fixation, cells were stained for accumulation of endogenous RPA and polκ. In XP2YO XPF WT cells, endogenous polκ co-localises with RPA. This co-localisation is not observed in the absence of functional nuclease, as observed in XP2YO and XP2YO D676A cells. Accumulation of protein is indicated by the white arrows.

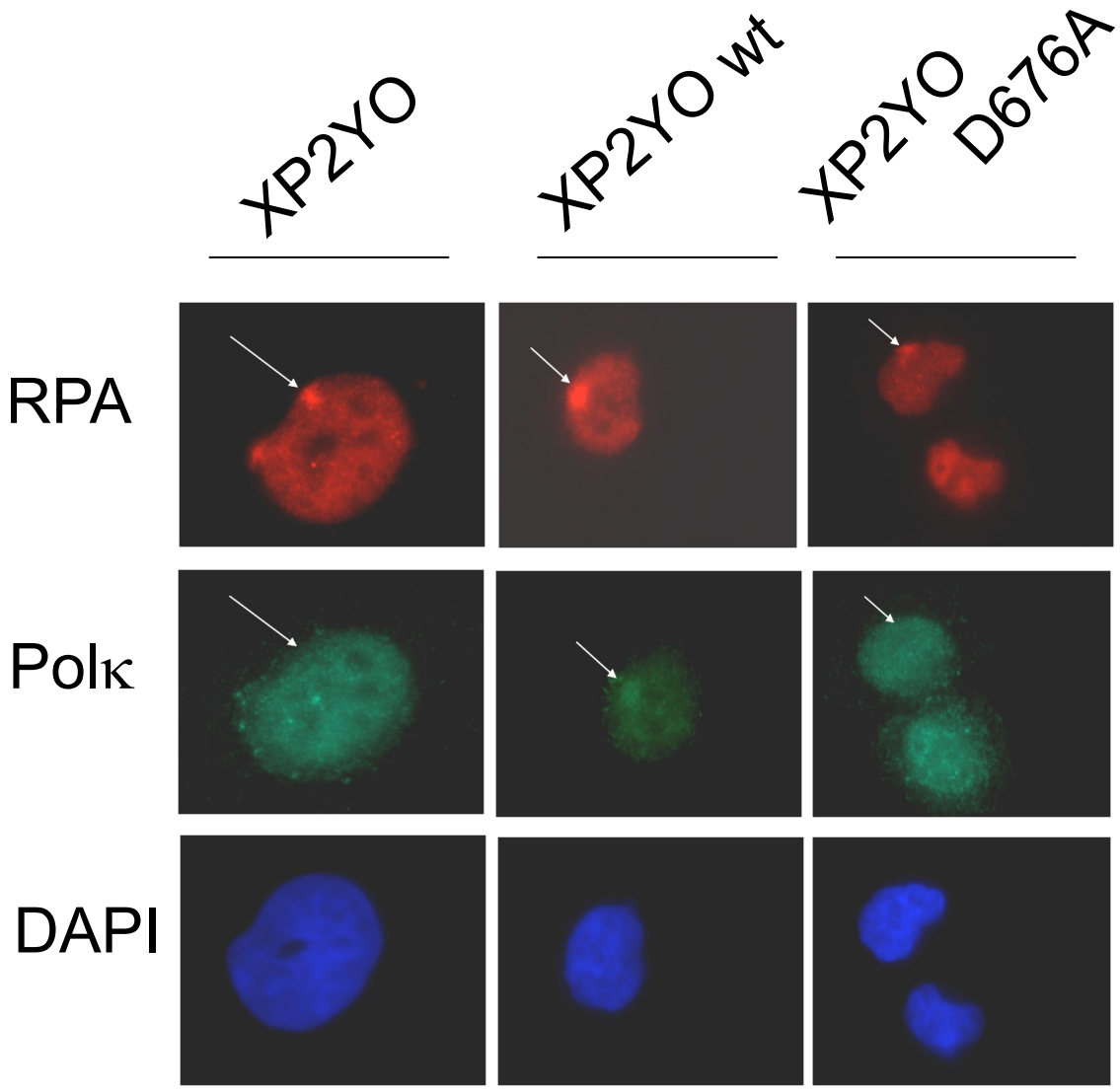
XP2YO
XP2YO wt
XP2YO D676A
RPA
Polκ
DAPI

Figure 5.4 Accumulation of Endogenous Polκ is Observed Independent of XPG Performing the 3' Incision

XPCS1RO and derived lines cells were grown on a coverslip and exposed to UV irradiation through at 5μm pore filter. Following fixation, cells were stained for accumulation of endogenous RPA and polκ. In XPCS1RO XPG WT and XPCS1RO E791A cells, endogenous polκ co-localises with RPA. Accumulation is not dependent on a functional nuclease This co-localisation is observed in the absence of catalytic nuclease, as observed in XPCS1RO E791A cells. Accumulation of protein is indicated by the white arrows.

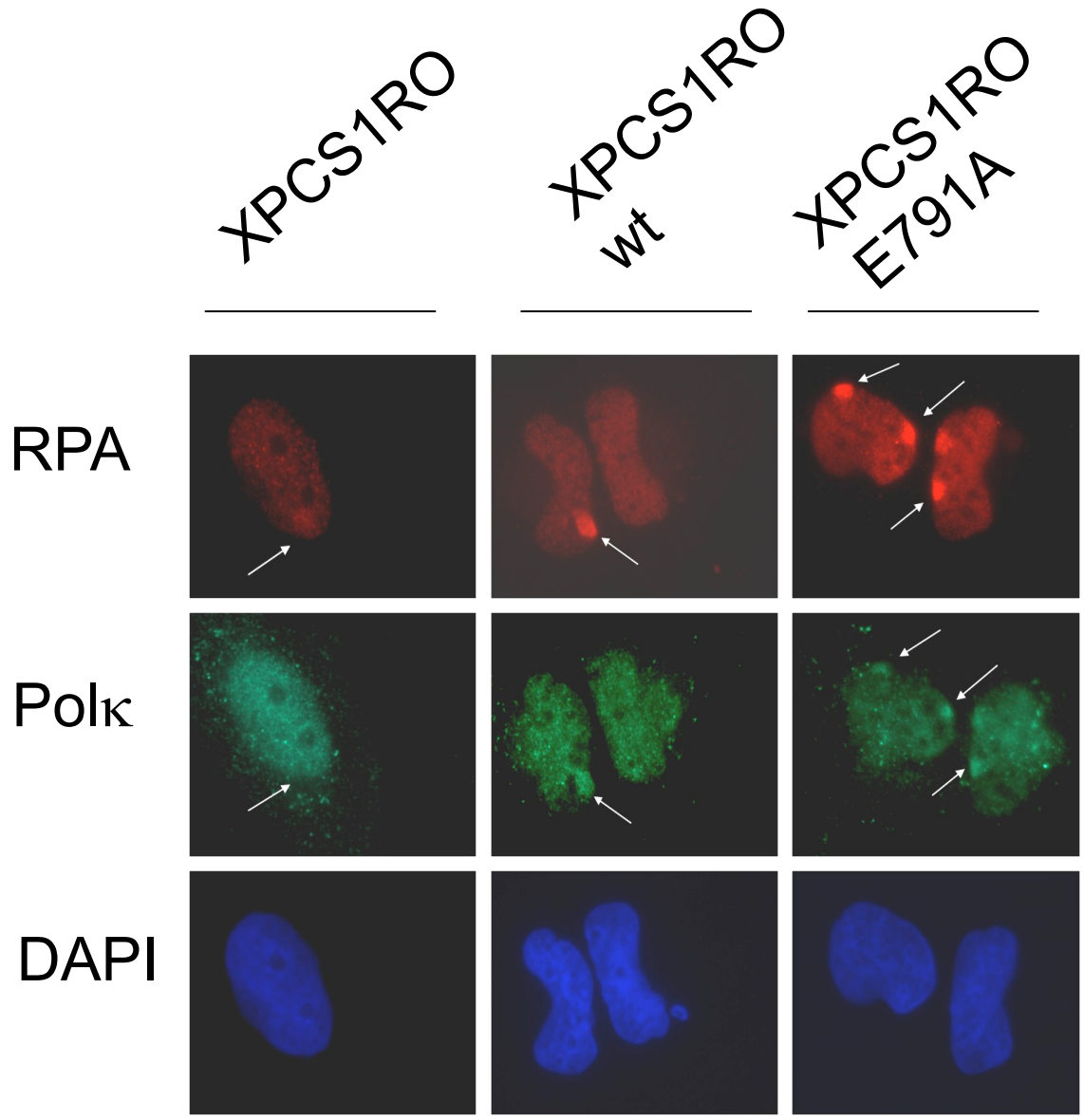
XPCS1RO
XPCS1RO wt
XPCS1RO E791A
RPA
Polκ
DAPI

damage was induced and no staining was used other than DAPI. As can be seen, both cell lines are successfully transfected and express GFP after calcium phosphate treatment (Fig 5.5). Presumably this would apply to the cell lines derived from XP2YO and XPCS1RO and work went forward to re-attempt visualising the accumulation of GFP-polκ following DNA damage in all six cell lines.

As can now be clearly seen, the accumulation of GFP-polκ is different depending on when the incision by the NER nuclease is made. XPA was used as an internal control for NER in these cell lines as RPA accumulation under these conditions was found to be weaker than expected in the XP2YO and XPCS1RO lines and the ones complemented with defective nucleases. GFP-polκ accumulates as previously observed in the cell lines complemented for wild type nucleases, XP2YO wild-type and XPCS1RO wild-type. In XP2YO cells, which are deficient for the 5' nuclease XPF, no accumulation of GFP-polκ is observed. Similar lack of accumulation is seen in the XP2YO cell line complemented with the nuclease dead mutant XPF D676A (Fig 5.6). In XPCS1RO, where XPG is physically absent, there is no observed accumulation of GFP-polκ following localised UV irradiation. Since XPG is physically required to prompt the incision by XPF, this lack of accumulation can be attributed to lack of the 5' incision opening access to the NER gap for the repair synthesis machinery. However, in XPCS1RO E791A, GFP-polκ accumulation is clearly evident and co-localised with XPA. This nuclease-dead mutant of XPG is unable to undertake 3' incision of the DNA backbone but can prompt XPF to cut 5' of the lesion (Figure 5.7). Polκ can therefore be recruited before excision of the damage containing strand is fully completed.

In a fully functional cell capable of carrying out NER with no restrictions on the actions of its nucleases, the coordination of the individual cuts by XPF and XPG is expected to be tightly controlled with minimal delay between the two events. However, these data show that recruitment of polκ can occur without dependency on the complete excision of the

Figure 5.5 XP2YO and XPCS1RO Cell Lines can be Successfully Transfected with Calcium Phosphate Methods

XPCS1RO and XP2YO cells were grown on a coverslip and transfected with plasmid expressing GFP using calcium phosphate. Cells were fixed and stained for DNA using DAPI. In both cell lines, a population of cells were successfully transfected and began to express GFP. Thus the cell lines that had proved refractory to transfection by other means were able to be transfected using the calcium phosphate method.

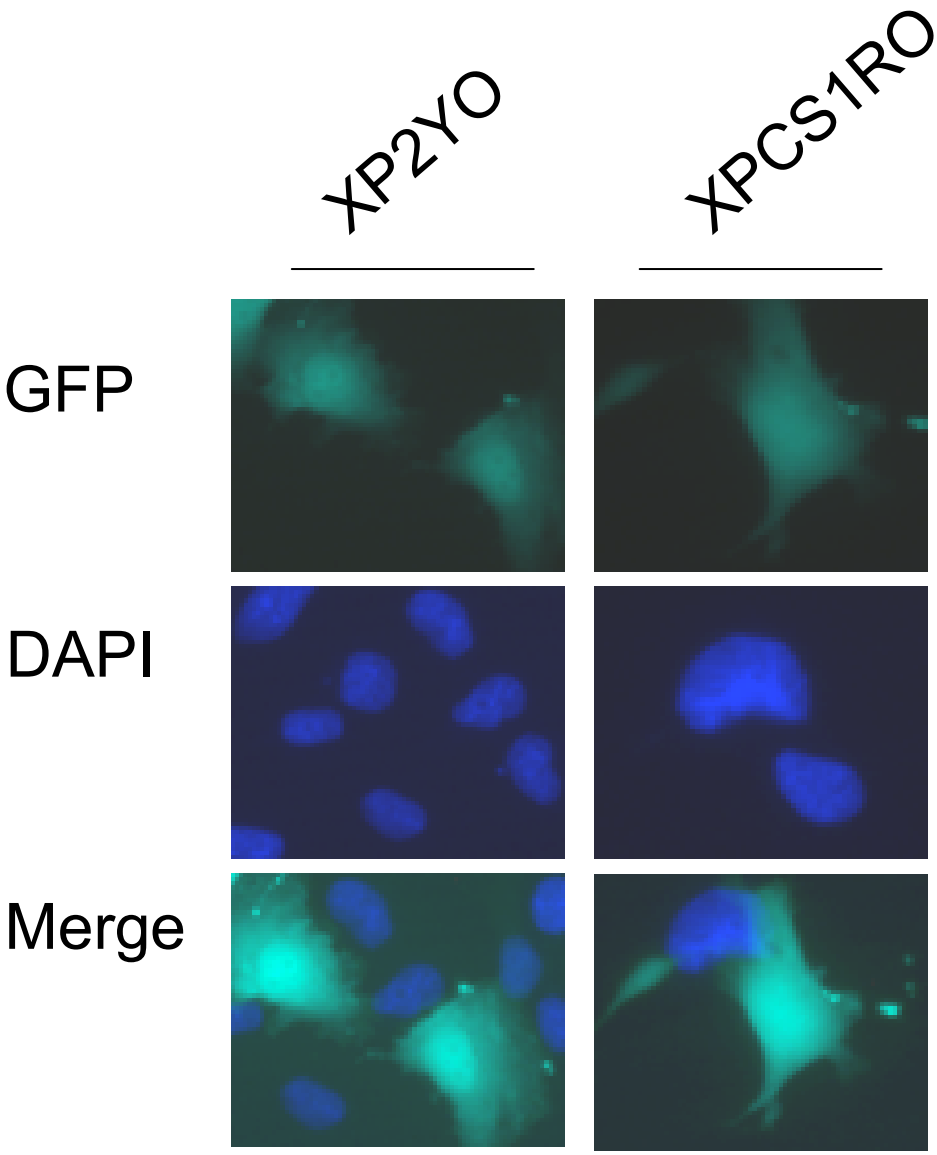
XP2YO
XPCS1RO
GFP
DAPI
Merge

Figure 5.6 Accumulation of Exogenous GFP-polκ is Only Observed When XPF is Able to Perform the 5' Incision

XP2YO and derived lines cells were grown on a coverslip, transfected with plasmid expressing GFP-polκ and exposed to UV irradiation through at 5μm pore filter. Following fixation, cells were stained for accumulation of endogenous XPA. As can now clearly be seen, GFP-polκ accumulation is dependent upon a functional nuclease to make the 5' incision. In cell lines lacking nuclease, XP2YO, or with a non-functional mutant, XP2YO D676A, no accumulation of polymerase is observed. Accumulation is marked out with white arrows.

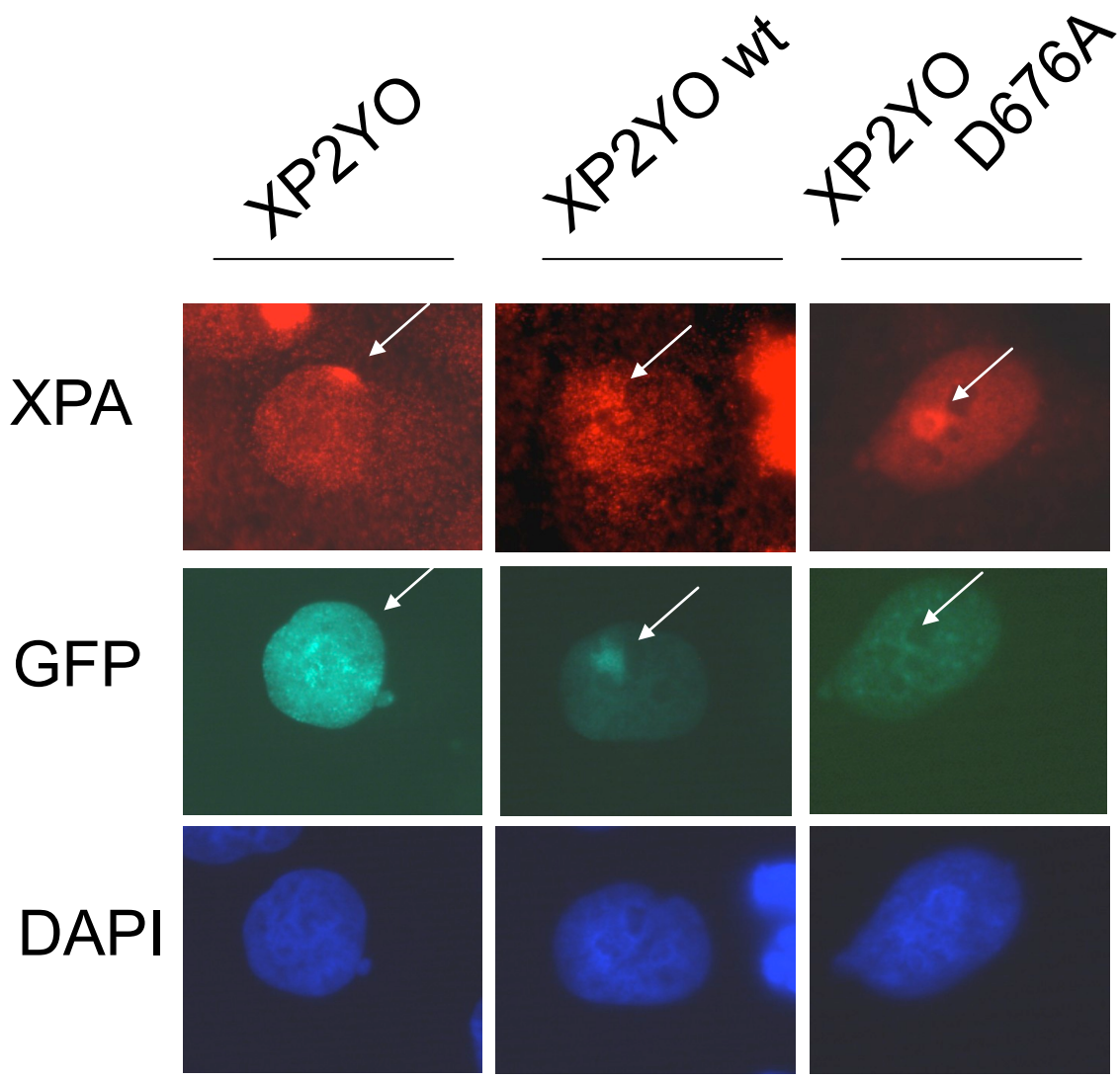
XP2YO
XP2YO wt
XP2YO D676A
XPA
GFP
DAPI

Figure 5.7 Accumulation of Exogenous GFP-polκ is Observed Independent of XPG Performing the 3' Incision

XPCS1RO and derived lines cells were grown on a coverslip, transfected with plasmid expressing GFP-polκ and exposed to UV irradiation through at 5μm pore filter. Following fixation, cells were stained for accumulation of endogenous XPA. As can now clearly be seen, GFP-polκ accumulation is dependent upon the 5' incision but not the 3' incision. Cell lines with functional XPG, XPCS1RO wt, or non-catalytic XPG, XPCS1RO E791A, GFP-Polk accumulates following damage. In cell lines lacking nuclease XPCS1RO, no accumulation of polymerase is observed. Accumulation is marked out with white arrows.

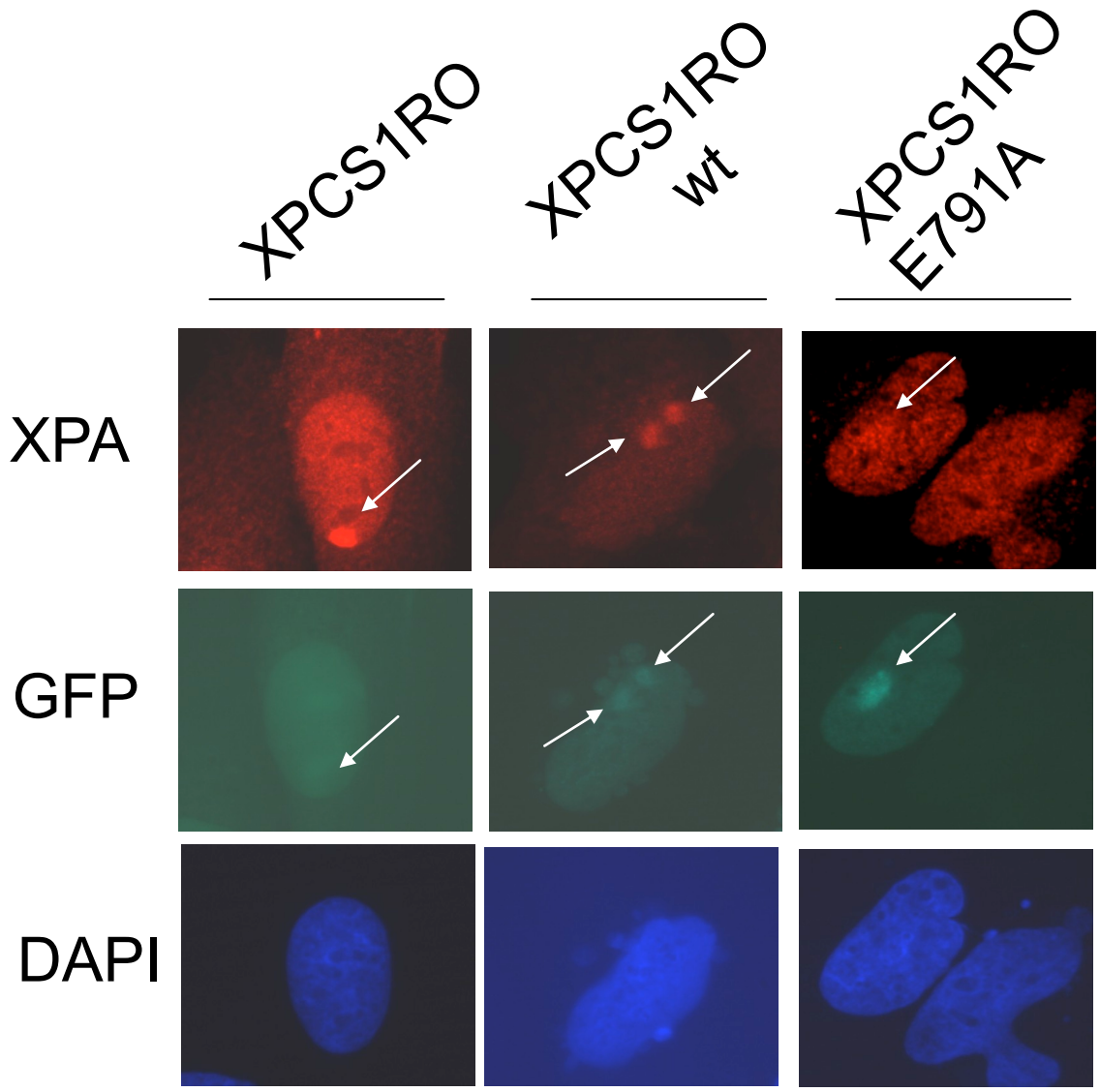
XPCS1RO
XPCS1RO wt
XPCS1RO E791A
XPA
GFP
DAPI

damaged DNA. This raises the possibility that repair synthesis can begin before the NER excision process is fully completed (Fig 5.1, right side of branched pathway).

5.3 Discussion

The main emphasis of this thesis has been the investigation of the role of the identified conserved residues in human polκ. Also addressed is the recruitment of the polymerase dependent on the coordinated actions of the nucleases XPG and XPF. This built on work done by Staresincic *et al* which used cell lines deficient in, or complemented with wild-type or mutant nucleases to separate temporally the order of excision and recruitment of resynthesis factors (Staresincic et al., 2009). It was observed that XPF nuclease made a 5' incision independent of nicking on the 3' side by XPG but this was dependent on the physical presence of the XPG nuclease. It was further observed by Staresincic *et al.* that various repair synthesis factors such as polδ and PCNA were recruited following the incision by XPF but did not require the full excision of the damage-containing strand by the subsequent incision by XPG. This work, together with the role for polκ in repair synthesis suggested by Ogi *et al.*, led us to propose that recruitment of polκ might also proceed in the same manner.

Though the cell lines XP2YO and XPCS1RO and their derivatives proved remarkably resistant against lipid/polymer transfection reagents, the recruitment of polκ was initially observed using antibody against endogenous polymerase and then confirmed using transfection with the calcium phosphate method. The reasons for this refractory nature against commonly used transfection reagents are unknown, though it is probably as straightforward as a simple 'quirk' of the cell lines. Since the antibody based immunofluoresence and the expression of transiently transfected GFP-polκ wild-type both resulted in the same outcome, they will be considered together.

It would probably be most straightforward to analyse the results broken down into the individual cell lines. Firstly, the XP2YO cell line which is deficient in the nuclease XPF and,

as such, cannot make the 5' incision in NER. No accumulation of polymerase was seen in this cell line whereas the accumulation of upstream factors that are recruited during the unwinding phase of NER (RPA, XPB, XPA, etc) was observed. If the cell line is complemented with wild-type XPF nuclease and is fully competent in NER, then polκ is seen to accumulate at localised damage as in other NER wild-type cell lines. If this complementation is replaced with XPF D676A, which has had its catalytic site disabled, then the physical presence is not sufficient to recruit the polymerase (Fig 5.3 and 5.6). In the XPCS1RO cell line, the lack of XPG prevents the recruitment of polκ. When the cell line expresses wild-type XPG, recruitment of the polymerase is seen as expected. If this nuclease is replaced with XPG E791A, abrogated in its nuclease activity, the recruitment of the polymerase is still observed (Fig 5.4 and 5.7). This is consistent with the results of other resynthesis factors seen by Staresincic *et al.* in which it is the physical presence of the XPG that licences the XPF to proceed with its incision. This 5' incision is not reliant on the 3' incision being made at all. Once the 5' incision has been made, this would open up a flap structure in the DNA with a double stranded/single stranded junction that would act as a site of loading for repair resynthesis factors. Combining these data with observations from Staresincic *et al*, Overmeer *et al*, Giannattasio *et al* and Sertic *et al* it strongly suggests a model where no single-stranded gap is ever generated during 'normal' NER (Giannattasio et al., 2010; Overmeer et al., 2011; Sertic et al., Manuscript in Preperation; Staresincic et al., 2009) Immediately after the 5' incision by XPF, resynthesis factors are recruited to the dsDNA-ssDNA junction and begin to restore the excised DNA. The absence of a successful 3' incision by XPG creates an opportunity for extensive digestion by the nuclease exo1, exposing a long ssDNA region capable of triggering the checkpoint.

Under the model of polκ involvement in NER as proposed by Ogi *et al*, polκ is recruited to sites of NER by interaction with ubiquitinated PCNA and the scaffolding protein XRCC1, which also recruits the ligase Lig3 (Ogi et al., 2010). It is tempting to envisage a scenario where arrival of the repair synthesis factors can then induce XPG to make the 3' incision, coupling the completion of excision to the completion of DNA synthesis. If this

completion is competing against digestion by exo1, the timely arrival of the repair synthesis machinery would be important to avoid undue digestion and checkpoint activation. This supports a proposed role of polκ for NER under low nucleotide conditions. The k_{cat}/K_m of polκ is 0.86-2.15; polκ is substantially more efficient under low nucleotide conditions than that of the replicative polymerases (Haracska et al., 2002; Suzuki et al., 2001). Polκ may play a role in taking over from an inefficient replicative polymerase to complete repair synthesis and prevent inappropriate activation of the checkpoint. Even in non-dividing cells, checkpoint activation can lead to downstream events detrimental to the cell.

However, this outlined model is difficult to reconcile with the observations of Overmeer *et al*, who showed that XPG can disassociate from NER complexes independent of the completion of repair synthesis and that inhibition with HU or ligase inhibitors can stall the repair synthesis factors at sites of damage for up to 20 hrs. XPG may only have a limited window of time to make its incision before dissociating from the repair site. The extended accumulation of repair synthesis factors at late time points may either represent genuinely stalled repair or could be repair synthesis machinery unable to continue resynthesis and subsequently out competed by the Exo1 nuclease.

Chapter 6 – Interactions Between Human DNA Polκ and Ubiquitinated Proteins

Prior experiments detailed in this thesis have established a requirement for conserved residues inside the UBZ domains of human polκ for successful recruitment to sites of NER following UV irradiation. Conversely, depletion of the pool of free ubiquitin impaired recruitment of the wild-type polymerase. This was expanded upon by the use of cell lines created to stably express GFP-tagged polκ either in with its wild-type sequence or with mutations to conserved residues. These experiments showed a reliance on functional UBZ domains for long term survival following UV, implicating a vital role in global genomic repair. Curiously, these residues were not required for transcription-coupled repair involvement. Thus it appears that for successful involvement of the polymerase in NER, there is a need for a polκ to interact with an ubiquitinated protein.

Several previous studies have established that murine and human polκ interact with ubiquitinated PCNA following DNA damage. Murine polκ was shown by Guo *et al* to interact with mono-ubiquitinated PCNA in a manner that was dependent on intact UBZ domains. However, it should be noted that they tested for interaction eight to sixtheen hours after incubation, at which time a large proportion of the DNA damage would have been repaired by NER. Thus the interaction seen by Guo might represent the interaction between ubiquitinated PCNA and murine polκ in a TLS context as opposed to a NER context (Guo et al., 2008). More recently, Ogi *et al* tested human polκ involvement in NER and used ChIP techniques to determine which proteins were required for the involvement of the polymerase in NER. The ubiquitinated species of PCNA was observed following UV irradiation and after only one hour recovery time. This work clearly established an involvement for ubiquinated PCNA in NER as a scaffold for human polκ (Ogi et al., 2010).

Is this interaction between human polκ and ubiquitinated PCNA mediated directly through the UBZ domains? Might other ubiquitinated species interact with polκ through its UBZ domains? To identify ubiquitinated proteins that interact with polκ and to test if those

interactions are disrupted by mutations in the UBZ domains of human polκ, I have attempted to purify either wild-type GFP-tagged polκ or the D676AD799A and C779AC782A mutants and compare what ubiquitinated proteins co-purify with each construct.

6.1 Isolation of Wild-type GFP-polκ from Transfected HEK293 Cells

Initial steps to determine the feasibility of the experiment required a determination of the ability to recover GFP-polκ followed by screening for associated proteins. Initially I attempted to transfect human embryonic kidney (HEK293) cells with GFP-polκ and IP from cell extracts with anti-GFP to isolate the polymerase and any associated proteins. Ubiquitinated species could then be detected through western blotting for ubiquitin. However, the results obtained were unsatisfactory and may have been biased toward free GFP-polκ. If only a small subset of the over-expressed protein is associated with endogenous partner proteins following damage, then this would increase the difficulty of detection following the IP.

To overcome this difficulty, a two-stage purification was proposed. The HEK293 cells would be co-transfected with plasmids carrying *gfp-polκ* and a plasmid carrying *6xhis-ubiquitin* respectively. Following UV damage, treatment with hydroxyurea and cross-linking, the lysates would be allowed to bind to nickel nitrilotriacetic acid agarose beads (NiNTA beads). From work by Ogi *et al*. and expanded upon by Overmeer *et al.,* the inclusion of HU was intended to stall the completion of repair synthesis in an attempt to increase the duration of polκ at NER events. If, as work by Ogi *et al* had indicated, a relatively stronger preference for the use of polκ under low nucleotide conditions existed, the application of HU could help prompt the participation of polκ in the repair process during the recovery period. Additionally, work by Overmeer *et al* showed that HU stalled the resynthesis step and thus halted the completion of the repair process (Overmeer et al.,

2011). This would also help recovery of polκ by stalling the dissociation of resynthesis factors.

If 6xhis-ubiquitin was present and cross-linking successful, then GFP-polκ should be able to be successfully recovered from the elutions of the NiNTA beads. Additionally, this would enrich the elution for 6xhis-ubiquitin and proteins that had been post-translationally modified by 6xhis-ubiquitin, aiding detection for proteins associated with polκ at subsequent points in the investigation.

Firstly, it was necessary to verify whether GFP-polκ itself had any non-specific binding to the NiNTA beads. To accomplish this, HEK293 cells were transfected with eGFP-C3 plasmid containing either *gfp* or *gfp-polκ*. In addition, all cells were transfected with the plasmid pMSCV, which carries no genes to be expressed, in place of the *6xhis-ubiquitin* vector. This ensured that the amount of DNA was equivalent between experiments. The cells expressing GFP-polκ were divided into two groups, which were either unirradiated or treated with UV radiation. Following the UV irradiation, the media on all plates was changed to DMEM supplemented with 10% FCS and 10mM hydroxyurea.

Proteins bound and eluted from the NiNTA beads were analysed by SDS-PAGE (Figure 6.1). No proteins were detected by Western Blot in lysates from cells over-expressing GFP (lanes 1-4). Over-expression of GFP-polκ shows some degree of unspecific binding (lane 8), which had also been observed using other Y-family polymerases purified from NiNTA beads (S. Sabbionedda – personal communication).

Alongside these transfections, cells on an identical set of plates were co-transfected with the vector containing *6xhis-ubiquitin* instead of the vector pMSCV. These plates were treated identically to the previous set. As can be seen (Figure 6.2), once again there is no recovery of GFP from the NiNTA beads even when 6xhis-ubiquitin is co-expressed (lane 4).

H

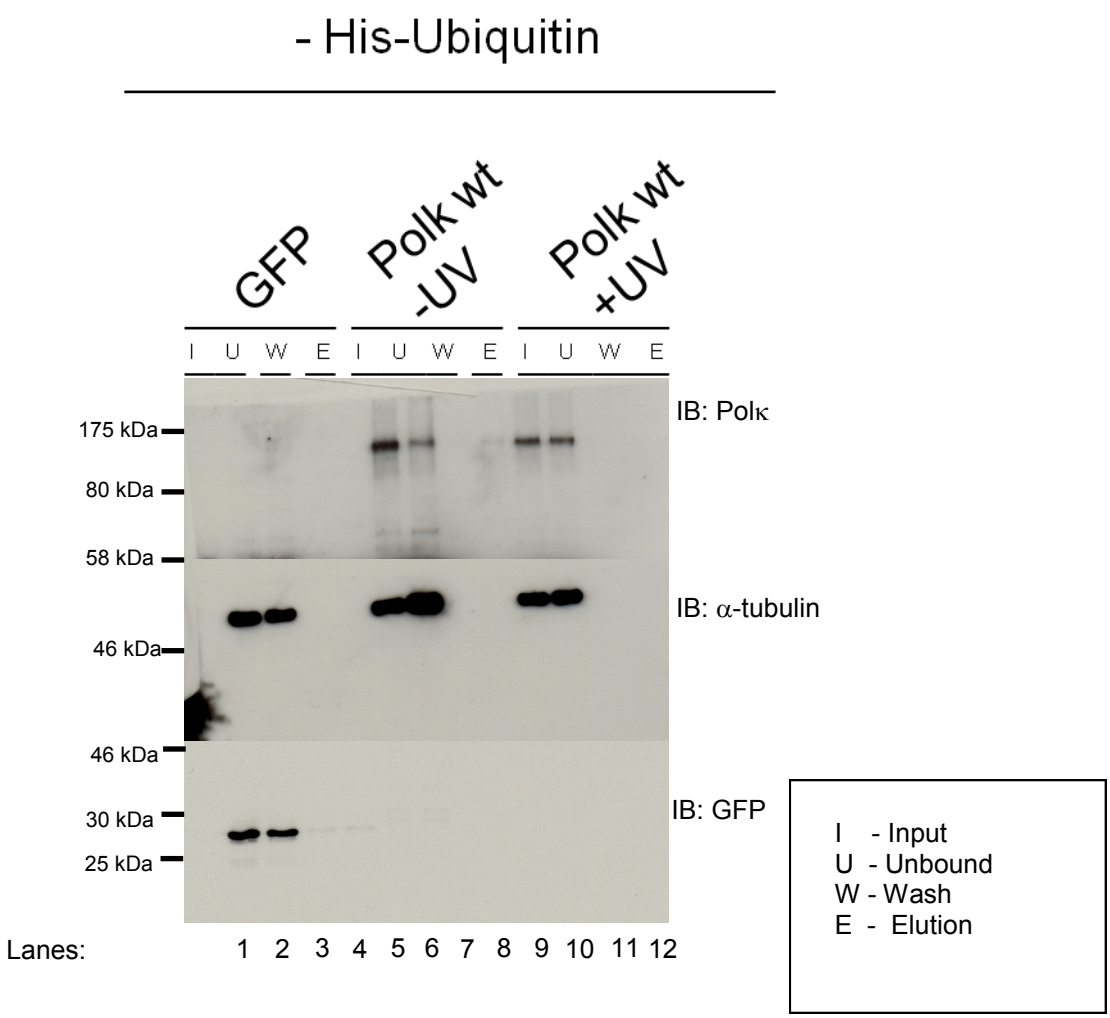

Figure 6.1 - Elution of GFP-Polκ wt from NiNTA Beads Transfected without 6xHis-Ubiquitin

HEK293 cells were transfected with pMSCV and plasmids carrying *gfp* or *gfp-polκ* and proteins were crosslinked and purified on nickel agarose beads. GFP does not bind to the beads. GFP-polκ demonstrates a limited degree of non-specific binding to nickel beads however the retention is minimal. Tubulin is included as a loading control.

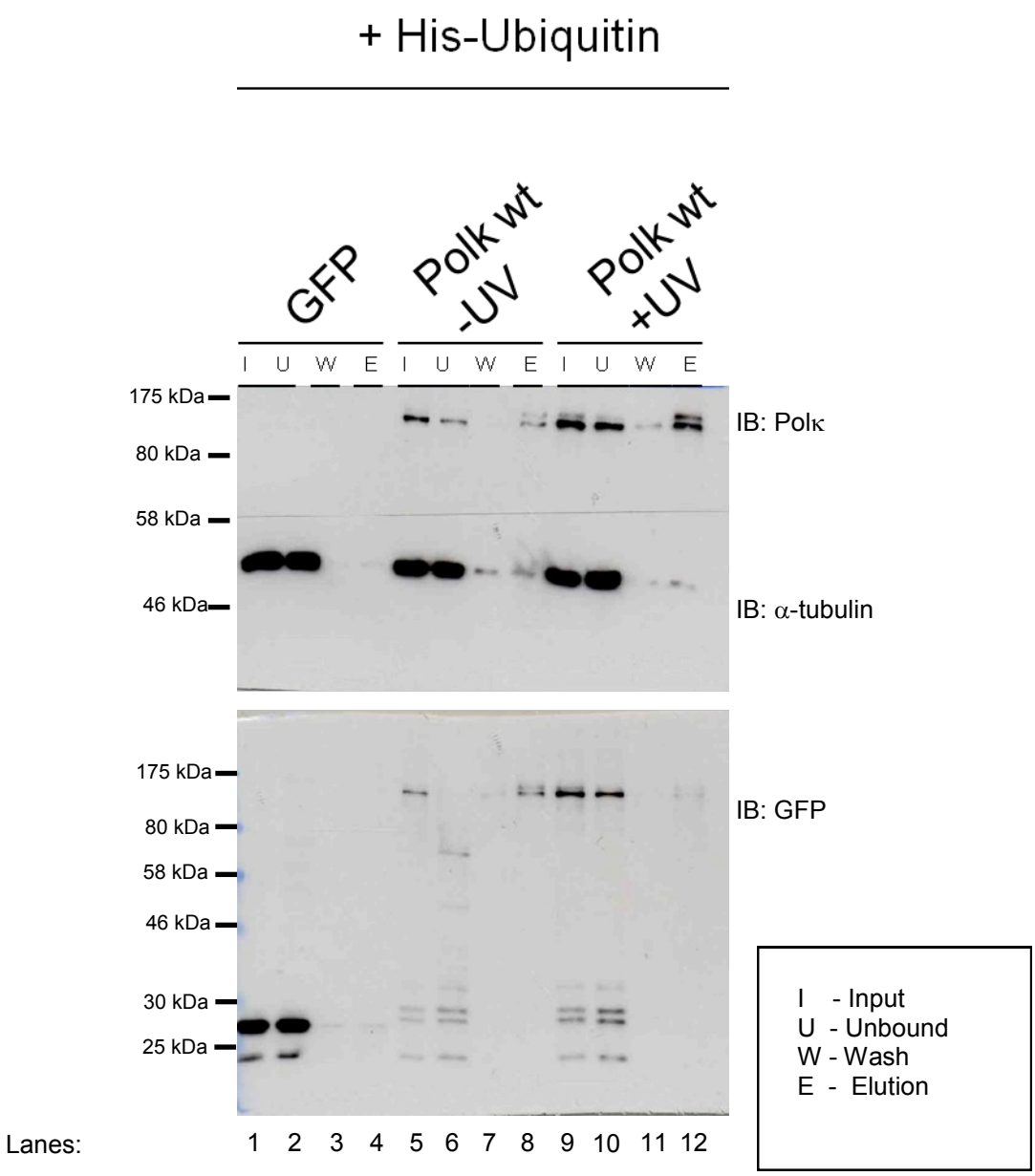

Figure 6.2 - Nickel Purification of GFP-Polκ from HEK 293 Cells Transfected with his-Ubiquitin

HEK293 cells were co-transfected with plasmid carrying his-tagged *ubiquitin* and *gfp* or *gfp-polκ* before crosslinking and purification using nickel agarose beads. However, GFP-polκ is now enriched in the elution fraction when co-expressed with his-ubiquitin.

owever, bands representing GFP-polκ eluted from the beads were detected, whether or not the cells have been exposed to UV (lanes 8, 12) (Figure 6.2).

6.2 Pulldown of GFP-polκ UBZ Mutants from Transfected HEK293 Cells

The previous experiment indicated an enhanced recovery of GFP-polκ when co-transfected with 6xhis-ubiquitin, though a degree of unspecific binding was noted when the co-transfectant was the empty vector pMSCV. To see if this yield is similar in variants of the polymerase with mutations in the UBZ domains the experiment was repeated with plasmids carrying *gfp-polκ wild-type*, *gfp-polκ D644AD799A* or *gfp-polκ C779AC782A* respectively. In all transfections, the plasmid carrying 6xhis-ubiquitin was co-transfected.

Again, the wild-type GFP-polκ was successfully recovered from the NiNTA beads (Figure 6.3, lanes 4, 8). Comparatively less was recovered from the beads incubated with lysates containing GFP-polκ D644AD799A (lanes 12, 16). This limited recovery may represent non-specific binding of polκ to the beads seen previously in the absence of 6xhis-ubiquitin (Figure 6.1). Equally, polκ is ubiquitinated itself and this ubiquitination appears not to depend on the conserved residues in the UBZ domains. This 6xhis-ubiquitinated polκ would interact with the NiNTA beads and be recovered following elution. Intriguingly, there was a partially greater recovery of GFP-polκ C779AC782A compared to the other UBZ mutation bearing protein but not as substantial as that seen with the wild-type polymerase. This recovery may be explained by the mutations in GFP-polκ C779AC782A only affecting one of the UBZ domains; thus, the unaltered domain might still be able to have some degree of binding to 6xhis-ubiquitin-tagged proteins under these *in vitro* conditions while still rendering the polymerase dysfunctional under *in vivo* circumstances (Figure 6.3).

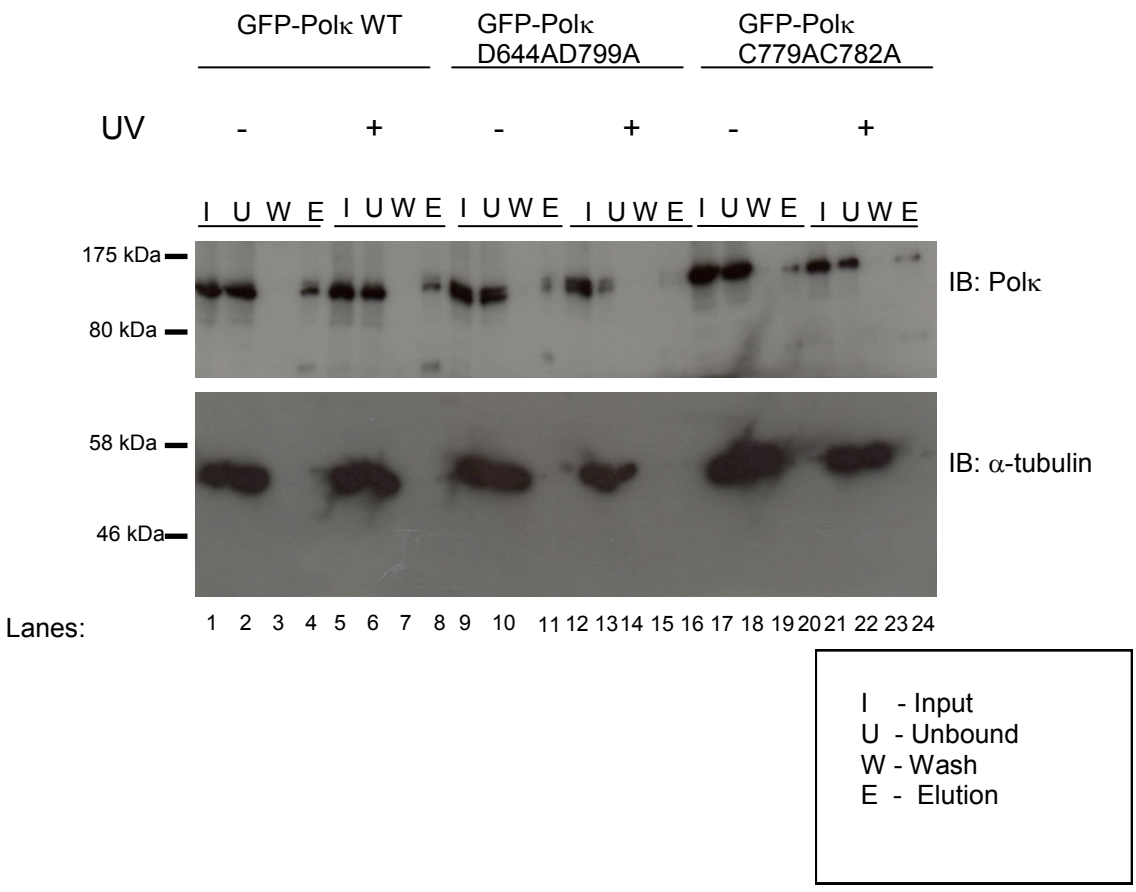

Figure 6.3 - Nickel Purification of GFP-polκ UBZ Domain Mutants from HEK 293 Cells Transfected with his-Ubiquitin

HEK293 cells were transfected with plasmid carrying his-tagged *ubiquitin* and plasmid carrying either *gfp-polκ* or the two zinc finger ubiquitin binding motif mutants before crosslinking and purification on nickel agarose beads. As previously shown, the wild-type GFP-polκ is enriched in the elution fraction. The mutant polymerases show a degree of binding to the nickel agarose beads but at a reduced level comparative to wild-type.

6.3 Isolation of GFP-tagged Proteins from Elutions off NiNTA Beads

Out of the total population of proteins present in the co-transfected HEK293 cell lysates, the pulldown from the NiNTA beads served to isolate the fraction of proteins that had been modified with 6xhis-ubiquitin and any proteins in local proximity that were cross-linked together. From the elutions obtained off these beads, it should then be possible to collect the subpopulation of 6xhis-ubiquitin modified proteins cross-linked to GFP-polκ specifically by immunoprecipitation with an antibody targeted against GFP. The elutions were increased to a final volume of 500 µl with IP buffer to dilute the imidazole and adjust the salt and pH levels appropriate for use on the magnetic Dynabeads. The *IP Inputs* were incubated with GFP antibody and then bound to the Dynabeads. After washing, the bound proteins were eluted by boiling in SDS-containing loading buffer and run on a SDS-PAGE gel to determine the recovery of GFP-polκ.

As expected, a larger amount of GFP-polκ is evident in the input from the sample obtained from the co-transfection of *gfp-polκ* with *6xhis-ubiquitin* bearing plasmids (Figure 6.4, lanes 1, 4). However, there was still a substantial recovery of GFP-polκ from the sample lacking 6xhis-ubiquitin, presumably due to the presence of GFP-polκ in the input due to the unspecific binding to the NiNTA beads that was observed (Figure 6.1, lanes 8, 12).

6.4 Screening of Bound Fractions from Dynabeads for 6xhis-Ubiquitin tagged Proteins

Having observed that it is possible to recover GFP-polκ after two separate purification steps, the elutions were analysed to determine what other proteins may have been recovered from the IP. My goal was to identify proteins modified with 6xhis-ubiquitin that interact with polκ, but not if the polκ was mutated in the UBZ domains. The eluted samples were run on SDS-PAGE gels and probed with antibodies against histidine and ubiquitin respectively.

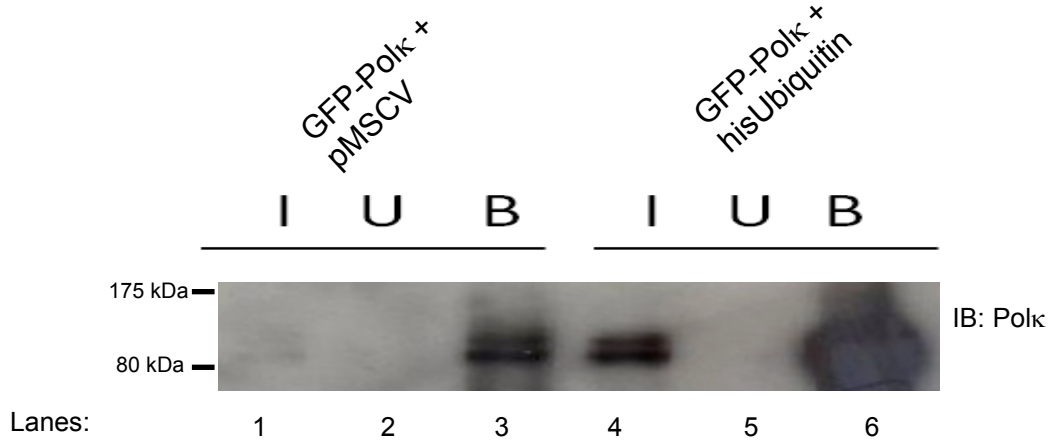

I - Input
U - Unbound
B - Bound

Figure 6.4 - Immunoprecipitation of GFP-Polκ

From the fractions eluted off of the nickel agarose beads, samples were diluted in IP Buffer and incubated with anti-GFP and Dynabeads overnight to isolate the GFP-polκ containing fraction. On a 8% gel the *input*, *unbound* and *bound* fractions were probed with antibody against polκ to verify the purification.

As can be seen (Figure 6.5), when the elutions are probed with anti-histidine, there are strong bands corresponding to the heavy and light IgG chains of the antibody used for the IP. These chains were present in all samples that had been purified by IP and where their presence was not alleviated by use of TrueBlot (a horseradish peroxidase conjugated secondary antibody that, in theory, only recognises intact antibodies and not the denatured chains present in the fractions bound to the Dynabeads) or by changing the species that the primary antibody was derived from. Despite this, it is possible to see in the wild-type GFP-polκ lanes a band that is absent in the samples expressing UBZ domain mutant of the polymerase (lanes 1 and 2). This band is stronger in the sample in which the cells had been UV irradiated prior to cross-linking and purification. Included is a sample derived from a stable cell line expressing 6xhis-PCNA to help aid in determining the size of any bands observed and for recovery of 6xhis-tagged proteins (Figure 6.5).

Samples were then re-run on a fresh gel and the subsequent membrane was probed with antibody against ubiquitin to confirm the presence of the band seen when probed with anti-histidine. Again, there appears to be a band present in the wild-type GFP-polκ samples that may not be present in the samples lacking 6xhis-ubiquitin (lanes 3 and 4). However, identification is difficult due to the presence of the IgG bands and their reactivity to the secondary antibody (Figure 6.6).

The size of the band falling between 25kDa and 50kDa suggested that it might potentially be the ubiquinated species of PCNA. To investigate, the fractions obtained from the Dynabeads were run on an SDS-PAGE gel and the membrane probed with an antibody raised against PCNA. This time, in an attempt to avoid saturation of the signal by the bands corresponding to the IgG chains, the areas of the membrane corresponding to those bands were excised prior to incubation with primary antibody. However, no band corresponding to PCNA is visible in the fractions obtained from the Dynabeads, whereas a strong band was obtained from a control sample consisting of lysate from an MRC5 line expressing both endogenous PCNA and a 6xhis-PCNA stable integration (Figure 6.7).

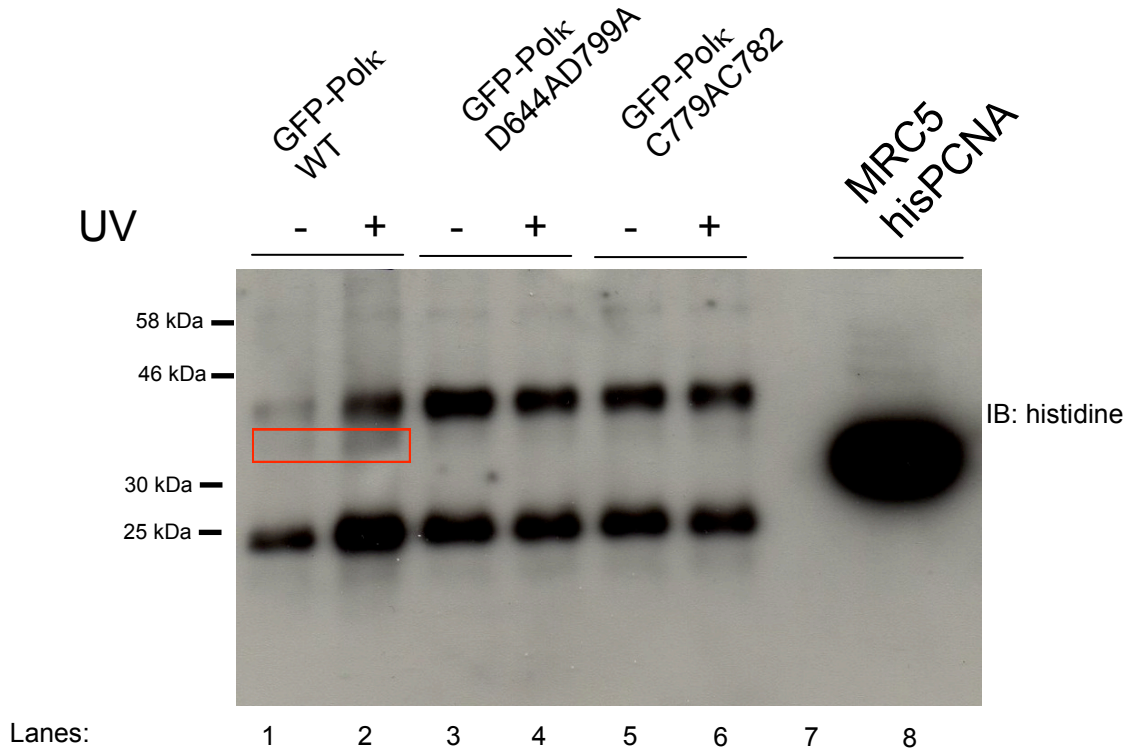

Figure 6.5 - Identification of Cross-linked Proteins – Probing with Anti-Histidine

Eluted fractions from the anti-GFP IP were run on a 15% SDS-PAGE gel and probed with antibody against histidine. Despite the strong presence of IgG light and heavy chain bands, a band is visible in the wild-type GFP-polκ sample that is not present in samples bearing UBZ mutations. A sample of MRC5V1 expressing his-tagged PCNA is run alongside as a control for detection of his-tagged proteins and for size comparison of identified proteins.

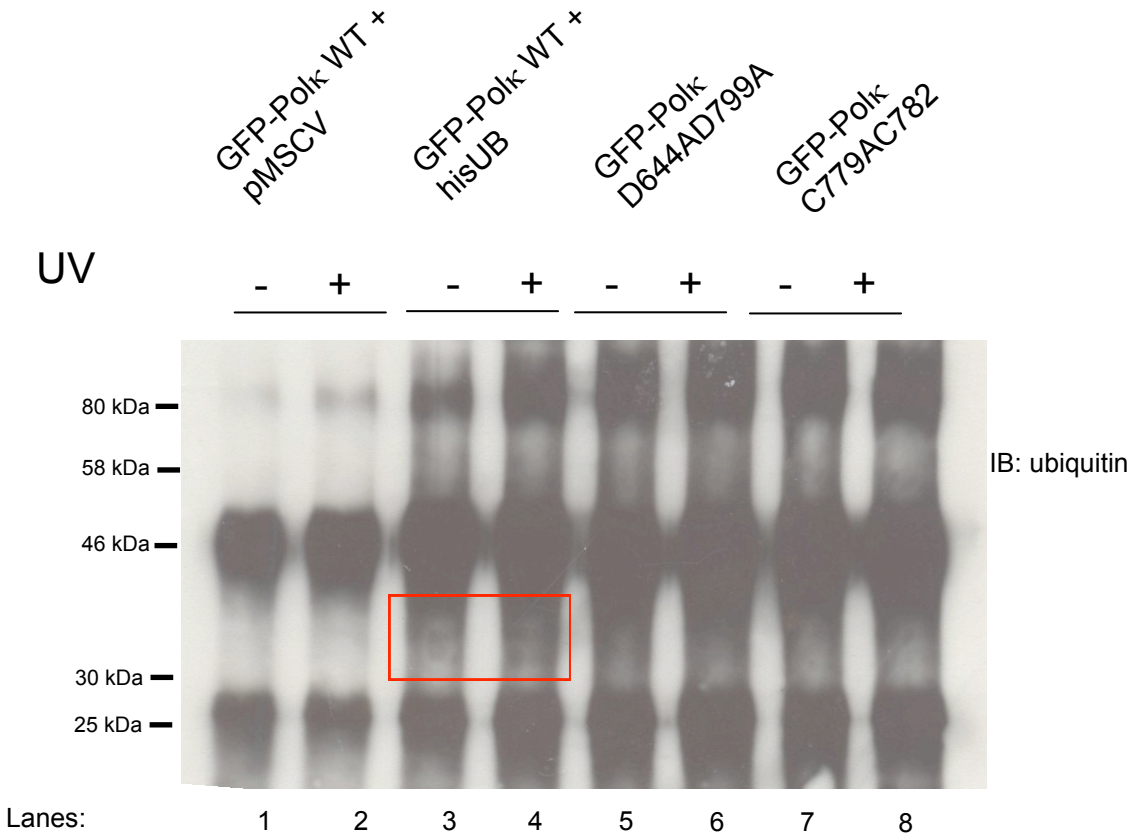

Figure 6.6 - Identification of Cross-linked Proteins – Probing with Anti-Ubiquitin

Elutioned fractions from the anti-GFP IP were run on a 10% gel and probed with an antibody raised against ubiquitin. Despite the strong presence of IgG light and heavy chain bands, a band is visible in wild-type GFP-polκ that is not present in the UBZ mutation bearing constructs or in the wild-type GFP-polk co-transfected with pMSCV.

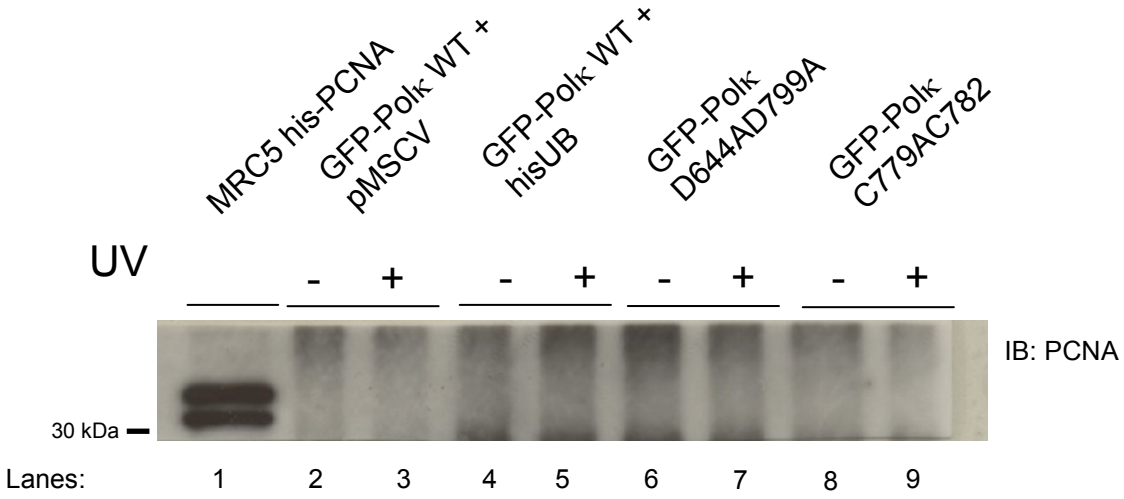

Figure 6.7 - Identification of Cross-linked Proteins – Probing with Anti-PCNA

Based on the observations in previous blots where a band was visible in the region between the 46 and 30 kDa markers, the elutions from the IP were probed for species of PCNA with the IgG light and heavy chain regions removed to reduce the signal from being overpowered. Unfortunately when tested directly for PCNA species, no band was visible in the region.

6.5 Screening of Bound Fractions from GFP-TRAP Beads for 6xhis-Ubiquitin tagged Proteins

The inability to remove the IgG chain signals by changing primary or secondary antibody represented a major obstacle to proper identification of any bands in the regions of approximately 25kDa to 50kDa. To overcome this limitation, it was suggested to use beads where the anti-GFP was covalently bound to the sepharose. This should drastically limit or eliminate any problem with antibody chains. GFP-Trap beads were obtained from Chromotek and substituted for the Dynabeads in the purification protocol.

When the experiment was re-run with all plates UV irradiated, successful recovery of wild-type GFP-polκ from the NiNTA beads is observed (lane 8), with some recovery from samples lacking 6xhis-ubiquitin (lane 4) or the modified UBZ domains (lanes 12, 16) as was observed previously. These elutions were then diluted as before and incubated with the GFP-Trap beads. As can be seen, a successful recovery of GFP-polκ was observed (Figure 6.8).

With the successful recovery of GFP-polκ from the GFP-Trap beads following purification from NiNTA beads, the bound fractions were fractionated on SDS-PAGE gels and probed with antibodies against PCNA, as attempted previously. Unmodified PCNA and post-translationally modified PCNA were clearly detected (Fig 6.9). Using a sample of a cell line expressing 6xhis-tagged PCNA alongside endogenous PCNA as a control for detection and a guide to size identification, the following can now be seen clearly: firstly, as expected, there is no band that corresponds with the size of 6xhis-ubiquitin-PCNA from cells expressing wild-type GFP-polκ but 6xhis-ubiquitin was not co-expressed (lane 9). Secondly, a band of appropriate size is now prominent when 6xhis-ubiquitin is co-expressed with wild-type GFP-polκ (lane 10). This band is markedly reduced in the samples in which wild-type GFP-polκ was replaced with the UBZ domain mutant constructs (lanes 11, 12). While the recovery of the D644AD799A construct was reduced, the C779AC782A construct had a yield equivalent to the wild-type polymerase while also

Figure 6.8- Use of Chromotek GFP-Trap Beads to Isolate Cross-linked Proteins

To eliminate the overexposure of IgG light and heavy chains, GFP-TRAP beads with covalently bound anti-GFP were used in place of Dynabeads.

A) HEK293 cells were transfected as before and the his-tagged fraction of proteins were isolated by use of nickel agarose beads. As seen previously, wild-type GFP-polκ co-transfected with his-tagged ubiquitin is recovered to a greater extent than when no his-tagged ubiquitin is present or in the GFP-polκ constructs with mutations to the UBZ domains.

B) The elutions from the nickel agarose beads were then incubated with the GFP-TRAP beads and bound proteins were eluted. As previously, the bound fraction shows a strong enrichment for GFP-polκ. The Input lanes contain 1% of the Input fraction. 10% of the Bound fraction was loaded into the corresponding lane.

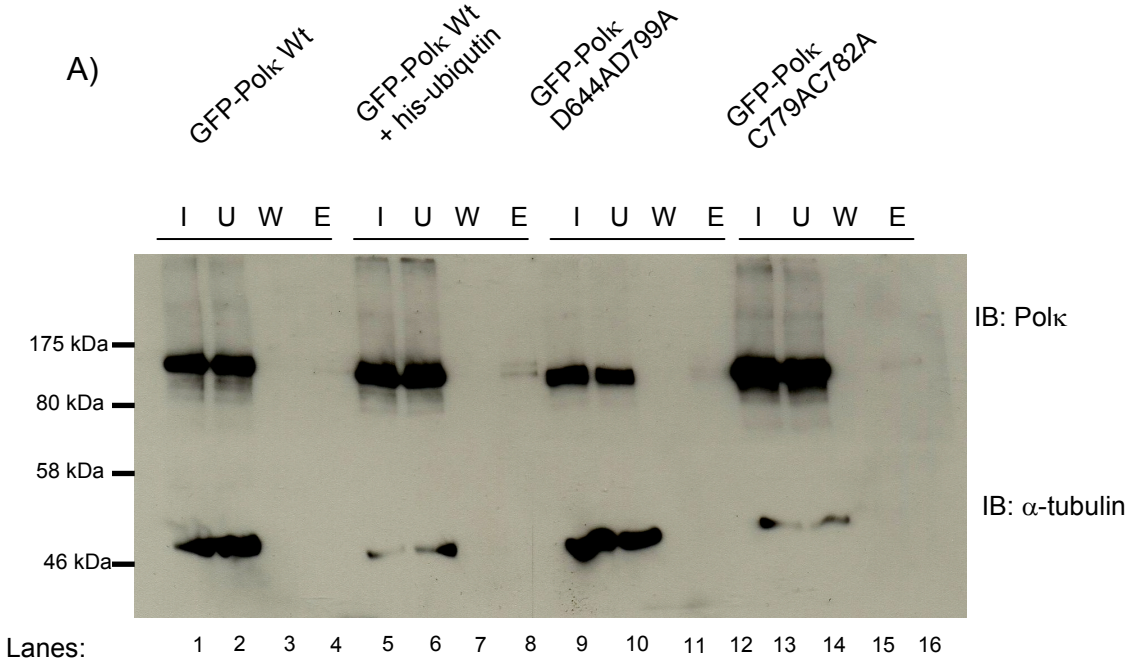

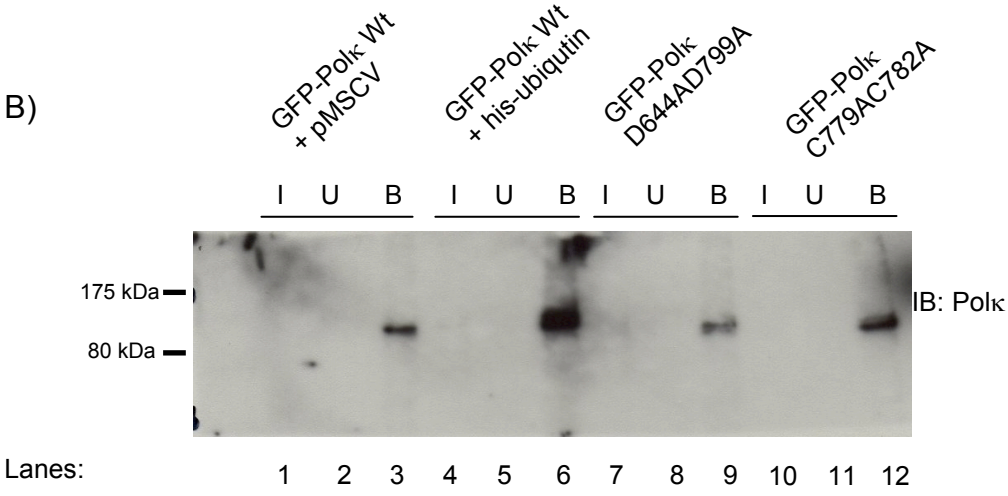

I - Input
U - Unbound
W - Wash
E - Elution
B - Bound

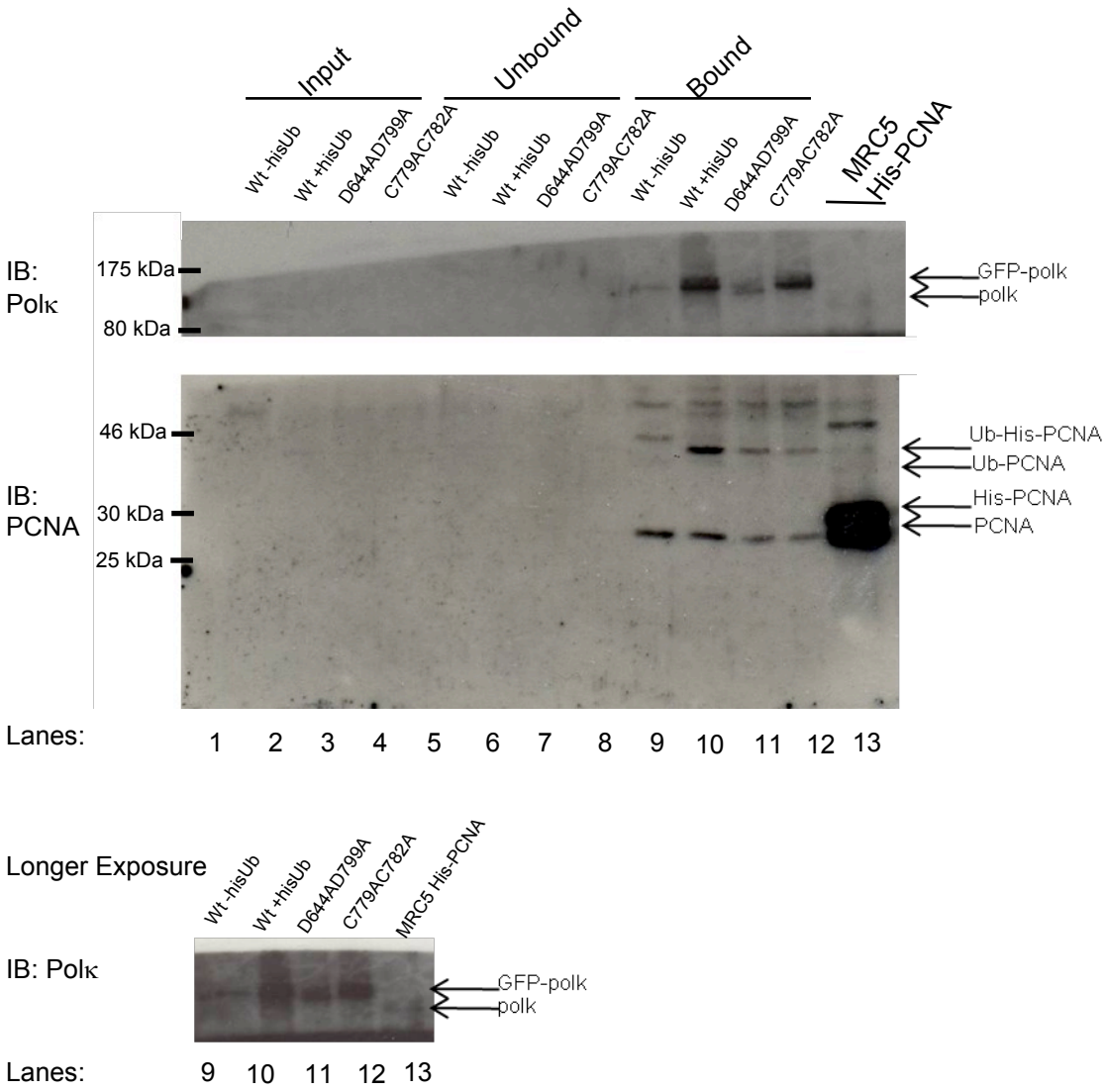

Figure 6.9 - Identification of Cross-linked Proteins From GFP-TRAP Purification – Probing with Anti-PCNA

Samples purified using the NiNTA beads and the GFP-Trap beads were probed for the recovery of GFP-polκ and any enrichment of PCNA. The lanes where cells expressed wild-type GFP-polκ and 6xhis-ubiquitin show a stronger enrichment for 6xhis-ubiquitin-PCNA than the UBZ domain mutants (compare lane 10 with 11,12). This band is missing entirely when 6xhis-ubiquitin is replaced with a non-expressed empty vector (lane 9)

having a markedly reduced recovery of 6xhis-ubiquitin-PCNA (lane 10 compared to lane 12) (Figure 6.9). The comparatively greater yield from C779AC782A was not unexpected given that a greater amount of protein was seen to be retrieved from the initial purification from the NiNTA beads (Figure 6.3).

6.6 Silver Stained SDS-PAGE Gel for Protein Identification

The use of GFP-Trap beads had allowed the identification of modified and unmodified PCNA when the samples were purified for GFP-polκ. To try and identify other proteins that could also be recovered from the elutions, the experiment was repeated and the entirety of the fraction recovered from the GFP-Trap beads was run on a SDS-PAGE gel and then stained with silver nitrate. As shown, many of the bands are present in all the samples, representing proteins not 6xhis-ubiquitin modified but presumably recovered due to the non-specific binding of GFP-polκ to the NiNTA beads. Several bands initially appeared fainter in the elutions from lysates with the polκ UBZ domain mutations, corresponding to the right size to be species of PCNA. However, in repeats of the experiment no differences were then observed (Figure 6.10).

6.7 Discussion

Several previous studies had investigated the interactions of polκ with other proteins that are necessary for the involvement of the polymerase in its biological functions. Of note, Guo *et al* demonstrated the interaction between murine polκ and ubiquitinated PCNA, while Ogi *et al* was able to detect interactions between human polκ, XRCC1, ubiquitinated PCNA, polδ, and RPA using ChIP in UV-irradiated cells (Guo et al., 2008; Ogi et al., 2010). Given the defects in accumulating at localised UV damage and the sensitivity to global UV irradiation when mutations are made in the UBZ domains of the polymerase, we decided to explore what interactions are potentially disrupted by these domain mutations. Guo *et al* had noted that disruptions to murine polκ UBZ domains disrupted the ability to bind ubiquitinated PCNA which raised the possibility that this extended to human polκ as well

Figure 6.10 - Silver Stain of GFP-TRAP Bound Fractions Show No Differences

A) Lysates from HEK293 cells were transfected and prepared as previously described. Samples from Input, Unbound and Bound fractions were run on a 10% SDS-PAGE gel and stained with $AgNO_3$.

B) The Bound lane magnified to compare and contrast the UBZ domain mutants with the wild-type samples. No differences can be observed.

A)

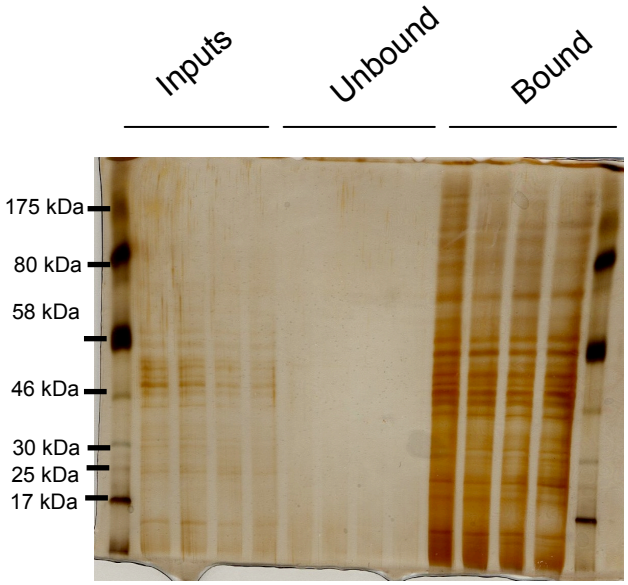
Inputs
Unbound
Bound
175 kDa
80 kDa
58 kDa
46 kDa
30 kDa
25 kDa
17 kDa

B)

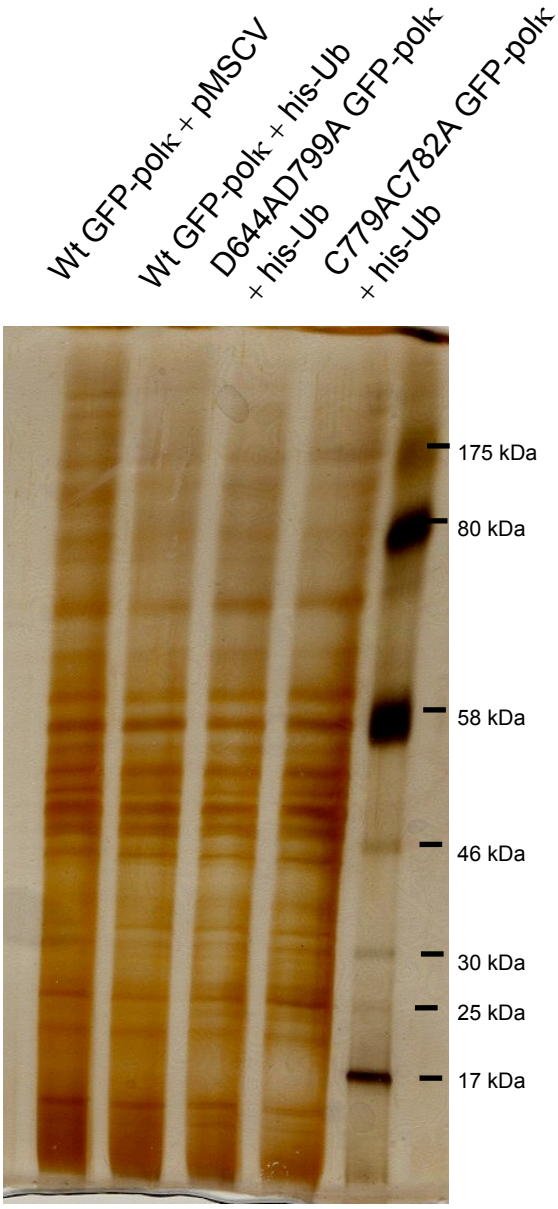
Wt GFP-polκ + pMSCV
Wt GFP-polκ + his-Ub
D644AD799A GFP-polκ + his-Ub
C779AC782A GFP-polκ + his-Ub
175 kDa
80 kDa
58 kDa
46 kDa
30 kDa
25 kDa
17 kDa

(Guo et al., 2008). In addition, we could also investigate if the UBZ domain mutations disrupted interaction with other ubiquitinated proteins.

Initial experiments that had attempted to IP GFP-polκ from cross-linked HEK293 cell extract using a polyclonal antibody against GFP did not produce usable results. The yield of GFP-polκ recovered and consequently associated proteins was low, and when western blots were probed with antibody against ubiquitin, bands were difficult to detect. We decided to address this issue in two ways: firstly, by using a five-fold increase in the quantity of HEK293 cells and to co-transfect with 6xhis-tagged ubiquitin. The addition of 6xhis-ubiquitin would then allow an initial purification using nickel agarose beads. This would increase the concentration and purification of 6xhis-ubiquitinated proteins and then be followed by an IP against GFP, isolating GFP-polκ and its partner proteins specifically from this pool of 6xhis-ubiquitinated proteins.

Initially it was necessary to determine if wild-type GFP-polκ and associated proteins could be recovered from the NiNTA beads while also ruling out non-specific interactions. When HEK293 cells are expressing GFP, no recovery of GFP is possible with or without the co-expression of 6xhis-ubiquitin. When wild-type GFP-polκ is expressed alone, there is some degree of non-specific binding to the NiNTA beads. Similar results had been described by colleagues attempting to nickel purify the Y-family polymerase polη. However, when wild-type GFP-polκ is co-expressed with 6xhis-ubiquitin, there is a much greater recovery of the polymerase (compare Fig 6.1 with 6.2). Therefore, even though the polymerase may bind non-specifically to the NiNTA beads to a degree, when there is 6xhis-ubiquitin present, it exhibits a much stronger binding. This could be through one of two ways: GFP-polκ is ubiquitinated and this band is present, and enriched, in the elution fraction. This 6xhis-ubiquitin modified polymerase would bind to the NiNTA beads independently of any other protein-protein interactions. Secondly, the HEK293 cells are cross-linked prior to the lysates being loaded onto the beads. Therefore, the wild-type GFP-polκ can also be

recovered through its interaction with a 6xhis-ubiquitin modified protein it is interacting with at the time of cross-linking.

Following the ability to recover wild-type GFP-polκ from NiNTA beads when co-expressed with 6xhis-ubiquitin, it was then decided to observe if the mutations made to the C-terminal domain of the protein abolished any protein-protein interactions. Based on the observed sensitivity to UV irradiation and failure to accumulate following localised damage, the UBZ domain mutations were candidates for disrupting interactions between the polymerase and associated proteins. When co-expressed with 6xhis-ubiquitin and eluted from NiNTA beads, several observations can be made. Firstly, the UBZ domain mutants still show the ubiquitination of human polκ. This is consistent with the work done by Guo *et al* who showed that in murine polκ the polymerase is ubiquitinated and that this ubiquitination is only abolished by complete deletion, removing both UBZ domains (Guo et al., 2008). This is further supported by studies done by Holler *et al* who observed that UBZ domain structures can support the auto-ubiquitination of the protein independent of an E3 ligase (Hoeller et al., 2007). Polκ is ubiquitinated independent of DNA damage. This modification is believed to be analogous to the ubiquitination of polη. Interactions between the ubiquitinated protein and its own UBZ domains would prevent interactions with ubiquitinated substrates except in response to specific stimuli which would prompt the de-ubiquitination of the protein (Bienko et al., 2010). A band of ubiquitinated polκ is recovered following UV damage. This is presumably from direct interactions between the 6xhis-ubiquitinated polκ and the NiNTA beads. Secondly, the UBZ domain mutations affect the interaction between GFP-polκ and its 6xhis-ubiquitinated partner. Compared to wild-type GFP-polκ, the UBZ domain mutants are only weakly recovered from the NiNTA beads, in a similar manner to when wild-type polκ is expressed without 6xhis-ubiquitin. There does appear to be a slightly greater recovery in the mutation C779AC782A compared to D644AD799A, though still less than wild-type. This is presumably due to the fact that the mutations affecting C779AC782A are confined to one UBZ domain while D644AD799A affect both UBZ domains of polκ (Fig 6.3), though

it must be noted that in *in vivo* experiments discussed in Chapter 3 and 4 the C779AC782A mutant phenotype is no different from what was observed with the other UBZ domain mutations. Therefore, a singular functional UBZ domain might still allow some recovery using *in vitro* techniques like the NiNTA beads but be detrimental in *in vivo* circumstances.

To follow the purification of 6xhis-ubiquitin tagged proteins, the elutions were then incubated with antibody raised against GFP before being immunoprecipitated using Dynabeads or GFP-Trap beads to isolate specifically the proteins associated with GFP-polκ. Purification was also possible on the sample in which 6xhis-ubiquitin was not expressed and on the UBZ domain mutants due to their lower but still existent binding to the NiNTA beads. GFP-polκ could be successfully recovered from this fraction. Firstly, membranes were probed with antibodies against ubiquitin, capable of recognising mono- and poly-ubiquitin conjugates, and histidine. From these blots, a band is visible in the UV irradiated wild-type GFP-polκ that is not visible in the other samples. The band falls between the 30kDa and 50 kDa markers, which would be the size expected for ubiquitinated PCNA (Fig. 6.5 and 6.6). When the samples were probed directly with antibody against PCNA however, no band was visible. Two explanations can be put forward: the antibody against PCNA may be much less sensitive than the ones used to detect ubiquitin or histidine. Secondly, the presence of the heavy chain IgG band is close enough in size to possible obscure any weak signal. I attempted to resolve this by using antibodies raised in different species or by using the secondary antibody TrueBlot, which should recognise only correctly folded antibody chains from the incubation with the primary antibody. Unfortunately, these attempts were unsuccessful in completely abolishing the IgG signal. GFP-Trap magnetic beads were used to try to resolve this issue. In Dynabeads, the GFP antibody is only bound to the beads through non-covalent interactions so the entire antibody disassociates and denatures when the samples are prepared by boiling in 1xSDS Laemmli buffer. Though it may have been possible to elute the purified proteins by incubating the Dynabeads with glycine, we decided to try a different bead system to avoid a loss of yield. The GFP-Trap beads have the GFP antibody covalently bound to the beads

themselves, leading to massively decreased contamination with unwanted IgG chains. These beads functioned at least as well as the Dynabeads in recovering GFP-polκ from the first round of purification. With the decrease in background signal, samples from the GFP-Trap beads were reprobed with antibody against PCNA. As could now be clearly seen, there is a marked increase in the recovery of his-tagged ubiquitinated PCNA in the sample where GFP-polκ and 6xhis-ubiquitin were co-expressed. This band is missing entirely when 6xhis-ubiquitin is not co-expressed. The UBZ domain mutants show less recovery of 6xhis-ubiquitinated PCNA (Fig 6.9). Though the yield of the D644AD799A construct was poor, the C779AC782A construct has a yield comparable with the wild-type polymerase yet brings with it far less 6xhis-ubiquitinated PCNA. A band of unmodified PCNA can be seen in all samples. This would be present from unmodified monomers that are part of a trimer where one unit or more has been post-translationally modified in response to damage. The limited recovery of 6xhis-ubiquitinated PCNA in the UBZ domain mutants can be explained due to the presence of intact PCNA binding regions in the two constructs. This could allow some interaction with PCNA independent of being able to bind an ubiquitin moiety. Therefore the recovery of the 6xhis-ubiquitinated PCNA would be due to the polymerase interactions with unmodified monomers in the trimer; these interactions would be preserved by the cross-linking carried out at the start of the purification. Furthermore, this limited interaction can also explain the weak accumulation at localised UV damage sometimes observed in previous experiments. Interaction with PCNA could be enough to have weak accumulation but intact UBZ domains are required for accurate localisation at sites of NER damage. These results coincide nicely with previous work from other laboratories. Ogi *et al*. observed the co-immunoprecipitation of wild-type polκ and ubiquitinated PCNA with chromatin immunoprecipitation after UV irradiation. When Rad18 was reduced using siRNA techniques or, as presented in Chapter 3 of this thesis, when the UBZ domains of polκ were mutated the localisation of polκ at NER sites was reduced (Ogi et al., 2010). With murine polκ, Guo *et al.* had found an interaction between the polymerase and ubiquitinated PCNA that was lost by mutation to conserved residues in the UBZ domains (Guo et al., 2008). This work recapitulates that

effect for human polκ and links the conserved UBZ domain residues with ubiquitinated PCNA interaction in an NER context.

To further investigate the interactions that may be disrupted by the mutations to the UBZ domains, the entirety of the purified proteins was examined by running a SDS-PAGE gel and using a silver stain to identify all the protein bands present. From the silver stained SDS-PAGE gel, the non-specific binding of proteins to the NiNTA beads represented a large obstacle to identification of interaction partners. As was observed in previous western blots, GFP-polκ itself exhibits a degree of non-specific binding to the NiNTA beads as seen in samples co-transfected with pMSCV in the place of the *6xhis-ubiquitin* plasmid. This would lead to the inadvertent purification of proteins associated with GFP-polκ, including ubiquitinated proteins. Distinguishing these proteins from 6xhis-ubiquitin modified species in the other samples would be difficult due to the small size of the 6xhis tag and the breadth of proteins visible on the silver stain. As can be seen, all samples transfected with GFP-polκ share nearly all bands in common. Repeated attempts at the experiment failed to resolve any differences between the samples. Given the extent of bands resolved even after two rounds of purification, staining with silver is an overly general method of protein identification that would not aid in identifying proteins. Until a higher degree of purity can be obtained, investigating specific proteins through immunoblotting with antibodies remains the best route to identify affected interactions.

To overcome the problems experienced, future work should move away from a transient transfection of HEK293 cells and instead focus on creating a stable cell line expressing the 6xhis-ubiquitin and GFP-polκ either as the wild-type polymerase or the UBZ domain mutations. Though the expression of a stably integrated gene is never as high when a plasmid is transfected and expressed in a transient manner, the creation of a stable cell line would be beneficial in two ways: firstly, the FACS Aria system could be used to select for cells of a specific level of expression; secondly, a cell line stably expressing the exogenous gene could be rapidly and efficiently expanded in quantity. This would greatly

expand the available quantities of protein to purify which would aid in indentifying transient interactions or ones present only in minute quantities.

Chapter 7 : Conclusion

7.1 : Conclusions and Future Work

An analysis of conserved residues in the C-terminal domain of human polκ has shown an essential role for the aspartic acid and cysteine residues located inside the ubiquitin binding zinc finger domains. When these amino acids are mutated to alanines, several effects are observed. Firstly, these mutants fail to accumulate at sites of NER following localised UV damage. Secondly, cells that stably express these mutants are sensitive to UV irradiation. Thirdly, these mutants do not interact to the same extent with the same proteins that the wild-type polymerase does. These mutations disrupt interactions with ubiquitinated PCNA. Disruption to the ubiquitin binding domains or prevention of ubiquitination of PCNA severely disrupts the ability of polκ to engage in NER and sensitises the cell to the lethal effects of UV irradiation through failure to complete the repair process. Conversely, mutations in conserved residues outside the UBZ domains do not affect the engagement of the polymerase in NER or the viability of the cell. Curiously, the UBZ domain mutations do not appear to affect the involvement of polκ in TCR as measured by recovery of RNA synthesis (Figure 7.1).

There are several potential areas for future investigation that could extend the scope of this work. Firstly, for nothing more than a matter of thoroughness, it would be beneficial to have established a stable cell line expressing GFP-polκ S824AS825A to see if it behaved in the same manner as the other C-terminal mutations that accumulate at localised UV damage. With this and the other cell lines that stably express GFP-polκ, a further investigation of the effect the mutations have on NER could be attempted. This would include a more sensitive detection of repair synthesis using caesium chloride gradients and exploring the apparent dispensability of UBZ domains for the involvement of the polymerase in transcription-coupled repair. As observed, the stable cell lines expressing GFP-polκ Q835AK836A repeatedly exhibited sensitivity to UV at low UV doses when assayed for clonogenic survival but an increase in RNA synthesis from the same level of

Figure 7.1: A model for the Involvement of Human DNA Polκ in Nucleotide Excision Repair

Following detection and verification, the two nucleases coordinate to excise the damage containing strand. The 5' incision is made firstly by XPF. This allows the recruitment of repair synthesis factors. In 50% of NER events, resynthesis of DNA involves polε (Ogi *et al.* 2010). The remaining 50% involves cooperation between polδ and polκ. The accumulation of polκ at NER sites requires the conserved residues in the ubiquitin binding zinc fingers of the polymerase. Mutations of these conserved residues prevent interaction with ubiquitinated PCNA and limit the presence of the polymerase at the repair site. Failure to associate with ubiquitinated PCNA limits completion of repair and sensitises the cells to the lethal effects of UV exposure.

Conversely, mutations to conserved residues outside the UBZ domains do not impair the ability of the polymerase to engage in NER repair synthesis. Nor do any of the mutations constructed cause a defect in the ability of the cell to recover its RNA synthesis levels in a transcription-coupled repair manner.

For the purposes of clarity, many necessary loading and scaffolding factors such as RFC1-RFC, XRCC1, Lig1 and Lig3 have been omitted.

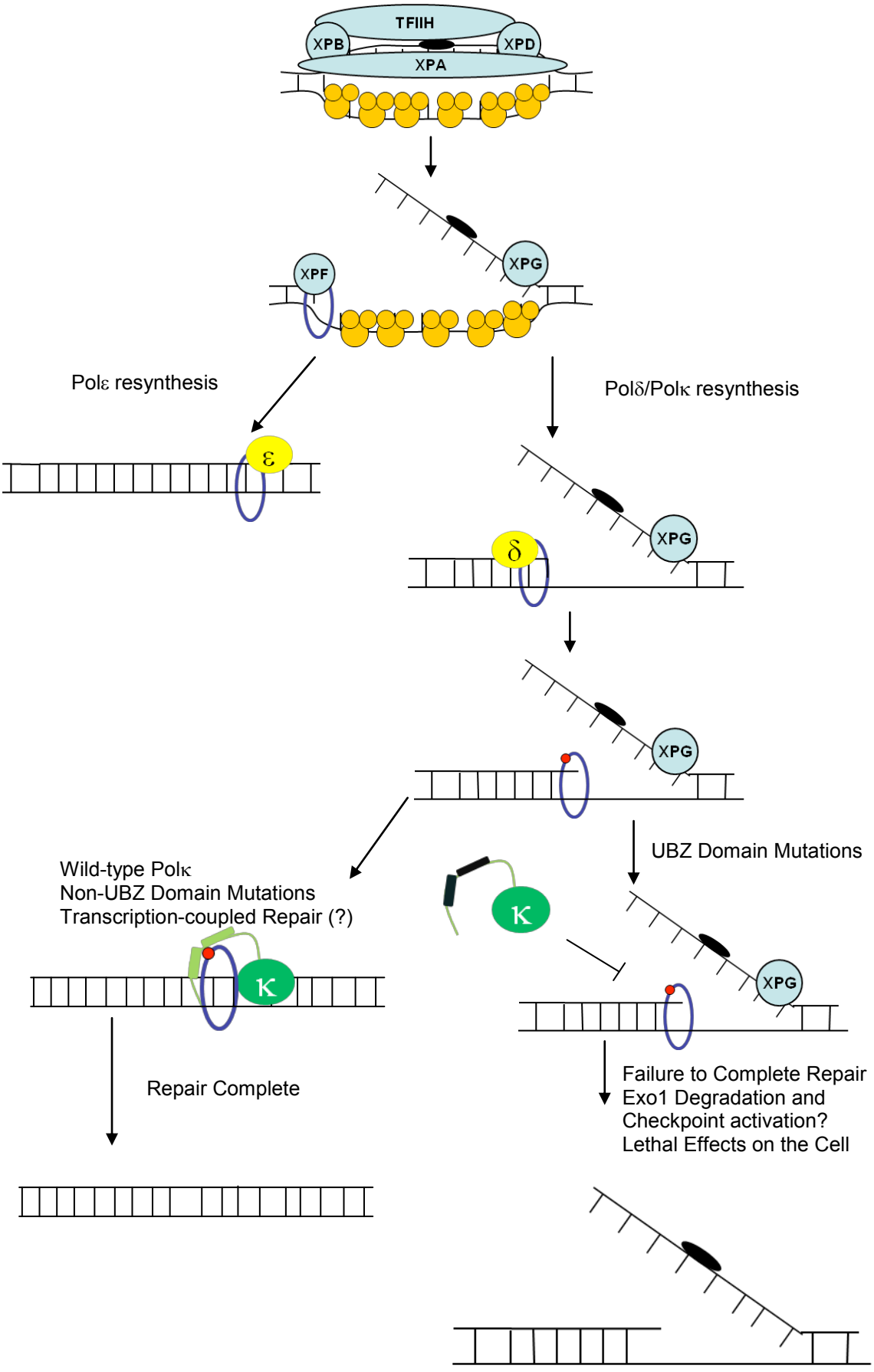
TFIIH
XPB
XPD
XPA
XPG
XPF
Polε resynthesis
Polδ/Polκ resynthesis
ε
δ
XPG
XPG
UBZ Domain Mutations
Wild-type Polκ
Non-UBZ Domain Mutations
Transcription-coupled Repair (?)
κ
κ
XPG
Repair Complete
Failure to Complete Repair
Exo1 Degradation and
Checkpoint activation?
Lethal Effects on the Cell

exposure. What underlies this observation? Does K836 represent a possible site of post-translational modification? Finally, what other protein-protein interactions are disrupted by the mutations to the UBZ domains? Mass spectrometry analysis of the purified complexes could help to expand the list of proteins that polκ interacts with and which interactions are abolished by specific mutations.

Appendix A: Primers

Name	Sequence[3]	Purpose
D799A_fw	5'-CCCTGTTCAATGTGCATGTGG CTGTTTGCTTAAATAAAAGTTTT-3'	Introduces the D799A mutation
D799A_rv	5'-AAAACTTTTATTTAAGCAAACA GCCACATGCACATTGAACAGGG-3'	
D644A_fw	5'-GCCTTGAATAAACATGTA GCTGAATGTCTTGATGGACC-3'	Introduces the D644A mutation.
D644A_rv	5'-GGTCCATCAAGACATTCA GCTACATGTTTATTCAAGGC-3'	
C779A_fw	5'-GTGAAAACAGGCCAAGCTCTA GTTGCTCCTGTTGCTAACGTAG-3'	Introduces the C779A mutation. Preserves the C782A mutation.
C779A_rv	5'-CTACGTTAGCAACAGGAGCAA CTAGAGCTTGGCCTGTTTTCAC-3'	
C782A_fw	5'-CCAAGCTCTAGTTTGTCCTGTTGCT AACGTAGAACAAAAGACTTC -3'	Introduces the C782A mutation
C782A_rv	5'-TGAAGTCTTTTGTTCTACGTTAGCAA CAGGACAAACTAGAGCTTGG -3'	
IQEL807AAAA_fw	5'-GTTTGCTTAAATAAAAGTTTTGCCGCC GCCGCCAGAAAGGATAAATTTAACCC -3'	Introduces the IQEL807-810AAAA mutation
IQEL807AAAA_rv	5'- GGGTTAAATTTATCCTTTCTGGCGG CGGCGGCAAAACTTTTATTTAAGCAAAC -3'	
Fusion_fw	5'-CTATATAAGCAGAGCTGG TTTAGTGAACCGTCAGATCC-3'	Amplifies the region of *polκ* surrounding the IQEL807-810AAAA mutation
Fusion_rv	5'-GGTATGGCTGATTATGAT CAGTTATCTAGATCCGG-3'	

[3] Mismatched bases for the creation of site directed mutations are highlighted in red

Q835A_fw	5’-GTACTGGTAGCTCAAGTGGAGTAG CCAAGGCTGTAACAAGAACA -3’	Introduces the Q835A mutation
Q835A_rv	5’-TGTTCTTGTTACAGCCTTGGCTA CTCCACTTGAGCTACCAGTAC -3’	
K836A_fw	5’-GGTAGCTCAAGTGGAGTAGCCGC CGCTGTAACAAGAACAAAAA -3’	Introduces the K836A mutation. Preserves the Q835A mutation
K836A_rv	5’- TTTTTGTTCTTGTTACAGCGGCG GCTACTCCACTTGAGCTACC -3’	
S824A_fw	5’-ATTTAACCCAGTTAATCAACCCAAA GAAGCCTCCAGAAGTACTGG -3’	Introduces the S824A mutation
S824A_rv	5’-CCATGACTTCTGGAGGCTTCTTTGGG TTGATTAACTGGGTTAAAT -3’	
S825A_fw	5’-CAGCCGAAAGAAGCCGCC CGTAGCACCGGCAG -3’	Introduces the S825A mutation. Preserves the S824A mutation.
S825A_rv	5’ CTGCCGGTGCTACGGGCG GCTTCTTTCGGCTG-3’	

Appendix B: Plasmids

Name	Distinguishing Characteristics
eGFP-C3 (Clontech)	Expression vector for GFP
eGFP-polκ wt	Expression vector for GFP-tagged polκ wild-type
eGFP-polκ D799A	Expression vector for GFP-tagged polκ D799A
eGFP-polκ D644AD799A	Expression vector for GFP-tagged polκ D644AD799A
eGFP-polκ C779AC782A	Expression vector for GFP-tagged polκ C779AC782A
eGFP-polκ Q835AK826A	Expression vector for GFP-tagged polκ Q835AK826A
eGFP-polκ IQEL807-810AAAA	Expression vector for GFP-tagged polκ IQEL807-810AAAA
eGFP-polκ S824AS825A	Expression vector for GFP-tagged polκ S824AS825A
pMSCV	Empty vector carrying puromycin resistance
pMSCV- eGFP-polκ wt	Expression vector for GFP-tagged polκ wild-type used to create stable cell lines
pMSCV- eGFP-polκ D644AD799A	Expression vector for GFP-tagged polκ D644AD799A used to create stable cell lines
pMSCV- eGFP-polκ C779AC782A	Expression vector for GFP-tagged polκ C779AC782A used to create stable cell lines
pMSCV- eGFP-polκ Q835AK826A	Expression vector for GFP-tagged polκ Q835AK826A used to create stable cell lines
pMSCV- eGFP-polκ IQEL807-810AAAA	Expression vector for GFP-tagged polκ IQEL807-810AAAA to create stable cell lines

pGEMT-easy (Promega)	Linear vector for cloning of PCR products
6xHis-Ubiquitin	Expression vector for 6xHis-tagged ubiquitin

Appendix C: Cell Lines

Name	**Cell Type**	**Distinguishing Characteristics**
MRC5V1	Human Lung Fibroblasts	Immortalised
HEK293	Human Embryonic Kidneys	Immortalised
M1	Mouse Embryonic Fibroblasts	*Polκ*$^{+/+}$
M6	Mouse Embryonic Fibroblasts	*Polκ*$^{-/-}$
WT3 / WT	Mouse Embryonic Fibroblasts (Derived from M6)	Stably expresses GFP-polκ wild-type
DD3 / DD7	Mouse Embryonic Fibroblasts (Derived from M6)	Stably expresses GFP-polκ D644AD799A
CC4 / CC1	Mouse Embryonic Fibroblasts (Derived from M6)	Stably expresses GFP-polκ C779AC782A
QK1 / QK5	Mouse Embryonic Fibroblasts (Derived from M6)	Stably expresses GFP-polκ Q835AK836A
IQEL16 / IQEL7	Mouse Embryonic Fibroblasts (Derived from M6)	Stably expresses GFP-polκ IQEL807-810AAAA
MRC5V1 PCNA-K164R	Human Lung Fibroblasts (Derived from MRC5V1)	Stably expresses 6xHis-PCNA with K164R mutation
XP2YO	Human Fibroblast	XPF$^{-/-}$

XP2YO Wild-type XPF	Human Fibroblast (Derived from XP2YO)	Expresses wild-type XPF
XP2YO D676A XPF	Human Fibroblast (Derived from XP2YO)	Expresses XPF with the nuclease dead mutation D676A
XPCS1RO	Human Fibroblast	$XPG^{-/-}$
XPCS1RO Wild-type XPG	Human Fibroblast (Derived from XPCS1RO)	Expresses wild-type XPG
XPCS1RO E791A XPG	Human Fibroblast (Derived from XPCS1RO)	Expresses XPG with the nuclease dead mutation E791A

Appendix D: UV Survival Data

Cell line / UV (J/m^2)	M1	M6	WT3	DD3	CC4	QK1	IQEL16
0	100.000	100.000	100.000	100.000	100.000	100.000	100.000
5	49.315	17.456	23.810	9.703	5.684	16.541	22.751
10	7.306	0.450	3.889	0.504	0.698	1.520	2.344
15	2.151	0.276	0.823	0.153	0.482	0.936	0.904

Cell line / UV (J/m^2)	M1	M6	WT3	DD3	CC4	QK1	IQEL16
0	100.000	100.000	100.000	100.000	100.000	100.000	100.000
5	33.815	20.381	22.276	8.038	2.875	21.617	28.780
10	11.985	2.253	3.932	0.823	0.784	4.145	4.274
15	1.365	0.529	0.422	0.118	0.314	2.142	1.221

Cell line / UV (J/m^2)	M1	M6	WT3	DD3	CC4	QK1	IQEL16
0	100.000	100.000	100.000	100.000	100.000	100.000	100.000
5	14.566	12.254	13.948	8.793	4.131	18.084	24.351
10	2.353	2.283	3.360	0.950	0.083	3.006	4.358
15	0.566	0.062	0.420	0.176	0.184	0.591	0.869

Cell line / UV (J/m^2)	M1	M6	WT3	DD3	CC4	QK1	IQEL16
0	100.00	100.00	100.00	100.00	100.00	100.00	100.00
5	32.02	15.58	20.48	8.51	6.44	13.31	25.47
10	6.31	1.94	4.01	0.81	1.00	2.29	4.89
15	1.34	0.26	0.58	0.13	0.29	0.88	1.27

Appendix E: UV Survival Data – Alternative MEF Cell Line Clones

Cell line / UV (J/m^2)	M1	M6	WT	DD7	CC1	QK5	IQEL7
0	100.000	100.000	-	-	-	-	100.000
5	37.256	6.553	-	-	-	-	24.088
10	8.987	0.609	-	-	-	-	2.120
15	1.057	0.077	-	-	-	-	0.214

Cell line / UV (J/m^2)	M1	M6	WT	DD7	CC1	QK5	IQEL7
0	100.000	100.000	-	-	100.000	100.000	-
5	41.947	-	-	-	8.710	18.879	-
10	10.748	3.489	-	-	1.045	5.756	-
15	1.847	0.044	-	-	0.071	0.757	-

Cell line / UV (J/m^2)	M1	M6	WT	DD7	CC1	QK5	IQEL7
0	100.000	100.000	100.000	100.000	100.000	100.000	-
5	38.095	19.836	32.468	1.883	7.744	-	-
10	35.000	0.714	22.857	0.147	0.377	4.716	-
15	4.444	0.173	1.818	0.142	0.092	-	-

Cell line / UV (J/m^2)	M1	M6	WT	DD7	CC1	QK5	IQEL7
0	100.000	100.000	100.000	100.000	-	-	-
5	55.300	8.523	52.949	3.508	-	-	-
10	16.774	0.313	16.881	1.052	-	-	-
15	5.161	0.208	6.197	0.017	-	-	-

Cell line / UV (J/m^2)	M1	M6	WT	DD7	CC1	QK5	IQEL7
0	100.000	100.000	100.000	-	-	100.000	100.000
5	20.000	7.879	1.758	-	-	1.884	21.946
10	6.000	1.000	0.615	-	-	-	0.904
15	0.889	0.053	-	-	-	0.193	0.100

Cell line / UV (J/m^2)	M1	M6	WT	DD7	CC1	QK5	IQEL7
0	100.000	100.000	100.000	100.000	100.000	100.000	100.000
5	-	-	-	1.617	11.672	13.538	33.580
10	-	3.489	1.194	1.512	0.921	0.771	5.674
15	1.437	0.044	0.929	0.523	0.102	0.318	0.931

Appendix F: Recovery of RNA Synthesis Data

Cell line / UV (J/m^2)	M1	M6	WT3	DD3	CC4	QK1	IQEL16
0	100.000	100.000	100.000	100.000	100.000	100.000	100.000
5	74.393	59.718	127.782	86.354	79.322	112.211	76.480
10	27.621	19.722	96.721	35.593	46.440	34.378	35.856
15	17.159	7.558	37.941	16.241	20.813	17.249	14.314

Cell line / UV (J/m^2)	M1	M6	WT3	DD3	CC4	QK1	IQEL16
0	100.000	100.000	100.000	-	100.000	100.000	-
5	56.461	47.284	60.243	-	70.264	142.707	-
10	30.473	13.078	9.449	-	37.489	30.581	-
15	13.471	4.322	-10.567	-	20.498	19.913	-

Cell line / UV (J/m^2)	M1	M6	WT3	DD3	CC4	QK1	IQEL16
0	100.000	100.000	-	-	-	-	100.000
5	91.292	71.796	-	-	-	-	134.259
10	38.913	25.153	-	-	-	-	97.311
15	20.756	12.449	-	-	-	-	55.552

Cell line / UV (J/m^2)	M1	M6	WT3	DD3	CC4	QK1	IQEL16
0	100.000	100.000	100.000	100.000	100.000	100.000	100.000
5	95.840	72.532	84.194	98.185	62.557	138.044	61.122
10	57.344	25.764	51.369	82.178	43.447	45.726	26.983
15	42.628	11.162	35.831	35.438	30.730	25.742	21.543

Cell line / UV (J/m^2)	M1	M6	WT3	DD3	CC4	QK1	IQEL16
0	100.000	100.000	-	100.000	-	-	-
5	90.957	72.241	-	66.426	-	-	-
10	59.044	48.798	-	33.779	-	-	-
15	21.897	24.047	-	19.608	-	-	-

Appendix G: Data Averages

Table 9: UV Survival Data Averages[4]

Cell line / UV (J/m^2)	M1		M6		WT3		DD3		CC4		QK1		IQEL16	
	AVG	% M1	AVG	% M1	AVG	% M1	AVG	% M1	AVG	% M1	AVG	% M1	AVG	% M1
0	100.00	100 ± 0	100.00	100± 0	100.00	100± 0	100.00	100± 0	100.00	100± 0	100.00	100± 0	100.00	100± 0
5	32.02	100 ± 0	15.58	55± 22	20.48	71± 17	8.51	35± 18	6.44	23± 16	13.31	62± 75	25.47	96± 51
10	6.31	100 ± 0	1.94	50± 44	4.01	91± 49	0.81	24± 14	1.00	22± 31	2.29	63± 47	4.89	123± 105
15	1.34	100 ± 0	0.26	19± 13	0.58	49± 16	0.13	18± 13	0.29	23± 8	0.88	89± 53	1.27	112± 57

Table 10: UV Survival Data Averages - Alternative Clones[4]

Cell line / UV (J/m^2)	M1		M6		WT3		DD7		CC1		QK5		IQEL7	
	AVG	% M1	AVG	% M1	AVG	% M1	AVG	% M1	AVG	% M1	AVG	% M1	AVG	% M1
0	100.000	100 ± 0	100.000	100± 0	100.000	100± 0	100.000	100± 0	100.000	100± 0	100.000	100± 0	100.000	100± 0
5	39.099	100 ± 0	11.638	31± 18	29.058	63± 47	2.336	6± 1	9.376	21± 4	11.433	27± 25	26.538	871± 32
10	18.245	100 ± 0	0.545	12± 13	13.644	59± 46	0.904	3± 4	0.781	5± 6	3.748	34± 28	2.899	19± 6
15	2.449	100 ± 0	0.153	4± 2	2.981	75± 56	0.227	13± 20	0.088	4± 3	0.423	28± 14	0.415	32± 29

[4] Data is presented as the average survival of 3 or more experiments. Highlighted columns present the average of each experiment normalised to M1 values ± standard deviation of the experimental values.

Table 11: Recovery of RNA Synthesis Data Averages[5]

Cell line / UV (J/m^2)	M1		M6		WT3		DD3		CC4		QK1		IQEL16	
	AVG	% M1	AVG	% M1	AVG	% M1	AVG	% M1	AVG	% M1	AVG	% M1	AVG	% M1
0	100.00	100 ± 0	100.00	100± 0	100.00	100± 0	100.00	100± 0	100.00	100± 0	100.00	100± 0	100.00	100± 0
5	81.79	100 ± 0	62.83	80± 3	90.74	122± 44	83.65	97± 23	70.71	99± 30	130.99	183± 61	90.62	105± 42
10	42.68	100 ± 0	20.93	61± 17	52.51	157± 170	50.52	110± 46	42.46	122± 46	36.89	102± 22	53.38	142± 102
15	23.18	100 ± 0	8.87	54± 34	21.07	76± 150	23.76	89± 6	24.01	115± 40	20.97	103± 44	30.47	134± 117

[5] Data is presented as the average of 3 or more experiments. Highlighted columns present the average of each experiment normalised to M1 values ± standard deviation of the experimental values.

References

Anindya, R., Mari, P.-O., Kristensen, U., Kool, H., Giglia-Mari, G., Mullenders, L.H., Fousteri, M., Vermeulen, W., Egly, J.-M., and Svejstrup, J.Q. (2010). A Ubiquitin-Binding Domain in Cockayne Syndrome B Required for Transcription-Coupled Nucleotide Excision Repair. Mol Cell *38*, 637-648.

Auclair, Y., Rouget, R., Affar, E.B., and Drobetsky, E.A. (2008). ATR kinase is required for global genomic nucleotide excision repair exclusively during S phase in human cells. Proc Natl Acad Sci U S A *105*, 17896-17901.

Bakkenist, C.J., and Kastan, M.B. (2003). DNA damage activates ATM through intermolecular autophosphorylation and dimer dissociation. Nature *421*, 499-506.

Barnes, D.E., and Lindahl, T. (2004). Repair and Genetic Consequences of Endogenous DNA Base Damage in Mammalian Cells. Annu Rev Genet *38*, 445-476.

Bassing, C.H., Swat, W., and Alt, F.W. (2002). The Mechanism and Regulation of Chromosomal V(D)J Recombination. Cell *109*, 45-S55.

Batty, D., Rapic'-Otrin, V., Levine, A.S., and Wood, R.D. (2000). Stable Binding of Human XPC Complex to Irradiated DNA Confers Strong Discrimination for Damaged Sites. J Mol Biol *300*, 275-290.

Bergmann, E., and Egly, J.-M. (2001). Trichothiodystrophy, a transcription syndrome. Trends Genet *17*, 279-286.

Bergoglio, V., Bavoux, C., Verbiest, V., Hoffmann, J.-S., and Cazaux, C. (2002). Localisation of human DNA polymerase κ to replication foci. J Cell Sci *115*`, 4413-4418.

Bi, X., Barkley, L.R., Slater, D.M., Tateishi, S., Yamaizumi, M., Ohmori, H., and Vaziri, C. (2006). Rad18 Regulates DNA Polymerase κ and Is Required for Recovery from S-Phase Checkpoint-Mediated Arrest. Mol Cell Biol *26*, 3527-3540.

Bienko, M., Green, C.M., Crosetto, N., Rudolf, F., Zapart, G., Coull, B., Kannouche, P., Wider, G., Peter, M., Lehmann, A.R.*, et al.* (2005). Ubiquitin-Binding Domain in Y-Family Polymerases Regulate Translesion Synthesis. Science *310*, 1821 - 1824.

Bienko, M., Green, C.M., Sabbioneda, S., Crosetto, N., Matic, I., Hibbert, R.G., Begovic, T., Niimi, A., Mann, M., Lehmann, A.R.*, et al.* (2010). Regulation of Translesion Synthesis DNA Polymerase [eta] by Monoubiquitination. Mol Cell *37*, 396-407.

Bolderson, E., Tomimatsu, N., Richard, D.J., Boucher, D., Kumar, R., Pandita, T.K., Burma, S., and Khanna, K.K. (2010). Phosphorylation of Exo1 modulates homologous recombination repair of DNA double-strand breaks. Nucleic Acids Res *38*, 1821-1831.

Bomar, M.G., Pai, M.-T., Tzeng, S.-R., Li, S.S.-C., and Zhou, P. (2007). Structure of the ubiquitin-binding zinc finger domain of human DNA Y-polymerase [eta]. EMBO Rep *8*, 247-251.

Bomgarden, R.D., Lupardus, P.J., Soni, D.V., Yee, M.-C., Ford, J.M., and Cimprich, K.A. (2006). Opposing effects of the UV lesion repair protein XPA and UV bypass polymerase [eta] on ATR checkpoint signaling. EMBO J *25*, 2605-2614.

Boom, V.v.d., Citterio, E., Hoogstraten, D., Zotter, A., Egly, J.-M., Cappellen, W.A.v., Hoeijmakers, J.H.J., Houtsmuller, A.B., and Vermeulen, W. (2004). DNA damage stabilizes interaction of CSB with the transcription elongation machinery. J Cell Biol *166*, 27-36.

Bunick, C.G., and Chazin, W.J. (2005). Two Blades of the [Ex]Scissor. Structure *13*, 1740-1741.

Caldecott, K.W. (2008). Single-strand break repair and genetic disease. Naure Rev Genet *9*, 619-631.

Carlson, K.D., Johnson, R.E., Prakash, L., Prakash, S., and Washington, M.T. (2006). Human DNA polymerase κ forms nonproductive complexes with matched primer termini but not with mismatched primer termini. Proc Natl Acad Sci U S A *103*, 15776-15781.

Carty, M.P., Zernik-Kobak, M., McGrath, S., and Dixon, K. (1994). UV light-induced DNA synthesis arrest in HeLa cells is associated with changes in phosphorylation of human single-stranded DNA-binding protein. EMBO J *13*, 2114-2123.

Chen, X.-B., Melchionna, R., Denis, C.-M., Gaillard, P.-H.L., Blasina, A., Van de Weyer, I., Boddy, M.N., Russell, P., Vialard, J., and McGowan, C.H. (2001). Human Mus81-Associated Endonuclease Cleaves Holliday Junctions In Vitro. Mol Cell *8*, 1117-1127.

Chiu, R.K., Brun, J., Ramaekers, C., Theys, J., Weng, L., Lambin, P., Gray, D.A., and Wouters, B.G. (2006). Lysine 63-polyubiquitination guards against translesion synthesis-induced mutations. PLoS Genet *2*, 1070-1083.

Ciccia, A., and Elledge, S.J. (2010). The DNA Damage Response: Making It Safe to Play with Knives. Mol Cell *40*, 179-204.

Cohn, M.A., Kowai, P., Yang, K., Haas, W., Huang, T.T., Gygi, S.P., and D'Andrea, A.D. (2007). A UAF1-Containing Multisubunit Protein Complex Regulates the Fanconi Anemia Pathway. Mol Cell *28*, 786-797.

Coin, F., Oksenych, V., and Egly, J.-M. (2007). Distinct Roles for the XPB/p52 and XPD/p44 Subcomplexes of TFIIH in Damaged DNA Opening during Nucleotide Excision Repair. Mol Cell *26*, 245-256.

Coin, F., Oksenych, V., Mocquet, V., Groh, S., Blattner, C., and Egly, J.M. (2008). Nucleotide Excision Repair Driven by the Dissociation of CAK from TFIIH. Mol Cell *31*, 9-20.

Davies, A.A., Huttner, D., Daigaku, Y., Chen, S., and Ulrich, H.D. (2008). Activation of Ubiquitin-Dependent DNA Damage Bypass Is Mediated by Replication Protein A. Mol Cell *29*, 625-636.

Day, T.A., Palle, K., Barkley, L.R., Kakusho, N., Zou, Y., Tateishi, S., Verreault, A., Masai, H., and Vaziri, C. (2010). Phosphorylated Rad18 directs DNA Polymerase η to sites of stalled replication. J Cell Biol *191*, 953-966.

Edmunds, C.E., Simpson, L.J., and Sale, J.E. (2008). PCNA Ubiquitination and REV1 Define Temporally Distinct Mechanisms for Controlling Translesion Synthesis in the Avian Cell Line DT40. Mol Cell *30*, 519-529.

Eker, A., Quayle, C., Chaves, I., and van der Horst, G. (2009). DNA Repair in Mammalian Cells. CMLS *66*, 968-980.

Evans, E., Moggs, J.G., Hwang, J.R., Egly, J.-M., and Wood, R.D. (1997). Mechanism of open complex and dual incision formation by human nucleotide excision repair factors. EMBO J *16*, 6559-6573.

Fan, L., Fuss, J.O., Cheng, Q.J., Arvai, A.S., Hammel, M., Roberts, V.A., Cooper, P.K., and Tainer, J.A. (2008). XPD Helicase Structures and Activities: Insights into the Cancer and Aging Phenotypes from XPD Mutations. Cell *133*, 789-800.

Fan, W., and Luo, J. (2010). SIRT1 Regulates UV-induced DNA Repair through Deacetylating XPA. Mol Cell *39*, 247-258.

Fousteri, M., and Mullenders, L.H. (2008). Transcription-coupled nucleotide excision repair in mammalian cells: molecular mechanism and biological effects. Cell Res *18*, 73-84.

Fousteri, M., Vermeulen, W., Zeeland, A.A.v., and Mullendera, L.H.F. (2006). Cockayne Syndrome A and B Proteins Differentially Regulate Recruitment of Chromatin Remodeling and Repair Factors to Stalled RNA Polymerase II In Vivo. Mol Cell *23*, 471-482.

Friedberg, E.C., Wagner, R., and Radman, M. (2002). Specialized DNA Polymerases, Cellular Survival, and the Genesis of Mutations. Science *296*, 1627-1630.

Gerlach, V.L., Aravind, L., Gotway, G., Schultz, R.A., Koonin, E.V., and Freidberg, E.C. (1999). Human and mouse homologs of *Escherichia coli* DinB (DNA polymerase IV), members of the UmuC/DinB superfamily. Proc Natl Acad Sci U S A *96*, 11922-11927.

Giannattasio, M., Follonier, C., Tourrière, H., Puddu, F., Lazzaro, F., Pasero, P., Lopes, M., Plevani, P., and Muzi-Falconi, M. (2010). Exo1 Competes with Repair Synthesis, Converts NER Intermediates to Long ssDNA Gaps, and Promotes Checkpoint Activation. Mol Cell *40*, 50-62.

Giannattasio, M., Lazzaro, F., Longhese, M.P., Plevani, P., and Muzi-Falconi, M. (2004). Physical and functional interactions between nucleotide excision repair and DNA damage checkpoint. EMBO J *23*, 429-438.

Giglia-Mari, G., Coin, F., Ranish, J.A., Hoogstraten, D., Theil, A., Wijgers, N., Jaspers, N.G.J., Raams, A., Argentini, M., van der Spek, P.J.*, et al.* (2004). A new, tenth subunit of TFIIH is responsible for the DNA repair syndrome trichothiodystrophy group A. Nat Genet *36*, 714-719.

Godoy, V.G., Jarosz, D.F., Walker, F.L., Simmons, L.A., and Walker, G.C. (2006). Y-family DNA polymerases respond to DNA damage-independent inhibition of replication fork progression. EMBO J *25*, 868-879.

Göhler, T., Sabbioneda, S., Green, C.M., and Lehmann, A.R. (2011). ATR-mediated phosphorylation of DNA polymerase η is needed for efficient recovery from UV damage. J Cell Biol *192*, 219-227.

Goodarzi, A.A., Noon, A.T., Deckbar, D., Ziv, Y., Shiloh, Y., Löbrich, M., and Jeggo, P.A. (2008). ATM Signaling Facilitates Repair of DNA Double-Strand Breaks Associated with Heterochromatin. Mol Cell *31*, 167-177.

Green, C.M., and Almouzni, G. (2003). Local action of the chromatin assembly factor CAF-1 at sites of nucleotide excision repair *in vivo*. EMBO J *22*, 5163-5174.

Groisman, R., Polanowska, J., Kuraoka, I., Sawada, J.-i., Saijo, M., Drapkin, R., Kisselev, A.F., Tanaka, K., and Nakatani, Y. (2003). The Ubiquitin Ligase Activity in the DDB2 and CSA Complexes Is Differentially Regulated by the COP9 Signalosome in Response to DNA Damage. Cell *113*, 357-367.

Guo, C., Tang, T.-S., Bienko, M., Dikic, I., and Friedberg, E.C. (2008). Requirements for the Interaction of Mouse Polκ with Ubiquitin and Its Biological Significance. J Biol Chem *283*, 4658-4664.

Guo, R., Chen, J., Mitchell, D.L., and Johnson, D.G. (2010). GCN5 and E2F1 stimulate nucleotide excision repair by promoting H3K9 acetylation at sites of damage. Nucleic Acids Res, 1390-1397.

Haracska, L., Unk, I., Johnson, R.E., Phillips, B.B., Hurwitz, J., Prakash, L., and Prakash, S. (2002). Stimulation of DNA Synthesis Activity of Human DNA Polymerase κ by PCNA. Mol Cell Biol *22*, 784-791.

Hasegawa, K., Yoshiyama, K., and Maki, H. (2008). Spontaneous mutagenesis associated with nucleotide excision repair in *Escherichia coli*. Genes Cells *13*, 459-569.

Herrlich, P., Karin, M., and Weiss, C. (2008). Supreme EnLIGHTenment: Damage Recognition and Signaling in the Mammalian UV Response. Mol Cell *29*, 279-290.

Hoeijmakers, J.H.J. (2001). Genome maintenance mechanisms for preventing cancer. Nature *411*, 366-374.

Hoeller, D., Hecker, C.-M., Wagner, S., Rogov, V., Dötsch, V., and Dikic, I. (2007). E3-Independent Monoubiquitination of Ubiquitin-Binding Proteins. Molecular Cell *26*, 891-898.

Huang, T.T., Nijman, S.M.B., Mirchandani, K.D., Galardy, P.J., Cohn, M.A., Haas, W., Gygi, S.P., Ploegh, H.L., Bernards, R., and D'Andrea, A.D. (2006). Regulation of monoubiquitinated PCNA by DUB autocleavage. Nature Cell Biol *8*, 341-347.

Huen, M.S.Y., Grant, R., Manke, I., Minn, K., Yu, X., Yaffe, M.B., and Chen, J. (2007). RNF8 Transduces the DNA-Damage Signal via Histone Ubiquitylation and Checkpoint Protein Assembly. Cell *131*, 901-914.

Hurley, J.H., Lee, S., and Prag, G. (2006). Ubiquitin-binding domains. Biochem J *399*, 361-372.

Ip, S.C.Y., Rass, U., Blanco, M.G., Flynn, H.R., Skehel, J.M., and West, S.C. (2008). Identification of Holliday junction resolvases from humans and yeast. Nature *456*, 357-361.

Jentsch, S., and Pyrowolakis, G. (2000). Ubiquitin and its kin: how close are the family ties? Trends Cell Biol *10*, 335-342.

Jiang, G., and Sancar, A. (2006). Recruitment of DNA Damage Checkpoint Proteins to Damage in Transcribed and Nontranscribed Sequences. Mol Cell Biol *26*, 39-49.

Jiang, Y., Wang, X., Bao, S., Guo, R., Johnson, D.G., Shen, X., and Li, L. (2010). INO80 chromatin remodeling complex promotes the removal of UV lesions by the nucleotide excision repair pathway. Proc Natl Acad Sci U S A *107*, 17274-17279.

Johnson, R.E., Prakash, S., and Prakash, L. (2000a). The human *DINB1* gene encodes the DNA polymerase Polθ. Proc Natl Acad Sci U S A *97*, 3838-3843.

Johnson, R.E., Washington, M.T., Haracska, L., Prakash, S., and Prakash, L. (2000b). Eukaryotic polymerases ι and ζ act sequentially to bypass DNA lesions. Nature *406*, 1015-1019.

Kang, T.-H., Lindsey-Boltz, L.A., Reardon, J.T., and Sancar, A. (2010a). Circadian control of XPA and excision repair of cisplatin-DNA damage by cryptochrome and HERC2 ubiquitin ligase. Proc Natl Acad Sci U S A *107*, 4890-4895.

Kang, T.-H., Reardon, J.T., and Sancar, A. (2010b). Regulation of nucleotide excision repair activity by transcriptional and post-transcriptional control of the XPA protein. Nucleic Acids Res, 1-12.

Kannouche, P., Henestrosa, A.R.F.d., Coull, B., Vidal, A.E., Gray, C., Zicha, D., Woodgate, R., and Lehmann, A.R. (2003). Localization of DNA polymerase η and ι to the replication machinery is tightly co-ordinated in human cells. EMBO J *22*, 1223-1233.

Kannouche, P.L., Wing, J., and Lehmann, A.R. (2004). Interaction of Human DNA Polymerase η with Monoubiquitinated PCNA: A Possible Mechanism for the Polymerase Switch in Response to DNA Damage. Mol Cell *14*, 491-500.

Klungland, A., and Lindahl, T. (1997). Second pathway for completion of human DNA base excision-repair: reconstitution with purified proteins and requirement for DNase IV (FEN1). EMBO J *16*, 3341-3348.

Kraemer, K.H., Lee, M.M., and Scotto, J. (1987). Xeroderma Pigmentosum: Cutaneous, Ocular, and Neurologic Abnormalities in 830 Published Cases. Arch Dermatol *123*, 241-250.

Kubota, Y., Nash, R.A., Klungland, A., Schär, P., Barnes, D.E., and Lindahl, T. (1996). Reconstitution of DNA base excision-repair with purified human proteins: interaction between DNA polymerase beta and the XRCC1 protein. EMBO J *15*, 6662-6670.

Kunkel, T.A., and Burgers, P.M. (2008). Dividing the workload at a eukaryotic replication fork. Trends Cell Biol *18*, 521-527.

Lee, D.H., and Goldberg, A.L. (1998). Proteasome inhibitors: valuable new tools for cell biologists. Trends Cell Biol *8*, 397-403.

Lehmann, A.R. (2001). The xeroderma pigmentosum group D (XPD) gene: one gene, two functions, three diseases. Genes Dev *15*, 15-23.

Lehmann, A.R. (2002). Replication of damaged DNA in mammalian cells: new solutions to an old problem. Mutat Res *509*, 23-34.

Lehmann, A.R. (2003). DNA repair-deficient diseases, xeroderma pigmentosum, Cockayne syndrome and trichothiodystrophy. Biochimie *85*, 1101-1111.

Lehmann, A.R. (personal communication).

Lehmann, A.R., Niimi, A., Ogi, T., Brown, S., Sabbioneda, S., Wing, J.F., Kannouche, P.L., and Green, C.M. (2007). Translesion Synthesis: Y-family Polymerases and the polymerase switch. DNA Repair, 891-899.

Lemée, F., Bavoux, C., Pillaire, M., Bieth, A., Machado, C., Pena, S., Guimbaud, R., Selves, J., Hoffmann, J., and Cazoux, C. (2007). Characterization of promoter regulatory elements

involved in downexpression of the DNA polymerase κ in colorectal cancer. Oncogene *26*, 3387-3394.

Li, L., Elledge, S.J., Peterson, C.A., Bales, E.S., and Legerski, R.J. (1994). Specific association between the human DNA repair proteins XPA and ERCC1. Proc Natl Acad Sci U S A *91*, 5012-5016.

Limsirichaikul, S., Niimi, A., Fawcett, H., Lehmann, A., Yamashita, S., and Ogi, T. (2009). A rapid non-radioactive technique for measurement of repair synthesis in primary human fibroblasts by incorporation of ethynyl deoxyuridine (EdU). Nucleic Acids Res *37*, 1-10.

Lindahl, T. (1996). The Croonian Lecture, 1996: Endogenous Damage to DNA. Philos Trans R Soc Lond B Biol Sci *351*, 1529-1538.

Lindahl, T. (2000). Suppression of spontaneous mutagenesis in human cells by DNA base excision-repair. Mutat Res *462*, 129-135.

Liu, H., Rudolf, J., Johnson, K.A., McMahon, S.A., Oke, M., Carter, L., McRobbie, A.-M., Brown, S.E., Naismith, J.H., and White, M.F. (2008). Structure of the DNA Repair Helicase XPD. Cell *133*, 801-812.

Lone, S., Townson, S.A., Ujon, S.N., Johnson, R.E., Brahma, A., Nair, D.T., Prakash, S., Prakash, L., and Aggarwai, A.K. (2007). Human DNA Polymerase κ Encircles DNA: Implications for Mismatch Extension and Lesion Bypass. Mol Cell *25*, 601-614.

Maga, G., and Hübscher, U. (2003). Proliferating cell nuclear antigen (PCNA): a dancer with many partners. J Cell Sci *116*, 3051-3060.

Mahaney, B.L., Meek, K., and Lees-miller, S.P. (2009). Repair of ionizing radiation-induced DNA double-strand breaks by non-homologous end-joining. Biochem J *417*, 639-650.

Mailand, N., Bekker-Jensen, S., Faustrup, H., Melander, F., Bartek, J., Lukas, C., and Lukas, J. (2007). RNF8 Ubiquitylates Histones at DNA Double-Strand Breaks and Promotes Assembly of Repair Proteins. Cell *131*, 887-900.

Marini, F., Nardo, T., Giannattasio, M., Minuzzo, M., Stefanini, M., Plevani, P., and Falconi, M.M. (2006). DNA nucleotide excision repair-dependent signaling to checkpoint activation. Proc Natl Acad Sci U S A *103*, 17325-17330.

Masuda, Y., Ohmae, M., Masuda, K., and Kamiya, K. (2003). Structure and Enzymatic Properties of a Stable Complex of the Human REV1 and REV7 Proteins. J Biol Chem *278*, 12356-12360.

Masutani, C., Kusumoto, R., Yamada, A., Dohmae, N., Yokoi, M., Yuasa, M., Araki, M., Iwai, S., Takio, K., and Hanaoka, F. (1999). The XPV (xeroderma pigmentosum variant) gene encodes human DNA polymerase ε. Nature *399*, 700-704.

Masutani, C., Sugasawa, K., Yanagisawa, J., Sonoyama, T., Ui, M., Enomoto, T., Takio, K., Tanaka, K., Spek, P.J.v.d., Bootsma, D*., et al.* (1994). Purification and cloning of a nucleotide excision repair complex involving the xeroderma pigmentosum group C protein and a human homologue of yeast RAD23. EMBO J *13*, 1831-1843.

Mathieu, N., Kaczmarek, N., and Naegeli, H. (2010). Strand- and site-specific DNA lesion demarcation by the xeroderma pigmentosum group D helicase. Proceedings of the National Academy of Sciences *107*, 17545-17550.

Matsumoto, M., Yaginuma, K., Igarashi, A., Imura, M., Hasegawa, M., Iwabuchi, K., Date, T., Mori, T., Ishizaki, K., Yamashita, K*., et al.* (2007). Perturbed gap-filling synthesis in nucleotide excision repair causes histone H2AX phosphorylation in human quiescent cells. J Cell Sci *120*, 1104-1112.

Matsumura, Y., Nishigori, C., Yagi, T., Imamura, S., and Takebe, H. (1998). Characterization of Molecular Defects in Xeroderma Pigmentosum Group F in Relation to Its Clinically Mild Symptoms. Hum Mol Genet *7*, 969-974.

Mayne, L.V., and Lehmann, A.R. (1982). Failure of RNA Synthesis to Recover after UV Irradiation: An Early Defect in Cells from Individuals with Cockayne's Syndrome and Xeroderma Pigmentosum. Cancer Res *42*, 1473-1478.

McCulloch, S.D., Kokoska, R.J., Masutani, C., Iwai, S., Hanaoka, F., and Kunkel, T.A. (2004). Preferential cis-syn thymine dimer bypass by DNA polymerase [eta] occurs with biased fidelity. Nature *428*, 97-100.

Mellon, I., Spivak, G., and Hanawalt, P.C. (1987). Selective removal of transcription-blocking DNA damage from the transcribed strand of the mammalian DHFR gene. Cell *51*, 241-249.

Mimitou, E.P., and Symington, L.S. (2009). DNA end resection: Many nucleases make light work. DNA Repair *8*, 983-995.

Min, J.-H., and Pavletich, N.P. (2007). Recognition of DNA damage by the Rad4 nucleotide excision repair protein. Nature *449*, 570-575.

Minko, I.G., Harbut, M.B., Kozekov, I.D., Kozekova, A., Jakobs, P.M., Olson, S.B., Moses, R.E., Harris, T.M., Rizzo, C.J., and Lloyd, R.S. (2008). Role for DNA Polymerase κ in the Processing of N2-N2-Guanine Interstrand Cross-links. J Biol Chem *283*, 17075-17082.

Mocquet, V., Lainé, J.P., Riedl, T., Yajin, Z., Lee, M.Y., and Egly, J.M. (2008). Sequential recruitment of the repair factors during NER: the role of XPG in initiating the resynthesis step. EMBO J *27*, 155-167.

Modrich, P. (2006). Mechanisms in Eukaryotic Mismatch Repair. J Biol Chem *281*, 30305-30309.

Moldovan, G.-L., Pfander, B., and Jentsch, S. (2007). PCNA. the Maestro of the Replication Fork. Cell *129*, 665-679.

Moser, J., Kool, H., Giakzidis, I., Caldecott, K., Mullenders, L.H.F., and Fousteri, M.I. (2007). Sealing of Chromosomal DNA Nicks during Nucleotide Excision Repair Requires XRCC1 and DNA Ligase IIIα in a Cell-Cycle-Specific Manner. Mol Cell *27*, 311-323.

Naegeli, H., Bardwell, L., and Friedberg, E.C. (1992). The DNA helicase and adenosine triphosphatase activities of yeast Rad3 protein are inhibited by DNA damage. A potential mechanism for damage-specific recognition. J Biol Chem *267*, 392-398.

Nardo, T., Oneda, R., Spivak, G., Vaz, B., Mortier, L., Thomas, P., Orioli, D., Laugel, V., Stary, A., Hanawalt, P.C.*, et al.* (2009). A UV-sensitive syndrome patient with a specific CSA mutation reveals separable roles for CSA in response to UV and oxidative DNA damage. Proc Natl Acad Sci U S A *106*, 6209-6214.

Nelson, J.R., Lawrence, C.W., and Hinkle, D.C. (1996a). Deoxycytidyl transferase activity of yeast *REV1* protein. Nature *382*, 729-731.

Nelson, J.R., Lawrence, C.W., and Hinkle, D.C. (1996b). Thymine-Thymine Dimer Bypass by Yeast DNA Polymerase ζ. Science *272*, 1646-1649.

Niedernhofer, L.J., Garinis, G.A., Raams, A., Lalai, A.S., Robinson, A.R., Appeldoorn, E., Odijk, H., Oostendorp, R., Ahmad, A., van Leeuwen, W.*, et al.* (2006). A new progeroid syndrome reveals that genotoxic stress suppresses the somatotroph axis. Nature *444*, 1038-1043.

Niimi, A., Brown, S., Sabbioneda, S., Kannouche, P.L., Scott, A., Yasui, A., Green, C.M., and Lehmann, A.R. (2008). Regulation of proliferating cell nuclear antigen ubiquitination in mammalian cells. Proc Natl Acad Sci U S A *105*, 16125-16130.

Noon, A.T., Shibata, A., Rief, N., Lobrich, M., Stewart, G.S., Jeggo, P.A., and Goodarzi, A.A. (2010). 53BP1-dependent robust localized KAP-1 phosphorylation is essential for heterochromatic DNA double-strand break repair. Nat Cell Biol *12*, 177-184.

O'Donovan, A., Davies, A.A., Moggs, J.G., West, S.C., and Wood, R.D. (1994). XPG endonuclease makes the 3[prime] incision in human DNA nucleotide excision repair. Nature *371*, 432-435.

O'Driscoll, M., Ruiz-Perez, V.L., Woods, C.G., Jeggo, P.A., and Goodship, J.A. (2003). A splicing mutation affecting expression of ataxia-telangiectasia and Rad3-related protein (ATR) results in Seckel syndrome. Nat Genet *33*, 497-501.

O-Wang, J., Kawamura, K., Tada, Y., Ohmori, H., Kimura, H., Sakiyama, S., and Tagawa, M. (2001). DNA Polymerase κ, Implicated in Spontaneous and DNA Damage-induced Mutagenesis, is Overexpressed in Lung Cancer. Cancer Res *61*, 5366-5369.

Ogi, T., Kannouche, P., and Lehmann, A.R. (2005). Localisation of human Y-family DNA polymerase κ: relationship to PCNA foci. J Cell Sci *118*, 129-136.

Ogi, T., Kato, T., Kato, T., and Ohmori, H. (1999). Mutation enhancement by DINB1, a mammalian homologue of the Escherichia coli mutagenesis protein DinB. Genes Cells *4*, 607-618.

Ogi, T., and Lehmann, A.R. (2006). The Y-family DNA polymerase κ (pol κ) functions in mammalian nucleotide-excision repair. Nature Cell Biol *8*, 640-642.

Ogi, T., Limsirichaikul, S., Overmeer, R.M., Volker, M., Takenaka, K., Cloney, R., Nakazawa, Y., Niimi, A., Miki, Y., Jaspers, N.G.*, et al.* (2010). Three DNA Polymerases, Recruited by Different Mechanisms, Carry Out NER Repair Synthesis in Human Cells. Mol Cell *37*, 714-727.

Ogi, T., Mimura, J., Hikida, M., Fujimoto, H., Fujii-Kuriyama, Y., and Ohmori, H. (2001). Expression of human and mouse genes encoding polκ κ : testis-specific developmental regulation and AhR-dependent inducible transcription. Genes Cells *6*, 943-953.

Ogi, T., Shinkai, Y., Tanaka, K., and Ohmori, H. (2002). Polkappa protects mammalian cells against the lethal and mutagenic effects of benzo[a]pyrene. Proc Natl Acad Sci U S A *99*, 15548-15553.

Ohashi, E., Bebenek, K., Matsuda, T., Feaver, W.J., Gerlach, V.L., Friedberg, E.C., Ohmori, M., and Kunkel, T.A. (2000a). Fidelity and Processivity of DNA Synthesis by DNA Polymerase κ, the Product of the Human *DIBN1* Gene. J Biol Chem *275*, 39678-39684.

Ohashi, E., Hanafusa, T., Kamei, K., Song, I., Tomida, J., Hashimoto, H., Vaziri, C., and Ohmori, H. (2009). Identification of a novel REV1-interacting motif necessary for DNA polymerase κ function. Genes Cells *14*, 101-111.

Ohashi, E., Murakumo, Y., Kanjo, N., Akagi, J.-i., Masutani, C., Hanaoka, F., and Ohmori, H. (2004). Interaction of hREV1 with three human Y-family DNA polymerases. Genes Cells *9*, 523-531.

Ohashi, E., Ogi, T., Kusumoto, R., Iwai, S., Masutani, C., Hanaoka, F., and Ohmori, H. (2000b). Error-prone bypass of certain DNA lesion by the human DNA polymerase κ. Genes Dev *14*, 1589-1594.

Ohmori, H., Friedberg, E.C., Fuchs, R.P., Goodman, M.F., Hanaoka, F., Hinkle, D., Kunkel, T.A., Lawrence, C.W., Livneh, Z., Nohmi, T*., et al.* (2001). The Y-family of DNA polymerases. Mol Cell *8*, 7-8.

Okada, T., Sonoda, E., Yamashita, Y.M., Koyoshi, S., Tateishi, S., Yamaizumi, M., Takata, M., Ogawa, O., and Takeda, S. (2001). Involvement of Vertebrate Polκ in Rad18-independent Postreplication Repair of UV Damage. J Biol Chem *227*, 48690-48695.

Overmeer, R.M., Moser, J., Volker, M., Kool, H., Tomkinson, A.E., van Zeeland, A.A., Mullenders, L.H.F., and Fousteri, M. (2011). Replication protein A safeguards genome integrity by controlling NER incision events. J Cell Biol, 401-415.

Pagès, V., and Fuchs, R.P. (2002). How DNA lesions are turned into mutations within cells? Oncogene *21*, 8957-8966.

Park, C.-H., Mu, D., Reardon, J.T., and Sancar, A. (1995). The General Transcription-Repair Factor TFIIH Is Recruited to the Excision Repair Complex by the XPA Protein Independent of the TFIIE Transcription Factor. J Biol Chem *270*, 4896-4902.

Park, C.-J., and Choi, B.-S. (2006). The protein shuffle: Sequential interactions among components of the human nucleotide excision repair pathway. FEBS J *273*, 1600-1606.

Park, C.H., and Sancar, A. (1994). Formation of a ternary complex by human XPA, ERCC1, and ERCC4(XPF) excision repair proteins. Proc Natl Acad Sci U S A *91*, 5017-5021.

Petta, T.B., Nakajima, S., Zlatanou, A., Despras, E., Couve-Privat, S., Ishchenko, A., Sarasin, A., Yasui, A., and Kannouche, P. (2008). Human DNA polymerase iota protects cells against oxidative stress. EMBO J *27*, 2883-2895.

Phillips, L.G., and Sale, J.E. (2010). The Werner's Syndrome protein collaborates with REV1 to promote replication fork progression on damaged DNA. DNA Repair *9*, 1064-1072.

Pickart, C.M., and Eddins, M.J. (2004). Ubiquitin: structures, functions, mechanisms. Biochim Biophys Acta *1695*, 55-72.

Povirk, L.F., Zhou, T., Zhou, R., Cowan, M.J., and Yannone, S.M. (2007). Processing of 3′-Phosphoglycolate-terminated DNA Double Strand Breaks by Artemis Nuclease. J Biol Chem *282*, 3547-3558.

Proietti-De-Santis, L., Drané, P., and Egly, J.-M. (2006). Cockayne syndrome B protein regulates the transcriptional program after UV irradiation. EMBO J *25*, 1915-1923.

Ray, A., Mir, S.N., Wani, G., Zhao, Q., Battu, A., Zhu, Q., Wang, Q.-E., and Wani, A.A. (2009). Human SNF5/IN11, a Component of the Human SWI/SNF Chromatin Remodelling Complex, Promotes Nucleotide Excision Repair by Influencing ATM Recruitment and Downstream H2AX Phosphorylation. Mol Cell Biol *29*, 6209-6219.

Roberts, S.A., Strande, N., Burkhalter, M.D., Strom, C., Havener, J.M., Hasty, P., and Ramsden, D.A. (2010). Ku is a 5[prime]-dRP/AP lyase that excises nucleotide damage near broken ends. Nature *464*, 1214-1217.

Rogakou, E.P., Pilch, D.R., Orr, A.H., Ivanova, V.S., and Bonner, W.M. (1998). DNA Double-stranded Breaks Induce Histone H2AX Phosphorylation on Serine 139. J Biol Chem *273*, 5858-5868.

Ross, A.-L., Simpson, L.J., and Sale, J.E. (2005). Vertebrate DNA damage tolerance requires the C-terminus but not BRCT or transferase domains of REV1. Nucleic Acids Research *33*, 1280-1289.

Rudolf, J., Rouillon, C., Schwarz-Linek, U., and White, M.F. (2010). The helicase XPD unwinds bubble structures and is not stalled by DNA lesions removed by the nucleotide excision repair pathway. Nucleic Acids Res *38*, 931-941.

Sabbioneda, S., Gourdin, A.M., Green, C.M., Zotter, A., Giglia-Mari, G., Houtsmuller, A., Vermeulen, W., and Lehmann, A.R. (2008). Effect of Proliferating Cell Nuclear Antigen Ubiquitination and Chromatin Structure on the Dynamic Properties of the Y-family DNA Polymerases. Mol Biol Cell *19*, 5193-5202.

Sabbioneda, S., Green, C.M., Bienko, M., Kannouche, P., Dikic, I., and Lehmann, A.R. (2009). Ubiquitin-binding motif of human DNA polymerase η is required for correct localization. Proc Natl Acad Sci USA *106*, E20.

Saijo, M., Takedachi, A., and Tanaka, K. (2011). Nucleotide Excision Repair by Mutant Xeroderma Pigmentosum Group A (XPA) Proteins with Deficiency in Interaction with RPA. J Biol Chem *286*, 5476-5483.

Sarkar, S., Davies, A.A., Ulrich, H.D., and McHugh, P.J. (2006). DNA interstrand crosslink repair during G1 involves nucleotide excision repair and DNA polymerase [zeta]. EMBO J *25*, 1285-1294.

Sarkar, S., Kiely, R., and McHugh, P.J. (2010). The Ino80 chromatin-remodeling complex restores chromatin structure during UV DNA damage repair. J Cell Biol *191*, 1061-1068.

Sarkies, P., Reams, C., Simpson, L.J., and Sale, J.E. (2010). Epigenetic Instability due to Defective Replication of Structured DNA. Molecular Cell *40*, 703-713.

Sartori, A.A., Lukas, C., Coates, J., Mistrik, M., Fu, S., Bartek, J., Baer, R., Lukas, J., and Jackson, S.P. (2007). Human CtIP promotes DNA end resection. Nature *450*, 509-514.

Sassa, A., Niimi, N., Fujimoto, H., Katafuchi, A., Grúz, P., Yasui, M., Gupta, R.C., Johnson, F., Ohta, T., and Nohmi, T. (2011). Phenylalanine 171 is a molecular brake for translesion synthesis across benzo[a]pyrene-guanine adducts by human DNA polymerase kappa. Mutat Res-Gen Tox En *718*, 10-17.

Schaeffer, L., Moncollin, V., Roy, R., Staub, A., Mezzina, M., Sarasin, A., Weeda, G., Hoeijmakers, J.H.J., and Egly, J.M. (1994). The ERCC2/DNA repair protein is associated with the class II BTF2/TFIIH transcription factor. EMBO J *13*, 2388-2392.

Schaeffer, L., Roy, R., Humbert, S., Moncollin, V., Vermeulen, W., Hoeijmakers, J.H.J., Chambon, P., and Egly, J.-M. (1993). DNA Repair Helicase: A Component of BTF2 (TFIIH) Basic Transcription Factor. Science *260*, 58-63.

Schärer, O.D. (2008). The molecular basis for different disease states caused by mutations in TFIIH and XPG. DNA Repair *7*, 339-344.

Schenten, D., Gerlach, V.L., Guo, C., Velasco-Miguel, S., Hladik, C.L., White, C.L., Friedberg, E.C., Rajewsky, K., and Esposito, G. (2002). DNA polymerase κ deficiency does not affect somatic hypermutation in mice. Eur J Immunol *32*, 3152-3160.

Schofield, M.J., and Hsieh, P. (2003). DNA Mismatch Repair: Molecular Mechanisms and Biological Function. Annu Rev Microbiol *57*, 579-608.

Schreiber, V., Dantzer, F., Ame, J.-C., and de Murcia, G. (2006). Poly(ADP-ribose): novel functions for an old molecule. Nature Rev Mol Cell Biol *7*, 517-528.

Scrima, A., Konícková, R., Czyzewski, B.K., Kawasaki, Y., Jeffrey, P.D., Groisman, R., Nakatani, Y., Iwai, S., Pavletich, N.P., and Thomä, N.H. (2008). Structural Basis of UV DNA-Damage Recognition by the DDB1-DDB2 Complex. Cell *135*, 1213-1223.

Seki, M., Gearhart, P.J., and Wood, R.D. (2005). DNA polymerases and somatic hypermutation of immunoglobulin genes. EMBO Rep *6*, 1143-1148.

Sertic, S., Cloney, R., Lehman, A.R., Marini, F., Plevani, P., and Muzi-Falconi, M. (Manuscript in Preperation). Human Exonuclease 1 connects NER processing with checkpoint activation in response to UV irradiation.

Shimizu, T., Azuma, T., Ishiguro, M., Kanjo, N., Yamada, S., and Ohmori, H. (2005). Normal immunoglobulin gene somatic hypermutation in Polκ-Polι double-deficient mice. Immunol Lett *98*, 259-264.

Shimizu, T., Shinkai, Y., Ogi, T., Ohmori, H., and Azuma, T. (2003). The absence of DNA polymerase κ does not affect somatic hypermutation of the mouse immunoglobulin heavy chain gene. Immunol Lett *86*, 265-270.

Shuck, S.C., Short, E.A., and Turchi, J.J. (2008). Eukaryotic nucleotide exicision repair: from understanding mechanisms to influencing biology. Cell Res *18*, 64-72.

Sigurdsson, S., Van Komen, S., Bussen, W., Schild, D., Albala, J.S., and Sung, P. (2001). Mediator function of the human Rad51B–Rad51C complex in Rad51/RPA-catalyzed DNA strand exchange. Genes Dev *15*, 3308-3318.

Smerdon, M.J., and Thoma, F. (1990). Site-specific DNA repair at the nucleosome level in a yeast minichromosome. Cell *61*, 675-684.

Stancel, J.N.K., McDaniel, L.D., Velasco, S., Richardson, J., Guo, C., and Friedberg, E.C. (2009). Polk mutant mice have a spontaneous mutator phenotype. DNA Repair *8*, 1355-1362.

Staresincic, L., Fagbemi, A.F., Enzlin, J.H., Gourdin, A.M., Wijgers, N., Dunand-Sauthier, I., Giglia-Mari, G., Clarkson, S.G., Vermeulen, W., and Shärer, O.D. (2009). Coordination of dual incision and repair synthesis in human nucleotide excision repair. EMBO J *28*, 1111-1120.

Sugasawa, K., Akagi, J.-i., Nishi, R., Iwai, S., and Hanaoka, F. (2009). Two-Step Recognition of DNA Damage for Mammalian Nucleotide Excision Repair: Directional Binding of the XPC Compex and DNA Strand Scanning. Mol Cell *38*, 642-653.

Sugasawa, K., Masutani, C., Uchida, A., Maekawa, T., van der Spek, P., Bootsma, D., Hoeijmakers, J., and Hanaoka, F. (1996). HHR23B, a human Rad23 homolog, stimulates XPC protein in nucleotide excision repair in vitro. Mol Cell Biol *16*, 4852-4861.

Sugasawa, K., Okamoto, T., Shimizu, Y., Masutani, C., Iwai, S., and Hanaoka, F. (2001). A multistep damage recognition mechanism for global genomic nucleotide excision repair. Genes Dev *15*, 507-521.

Sugasawa, K., Okuda, Y., Saijo, M., Nishi, R., Matsuda, N., Chu, G., Mori, T., Iwai, S., Tanaka, K., Tanaka, K*., et al.* (2005). UV-Induced Ubiquitylation of XPC Protein Mediated by UV-DDB-Ubiquitin Ligase Complex. Cell *121*, 387-400.

Sugasawa, K., Shimizu, Y., Iwai, S., and Hanaoka, F. (2002). A molecular mechanism for DNA damage recognition by the xeroderma pigmentosum group C protein complex. DNA Repair *1*, 95-107.

Suzuki, N., Ohashi, E., Hayashi, K., Ohmori, H., Grollman, A.P., and Shibutani, S. (2001). Translesional Synthesis Past Acetylaminofluorene-Derived DNA Adducts Catalyzed by Human DNA Polymerase κ and Escherichia coli DNA Polymerase IV. Biochem *40*, 15176-15183.

Takedachi, A., Saijo, M., and Tanaka, K. (2010). DDB2 Complex-Mediated Ubiquitylation around DNA Damage Is Oppositely Regulated by XPC and Ku and Contributes to the Recruitement of XPA. Mol Cell Biol *30*, 2708-2723.

Tang, M., Pham, P., Shen, X., Taylor, J.-S., O'Donnell, M., Woodgate, R., and Goodman, M.F. (2000). Roles of E. coli DNA polymerases IV and V in lesion-targeted and untargeted SOS mutagenesis. Nature *404*, 1014-1018.

Teng, Y., Yu, Y., and Waters, R. (2002). The *Saccharomyces cerevisiae* Histone Acetyltransferase Gcn5 has a Role in the Photoreactivation and Nucleotide Excision Repair of UV-induced Cyclobutane Pyrimidine Dimers in the *MFA2* Gene. J Mol Biol *316*, 489-499.

Tissier, A., McDonald, J.P., Frank, E.G., and Woodgate, R. (2000). polι, a remarkably error-prone human DNA polymerase. Genes Dev *14*, 1642-1650.

Truglio, J.J., Croteau, D.L., Houten, B.V., and Kisker, C. (2006). Prokaryotic Nucleotide Excision Repair: The UvrABC System. Chem Rev *106*, 233-252.

Uljon, S.N., Johnson, R.E., Edwards, T.A., Prakash, S., Prakash, L., and Aggarwal, A.K. (2004). Crystal Structure of the Catalytic Core of Human DNA Polymerase Kappa. Structure *12*, 1395-1404.

Vaisman, A., Tissier, A., Frank, E.G., Goodman, M.F., and Woodgate, R. (2001). Human DNA Polymerase ι Promiscuous Mismatch Extension. J Biol Chem *276*, 30615-30622.

Velasco-Miguel, S., Richardson, J.A., Gerlach, V.L., Lai, W.C., Gao, T., Russell, L.D., Hladik, C.L., III, C.L.W., and Friedberg, E.C. (2003). Constitutive and regulated expression of the mouse *DinB* (*Polκ*) gene encoding DNA polymerase kappa. DNA Repair *2*, 91-106.

Volker, M., Moné, M.J., Karmakar, P., Hoffen, A.v., Schul, W., Vermeulen, W., Hoeijmakers, J.H.J., Driel, R.v., Zeeland, A.A.v., and Mullenders, L.H.F. (2001). Sequential Assembly of the Nucleotide Excision Repair Factors In Vivo. Mol Cell *8*, 213-224.

Vrouwe, M.G., Pines, A., Overmeer, R.M., Hanada, K., and Mullenders, L.H.F. (2011). UV-induced photolesions elicit ATR-kinase-dependent signaling in non-cycling cells through nucleotide excision repair-dependent and -independent pathways. J Cell Sci *124*, 435-446.

Wakasugi, M., Reardon, J.T., and Sancar, A. (1997). The Non-catalytic Function of XPG Protein during Dual Incision in Human Nucleotide Excision Repair. J Biol Chem *272*, 16030-16034.

Walker, J.R., Corpina, R.A., and Goldberg, J. (2001). Structure of the Ku heterodimer bound to DNA and its implications for double-strand break repair. Nature *412*, 607-614.

Wang, B., Hurov, K., Hofmann, K., and Elledge, S.J. (2009). NBA1, a new player in the Brca1 A complex, is required for DNA damage resistance and checkpoint control. Genes Dev *23*, 729-739.

Wang, Y. (2007). Bulky DNA Lesions Induced by Reactive Oxygen Species. Chem Res Toxicol *21*, 276-281.

Warbrick, E. (2000). The puzzle of PCNA's many partners. BioEssays *22*, 997-1006.

Warbrick, E. (2006). A Functional analysis of PCNA-binding peptides derived from protein sequence, interaction screening and rational design. Oncogene *25*, 2850-2850.

Watanabe, K., Tateishi, S., Kawasuji, M., Tsurimoto, T., Inoue, H., and Yamaizumi, M. (2004). Rad18 guides pol[eta] to replication stalling sites through physical interaction and PCNA monoubiquitination. EMBO J *23*, 3886-3896.

Weissman, A.M. (2001). Themes and variations on ubiquitylation. Nature Rev Mol Cell Biol *2*, 169-178.

Williams, R.S., Williams, J.S., and Tainer, J.A. (2007). Mre11-Rad50-Nbs1 is a keystone complex connecting DNA repair machinery, double-strand break signaling, and the chromatin template. Biochem Cell Biol *85*, 509-520.

Wolski, S.C., Kuper, J., Hänzelmann, P., Truglio, J.J., Croteau, D.L., Houten, B.V., and Kisker, C. (2008). Crystal Structure of the FeS Cluster–Containing Nucleotide Excision Repair Helicase XPD. PLoS Biol *6*, 1332-1342.

Wu, F., Lin, X., Okuda, T., and Howell, S.B. (2004). DNA Polymerase ζ Regulates Cisplatin Cytotoxicity, Mutagenicity, and The Rate of Development of Cisplatin Resistance. Cancer Res *64*, 8029-8035.

Wu, L., and Hickson, I.D. (2003). The Bloom's syndrome helicase suppresses crossing over during homologous recombination. Nature *426*, 870-874.

Wu, X., Shell, S.M., Yang, Z., and Zou, Y. (2006). Phosphorylation of Nucleotide Excision Repair Factor Xeroderma Pigmentosum Group A by Ataxia Telangiectasia Mutated and Rad3-Related–Dependent Checkpoint Pathway Promotes Cell Survival in Response to UV Irradiation. Cancer Res *66*, 2997-3005.

Yoo, S., and Dynan, W.S. (1999). Geometry of a complex formed by double strand break repair proteins at a single DNA end: Recruitment of DNA-PKcs induces inward translocation of Ku protein. Nucleic Acids Res *27*, 4679-4686.

Zhao, Q., Wang, Q.-E., Ray, A., Wani, G., Han, C., Milum, K., and Wani, A.A. (2009). Modulation of Nucleotide Excision Repair by Mammalian SWI/SNF Chromatin-remodeling Complex. J Biol Chem *284*, 30424-30432.

Zhu, Q., Wani, G., Arab, H.H., El-Mahdy, M.A., Ray, A., and Wani, A.A. (2009). Chromatin restoration following nucleotide excision repair involves the incorporation of ubiquitinated H2A at damaged genomic sites. DNA Repair *8*, 262-273.

Zhuang, Z., Johnson, R.E., Haracska, L., Prakash, L., Prakash, S., and Benkovic, S.J. (2008). Regulation of polymerase exchange between Poleta and Poldelta by monoubiquitination

of PCNA and the movement of DNA polymerase holoenzyme. Proc Natl Acad Sci U S A *105*, 5361-5366.

Ziv, O., Geacintov, N., Nakajima, S., Yasui, A., and Livneh, Z. (2009). DNA polymerase ζ cooperates with polymerases κ and ι in translesion DNA synthesis across pyrimidine photodimers in cells from XPV patients. Proc Natl Acad Sci U S A *106*, 11552-11557.

Molecular Cell
Article

Three DNA Polymerases, Recruited by Different Mechanisms, Carry Out NER Repair Synthesis in Human Cells

Tomoo Ogi,[1,*] Siripan Limsirichaikul,[1,2,8] René M. Overmeer,[3,8] Marcel Volker,[4,8] Katsuya Takenaka,[5,8] Ross Cloney,[4,8] Yuka Nakazawa,[1,8] Atsuko Niimi,[1,4] Yoshio Miki,[5] Nicolaas G. Jaspers,[6] Leon H.F. Mullenders,[3,9] Shunichi Yamashita,[1,9] Maria I. Fousteri,[3,7,9] and Alan R. Lehmann[4,*]

[1]Department of Molecular Medicine, Atomic Bomb Disease Institute, Graduate School of Biomedical Sciences, Nagasaki University, 1-12-4, Sakamoto, Nagasaki 852-8523, Japan
[2]Department of Biopharmacy, Faculty of Pharmacy, Silpakorn University, Nakhon Pathom 73000, Thailand
[3]Department of Toxicogenetics, Leiden University Medical Center, Einthovenweg 20, 2333 ZC Leiden, Netherlands
[4]Genome Damage and Stability Centre, University of Sussex, Falmer, Brighton BN1 9RQ, UK
[5]Department of Molecular Genetics, Medical Research Institute, Tokyo Medical and Dental University, 1-5-45, Yushima, Bunkyo-ku, Tokyo 113-8510, Japan
[6]Department of Genetics, Erasmus University Medical Centre, Erasmus MC, 3000 CA Rotterdam, Netherlands
[7]Biomedical Sciences Research Center "Alexander Fleming," Vari 166-72, Greece
[8]These authors contributed equally to this work
[9]These authors contributed equally to this work
*Correspondence: togi@nagasaki-u.ac.jp (T.O.), a.r.lehmann@sussex.ac.uk (A.R.L.)
DOI 10.1016/j.molcel.2010.02.009

SUMMARY

Nucleotide excision repair (NER) is the most versatile DNA repair system that deals with the major UV photoproducts in DNA, as well as many other DNA adducts. The early steps of NER are well understood, whereas the later steps of repair synthesis and ligation are not. In particular, which polymerases are definitely involved in repair synthesis and how they are recruited to the damaged sites has not yet been established. We report that, in human fibroblasts, approximately half of the repair synthesis requires both polκ and polδ, and both polymerases can be recovered in the same repair complexes. Polκ is recruited to repair sites by ubiquitinated PCNA and XRCC1 and polδ by the classical replication factor complex RFC1-RFC, together with a polymerase accessory factor, p66, and unmodified PCNA. The remaining repair synthesis is dependent on polε, recruitment of which is dependent on the alternative clamp loader CTF18-RFC.

INTRODUCTION

Nucleotide excision repair (NER) is the most versatile DNA repair system that deals with both of the major UV photoproducts in DNA, as well as many other DNA adducts (Friedberg et al., 2005b). Most cases of xeroderma pigmentosum (XP), an extremely sunlight-sensitive and cancer-prone hereditary disease, result from a deficiency in one of the genes involved in NER (Andressoo and Hoeijmakers, 2005). The NER pathway can be divided into early and late steps: the molecular mechanism of the former, which involves sequential actions of XP proteins that recognize, unwind, and incise the damage, has been well characterized from bacteria to humans. However, the latter step, comprising gap-filling repair synthesis, in which DNA replication proteins fill in the ~30 nucleotide gap, and ligation, has not yet been defined in higher eukaryotes (reviewed in Gillet and Scharer, 2006; Hanawalt and Spivak, 2008).

Research on the postincision steps of human NER has been carried out mainly with in vitro reconstituted systems with recombinant proteins and/or tissue culture cell lysates (Aboussekhra et al., 1995; Araujo et al., 2000; Nishida et al., 1988). In these systems, the proteins that are involved in replicative DNA synthesis (or even bacterial or viral DNA replication proteins) can carry out the NER resynthesis reaction. Based on the findings of these studies, it has been assumed that both of the replicative DNA polymerases, polδ and polε, are responsible for repair synthesis in vivo and that the nick sealing is carried out by DNA Ligase I, similar to S phase DNA replication (see reviews). Since NER is considered a non-mutagenic process, the above model that the gap-filling step is performed by the high-fidelity B family DNA polymerases has been widely accepted (Wood and Shivji, 1997), despite the lack of definitive evidence to support this hypothesis.

Contrary to these assumptions, however, our groups have recently reported that an error-prone Y family DNA polymerase, polκ, is also involved in NER in mouse cells (Ogi and Lehmann, 2006) and that the XRCC1/Ligase III complex, which interacts with polβ and is involved in single-strand break repair and base-excision repair, is largely responsible for the NER nick ligation process in human cells (Moser et al., 2007).

DNA polymerase loading mechanisms in human cells have been extensively investigated with in vitro systems (reviewed in Johnson and O'Donnell, 2005). During DNA replication,

proliferating cell nuclear antigen (PCNA) is loaded by the replication factor C (RFC) clamp loader complex at the double-strand/single-strand DNA template-primer terminus in an ATP-dependent manner (Majka and Burgers, 2004). Subsequent to PCNA loading, the replicative DNA polymerase can access the replication site through an interaction with PCNA. A similar molecular mechanism has been assumed for NER repair synthesis as the gap remaining after damage incision and removal by XP proteins leaves a free 3′-OH terminus with an intact template, which is structurally similar to the replication elongation intermediate (Gillet and Scharer, 2006). In contrast, translesion synthesis (TLS), the bypass of DNA lesions that block replication by normal replicative DNA polymerases, involves a polymerase switch from the replicative to a specialized DNA polymerase (Friedberg et al., 2005a). Ubiquitination of PCNA, which is dependent on the E3 ubiquitin ligase RAD18, facilitates this process (Moldovan et al., 2007). All Y family polymerases have both PCNA-binding and ubiquitin-binding motifs, so ubiquitination of PCNA increases its affinity for these polymerases, thereby mediating the polymerase switch (Bienko et al., 2005; Kannouche et al., 2004; Plosky et al., 2006; Watanabe et al., 2004).

Clamp loaders are heteropentamers comprising four small subunits, RFC2–5, common to all clamp loaders and a large subunit that varies between complexes (Majka and Burgers, 2004). The classical RFC1–5 pentamer loads PCNA onto the DNA during replication. Because of their ability to interact with DNA polymerases, RFC complexes have been often implicated in loading different DNA polymerases themselves as well as loading PCNA and the alternative sliding clamp 9-1-1 (Kai and Wang, 2003; Masuda et al., 2007; Shiomi et al., 2007). The polκ homolog in *S. pombe*, DinB, is reported to be recruited to the replication fork by the 9-1-1 checkpoint clamp and RAD17 clamp loader complex, when the replication machinery encounters DNA damage (Kai and Wang, 2003).

Here we describe roles of three DNA polymerases, polδ, polε, and polκ, which we show are responsible for human NER repair synthesis in vivo. siRNA depletion of these polymerases diminished the repair synthesis activity in vivo. Recruitment of these polymerases into NER repair sites is differentially regulated by the status of PCNA ubiquitination as well as by usage of distinct clamp loader complexes or the repair scaffolding protein XRCC1. Based on the above findings, we propose a model for the involvement of mutagenic and conventional DNA polymerases and their differential loading mechanisms in NER repair synthesis.

RESULTS

UV Damage Induces PCNA Ubiquitination in Quiescent Human Cells

In previous work we and many other groups have highlighted the importance of PCNA ubiquitination in the regulation of TLS during replication of damaged DNA (Lehmann et al., 2007). TLS usually uses Y family DNA polymerases (Ohmori et al., 2001), which are recruited to ubiquitinated PCNA because they have binding motifs for both PCNA (PIP box) and ubiquitin (UBZ motif) (Bienko et al., 2005). We were interested to discover if ubiquitinated PCNA might have functions outside of S phase, so we examined primary human fibroblasts that were maintained for several days in low serum to bring them into quiescence. Figure 1A shows that UV irradiation did indeed result in PCNA ubiquitination in normal (48BR) cells (lanes 2–4), albeit at much lower levels than in exponentially growing SV40-transformed MRC5V1 cells (lane 1). Remarkably, a similar induction of PCNA ubiquitination was observed in XP-A (Figure 1A, lanes 5–7) and XP-C cells (lanes 8–10), indicating that, although UV dependent, it was independent of incision during NER. In all cases, the ubiquitinated PCNA was resistant to extraction by Triton X-100, indicating that it was bound to chromatin (Figure 1B).

The number of S phase cells in these cultures was negligible, as measured by the expression of cycling marker ki67 and nucleoside incorporation (Supplemental Experimental Procedures, available online), so there could be no involvement in replication-associated processes. Furthermore, hydroxyurea treatment for up to 4 hr, which stalls cells in S phase, did not elicit the ubiquitination of PCNA in quiescent normal (Figure 1C, lanes 4 and 5) or XP (lanes 8 and 9 for XP-A and lanes 12 and 13 for XP-C) cells, though it did, as shown previously, induce PCNA ubiquitination in cycling populations in S phase (lane 2) (Bienko et al., 2005).

Ubiquitinated PCNA Is Associated with Proteins Involved in the Late Step of NER

Although the results of Figure 1A indicate that PCNA ubiquitination was not dependent on damage incision during NER, we were interested to discover if it might nevertheless play a role in later steps of NER. In previous work, we have used chromatin immunoprecipitation (ChIP) to identify protein complexes involved in different stages of NER (Fousteri et al., 2006; Moser et al., 2007). In particular we were able to identify a complex that was UV dependent and contained proteins involved in the late, postincision steps of NER, including RPA, XRCC1, and PCNA. Figures 1D and 1E show immunoblots revealing some of the components of this complex following ChIP with anti-PCNA antibody from normal cells under various different conditions. Remarkably, a band corresponding to ubiquitinated PCNA was easily observable in these ChIPs. This band was dependent on UV irradiation and could be observed both in serum-starved (G0) cells (Figures 1D and 1E, lanes 1 and 2) and cycling cells close to confluence (lanes 3 and 4). This represents a considerable enrichment of the ubiquitinated PCNA relative to unmodified PCNA (compare relative intensities of modified and unmodified bands in Figures 1D, 1E, and 1A). We noted in these complexes the presence of polδ both in G0 cells and in cycling cells (Figure 1D), consistent with our previous observations (Moser et al., 2007), and also polε only in cycling cells (Figure 1E). Both of these DNA polymerases have been previously implicated in NER repair synthesis in an in vitro reconstituted system (Araujo et al., 2000). Polη, which is involved in TLS of cyclobutane pyrimidine dimers, was barely detectable in the ChIP (Figure 1E, lane 4). Importantly, the complex also contained polκ (Figure 1D), which we have previously shown to be involved in NER in mouse embryonic fibroblasts (Ogi and Lehmann, 2006). The amount of polκ in the ChIP was significantly higher in G0 cells than in cycling cells (Figures 1D and 1E, compare lanes 2 and 4). The cellular dNTP levels are reduced in quiescent cells, so this finding supports

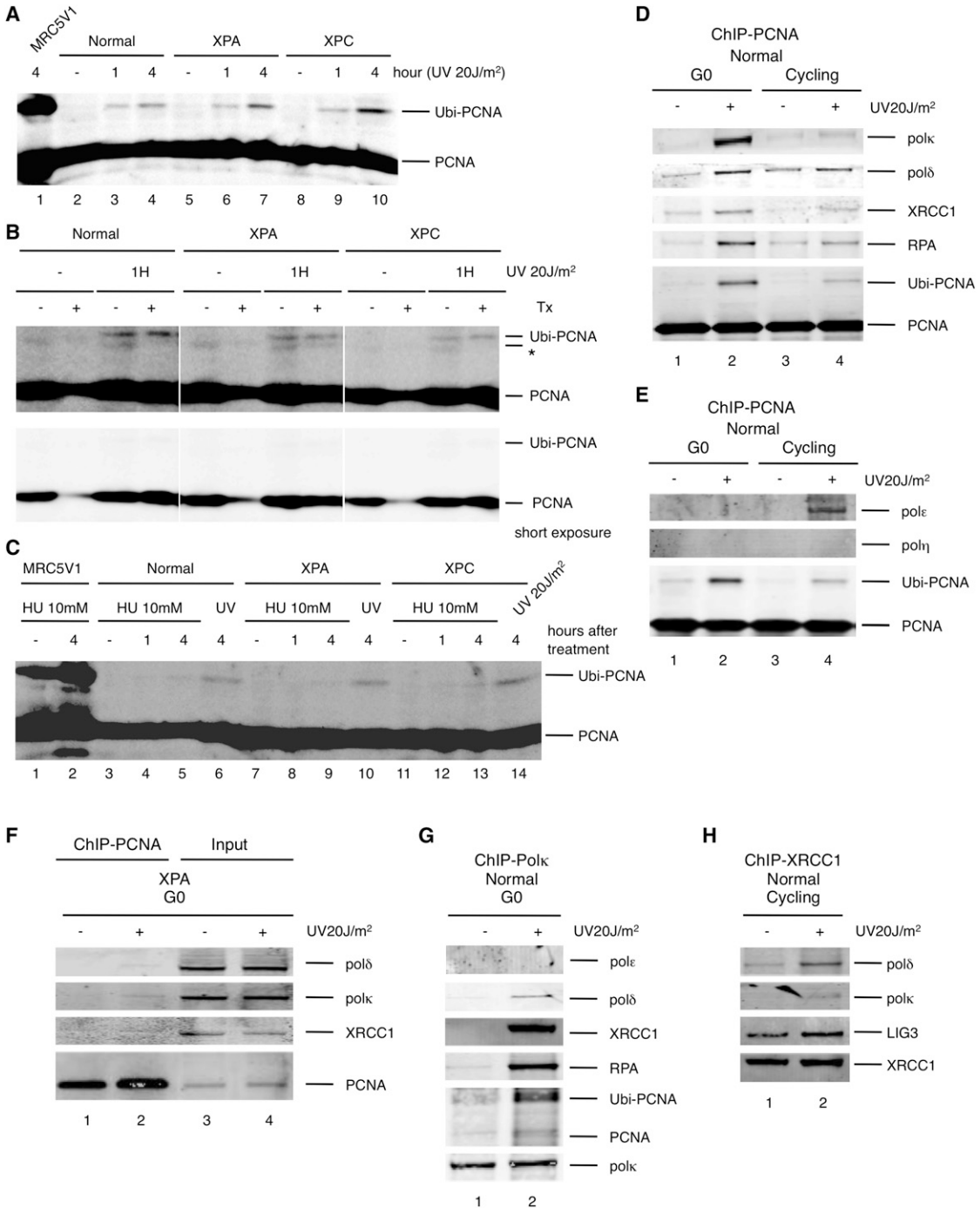

Figure 1. UVC Irradiation-Dependent PCNA Ubiquitination in Quiescent Cells and Interaction of DNA Polymerases with NER Postincision Machinery

(A–C) Western blot showing ubiquitination of PCNA at indicated times after 20 J/m^2 global UVC irradiation (A and B) or 10 mM hydroxyurea (HU) treatment (C) in quiescent cells. Normal (48BR), XPA (XP15BR), and XPC (XP21BR) are all quiescent primary fibroblasts (G0). −, without treatment. SV40-transformed MRC5 cells (MRC5V1) were used as a control. In (B), cells were extracted with Triton X-100 before harvesting (Tx).

(D–H) Normal (VH25) or XPA (XP25RO) primary fibroblasts that were either serum starved (G0) or close to confluent density (Cycling) were globally UVC irradiated (20 J/m^2) and incubated for 1 hr. Repair proteins were then crosslinked to DNA with formaldehyde treatment followed by ChIP with mouse anti-PCNA, PC-10 antibody (D–F), rabbit anti-polκ, K1 antibody (G), or mouse anti-XRCC1, 33-2-5 antibody (H). Coprecipitated proteins were analyzed by western blotting with the antibodies listed in the Supplemental Experimental Procedures. See also Figure S1.

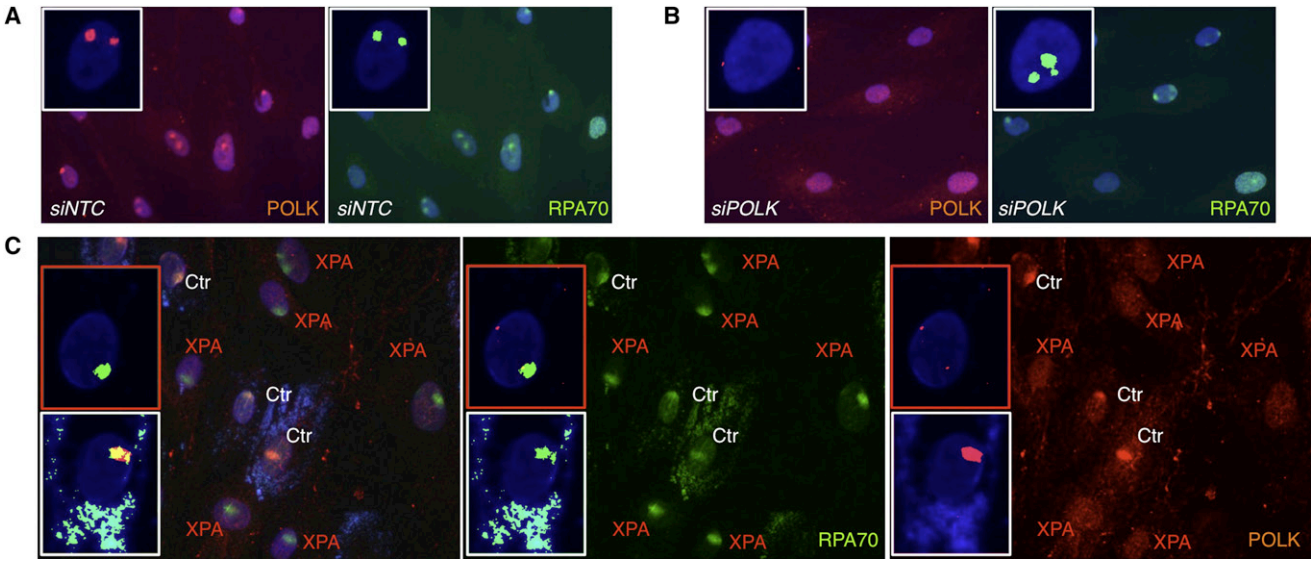

Figure 2. Polκ Accumulation at Local Damage Is Dependent on Early Steps of NER

(A and B) Non-dividing normal 48BR human primary fibroblasts were transfected with either *siNTC* non-targeting control (A) or *POLK* targeting siRNA (B), UVC irradiated (40 J/m^2) through a polycarbonate micropore filter (5 μm), followed by 30 min incubation with 10 mM hydroxyurea and immunostaining with mouse anti-RPA70 (RPA70-9; green) and rabbit anti-polκ (K1; red) antibodies. Blue, DAPI stain.

(C) XP15BR XP-A cells were cocultured with normal 48BR cells containing blue beads (Ctr), UVC irradiated and processed as in (A), except that the post-UVC incubation was for 1 hr without hydroxyurea. The insets in this and subsequent figures show enlarged images of individual cells. The inset in the white box is a normal cell and in the red box an XP cell. See also Figure S2.

our previous proposal that polκ might be the optimal polymerase for NER repair replication when dNTP concentrations are low (Ogi and Lehmann, 2006). Very little of the above proteins were precipitated from unirradiated cells (Figures 1D and 1E, lanes 1 and 3), confirming that these interactions were DNA damage specific. We did not observe any significant interaction in a similar ChIP with anti-PCNA antibody from NER-deficient non-dividing XPA cells (Figure 1F, lanes 1 and 2). Importantly, the same proteins were obtained in the converse experiment using anti-polκ (Figure 1G) as well as anti-XRCC1 (Figure 1H) antibodies for the ChIPs. In particular, Figure 1G shows that polκ and polδ are present in the same repair complex.

Recruitment of DNA Polymerase κ into Repair Sites Is Dependent on NER Damage Incision

To determine if ubiquitinated PCNA is required for recruitment of DNA polymerases to NER complexes, we used the technique of irradiation of non-dividing primary human fibroblasts through a micropore filter to generate damage in localized parts of the nucleus (Volker et al., 2001). We then analyzed the accumulation of polymerases at the sites of local damage (ALD). Using anti-polκ antibodies that detect endogenous levels of polκ (Figures S1A and S1B), we were able to observe polκ ALD following UV irradiation of confluent primary human fibroblasts, where it colocalized with DNA damage (Figure S2A) and with RPA (Figure 2A). Using *POLK* siRNA, we confirmed that these ALD "spots" did indeed represent polκ (Figure 2B and Figure S2B).

Polκ ALD could be observed either in quiescent cells or in cycling cells outside of S phase (Figure S2C), but was not seen in S phase cells (Figure S2D). We previously showed that polκ, unlike the other Y family polymerases, is rarely located in replication factories (Ogi et al., 2005). The intensity of the ALD spots could be amplified by incubation in hydroxyurea after UV irradiation (Figures S2E and S2F, right panels). We have occasionally used hydroxyurea in ALD experiments to obtain clearer images, but in all cases, we have observed similar phenomena with and without the inhibitor, any differences being quantitative rather than qualitative.

We next used XP cells from different complementation groups, whose gene products function in the preincision and dual incision steps of global NER. In XP-A (Figure 2C), -C, and -G cells, and in cells depleted of XPF (Figures S2G–2I), polκ ALD was abolished, whereas it did accumulate at damaged sites in cocultivated normal cells that were loaded with latex beads to distinguish them from the XP cells. Polκ ALD was not affected in Cockayne syndrome (CS-B) cells, which are defective in the transcription-coupled branch of NER (which only contributes to ~5% of the entire NER activity) (Figure S2J). These results show that in human primary fibroblasts, polκ is involved in a late stage of NER that is dependent on successful completion of the early incision steps.

Role of DNA Polymerase κ in NER Repair Synthesis Is Dependent on Its UBZ Zn Finger Domain and PCNA Ubiquitination by *RAD18*

We next examined if recruitment of polκ during NER was dependent on PCNA ubiquitination. A key enzyme required to ubiquitinate PCNA is the E3 ubiquitin ligase RAD18 (Hoege et al., 2002; Kannouche et al., 2004; Watanabe et al., 2004). In a previous report, RAD18 was shown to regulate polκ recruitment to stalled

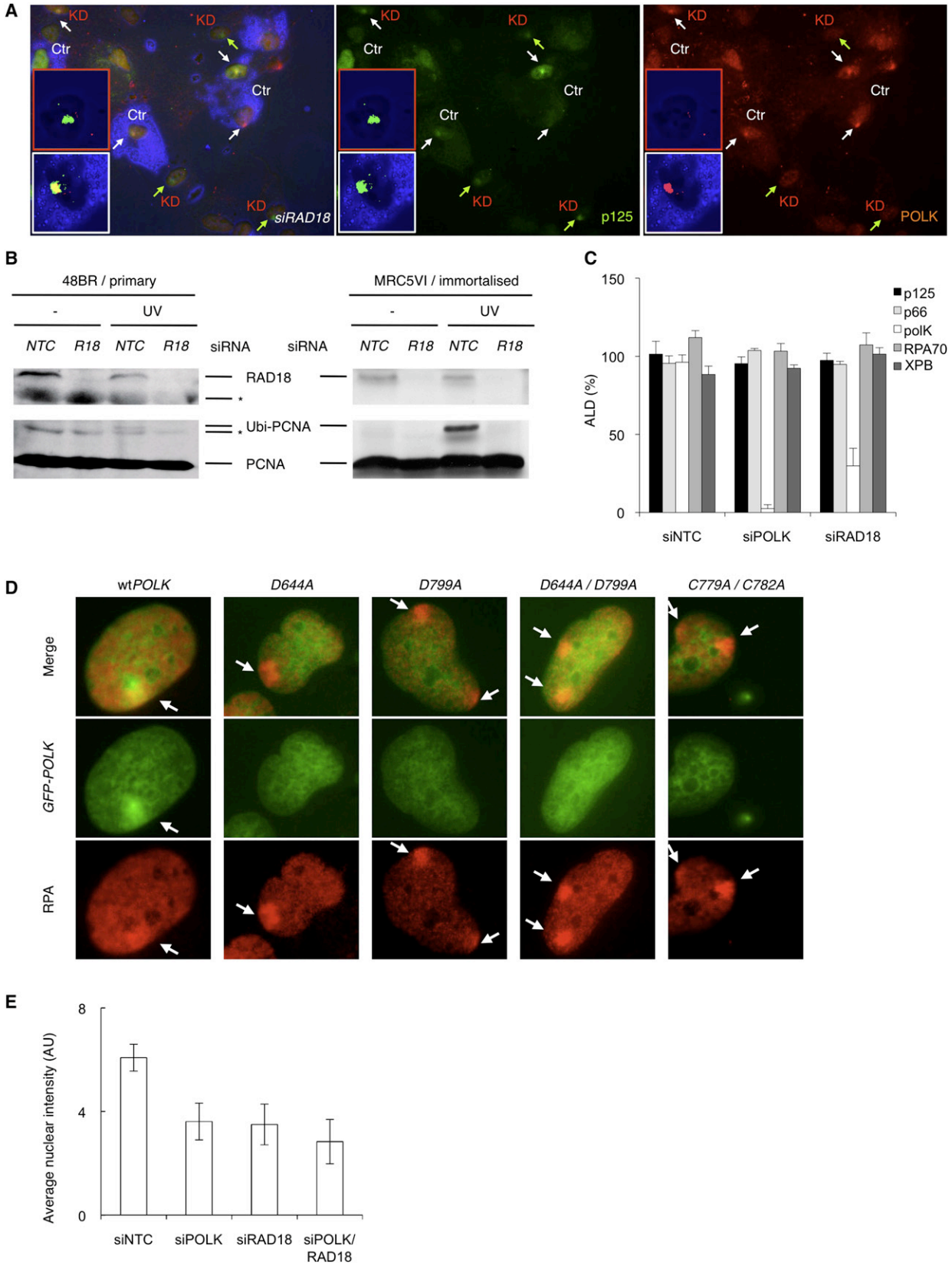
A
KD
Ctr
siRAD18
p125
POLK
B
48BR / primary
MRC5VI / immortalised
-
UV
NTC
R18
siRNA
RAD18
Ubi-PCNA
PCNA
C
ALD (%)
150
100
50
0
p125
p66
polK
RPA70
XPB
siNTC
siPOLK
siRAD18
D
wtPOLK
D644A
D799A
D644A / D799A
C779A / C782A
Merge
GFP-POLK
RPA
E
Average nuclear intensity (AU)
8
4
0
siNTC
siPOLK
siRAD18
siPOLK/
RAD18

replication forks during TLS of bulky DNA adducts (Bi et al., 2006). We therefore examined the effect of depleting RAD18 on ALD of polκ in NER repair synthesis. In these experiments, we cocultivated cells treated with a non-targeting control and loaded with latex beads with cells treated with a specific *RAD18* siRNA. Depletion of RAD18 resulted in a reduction in polκ ALD (Figure 3A, right panel, compare nuclei indicated with green [polκ ALD negative] and white [polκ ALD positive] arrows); we also confirmed that PCNA ubiquitination after UVC irradiation was completely abolished in the cells treated with *RAD18* siRNA (Figure 3B). The ALD data are quantitated in Figure 3C.

Polκ contains two C2HC ubiquitin-binding zinc finger (UBZ) motifs that are required for binding of polκ to ubiquitinated PCNA (Bienko et al., 2005; Guo et al., 2008). Apart from the cysteine residues, D644 and D799 are crucial aspartate residues that are essential for binding of the zinc finger to ubiquitin (Bienko et al., 2005). We mutated different residues in one or both of these motifs and found that this abolished polκ ALD (Figure 3D). (Figure S2K shows expression levels of the different GFP-polκ constructs. These varied about twofold between cells expressing different constructs, but there was no correlation between expression level and ALD.)

ALD and ChIP measure the recruitment of proteins to the sites of DNA damage but do not prove unequivocally that they are required for repair of the damage. We therefore measured the repair replication step of NER, using a recently developed fluorescence-based variation of the unscheduled DNA repair synthesis (UDS) assay by incorporation of a thymidine analog, ethynyl deoxyuridine (Figures S3A and S3B) (Limsirichaikul et al., 2009). As shown in Figure 3E and Figure S3C, depleting cells of polκ yielded a substantial reduction in UDS, similar to the reduction that we previously observed in *Polk*-deficient mouse embryonic fibroblasts (Ogi and Lehmann, 2006). Depletion of RAD18 resulted in a comparable level of reduction in UDS and depletion of both RAD18 and polκ resulted in only a slight further reduction. To rule out any off-target effects from these pools of four siRNAs, we also analyzed the effects of each siRNA individually. Figure S3D shows that each individual siRNA had a similar effect to the pool, ruling out any off-target effects. Taken together, the data of Figures 1–3 suggest that polκ is recruited to sites of NER by binding to ubiquitinated PCNA, where it is involved in repair synthesis at about 50% of the repair sites.

Polymerase δ and NER

Mammalian polδ contains four subunits, p125, p66, p50, and p12 (Podust et al., 2002). p125 and p50 are the catalytic-core subunits (Lee et al., 1991) and p66 is an accessory factor that binds to PCNA (Hughes et al., 1999). Confirming our previous results (Moser et al., 2007), polδ accumulates at local damage, as shown for both p125 and p66 in Figure 3A (middle for p125) and Figure 4A (top for p125 and middle for p66). In contrast to polκ, ALDs of p125 and p66 were unaffected by depletion of RAD18 (compare green and white arrows in Figure 3A; quantitation in Figure 3C), suggesting that ubiquitination of PCNA is not required for recruitment of polδ to NER sites following incision by the XP proteins.

We next investigated the interdependency of polκ and polδ for relocation to DNA damage. We anticipated that the localization of polκ might be dependent on the p66 subunit of polδ as p66 has been implicated in recruiting translesion polymerases to stalled replication forks in yeast (Gerik et al., 1998; Gibbs et al., 2005). Additionally, the contribution of p66 to recruiting the polδ catalytic core to PCNA loaded onto DNA is still contentious: Pol32p, the p66 subunit of yeast polδ, is dispensable for cell viability, suggesting that it is not essential for DNA synthesis itself (Gerik et al., 1998). Some in vitro evidence also suggests that DNA synthesis activity of polδ stimulated by PCNA may not be strongly dependent on p66 (Podust et al., 2002; Zhou et al., 1997), although contradictory data have also been reported (Ducoux et al., 2001; Masuda et al., 2007; Shikata et al., 2001). To determine the roles of p66 in NER repair synthesis, we examined the effects of siRNA depletion of *POLD3* (p66) as well as *POLD1* (p125) on ALD of the polymerases. Interestingly, ALD of polδ p125 catalytic core was dependent on the p66 subunit (Figure 4A, top right; and Figure 4B), whereas ALD of the p66 subunit was independent of p125 (middle center panel); this observation favors the previous reports suggesting that p66 is crucial for DNA synthesis (Ducoux et al., 2001; Masuda et al., 2007; Shikata et al., 2001). ALD of polκ was not dependent on either subunit of polδ (Figure 4A, bottom); in fact, depletion of

Figure 3. Role of Polκ in NER Is Dependent on PCNA Ubiquitination

(A) siRNA knockdown of RAD18 diminishes the ALD of polκ but not polδ. Cells incubated with blue beads and siRNA non-targeting control were cocultivated with cells incubated with *RAD18* siRNA and locally UVC irradiated (5 μm pores, 40 J/m^2), followed by 1 hr incubation without inhibitors. White arrows indicate polδ (p125; green) and polκ (red) double positive nuclei in cells treated with non-targeting control (also in inset in white box), whereas green arrows indicate nuclei with polδ spots only in cells treated with *RAD18* siRNA (also shown in inset in red box).

(B) Western blot showing that siRNA knockdown of RAD18 abolishes PCNA ubiquitination. Normal 48BR primary fibroblasts (left) or normal but SV40 immortalized MRC5VI cells (right) were transfected with either *siNTC* non-targeting control (*NTC*) or *RAD18* targeting (*R18*) siRNA and cultured at close to confluent density. Cells were globally UVC irradiated (10 J/m^2), followed by incubation for 1 hr without inhibitors. RAD18 and the ubiquitinated PCNA were respectively detected by rabbit anti-RAD18 (Abcam) and mouse anti-PCNA (PC-10) antibodies. Asterisks indicate non-specific bands.

(C) ALD of indicated NER proteins in 48BR cells depleted of RAD18 or polκ using siRNAs. Cells were locally UVC irradiated as in (A). Percentage of ALD represents the relative percentage of cells showing ALD of the indicated protein above a predetermined threshold compared with the percentage in relevant controls. Bars and error bars indicate, respectively, averages and standard deviations calculated from at least three independent experiments.

(D) ALD of wild-type or indicated mutants of polκ. SV40-transformed MRC5 cells were transfected with plasmid expressing either GFP-tagged wild-type human *POLK* or *POLK* with UBZ mutations at the indicated amino acid positions (GFP-POLK; green; see also Figure S2K). Cells were locally UVC irradiated as in (A), followed by immunostaining with anti-RPA antibody (RPA70-9; red).

(E) Effect of RAD18 and polκ depletion on UDS. 48BR cells were transfected with indicated siRNAs and UVC irradiated (10 J/m^2) followed by EdU incorporation for 2 hr. Bars and error bars, respectively, indicate averages and standard deviations of nuclear fluorescent intensity measured in at least 250 nuclei from at least five different positions. See also Figure S3.

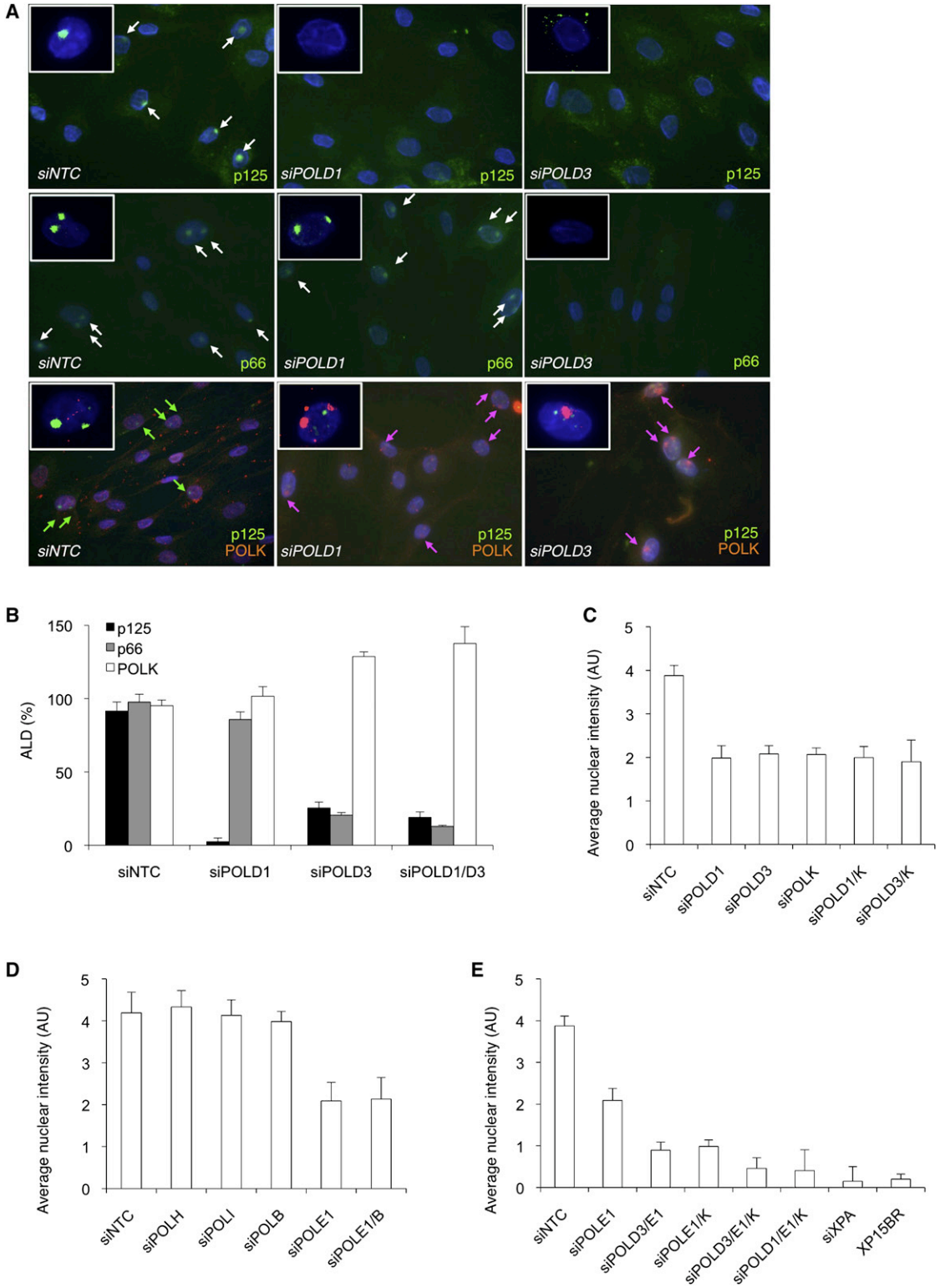

Figure 4. Effects of DNA Polymerase Knockdowns on UDS and ALD

(A) ALD of polδ p125 (A-9 antibody; top and bottom, green), p66 (3E2 antibody; middle, green), and polκ (K1 antibody; bottom, red) in primary 48BR cells treated with the indicated siRNA and locally UVC irradiated (40 J/m^2) followed by 30 min incubation. In the top and middle panels, white arrows represent nuclei with spots of indicated polδ subunit, whereas in the bottom panel, green and red arrows indicate nuclei with polδ p125 and polκ spots, respectively. Note that smaller sized green spots seen in the bottom panels are nonspecific nucleoli staining.

the polδ subunit(s) resulted in a modest increase in polκ ALD (Figure 4B). These data show that polκ and polδ are recruited to damage independently and that recruitment of polδ requires its p66 subunit.

DNA Polymerases δ, ε, and κ, but Neither β, η, nor ι, Are Responsible for NER Repair Synthesis

We next examined the effects of DNA polδ depletion on repair synthesis activity. As shown in Figure 4C (see also Figure S3C), depleting cells of the p125 (*POLD1*) or p66 (*POLD3*) subunits of polδ resulted in a 50% reduction in UDS, as observed with polκ depletion. However depletion of either subunit of polδ together with polκ had no further effect, suggesting that these two polymerases play roles in the same subpathway of repair replication. This conclusion is supported by the finding of both polymerases in the same repair complex, as shown above in Figure 1G. To determine which polymerase might be responsible for the remaining ~50% of UDS when both polκ and/or polδ are depleted, we examined the effects on UDS of depleting other polymerases. Polβ is well known to interact with the XRCC1/Lig3 complex, which we recently showed was involved in the ligation step of NER (Moser et al., 2007); however, in the same report, we failed to demonstrate the recruitment of polβ into NER repair sites (Moser et al., 2007). Consistent with this report, we found that depletion of polβ (*POLB*) had no significant effect on UDS, as was also the case for depletion of the Y family polη or polι (Figure 4D). In striking contrast, depletion of polε reduced UDS by about 50% (Figure 4D). Depletion of polε together with polβ did not elicit any further decrease (Figure 4D), but depletion of both polε and either polδ (*POLD3*) or polκ reduced UDS to about 25% and depletion of all three left only 10%–15% of the level in normal cells (Figure 4E). Since this is also the level that we observed in cells depleted of *XPA*, or a completely NER-defective XP-A cell strain (Figure 4E and Figures S3C and S3D; Limsirichaikul et al., 2009), we regard this as the detection limit of the technique and conclude that polε is indeed responsible for the repair synthesis that is not completed by polδ and polκ. Consistent with this we were able to detect ALD of polε under mild permeabilization conditions (Figure S4A). Whereas ALD of all other proteins was resistant to Triton X-100 extraction, polε that had accumulated at local damage was extracted by the same triton treatment (Figure S4B). This suggests that polε is less tightly bound to chromatin than other proteins or that it is bound more transiently. Taken together, our data show that three polymerases, polδ, polε, and polκ, are responsible for almost the entire repair synthesis in primary human cells.

Differential DNA Polymerase-Loading Mechanisms in NER Repair Synthesis

The above findings prompted us to consider differential polymerase recruitment mechanisms in NER repair synthesis, as the recruitment kinetics as well as the epistatic effects of polymerase depletions on UDS seemed different between polδ/κ and polε.

We first attempted to find out if any other clamps, clamp loaders, and scaffold proteins were required for recruitment of polδ and polκ during NER. We expected that the involvement of (unmodified) PCNA in the recruitment of polδ and of ubiquitinated PCNA in recruitment of polκ would implicate a clamp-loading complex in the recruitment of these polymerases. Although depletion of RFC1, RFC4, or both subunits reduced ALD of polδ-p125, surprisingly it had no effect on ALD of either polκ or polδ-p66 (Figures 5A and 5B). This finding indicates that the recruitment of DNA polymerases may not require post-UV loading of PCNA onto chromatin by the conventional RFC1-RFC. Additionally, RFC-independent p66 recruitment is consistent with a recent publication suggesting that p66 can compete with RFC and prevent pre-loaded PCNA being unloaded or relocated from the 3′ termini of replication sites by RFC (Masuda et al., 2007).

We next examined the effects of depleting either the checkpoint clamp loader RAD17 and also the checkpoint activator ATR. We found no significant effect on ALD of polκ or polδ (Figure 5A), in contrast to a report that the *S. pombe* ortholog of polκ is recruited to stalled replication forks by RAD17 and the 9-1-1 complex (Kai and Wang, 2003). Depletion of two other alternative clamp loader large subunits, CTF18 or FRAG1, had no effect on ALD of polκ, polδ-p66, or polδ-p125 (Figure 5A). In contrast, the scaffold protein XRCC1, previously shown to be a component of the postincision complex (Moser et al., 2007), was needed for ALD of polκ (Figures 5A and 5C). Depletion of any of the factors needed for ALD of polδ or polκ also resulted in a 50% reduction in UDS, whereas depletion of ATR or RAD17 had very little effect on repair synthesis (Figure 5D). In summary, these experiments suggest that polδ-p125 is loaded onto PCNA by RFC1-RFC and p66, whereas polκ is loaded onto ubiquitinated PCNA and requires XRCC1 but not RFC. Failure to load either of these polymerases results in a reduction in UDS to about 50% of its normal level, similar to that found by depleting the polymerases.

We have further examined whether any of the loading factors might also be needed for ALD of polε. As shown in Figure 5E, depletion of RAD18 did not elicit any reduction in polε ALD, suggesting that polε is loaded onto unmodified PCNA. Depletion of XRCC1 or the alternative clamp loader large subunits, RAD17 or FRAG1, did not affect polε ALD; however, depletion of either RFC4 or CTF18 resulted in a reduction in polε ALD, suggesting that CTF18-RFC is involved in loading polε in repair synthesis (Figures 5E and 5F). CTF18 is the human homolog of yeast Ctf18p, which is essential for accurate chromosome transmission, being implicated in sister chromatid cohesion (Hanna et al., 2001) and double strand break repair (Ogiwara et al., 2007). Additionally, recent reports demonstrated that CTF18-RFC can stimulate the activity of polη (Shiomi et al., 2007) as well as polδ (Bermudez

(B) Histogram analyses are shown. Bars and error bars indicate, respectively, averages and standard deviations of the percentages of ALD calculated from at least three independent experiments shown in (A).

(C–E) Effects of multiple DNA polymerase knockdowns on UDS. 48BR cells were transfected with indicated siRNAs and UVC irradiated (10 J/m^2) followed by EdU incorporation for 2 hr. Bars and error bars, respectively, indicate averages and standard deviations of nuclear fluorescent intensity measured in at least 250 nuclei from at least five different positions.

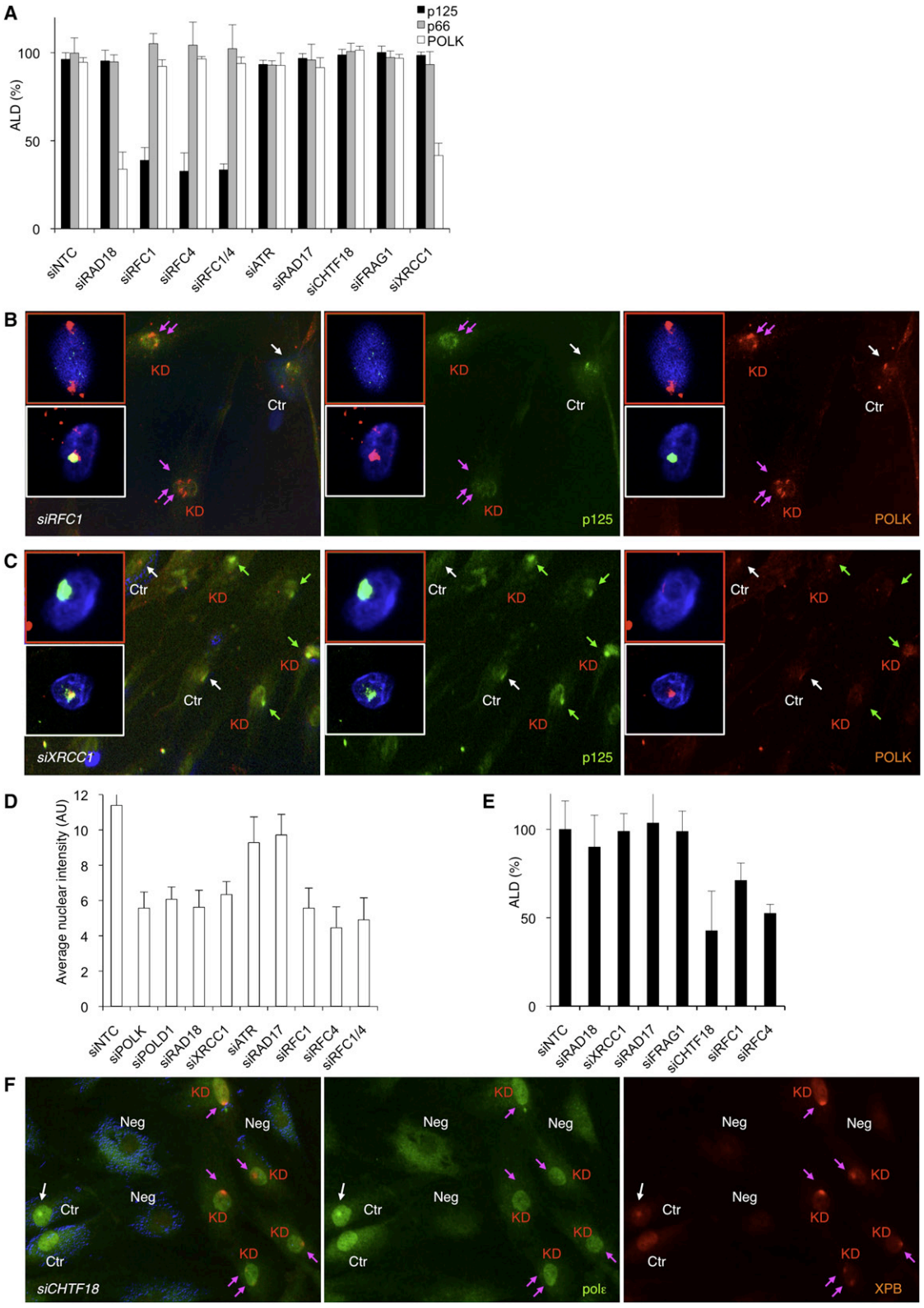

Figure 5. Differential Requirement of Repair Replication Factors for Recruitment of Gap-Filling DNA Polymerases

(A) ALD of polδ p125, p66, and polκ in 48BR cells depleted of indicated genes using siRNAs and local UVC irradiation (40 J/m^2) followed by 1 hr incubation without inhibitors. Bars and error bars indicate, respectively, averages and standard deviations of the percentages of ALD calculated from at least three independent experiments.

et al., 2003), suggesting that CTF18-RFC may play a role in loading specific polymerases during replication when needed.

We also observed a modest reduction of polε ALD in cells depleted of RFC1 (Figure 5E); however, because of the aforementioned technical issue, the experimental errors were substantially larger than errors in ALD measurements of the other proteins.

Considering these polε ALD results together, we propose that loading of polε onto PCNA is mainly dependent on the alternative clamp loader complex CTF18-RFC.

DISCUSSION

Our results have revealed an unexpected complexity in repair synthesis in human cells. Approximately 50% of the repair synthesis used polκ recruited by ubiquitinated PCNA and XRCC1, together with polδ recruited by the classical RFC complex. The remaining 50% is carried out by polε recruited by the CTF18-RFC complex. We propose the following model to explain our findings. RAD18 accumulates at sites of UV damage very rapidly and independently of NER-mediated dual incision (Figure 6A) (Nakajima et al., 2006; unpublished data). Ubiquitination of preloaded PCNA and repositioning of PCNA to the site of the lesion may therefore occur before completion of the preincision complex assembly (Figure 6B). In support of this suggestion, we have been able to detect low levels of ALD of PCNA (but not of polδ) in several NER-deficient XP primary fibroblasts (J. Moser, R.M.O., and M.I.F., unpublished data). Our results delineate two pathways for repair synthesis, following incision, one dependent on polε and the other requiring both polδ and polκ. One possibility is that the former deals with damage on the leading strand and the latter on the lagging strand. We consider, however, a more likely explanation to be that different mechanisms are used to deal with different conformations of the repair sites or of the chromatin structure around the damaged sites. We suggest that 50% of the sites are in an accessible configuration and polε can carry out repair synthesis rapidly (Figures 6Ca–6Ea). In mode 1, polε recruitment by CTF18-RFC occurs following conventional dual incision; possibly, recruitment of polδ and polκ might be inhibited (Figures 6Ca–6Da). After completion of repair synthesis, release of polε and recruitment of LigI occur (Figure 6Ea).

In the second pathway, for example, because of the conformation of the repair site or the chromatin structure, repair synthesis is more difficult, resulting in 3′ incision being delayed relative to 5′ incision (Figure 6Cb). This causes displacement synthesis, as was also proposed in early studies (Mullenders et al., 1985; Smith and Okumoto, 1984) and is consistent with the recent finding that XPF cleaves on the 5′ side of the damage prior to cleavage on the 3′ side by XPG, thereby leaving a 5′ flap to be displaced (Staresincic et al., 2009). This second mode (Figures 6Cb–6Eb) has more rigid requirements because of the surrounding steric hindrance; this mode involves both polδ and polκ. Recruitment of polδ occurs independently of PCNA ubiquitination status, but does depend on its accessory p66 subunit as well as the RFC complex (Figure 6Cb), whereas recruitment of polκ requires XRCC1 as well as ubiquitination of PCNA (Figure 6Db). Hydroxyurea prevents completion of repair synthesis, resulting in an accumulation of repair synthesis intermediates, perhaps because of displacement synthesis as suggested earlier (Mullenders et al., 1985; Smith and Okumoto, 1984), and an increased ALD of repair synthesis proteins.

XRCC1 appears to have a fairly direct, as yet undefined, role in recruiting polκ, and, after completion of repair synthesis, release of polymerases from the repair patch and XRCC1-dependent recruitment of LigIII occur (Figure 6Eb). Our data are consistent with a recent report suggesting that in vitro polδ is rather distributive, even in the presence of PCNA, whereas RFC remains at the primer terminus (Masuda et al., 2007). Which of the polymerases operates first in mode 2 and why both are needed will be the subject of future studies.

The major function of Y family DNA polymerases is believed to be in TLS, the bypass of DNA lesions that block replication by normal replicative DNA polymerases (Prakash et al., 2005). Because of this property, the replication fidelities of the Y family enzymes are very low (McCulloch and Kunkel, 2008). Polκ is specialized for TLS past bulky DNA lesions (Avkin et al., 2004; Ohashi et al., 2000b; Suzuki et al., 2002) and induces mutations when it acts on undamaged templates with a frequency of about 10^{-3} (Ohashi et al., 2000a; Zhang et al., 2000). We have considered the possibility that when there are two closely spaced lesions on opposite strands, repair synthesis on one strand will need to bypass the lesion on the opposite strand and that the role of polκ is to carry out this TLS step. Lam and Reynolds (1986) carried out a detailed analysis of the frequency of closely spaced lesions in human fibroblasts. After a dose of 40 J/m^{-2} used in our ALD experiments, they found that the proportion of overlapping lesions (0.8/10^8 daltons) represented only 0.5% of the total lesions (1.5/10^6 daltons). We think that this is unlikely to explain our data. There is increasing evidence that apart from their roles in TLS, Y family polymerases have other functions as well

(B) Depletion of RFC1 abolishes polδ ALD but does not affect polκ ALD. Cells with non-targeted siRNA cultured with blue beads were cocultured with cells in which RFC1 was depleted by siRNA. White arrow indicates polδ (p125; green) and polκ (red) double positive nuclei, whereas red arrows indicate nuclei with polκ spots only. KD, knockdown (also inset with red box); Ctr, control (also inset in white box).

(C) Depletion of XRCC1 abolishes polκ ALD but does not affect polδ ALD. White arrows indicate polδ (p125; green) and polκ (red) double positive nuclei, whereas green arrows indicate nuclei with polδ spots only.

(D) UDS following depletion of indicated genes. 48BR cells were transfected with indicated siRNAs and UVC irradiated (10 J/m^2) followed by EdU incorporation for 2 hr. Bars and error bars, respectively, indicate averages and standard deviations of nuclear fluorescent intensity measured in at least 250 nuclei from at least five different positions.

(E) ALD of polε in 48BR cells depleted of indicated genes using siRNAs. Cells were pre-fixed before immunostaining, as described in Figure S4. Bars and error bars indicate, respectively, averages and standard deviations of the percentages of ALD calculated from at least three independent experiments.

(F) Depletion of CTF18 inhibits polε ALD. Cells with non-targeted siRNA cultured with blue beads were cocultured with cells in which CTF18 was depleted by siRNA. As described in Figure S4, cells were pre-fixed before immunostaining. White arrow indicates polε (green) and XPB (red) double positive nuclei, whereas red arrows indicate nuclei with XPB spots only. Neg, polε negative non-cycling cells.

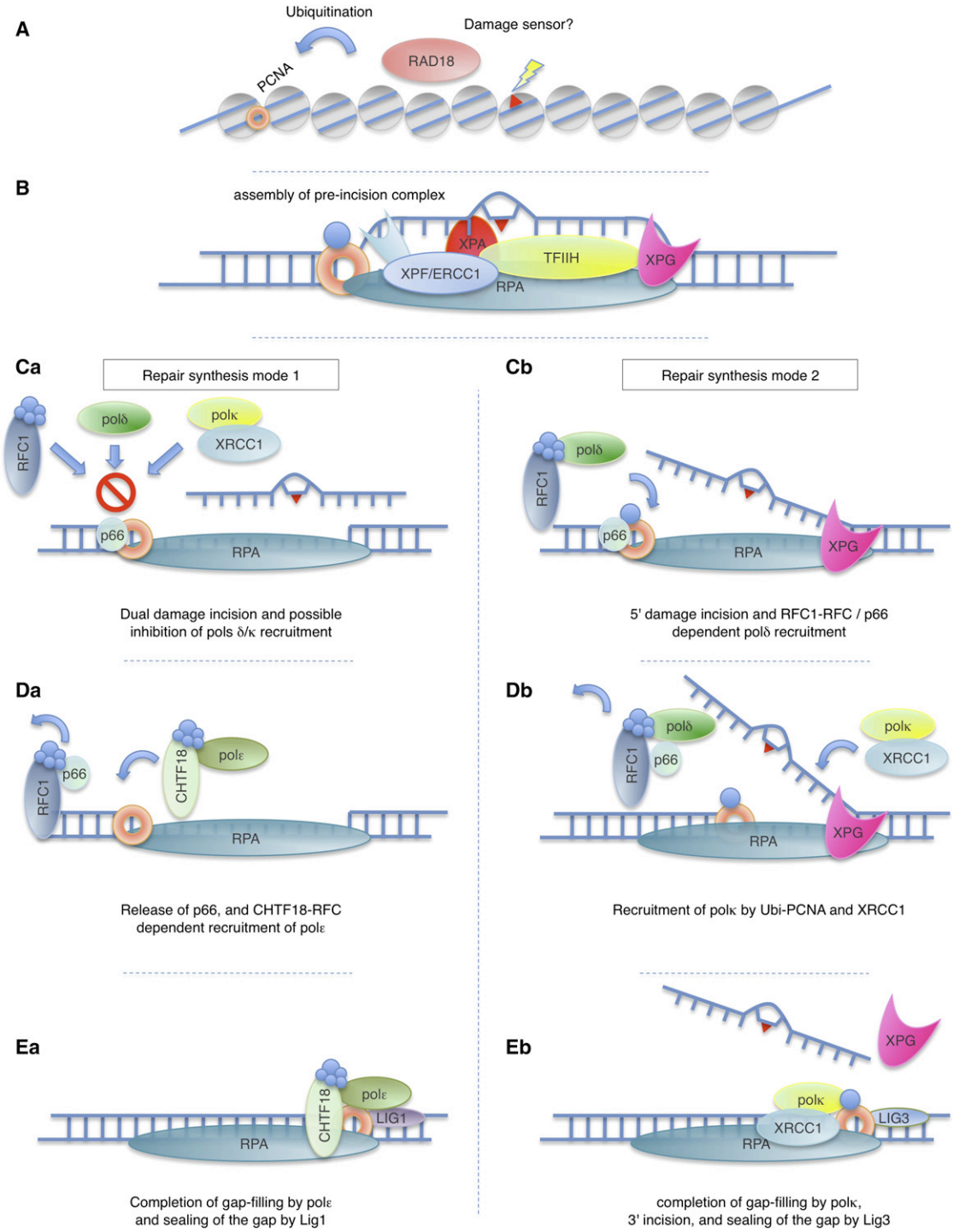

Figure 6. Model for Action of Polκ and Polδ during NER Gap-Filling DNA Synthesis

(A) Section of chromatin in quiescent cells with PCNA loaded on the DNA and damage sensed by RAD18, which is then able to ubiquitinate PCNA.

(B) Assembly of the preincision complex.

(Ca–Ea) In mode 1, following dual incisions to release the damaged fragment (Ca), polε is recruited by CTF18-RFC to fill the gap (Da), followed by Ligase I recruitment to seal the nick (Ea).

(Cb–Eb) In mode 2, 5′ incision is followed by recruitment of both polδ core by RFC and p66 (Cb) and polκ/XRCC1 by ubiquitinated PCNA (D2). (Eb) After completion of repair synthesis, polκ is released, XPG cleaves off the flap, and XRCC1 recruits Ligase III to seal the remaining nick.

(reviewed in Lehmann, 2006). At first sight it may seem strange that the cell uses an error-prone polymerase to carry out NER repair synthesis. However, we have previously speculated that the low K_m of polκ may make it especially suitable for use under conditions of low nucleotide concentration (Ogi and Lehmann, 2006). An error frequency of 10^{-3} together with a patch size of 30 nucleotides would result in about one error every 30 repair patches. This may be a price worth paying for the cell to carry out successful repair synthesis. We speculate that polκ may in this way contribute to UV-induced mutagenesis in normal human cells, especially in quiescence. Indeed, the bacterial homolog of polκ, DinB, is believed to be involved in untargeted mutagenesis in *E. coli*, a mutagenic process that occurs on non-damaged DNA templates—independently of TLS—under conditions of starvation (Brotcorne-Lannoye and Maenhaut-Michel, 1986).

Our results, though raising many new questions, give important insights into the complexity of repair synthesis and the role of different polymerases in this process.

EXPERIMENTAL PROCEDURES

Antibodies and Cell Lines

Antibodies and cell lines used in the study are described in detail in the Supplemental Experimental Procedures.

RNA Interference

All the siRNA oligos were purchased from Dharmacon (the sequences can be obtained from the authors upon request). Cells were transfected using HiPerfect (QIAGEN) according to the manufacturer's instruction. Immunostaining and UDS experiments were performed 48 hr after transfection. Knockdown efficiencies were confirmed by western blot and immunofluorescence.

ChIP Assay

Experimental details have been described previously (Fousteri et al., 2006; Moser et al., 2007). Confluent or serum-starved cells were UVC irradiated (20 J/m^2) and incubated for 1 hr prior to in vivo crosslinking (11 min, on ice) and ChIP. Antibodies used for the ChIP are described in the Supplemental Experimental Procedures.

Local UV Irradiation and Immunofluorescence

Experimental details have been described previously (Volker et al., 2001). Cells were grown on coverslips and locally UVC irradiated (40 J/m^2) through a polycarbonate filter (pore size of 5 μm), followed by incubation for 0.5 to 1 hr. Cells were fixed and stained with antibodies described in detail in Supplemental Experimental Procedures. Photographs were captured with a Zeiss Axioobserver microscope.

Unscheduled DNA Synthesis Assay

Experimental details have been described previously (Limsirichaikul et al., 2009). Cells were siRNA transfected and grown on coverslips before the experiments. Cells were globally UVC irradiated (10 J/m^2) and incubated for 2 hr in medium supplemented with 10 μM EdU. After EdU incorporation, coverslips were processed as described in detail in Supplemental Experimental Procedures. Photographs were captured with a KEYENCE BIOREVO BZ-9000 system.

More detailed and additional experimental procedures are described in the Supplemental Experimental Procedures.

SUPPLEMENTAL INFORMATION

Supplemental Information includes Supplemental Experimental Procedures and four figures and can be found with this article online at doi:10.1016/j.molcel.2010.02.009.

ACKNOWLEDGMENTS

This work was supported by Special Coordination Funds for Promoting Science and Technology from Japan Science and Technology Agency (JST), a Grant in aid for Scientific Research KAKENHI (20810021) from Japan Society for the Promotion of Science, a cancer research grant from the YASUDA Medical Foundation, a research grant from Uehara Memorial Foundation, a medical research grant from Takeda Science Foundation, a Grant in aid for Honeybee Research from Yamada Apiculture Center Inc., a Grant in aid for Seeds Innovation (Type-A) from JST, and a Butterfield Medical Award from the Great Britain Sasakawa Foundation to T.O.; a Global COE Program from the Ministry of Education, Culture, Sports, Sciences and Technology of Japan to T.O., S.L., Y.N., and S.Y.; a KAKENHI to K.T. and Y.M.; a Medical Research Council programme grant to A.R.L.; and an EC-RTN and integrated project to A.R.L. and L.M. We are grateful to Y. Gushiken for anti-polκ antibody purification. The anti-polε antibody, 3A3.2, is a kind gift from S. Linn (University of California, Berkeley).

Received: May 26, 2009
Revised: September 25, 2009
Accepted: December 21, 2009
Published: March 11, 2010

REFERENCES

Aboussekhra, A., Biggerstaff, M., Shivji, M.K., Vilpo, J.A., Moncollin, V., Podust, V.N., Protic, M., Hubscher, U., Egly, J.M., and Wood, R.D. (1995). Mammalian DNA nucleotide excision repair reconstituted with purified protein components. Cell *80*, 859–868.

Andressoo, J.O., and Hoeijmakers, J.H. (2005). Transcription-coupled repair and premature ageing. Mutat. Res. *577*, 179–194.

Araujo, S.J., Tirode, F., Coin, F., Pospiech, H., Syvaoja, J.E., Stucki, M., Hubscher, U., Egly, J.M., and Wood, R.D. (2000). Nucleotide excision repair of DNA with recombinant human proteins: definition of the minimal set of factors, active forms of TFIIH, and modulation by CAK. Genes Dev. *14*, 349–359.

Avkin, S., Goldsmith, M., Velasco-Miguel, S., Geacintov, N., Friedberg, E.C., and Livneh, Z. (2004). Quantitative analysis of translesion DNA synthesis across a benzo[*a*]pyrene-guanine adduct in mammalian cells: the role of DNA polymerase κ. J. Biol. Chem. *279*, 53298–53305.

Bermudez, V.P., Maniwa, Y., Tappin, I., Ozato, K., Yokomori, K., and Hurwitz, J. (2003). The alternative Ctf18-Dcc1-Ctf8-replication factor C complex required for sister chromatid cohesion loads proliferating cell nuclear antigen onto DNA. Proc. Natl. Acad. Sci. USA *100*, 10237–10242.

Bi, X., Barkley, L.R., Slater, D.M., Tateishi, S., Yamaizumi, M., Ohmori, H., and Vaziri, C. (2006). Rad18 regulates DNA polymerase κ and is required for recovery from S-phase checkpoint-mediated arrest. Mol. Cell. Biol. *26*, 3527–3540.

Bienko, M., Green, C.M., Crosetto, N., Rudolf, F., Zapart, G., Coull, B., Kannouche, P., Wider, G., Peter, M., Lehmann, A.R., et al. (2005). Ubiquitin-binding domains in Y-family polymerases regulate translesion synthesis. Science *310*, 1821–1824.

Brotcorne-Lannoye, A., and Maenhaut-Michel, G. (1986). Role of RecA protein in untargeted UV mutagenesis of bacteriophage λ: evidence for the requirement for the dinB gene. Proc. Natl. Acad. Sci. USA *83*, 3904–3908.

Ducoux, M., Urbach, S., Baldacci, G., Hubscher, U., Koundrioukoff, S., Christensen, J., and Hughes, P. (2001). Mediation of proliferating cell nuclear antigen (PCNA)-dependent DNA replication through a conserved p21(Cip1)-like PCNA-binding motif present in the third subunit of human DNA polymerase δ. J. Biol. Chem. *276*, 49258–49266.

Fousteri, M., Vermeulen, W., van Zeeland, A.A., and Mullenders, L.H. (2006). Cockayne syndrome A and B proteins differentially regulate recruitment of chromatin remodeling and repair factors to stalled RNA polymerase II in vivo. Mol. Cell *23*, 471–482.

Friedberg, E.C., Lehmann, A.R., and Fuchs, R.P. (2005a). Trading places: how do DNA polymerases switch during translesion DNA synthesis? Mol. Cell *18*, 499–505.

Friedberg, E.C., Walker, G.C., Siede, W., Wood, R.D., Schultz, R.A., and Ellenberger, T. (2005b). DNA Repair and Mutagenesis, Second Edition (Washington, DC: ASM Press).

Gerik, K.J., Li, X., Pautz, A., and Burgers, P.M. (1998). Characterization of the two small subunits of Saccharomyces cerevisiae DNA polymerase δ. J. Biol. Chem. *273*, 19747–19755.

Gibbs, P.E., McDonald, J., Woodgate, R., and Lawrence, C.W. (2005). The relative roles in vivo of Saccharomyces cerevisiae Pol η, Pol ζ, Rev1 protein and Pol32 in the bypass and mutation induction of an abasic site, T-T (6-4) photoadduct and T-T cis-syn cyclobutane dimer. Genetics *169*, 575–582.

Gillet, L.C., and Scharer, O.D. (2006). Molecular mechanisms of mammalian global genome nucleotide excision repair. Chem. Rev. *106*, 253–276.

Guo, C., Tang, T.S., Bienko, M., Dikic, I., and Friedberg, E.C. (2008). Requirements for the interaction of mouse Polκ with ubiquitin and its biological significance. J. Biol. Chem. *283*, 4658–4664.

Hanawalt, P.C., and Spivak, G. (2008). Transcription-coupled DNA repair: two decades of progress and surprises. Nat. Rev. Mol. Cell Biol. *9*, 958–970.

Hanna, J.S., Kroll, E.S., Lundblad, V., and Spencer, F.A. (2001). Saccharomyces cerevisiae CTF18 and CTF4 are required for sister chromatid cohesion. Mol. Cell. Biol. *21*, 3144–3158.

Hoege, C., Pfander, B., Moldovan, G.L., Pyrowolakis, G., and Jentsch, S. (2002). RAD6-dependent DNA repair is linked to modification of PCNA by ubiquitin and SUMO. Nature *419*, 135–141.

Hughes, P., Tratner, I., Ducoux, M., Piard, K., and Baldacci, G. (1999). Isolation and identification of the third subunit of mammalian DNA polymerase delta by PCNA-affinity chromatography of mouse FM3A cell extracts. Nucleic Acids Res. *27*, 2108–2114.

Johnson, A., and O'Donnell, M. (2005). Cellular DNA replicases: components and dynamics at the replication fork. Annu. Rev. Biochem. *74*, 283–315.

Kai, M., and Wang, T.S. (2003). Checkpoint activation regulates mutagenic translesion synthesis. Genes Dev. *17*, 64–76.

Kannouche, P.L., Wing, J., and Lehmann, A.R. (2004). Interaction of human DNA polymerase η with monoubiquitinated PCNA: a possible mechanism for the polymerase switch in response to DNA damage. Mol. Cell *14*, 491–500.

Lam, L.H., and Reynolds, R.J. (1986). A sensitive, enzymatic assay for the detection of closely opposed cyclobutyl pyrimidine dimers induced in human diploid fibroblasts. Mutat. Res. *166*, 187–198.

Lee, M.Y., Jiang, Y.Q., Zhang, S.J., and Toomey, N.L. (1991). Characterization of human DNA polymerase δ and its immunochemical relationships with DNA polymerase α and ε. J. Biol. Chem. *266*, 2423–2429.

Lehmann, A.R. (2006). New functions for Y family polymerases. Mol. Cell *24*, 493–495.

Lehmann, A.R., Niimi, A., Ogi, T., Brown, S., Sabbioneda, S., Wing, J.F., Kannouche, P.L., and Green, C.M. (2007). Translesion synthesis: Y-family polymerases and the polymerase switch. DNA Repair (Amst.) *6*, 891–899.

Limsirichaikul, S., Niimi, A., Fawcett, H., Lehmann, A., Yamashita, S., and Ogi, T. (2009). A rapid non-radioactive technique for measurement of repair synthesis in primary human fibroblasts by incorporation of ethynyl deoxyuridine (EdU). Nucleic Acids Res. *37*, e31.

Majka, J., and Burgers, P.M. (2004). The PCNA-RFC families of DNA clamps and clamp loaders. Prog. Nucleic Acid Res. Mol. Biol. *78*, 227–260.

Masuda, Y., Suzuki, M., Piao, J., Gu, Y., Tsurimoto, T., and Kamiya, K. (2007). Dynamics of human replication factors in the elongation phase of DNA replication. Nucleic Acids Res. *35*, 6904–6916.

McCulloch, S.D., and Kunkel, T.A. (2008). The fidelity of DNA synthesis by eukaryotic replicative and translesion synthesis polymerases. Cell Res. *18*, 148–161.

Moldovan, G.L., Pfander, B., and Jentsch, S. (2007). PCNA, the maestro of the replication fork. Cell *129*, 665–679.

Moser, J., Kool, H., Giakzidis, I., Caldecott, K., Mullenders, L.H., and Fousteri, M.I. (2007). Sealing of chromosomal DNA nicks during nucleotide excision repair requires XRCC1 and DNA ligase III α in a cell-cycle-specific manner. Mol. Cell *27*, 311–323.

Mullenders, L.H., van Kesteren-van Leeuwen, A.C., van Zeeland, A.A., and Natarajan, A.T. (1985). Analysis of the structure and spatial distribution of ultraviolet-induced DNA repair patches in human cells made in the presence of inhibitors of replicative synthesis. Biochim. Biophys. Acta *826*, 38–48.

Nakajima, S., Lan, L., Kanno, S., Usami, N., Kobayashi, K., Mori, M., Shiomi, T., and Yasui, A. (2006). Replication-dependent and -independent responses of RAD18 to DNA damage in human cells. J. Biol. Chem. *281*, 34687–34695.

Nishida, C., Reinhard, P., and Linn, S. (1988). DNA repair synthesis in human fibroblasts requires DNA polymerase δ. J. Biol. Chem. *263*, 501–510.

Ogi, T., and Lehmann, A.R. (2006). The Y-family DNA polymerase κ (pol κ) functions in mammalian nucleotide-excision repair. Nat. Cell Biol. *8*, 640–642.

Ogi, T., Kannouche, P., and Lehmann, A.R. (2005). Localisation of human Y-family DNA polymerase κ: relationship to PCNA foci. J. Cell Sci. *118*, 129–136.

Ogiwara, H., Ohuchi, T., Ui, A., Tada, S., Enomoto, T., and Seki, M. (2007). Ctf18 is required for homologous recombination-mediated double-strand break repair. Nucleic Acids Res. *35*, 4989–5000.

Ohashi, E., Bebenek, K., Matsuda, T., Feaver, W.J., Gerlach, V.L., Friedberg, E.C., Ohmori, H., and Kunkel, T.A. (2000a). Fidelity and processivity of DNA synthesis by DNA polymerase κ, the product of the human DINB1 gene. J. Biol. Chem. *275*, 39678–39684.

Ohashi, E., Ogi, T., Kusumoto, R., Iwai, S., Masutani, C., Hanaoka, F., and Ohmori, H. (2000b). Error-prone bypass of certain DNA lesions by the human DNA polymerase κ. Genes Dev. *14*, 1589–1594.

Ohmori, H., Friedberg, E.C., Fuchs, R.P., Goodman, M.F., Hanaoka, F., Hinkle, D., Kunkel, T.A., Lawrence, C.W., Livneh, Z., Nohmi, T., et al. (2001). The Y-family of DNA polymerases. Mol. Cell *8*, 7–8.

Plosky, B.S., Vidal, A.E., Fernandez de Henestrosa, A.R., McLenigan, M.P., McDonald, J.P., Mead, S., and Woodgate, R. (2006). Controlling the subcellular localization of DNA polymerases ι and η via interactions with ubiquitin. EMBO J. *25*, 2847–2855.

Podust, V.N., Chang, L.S., Ott, R., Dianov, G.L., and Fanning, E. (2002). Reconstitution of human DNA polymerase δ using recombinant baculoviruses: the p12 subunit potentiates DNA polymerizing activity of the four-subunit enzyme. J. Biol. Chem. *277*, 3894–3901.

Prakash, S., Johnson, R.E., and Prakash, L. (2005). Eukaryotic translesion synthesis DNA polymerases: specificity of structure and function. Annu. Rev. Biochem. *74*, 317–353.

Shikata, K., Ohta, S., Yamada, K., Obuse, C., Yoshikawa, H., and Tsurimoto, T. (2001). The human homologue of fission Yeast cdc27, p66, is a component of active human DNA polymerase δ. J. Biochem. *129*, 699–708.

Shiomi, Y., Masutani, C., Hanaoka, F., Kimura, H., and Tsurimoto, T. (2007). A second proliferating cell nuclear antigen loader complex, Ctf18-replication factor C, stimulates DNA polymerase η activity. J. Biol. Chem. *282*, 20906–20914.

Smith, C.A., and Okumoto, D.S. (1984). Nature of DNA repair synthesis resistant to inhibitors of polymerase α in human cells. Biochemistry *23*, 1383–1391.

Staresincic, L., Fagbemi, A.F., Enzlin, J.H., Gourdin, A.M., Wijgers, N., Dunand-Sauthier, I., Giglia-Mari, G., Clarkson, S.G., Vermeulen, W., and Scharer, O.D. (2009). Coordination of dual incision and repair synthesis in human nucleotide excision repair. EMBO J. *28*, 1111–1120.

Suzuki, N., Ohashi, E., Kolbanovskiy, A., Geacintov, N.E., Grollman, A.P., Ohmori, H., and Shibutani, S. (2002). Translesion synthesis by human DNA polymerase κ on a DNA template containing a single stereoisomer of dG-(+)- or dG-(-)-anti-N^2-BPDE (7,8-dihydroxy-anti-9,10-epoxy-7,8,9,10-tetrahydrobenzo[*a*]pyrene). Biochemistry *41*, 6100–6106.

Volker, M., Mone, M.J., Karmakar, P., van Hoffen, A., Schul, W., Vermeulen, W., Hoeijmakers, J.H., van Driel, R., van Zeeland, A.A., and Mullenders, L.H.

(2001). Sequential assembly of the nucleotide excision repair factors in vivo. Mol. Cell *8*, 213–224.

Watanabe, K., Tateishi, S., Kawasuji, M., Tsurimoto, T., Inoue, H., and Yamaizumi, M. (2004). Rad18 guides poleta to replication stalling sites through physical interaction and PCNA monoubiquitination. EMBO J. *23*, 3886–3896.

Wood, R.D., and Shivji, M.K. (1997). Which DNA polymerases are used for DNA-repair in eukaryotes? Carcinogenesis *18*, 605–610.

Zhang, Y., Yuan, F., Xin, H., Wu, X., Rajpal, D.K., Yang, D., and Wang, Z. (2000). Human DNA polymerase κ synthesizes DNA with extraordinarily low fidelity. Nucleic Acids Res. *28*, 4147–4156.

Zhou, J.Q., He, H., Tan, C.K., Downey, K.M., and So, A.G. (1997). The small subunit is required for functional interaction of DNA polymerase δ with the proliferating cell nuclear antigen. Nucleic Acids Res. *25*, 1094–1099.